Sir Herbert Duthie Library
Llyfrgell Syr Herbert Duthie

University Hospital
of Wales
Heath Park
Cardiff
CF14 4XN

Ysbyty Athrofaol Cymru
Parc y Mynydd Bychan
Caerdydd
CF14 4XN

029 2074 2875
duthieliby@cardiff.ac.uk

DNA repair and transcription of the yeast *MFA2* gene:

roles of Tup1p, Gcn5p and Rad16p

Hairong Liu

Department of Pathology

Wales college of Medicine

Cardiff University

A thesis submitted to Wales College of Medicine, Cardiff University for

the degree of Doctor of Philosophy

September 2005

ProQuest LLC
789 East Eisenhower Parkway
P.O. Box 1346
Ann Arbor, MI 48106-1346

ACKNOWLEDGEMENTS

I would like to sincerely thank my supervisor Professor Raymond Waters for his patience, support, encouragement and excellent guidance throughout this study. I still remember the moment that he agreed that I could join this group for my PhD study, I was so excited to have a chance to do research in molecular biology. I have still kept the text books which he lent to me about four years ago and hope I can keep them longer, with no penalty for them being overdue.

I must thank Dr. Yumin Teng, a talented senior colleague who I have worked with for the last four years. He has taught me techniques and given me important suggestions for my experiments. Many thanks also to Dr. Yachuan Yu, for his good suggestions and friendship.

I also wish to give many thanks to Dr. Simon Reed, who was happy to discuss NER with me, and to Dr. Shirong Yu, for help both in the lab and out of work, to Dr. Nerys Morse, Mrs. Charlotte O'connell, Dr. Sarah Forbes-Robertson, Dr. Kerenza Njoh and many others in the School of biological sciences in Swansea and Department of Pathology of the Medical School in Cardiff, for improving my English and enabling me to enjoy my life in Wales.

I must thank my husband, Zheng, for his love, warm support and fully understanding in the twelve years since we met. I need give special thanks to my lovely son, Zichi (Leo), a four and half year old gentleman, who is my source of happiness, and is always next to me when I have been writing my thesis.

Thanks to my parents, who have encouraged me to follow science from an early age, and try hard to in my studies. Also many thanks to my younger brother, Qiang, for as much support as he can possibly offer. And thanks to both my parents and parents-in-law. Without their help in caring for my son, I would not have finished my PhD study.

Also in memory of my deeply loved grandmother, who sadly passed away three years ago without having realized her dream of seeing me finish my PhD study.

Finally, I would like to acknowledge the Chinese government, University of Wales, Swansea and the Medical School, Cardiff for offering my PhD studentship.

SUMMARY

In this thesis, the effect of transcription and chromatin remodelling on the Nucleotide Excision Repair (NER) of UV induced Cyclobutane Pyrimidine Dimer (CPD) DNA damage in the yeast *Saccharomyces cerevisiae* was examined. The model gene *MFA2* is an **a**-mating type specific gene-active in **a**-cells and repressed in α-cells by the co-repressor Tup1p-Ssn6p. Deletion of *TUP1* can derepress *MFA2* in α-cells, and also enhance the NER in the regulatory region of *MFA2* in α-cells. Mutating the TATA box in a *Δtup1* α background can abolish the transcription of *MFA2* which was induced due to the absence of Tup1p. However, the accelerated NER still occurred in the regulating regions of both the Transcribed strand (TS) and Non-transcribed strand (NTS) of $\Delta tup1 mfa2^{TATA}$α-cells compared to wild type α-cells. These results were in accord with the nucleosome mapping data which showed that nucleosomes at *MFA2* were disrupted when deleting *TUP1*. Hence, the enhanced NER induced by *TUP1* deletion in the regulating region are the result of changes in chromatin structure and transcriptional regulation.

The deletion of *TUP1* in α-cells can partially suppress the absolute requisite of Rad16p in Global Genome Repair (GGR) at *MFA2*. Rad16p is deemed an essential protein for functional GGR in transcriptionally silenced regions. In a *Δtup1rad16* α strain, CPDs can be repaired at many nucleotide sites, however, the survival of this strain shows it is still as sensitive to UV irradiation as the *Δrad16* strain. This effect was not seen at the *RPB2* locus where Tup1p had no effect on GGR. Therefore, this is a local phenomenon.

To clarify the role of one of the general chromatin remodelling factors-the histone acetylase Gcn5p in NER, I undertook experiments with *Δgcn5* and *Δtup1gcn5* strains. In *Δgcn5* **a**-cells, the transcription level of *MFA2* was decreased to 20% of that in wild type **a**-cells, and there was no effect on the repression of *MFA2* in *Δgcn5* α-cells. Slower repair was observed in both **a**- and α-cells. However, deletion of *TUP1* in a *Δgcn5* background can actively transcribe *MFA2* in α-cells, and increase the repair rate in both TS and NTS of *MFA2* which was even faster than in wild type α-cells. These results showed that Gcn5p plays a role in transcription and NER at *MFA2* by remodelling the chromatin structure, and deletion of *TUP1* can influence the role of Gcn5p in regulation at *MFA2*.

ABBREVIATIONS

AP	Apurinic/Apyrimidinic
ACF	ATP-utilizing chromatin assembly and remodelling factor
BER	Base excision repair
CBP	CREB binding protein
COFS	Cerebro-oculofacio-skeletal syndrome
CPD	Cyclobutane pyrimidine dimer
CS	Cockayne syndrome
DNA	Deoxyribonucleic Acid
dRPase	Deoxyribophosphodiesterase
dsDNA	Double-stranded DNA
ERCC	Excision repair cross complementing protein
GGR	Global genome repair
HAT	Histone acetyltransferase
HDAC	Histone deacetylase
HhH motif	Helix-hairpin-helix motif
HR	Homologous recombination
ML endo	*Micrococcus luteus* CPD endonuclease
MPC	Magnetic particle concentrator
mRNA	Messenger RNA
NER	Nucleotide excision repair
NTS	Non-transcribed strand
NuRD	Nucleosome remodelling histone deacetylase complex
NURF	Nucleosome remodelling factor
PCR	Polymerase chain reaction
PCNA	Proliferating cell nuclear antigen
Pol I (II)	Polymerase I (II)
6-4PPs	Pyrimidine-pyrimidone (6-4) lesions
RFC	Replication factor C
RNA	Ribonucleic acid
RPA	Replication protein A
RSC	Remodel the structure of chromatin
RSF	Remodeling and Spacing factor
SAGA	Spt-Ada-Gcn5-Acetyltransferase
S. cerevisiae	*Saccharomyces cerevisiae*
SIR	Silent information regulator
ssDNA	Single-stranded DNA
SWI/SNF	Switch/Sucrose nonfermenting
TAF	TBP associated factor
TBP	TATA box binding protein
TCR	Transcription coupled repair
TFIIH	Transcription factor II H
TS	Transcribed strand
TTD	Trichothiodystrophy
URS	Upstream regulatory sequence
UV	Ultraviolet (light)
XP	Xeroderma pigmentosum
XP-DSC	XP with DeSanctis-Cacchione syndrome
YC	Yeast complete medium

CONTENTS

Chapter 1
General Introduction

1.1 DNA damages

The accumulation of DNA damage, fuelling genetic instability in cells, is one of the factors postulated to drive the processes of aging and cancer in organisms ranging from simple eukaryotes to humans. The fundamental axiom of genetic inheritance is that exceptional genetic stability must be successful over many generations of cells and organisms. However, DNA is constantly exposed to the damaging effects of normal metabolic processes and to genotoxic agents in the environment. Over time, DNA accumulates changes that activate protooncogenes, inactivate tumour-suppressor genes and contribute to age-related functional decline. Therefore, DNA repair — biochemical pathways by which damaged, inappropriate, and mispaired bases are restored to their native state — is an essential process for the survival of all kinds of cells and organisms (Friedberg 1995, 2001; Hoeijmakers, 2001; de Boer *et al.*, 2002; Hasty, 2002; Sancar *et al.*, 2005).

Lesions can be induced in DNA by both exogenous and endogenous damaging agents. Environmental agents such as the ultraviolet (UV) component of sunlight, ionizing radiation and numerous carcinogenic chemicals cause alterations in DNA structure; these may lead to mutations that enhance cancer risk. DNA bases can absorb UV light directly and these lesions are discussed later. Ionizing radiations,

such as X-ray, γ-ray *etc.*, erode DNA structure either directly, for example, by inducing single- and double- strand breaks (SSBs and DSBs), or indirectly through oxidative stress. Many chemicals that cause cancer can react with DNA. Only a few reactive electrophiles, eg. ethylmethane sulfonate (EMS), methyl nitrosourea (MNU), are direct-acting carcinogens. They modify the DNA structure by chemically reacting with nitrogen and oxygen atoms. There are also indirect-acting carcinogens that are unreactive, water-insoluble compounds which need to be activated by enzymes in metabolic processes or other oxidative pathways prior to reacting with DNA (Friedberg, 1995, 2001; Hoeijmakers, 2001; Lehmann, 2000).

Endogenous DNA changes can come from normal cellular metabolism, including replication, transcription and repair. For example, *via* misincorporation of nucleotides during DNA replication and uncompleted DNA repair. They can also arise through spontaneous alteration of chemical bonds in DNA. Metabolic products include reactive oxygen species (ROS), such as superoxide anions, hydroxyl radicals and hydrogen peroxide, derived from oxidative respiration and products of lipid peroxidation. More than 100 oxidative modifications have been identified in DNA. Hydrolysis of nucleotide residues also leaves non-instructive abasic sites. Examples of these spontaneous or induced alterations of the chemical structure of DNA include the deamination of cytosine, adenine, guanine or 5-methylcytosine, converting these bases to the miscoding uracil, hypoxanthine, xanthine and thymine, respectively (Lindahl, 1993; Friedberg, 1995; Hoeijmakers, 2001).

The research presented here focuses on UV induced DNA damage.

1.1.1 UV-induced DNA damage

UV radiation is a potent environmental agent that damages DNA. In humans it only penetrates our skin, yet it can induce acute and chronic reactions. The UV radiation spectrum has been subdivided into three wavelength bands designated UV-A (400 to 320nm), UV-B (320-290nm), and UV-C (290-100nm). UV-C light at or near 254nm is close to the maximum absorption spectrum of DNA (~260nm), and generates many lesions in this molecule. However, UV-A and UV-B are the main components of solar UV radiation, because wavelengths below 320nm do not easily penetrate the atmospheric ozone (Friedberg *et al.*, 1995). The existence of holes in the ozone layer, however, means such radiation is playing an increasing role (Diffey, 2004). UV-B is highly mutagenic and carcinogenic in animals, and it can cause DNA damage, including CPDs and (6-4) photoproducts. These lesions can lead to the development of skin cancer. The phototoxic effect of UV-A is much lower compared to UV-B, since DNA is not a chromophore of UV-A. Cyclobutane pyrimidine dimers (CPDs) and (6-4) photoproducts account for the majority (~95%) of UV induced lesions after exposure to UV-C, with CPDs predominating at levels of up to about 75% of the total damage. Other damages occurring at low frequency include purine or pyrimidine hydrates, thymine glycols, DNA cross-links and strand breaks (Friedberg *et al.*, 1995; Ichihashi *et al.*, 2003).

1.1.1.1 Cyclobutane Pyrimidine Dimers (CPDs)

When DNA is exposed to UV light at a wavelength approaching its absorption

maximum (~260nm), adjacent pyrimidines in the same strand can form two covalent bonds at C^5-C^5 and C^6-C^6 (Fig. 1.1), resulting in a four-membered ring due to saturation of the C^5=C^6 double bonds in both pyrimidines. The structure of this formed cyclobutyl ring is referred to as a Cyclobutane Pyrimidine Dimer (CPD). CPDs can theoretically have 12 isomeric forms. However, only four of them, with the configuration of *cis-syn*, *cis-anti*, *trans-syn*, and *trans-anti* can have significant yields. In the double stranded B-form of DNA, the *cis-syn* isomer is thought to be the major form of CPD induced by UV irradiation (Friedberg *et al.*, 1995).

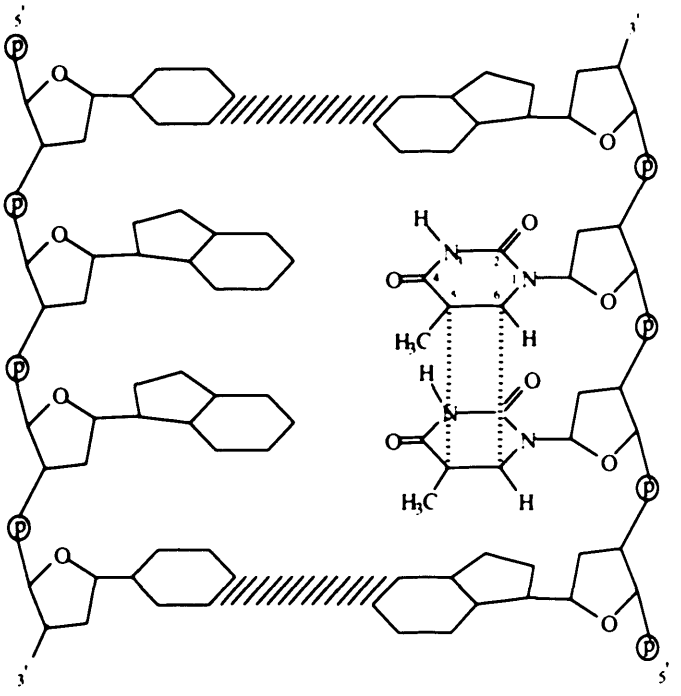

Figure 1.1 *Structure of a CPD.* Covalent interaction of two adjacent pyrimidines in the same polynucleotide chain forms a four-membered cyclobutyl ring linking the two pyrimidines. The formation of two new bonds (C^5-C^5, C^6-C^6) results from the saturation of the two C^5=C^6 double bonds in two pyrimidines. (Adapted from Friedberg *et al.*, 1995)

Traditionally, CPDs have been considered to be bulky, helix-distorting DNA damages (they induce a bend or kink of 7-9°), which are strictly uncoding and can

induce an obligatory arrest of replication and transcription, although this can be overcome in the case of replication (Wang and Taylor, 1991; Kim *et al.*, 1995; Friedberg *et al.*, 2004). The influence of these lesions on the local DNA structure is important because it is likely related to their recognition by repair enzymes or how they are dealt with in the template strand during replication (Seeberg and Fuchs, 1990; Sancar, 1994; Kusumoto *et al.*, 2001).

The yield of CPDs varies depending on the composition of DNA. Studies have showed the ratio of T=T to C=T to T=C to C=C is 68:13:16:3 in irradiated plasmid DNA. A similar trend has been found in human cells (Mitchell *et al.*, 1992; Tornaletti *et al.*, 1993). Formation of CPDs is also influenced by the flanking sequences for potential dimer sites. For example, the different sites of potential T=T at 5'ATTG3', 5'CTTC3' and 5'CTTTA3' reached different saturated levels that varied from 4% to 16%. Generally, the saturated level of dimers for TT sites at 5'ATTA3' is greater than that at 5'ATTG3' (Gordon and Haseltine, 1982). Moreover, CPD formation is also affected by the upstream and downstream sequences of the potential dimer sites, and is different in single- or double-stranded DNA (Friedberg *et al.*, 1995).

Additionally, the interaction between DNA and proteins affects the formation of CPDs, as reported for the *lac* repressor bound to the *lac* operator in *Escherichia coli* (Becker and Wang, 1984) and for several promoter elements that interact with sequences-specific proteins in yeast and mammalian cells. Transcription factors have direct effects on the induction and repair of CPDs (Selleck and Majors, 1987; Pfeifer *et al.*, 1992; Axelrod *et al.*, 1993; Tornaletti and Pfeifer, 1995). Whereas, chromatin

structure also can modulate damage formation induced by UV light. Bending DNA around the histone octamer facilitates inducing CPDs at sites where the DNA minor grooves face outside. Irrespective of the CPD modulation, CPDs can be detected throughout the nucleosome core. Thus, nucleosomes show a substantial degree of DNA flexibility as well as structural constraints, which modulates formation of DNA damage and also is essential for DNA repair (Thoma, 1999). Transcription factors and chromatin structure also influence CPD repair; this will be dealt with later.

1.1.1.2 Pyrimidine-Pyrimidone (6-4) photoproducts

Pyrimidine-Pyrimidone (6-4) photoproducts are the second most common type of UV- induced lesion, accounting for majority of the remaining 15-30% of DNA damage caused by UV (Mitchell and Nairn, 1989). These lesions occur at positions of cytosine (and much less frequently, thymine) located 3' to a pyrimidine nucleotide and introduce a major distortion (a bend or kink of about 44°) in the double helical structure of DNA by forming a stable bond between the two pyrimidines (5'C^6-$C^4$3') (Fig. 1.2) (Friedberg *et al.*, 1995; Kim *et al.*, 1995). (6-4) photoproducts occur mostly at TC sites, whereas there are relatively less at TT and CC. (Lippke *et al.*, 1981; Franklin *et al.*, 1985). In contrast to CPDs, (6-4) photoproduct distribution is not facilitated within nucleosomes (Gale and Smerdon, 1990). Apparently, there is no natural distortion in nucleosomal DNA which enables formation of the (6-4) photoproduct at any specific site. Hence, (6-4) photoproducts occur predominantly in linker DNA, where there is a higher flexibility compared to DNA folded in

nucleosomes (Niggli and Cerutti, 1982). It should also be noted that, proteins and protein complexes that disturb the B-form structure of DNA influence both the yields and the types of DNA damage including CPDs and (6-4) photoproducts (Becker and Wang, 1984).

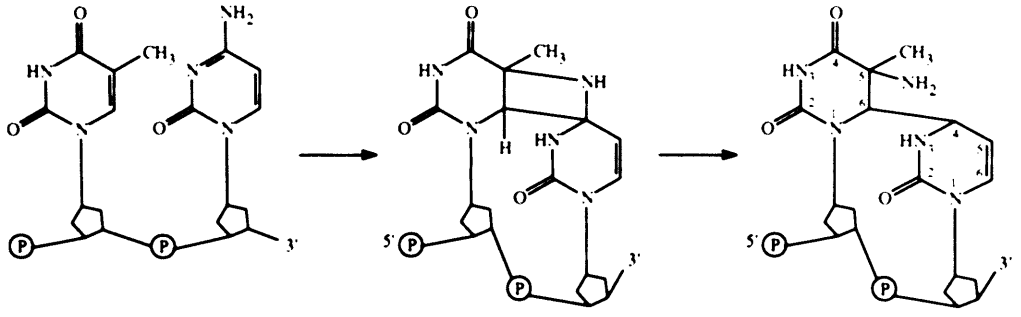

Figure 1.2 *Formation of the UV induced T-C (6-4) crosslink.* The covalent linkage between the C^6 position of one thymine and the C^4 position of the 3' adjacent cytosine forms due to UV radiation. It can be assumed that (6-4) photoproduct is a major distortion of the double helix. (Adapted from Friedberg *et al.*, 1995)

1.1.2 Cellular responses to DNA damage

The induction of DNA damage results in the transcriptional upregulation of a large number of genes, the precise functions of many of which remain to be established. Additionally, cells have evolved complex signaling pathways, consisting of sensors, transducers and effectors, to arrest the progression of the cell cycle in the presence of DNA damage, thereby providing increased time for repair and tolerance mechanisms to operate. When the burden of genomic damage is simply too large to be effectively met by the various responses, cells in multi-cellular eukaryotes are able to initiate programmed cell death (apoptosis), thereby eliminating themselves from a

population that otherwise might suffer serious pathological consequences (Zhou and Elledge, 2000; Friedberg, 2003).

1.2 DNA repair pathways

The initial reaction of a cell to DNA lesions is to repair the damage. DNA repair is the main defence process for cells to remove the lesions and help preserve the integrity of the whole genome. As soon as life began on earth it would have been subjected to exposure to agents that damage the genome, so DNA repair systems must have arisen early in evolution. As a result DNA repair pathways are highly conserved in both prokaryotes and eukaryotes. (Hoeijmakers, 2001)

DNA repair embraces the direct reversal of some types of damage, such as the enzymatic photoreactivation of CPDs, multiple distinct mechanisms for excising damaged bases, termed base excision repair (BER), nucleotide excision repair (NER) and mismatch repair (MMR), and repair mechanisms dealing with double strand breaks (DSBs), such as homologous recombination and non-homologous end joining. The principle of the mechanism of excision repair involves cutting out the damaged region as an oligonucleotide, inserting new bases to fill the gap using the opposite strand as a template, followed by ligation of the new DNA to the old (Friedberg, 2003; Sancar *et al.*, 2005). The research in this thesis focuses on excision repair, so BER and NER mechanism will be described further.

1.2.1 Base excision repair (BER)

BER repairs DNA lesions that arise from cellular hydrolytic events such as deamination or base loss, oxygen free radical attack or the methylation of ring nitrogens by endogenous agents (Lindahl, 1993). The main process in base excision repair is hydrolysis of the N-glycosyl bond linking a modified base to the deoxyribose-phosphate chain, which excises the base residue in the free form. The base release is catalyzed by DNA glycosylases, and there are specific enzymes for specific sets of lesions (Wood, 1996). The resulting apurinic or apyrimidinic (AP) sites (also another type of DNA damage) need to be processed by a second class of base excision repair enzymes called AP endonucleases. AP endonucleases produce incisions or nicks in duplex DNA through hydrolyzing the phosphodiester bonds close to 5' or 3' of each AP site, and generate 5' terminal deoxyribose-phosphate residues. Exonucleases can remove these residues by initiating the degradation of DNA at free ends. This process is accompanied by DNA repair synthesis and then ligation to complete BER (Friedberg *et al*, 1995; Sancar, 1995). An outline of the BER is shown in Fig. 1.3.

DNA Glycosylases

DNA glycosylases are DNA repair enzymes. They process damaged bases with a high specificity and have similar functions through a common intermediate by a similar chemistry, although they often share very little sequence homology. Generally, glycosylases are small proteins without subunit structure and they do not require any cofactors or exogenous energy source. (Lindahl, 1982; Friedberg *et al*, 1995; Krokan

et al., 1997) Here, the discussion of DNA glycosylases will focus on those involved in the repair of UV-induced DNA damage.

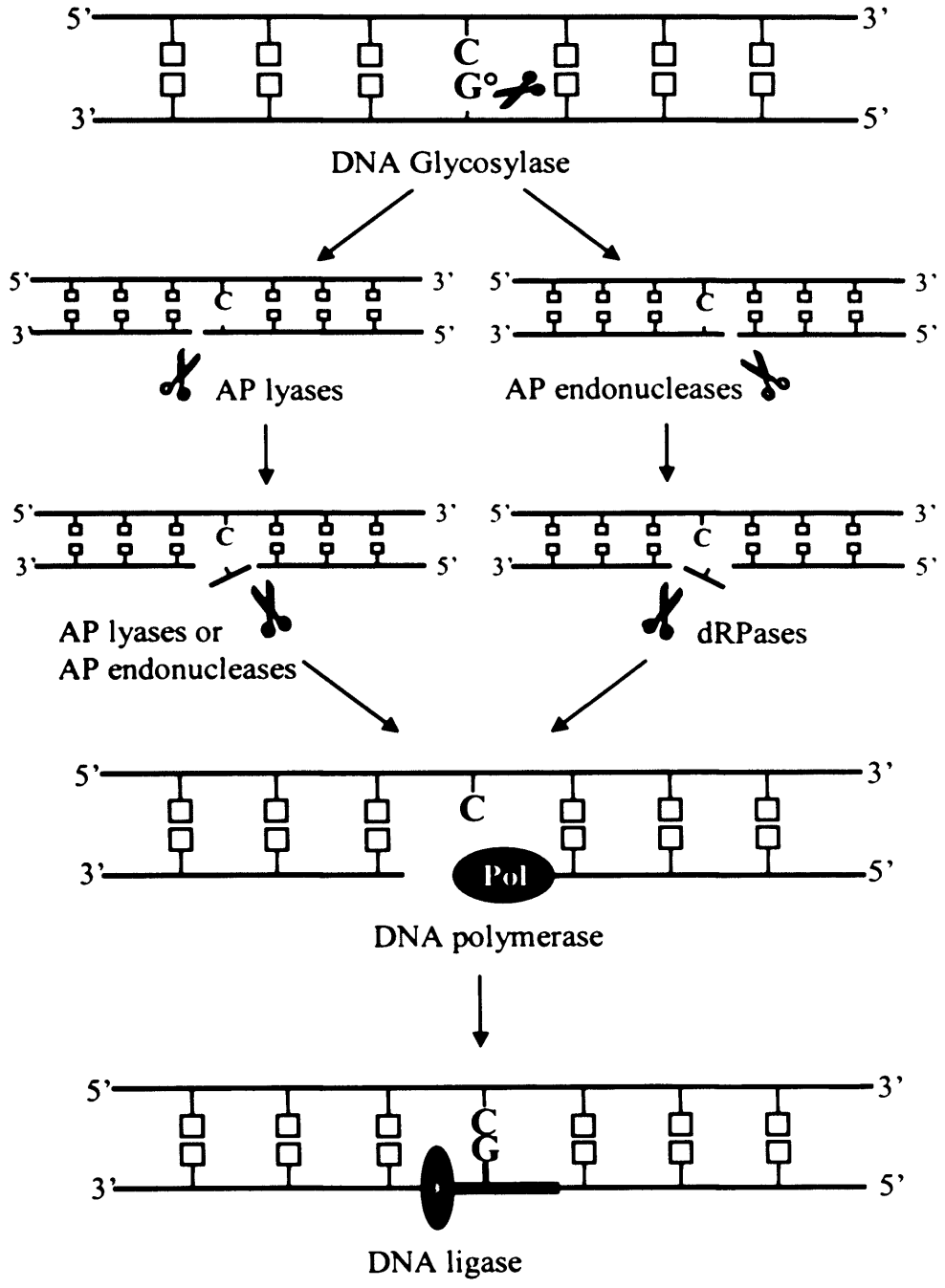

Figure 1.3 *The base excision repair (BER) pathway.* BER is initiated by a DNA glycosylase. The resulting AP site is removed either by an AP endonuclease and dRPase or by an AP lyase associated with the DNA glycosylases. Finally, the single nucleotide gap is filled by a DNA polymerase and sealed by DNA ligase. (Adapted from Yu [Ph.D thesis])

Pyrimidine dimer DNA glycosylases

Pyrimidine dimer DNA glycosylases, including T4 endonuclease V (T4 endo V) and *Micrococcus luteus* UV endonuclease, affect the hydrolysis of only one of the two glycosyl bonds in pyrimidine dimers. Thus, unlike other DNA glycosylases, they do not excise free bases, since the cyclobutane rings of CPDs are unaffected and still covalently bound to the DNA. Therefore, dimers are excised during the process of postincisional degradation as part of a nucleotide structure not as free bases (Friedberg *et al.*, 1995).

T4 endonuclease V

T4 endo V is a *cis-syn* CPD specific glycosylase with concomitant AP lyase activity. It is a small protein composed of 137 amino acids purified from bacteriophage T4. This protein consists of a single, compact domain containing three α-helices, and interacts with the pyrimidine dimers in the minor groove. (Slupphaug *et al.*, 1996; Krokan *et al.*, 1997; Lloyd, 1998) However, unlike other DNA glycosylases, T4 endo V does not flip the target bases out of the dsDNA helix, but instead flips an adenine which is complementary to the thymine of CPDs into a cavity on the enzyme surface. This alteration of flipping may help T4 endo V to differentiate damaged from normal DNA, and it also forms an empty space which will be occupied by its important catalytic residues.

Micrococcus luteus UV endonuclease

Micrococcus luteus UV endonuclease shares a common mechanism of catalysis with T4 endo V, in which it exclusively cleaves the 5'-bond in dimerized pyrimidines

and contains AP lyase activity. (Hamilton *et al.*, 1992; Krokan *et al.*, 1997; McCullough *et al.*, 1999) The protein is about 31-32kDa, with significant identity to the emerging family of DNA glycosylases containing a $[4Fe\text{-}4S]^{2+}$ cluster and a HhH motif. It exclusively cleaves the *cis-syn* thymine dimers and not *trans-syn*, (6-4) or Dewar dimers (Piersen *et al.*, 1995). This substrate specificity is similar to that of T4 endo V, except that the latter enzyme is also able to cleave *trans-syn* thymine dimers although only at a very low rate of ~1% that of cleavage of *cis-syn* dimers. (Smith and Taylor, 1993; Krokan *et al.*, 1997)

1.2.2 Nucleotide excision repair (NER)

Nucleotide excision repair (NER) is the most complicated excision repair process acting upon a wide range of alterations that result in large local distortions of DNA. It has also been reported to operate on some base damages that are substrates for BER. Thus some damages may be repairable by either mechanism. Following UV radiation the most relevant target lesions for NER are CPDs and (6-4) photoproducts. It also operates on numerous bulky chemical adducts as well as intrastrand crosslinks. Not all adducts are removed equally well. It is possible that the efficiency of NER may depend on the degree of structural difference from a normal base pair although other factors such as sequence context and chromatin structure also have roles. Defects in NER occur in humans suffering from the recessive cancer-prone genetic diseases, Xeroderma Pigmentosum (XP), Cockayne's Syndrome (CS) and trichothiodystrophy (TTD), *etc.*. These are characterized by sensitivity to sunlight and in the cases of XP,

high incidences of sunlight induced skin cancer (Lehmann, 2001; Hoeijmakers, 2001; Reed and Waters, 2003; Sancar, 2005)

Hence NER operates on a structurally diverse repertoire of DNA modifications and it might have to compete with other repair proteins that interact with structural alterations in DNA (de Laat *et al.*, 1999; Cline and Hanawalt, 2003).

In eukaryotes NER employs more than 30 proteins to remove damages from naked DNA *in vitro* and some of them also take part in other aspects of DNA metabolism such as replication and transcription (Petit and Sancar, 1999; Hoeijmakers, 2001).

NER operates in all free-living species tested, from the smallest life form of *Mycoplasma genitalium* to humans (Sancar, 1994). However, the subunits of excinucleases (see later) in prokaryotes do not share significant homology with any of those in eukaryotes. Bacteria recognize and excise bulky DNA modifications using the UvrABC complex, whereas, eukaryotes have evolved a more complicated NER mechanism comprised of numerous protein complexes with conserved functions from *S. cerevisiae* to human cells (Van Houten *et al.*, 2002; Costa *et al.*, 2003; Cline and Hanawalt, 2003). Next I will discuss in detail the NER process in the yeast *S. cerevisiae* and in humans.

1.3 Nucleotide excision repair *S. cerevisiae* and Humans

Eukaryotic NER is similar and conserved in organisms ranging from the yeast *S. cerevisiae* to *Drosophila, Xenopus,* and mammals. This high degree of conservation

has facilitated rapid progress in the field. The following discussion considers biochemical features of the most studied systems, those of the budding yeast *S. cerevisiae* and humans. Relevant proteins in human cells and yeast are summarized in Table 1. In yeast, cells with defects in NER proteins were first isolated as UV-sensitive *rad* mutants (named for radiation sensitive). In mammalian cells, NER mutants include human cells from individuals with one of the seven repair-deficient complementation groups A through G of XP, and those suffering with CS or TTD. Other important mutants are UV-sensitive rodent cell lines isolated in the laboratory, and which were complemented by human genes, namely excision repair cross-complementing (ERCC) genes. Some ERCC genes are identical to *XP* genes, in which case the *XP* designation is preferred (Lehmann *et al.*, 1994; Wood, 1996; Reed and Waters, 2003).

1.3.1 Genes required for NER in *S. cerevisiae* and humans

In *S. cerevisiae* there are two groups of genes involved in NER. The first group consists of *RAD1, RAD2, RAD3, RAD4, RAD10, RAD14* and *RAD25* genes, which are essential for all NER. The second group contains the *RAD7, RAD16, ABF1, RAD23* and *MMS19* genes. Mutations in the first group of genes confer a very high degree of sensitivity to UV light and cause a defect in the incision of DNA damage throughout the genome. Genes in the second group are not essential for all NER. Mutations in these cause a moderate degree of UV sensitivity and with respect to *RAD7, RAD16* and *ABF1*, are essential only for the repair of non-transcribed DNA and strands

(Verhage *et al.*, 1994; de Laat *et al.*, 1999; Wood, 1996, 1999; Reed *et al.*, 1998, 1999; Prakash and Prakash, 2000).

Except for *RAD7*, *RAD16*, *ABF1* and *MMS19*, homologues of all other mentioned yeast genes, have been identified in humans. Mutations in these human genes affect NER in a similar fashion to in yeast, with the exception of *XPC*, the human counterpart of the yeast *RAD4* gene. A *rad4* mutation shows the same high level of UV sensitivity as mutations of other first group genes and is completely defective in NER incision. However, XPC is only required for the repair of non-transcribed regions of the genome but not for the repair of the transcribed DNA strand of active genes. Contrarily in yeast, the repair of the transcriptionally inactive regions of whole genome has a specific dependence on the *RAD7*, *RAD16* and *ABF1* genes, whereas they play no role in the repair of the transcribed strand.

RAD26 and *RAD28* respectively represent the yeast counterparts of *CSB* and *CSA*, they function in transcription-coupled repair (TCR). However, only mutations of *RAD26*, but not of *RAD28*, affect TCR in yeast. Table 1 summarizes the NER proteins in yeast and human cells (Friedberg, 1996; Wood, 1996, 1999; Prakash and Prakash, 2000). The function of Rad26p in TCR is not clear. It has been considered that Rad26p can displace the RNA polymerase complex and recruit NER factors when transcription is arrested at a lesion (Friedberg, 1996; Tijsterman and Brouwer, 1999; de Boer and Hoeijmakers, 2000). Moreover, Rad26p was observed to promote efficient transcription through a damaged DNA strand. (Lee *et al.*, 2001, 2002; Woudstra *et al.*, 2002; Svejstrup *et al.*, 2002). Bucheli *et al.* (2001) had found that the

defect in the *rad26* mutant for TCR was dependent on the type of carbon source and disruption of *RAD26* leads to a specific defect in DNA repair and not transcription.

Table 1 Nucleotide excision repair genes in yeast and humans

S. cerevisiae	Human homolog	Activities
RAD14	*XPA*	binding DNA damage
RAD4	*XPC*	binding ssDNA with RAD23
RAD23	*HHR23B/A*	associated with RAD4
RAD1	*XPF*	DNA nuclease with RAD10 for 5'
RAD10	*ERCC1*	of damage
RAD2	*XPG*	DNA nuclease for 3' of damage
TFIIH		
RAD25/SSL2	*XPB*	3' to 5' DNA helicase
RAD3	*XPD*	5' to 3' DNA helicase
SSL1	*GTF2H2*	core TFIIH subunit p44
TFB1	*GTF2H1*	core TFIIH subunit p62
TFB2	*GTF2H4*	core TFIIH subunit p52
TFB4	*GTF2H3*	core TFIIH subunit p34
TFB3	*MAT1*	CDK assembly factor (MAT1)
RFA	*RPA*	binding to ssDNA
MMS19	*MMS19*	
RAD7	Not known	DNA dependent ATPase
RAD16	Not known	in Rad7-Rad16 complex
ABF1	Not known	
RAD26	*CSB*	DNA dependent ATPase
RAD28	*CSA*	
DEF1		DNA damage dependent ubiquitination

Woudstra *et al.* (2002) also identified that Def1p forms a complex with Rad26p in chromatin. The phenotypes of cells lacking *DEF1* are consistent with a role for this factor in the DNA damage response, but Def1p is not required for TCR. Rather, *Δdef1* cells are compromised for transcript elongation, and are unable to degrade RNA polymerase II in response to DNA damage. They suggested that RNA Pol II stalled at

a DNA lesion triggers a coordinated rescue mechanism that requires the Rad26p-Def1p complex, and that Def1p enables ubiquitination and proteolysis of RNA PolII when the lesion cannot be rapidly removed by Rad26-promoted DNA repair.

Proteasome and NER

Transcription and DNA repair are regulated through diverse mechanisms, including RNA synthesis, protein synthesis, posttranslational modification and protein degradation. The 26*S* proteasome, which can degrade a broad spectrum of proteins, has been shown to interact with several NER proteins, including XPB, Rad4p, and Rad23p. Rad4p and Rad23p form a complex that binds preferentially to UV-damaged DNA. Several lines of genetic evidence suggest a role for ubiquitylation and protein degradation in DNA repair (reviewed in Sweder and Madura, 2002). The 26*S* proteasome may regulate repair by degrading DNA repair proteins after repair is completed or, alternatively, the proteasome may act as a molecular chaperone to promote disassembly of the repair complex. In either case, the interaction between the proteasome and NER depends on proteins like Rad23p, whose ubiquitin-like domain can bind ubiquitin-conjugated proteins and the proteasome.

In addition to the role of 26S in protein degradation, Russell *et al.* (1999) have surprisingly reported that inhibition of protein degradation by the 26S proteasome does not affect the efficiency of NER. They suggest that the 19S regulatory complex of the 26S proteasome has a special function independent of protein degradation. Furthermore, Gillette *et al.* (2001) identified that the 19S regulatory subunit of the

26S proteasome can affect nucleotide excision repair independently of Rad23p. 19S regulatory complex can negatively regulate the rate of NER in yeast and suggest that Rad23p not only recruits the 19S regulatory complex, but also can mediate functional interactions between the 19S regulatory complex and the NER machinery. The 19S regulatory complex of the yeast 26S proteasome functions in NER independently of proteolysis.

1.3.2 The Molecular mechanism of Nucleotide Excision Repair

General NER is characterized by two typical features. First, incision of lesions is effected by the function of two endonucleases, each of which operates exclusively on one side of the lesion. Secondly, these incisions are located at characteristic distances from the damaged base. (Friedberg, 1996)

In *E. coli*, the 3' incision is located three or four nucleotides from the site of CPDs while normally the 5' incision is seven nucleotides away from damages. The distance between the damaged base and the 3' nick is conserved in yeast and human NER system. However, in such cells the 5' incision and the damaged base are separated by about 21 nucleotides (Sancar, 1994; Guzder *et al.*, 1995b). These characteristic spatial relationships are consistent with the notion that during general NER a region of the DNA in the immediate vicinity of a damaged base undergoes specific conformational changes effected by interactions with the NER machinery.

Genetic and biochemical studies in the yeast *S. cerevisiae* and humans have made major contributions in understanding the mechanism of dual incision of damaged DNA in eukaryotes, and they have also yielded important insights into the

diverse functions of NER proteins. Commonly, NER can be considered to occur in the following sequential steps:

(a) Damage recognition. The DNA lesions are sensed by specific protein complexes.

(b) Localized unwinding of DNA flanking such lesions, mediated by the helicase function of subunits of TFIIH.

(c) Dual incisions by endonucleases are introduced at both 5' and 3' ends to the lesions.

(d) Excision nucleases release the oligonucleotide containing the lesion.

(e) Repair synthesis to fill the resulting singled-strand gap and using the opposite undamaged strand as a template.

(f) Ligation of the newly synthesized fragment to seal the DNA gap.

1.3.2.1 NER in *S. cerevisiae*

NER is divided into two subpathways which have the majority of their components in common, but which differ with respect to the requirement of the previously mentioned genes. Damage in the transcribed strand, which blocks the elongation of RNA polymerases I or II, is removed by one NER subpathway called transcription-coupled repair (TCR). The second NER subpathway acts on the silent regions of the genome and in the non-transcribed strands of active genes, this is termed global genome repair (GGR).

Efficiency of GGR varies for different type of lesions, for example, 6-4PPs are eliminated from non-transcribed regions much faster than are CPDs (Mitchell and

Nairn, 1989). In contrast, TCR repairs different lesions at similar rates, and contributes to the rapid recovery of transcriptional activity after DNA has been damaged, thus ensuring the maintenance of transcription and survival of cells short term prior to DNA replication (Hanawalt and Mellon, 1993; van Hoffen *et al.*, 1995; Friedberg, 1996). The diversity between GGR and TCR efficiency may be related to how these respective subpathways recognize DNA damage.

Many transcriptionally active genes exhibit NER of UV-induced pyrimidine dimers which is several-fold faster in the transcribed strand (TS) when compared to the non-transcribed strand (NTS), or to both strands of inactive genes. (Mellon *et al.*, 1987; Smerdon and Thoma, 1990; Verhage *et al.*, 1994; Hanawalt, 1994, 2001, 2002; Teng *et al.*, 1997) Although these two subpathways utilize the same general NER machinery, some specific additional proteins are implicated in each of them, as shown in Fig 1.4. In the following sections, TCR and GGR will be discussed in detail.

DNA damage recognition

The recognition of DNA damage is an initial and essential step of NER, yet this activity is also the least well understood aspect of eukaryotic NER. GGR and TCR are considered to differ mainly in the early stage of damage recognition. During transcription elongation, a RNA polymerase stalled at a lesion has been proposed to constitute the signal for TCR (Bohr *et al.*, 1985; Friedberg *et al.*, 1995; Friedberg, 2001; Hanawalt, 2003; Svejstrup, 2003), although this may not always be the case as TCR has been reported in the absence of elongation (Li and Smerdon, 2002, 2004). It is possible TCR involves both the stalling of the polymerase and the chromatin

environment of the TS.

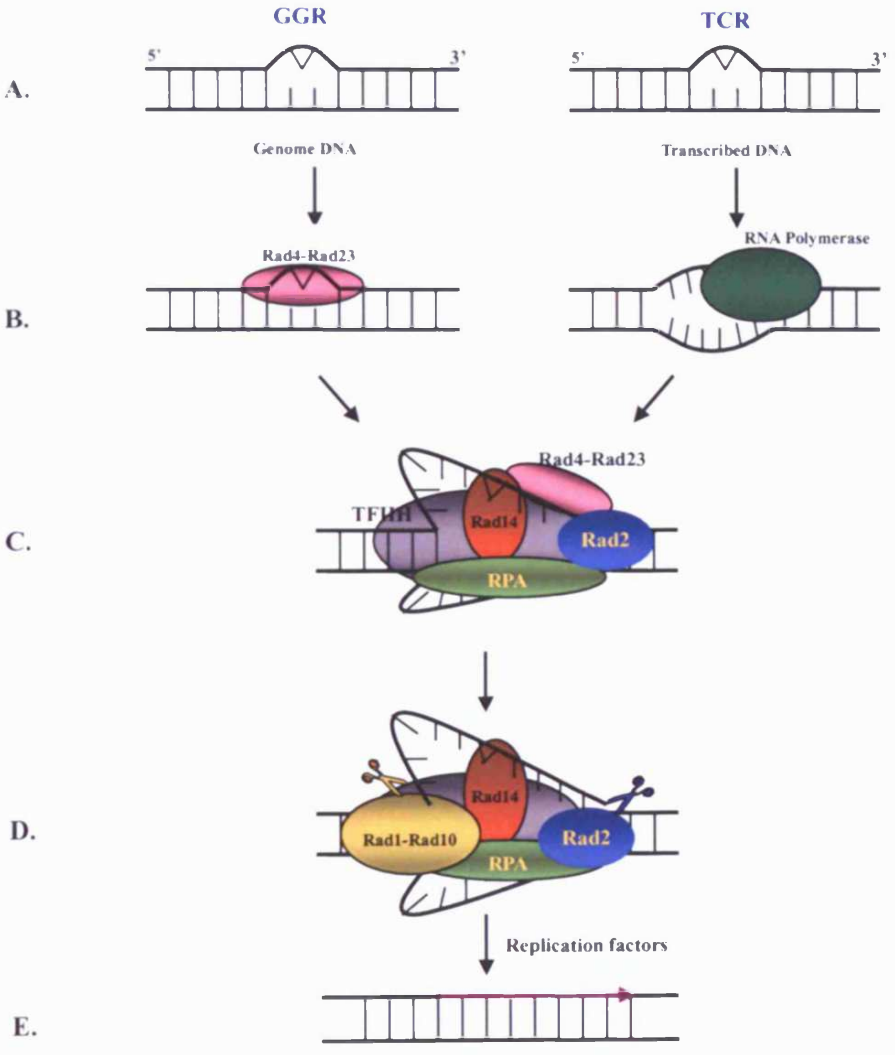

Figure 1.4 *Schematic presentation of NER in S. cerevisiae.* A: Formation of DNA lesion. B: damage recognition by Rad4p-Rad23p complex in GGR or RNA polymerase in TCR. C: Unwinding of DNA helix around the lesion with the Rad14p and RPA to stabilize an open structure. D: Incision of the lesion by Rad10p-Rad1p and Rad2p. E: the damaged fragment will be excised and the gap will be sealed by the normal DNA synthesis process.

Mutants of the *RAD26* gene (the yeast homolog of *CSB*) do not exhibit sensitivity to UV radiation, but still have reduced preferential repair of the transcribed strand (Tijsterman *et al.*, 1997; Teng *et al.*, 2000). However, cells lacking *RAD28*, the human *CSA* homolog, are not defective in TCR (Bhatia *et al.*, 1996).

GGR recognition

During GGR the Rad4p-Rad23p complex is considered to be the first damage sensor and to be the repair recruitment factor for GGR, this working even before Rad14p and RPA (replication protein A) are recruited. This association of proteins is then capable of recruiting the remainder of the repair machinery to the DNA damage (de Laat *et al.*, 1999; Prakash and Prakash, 2000). The Rad4p-Rad23p proteins exist as a heterodimeric complex, which binds UV damaged DNA specifically and shows no dependence on ATP. It is reported that Rad23p alone does not bind DNA, suggesting that either the damage binding activity may reside in Rad4p or that activation of the damage recognition is based on the formation of the Rad4p- Rad23p complex. (Guzder *et al.*, 1998b) Rad23p can interact with TFIIH and Rad14p (Guzder *et al.*, 1995a), consistent with the premise that the Rad4p-Rad23p complex links to other components of the incision machinery during repair.

Rad14p and RPA are two other ATP-independent binding proteins of the DNA damage recognition complex with a marked preference for damaged versus undamaged DNA (Jones and Wood, 1993; de Laat *et al.*, 1999). The Rad7p and Rad16p form an ATP-dependent complex now known to also contain Abf1p (Reed *et al.*, 1999). This complex is essential for GGR and it generates superhelicity in DNA

to remove the damage-containing oligonucleotide at a post incision stage (Yu *et al.*, 2004). Other studies show that a Rad7p and Rad16p heterodimer are involved in the early stages of damage recognition in GGR (Guzder *et al.*, 1997, 1998a; Prakash and Prakash, 2000).

Rad14p contains a 4-cysteine (C_4) zinc finger motif which allows it to bind one zinc atom (Guzder *et al.*, 1993). Because of its affinity for damaged DNA and its ability to interact with many core repair proteins, Rad14p and its human homologue XPA are considered to play a central role in positioning the repair machinery correctly around the damage (de Laat *et al.*, 1999; Prakash and Prakash, 2000).

RPA is a hetero-trimeric protein which binds to single stranded DNA with a defined polarity. It is required for the generation of full opening around the lesions in NER in which the complementary DNA strand need to separate at a certain stage (Evans *et al.*, 1997; Mu *et al.*, 1997; de Laat *et al.*, 1998). By binding to ssDNA, RPA is thought to stabilize intermediates that act along ssDNA and remove secondary structures (de Laat *et al.*, 1998). The size of the fully opened repair intermediate is ~30 nucleotides, which corresponds to the size of the optimal DNA-binding region of a single RPA heterotrimer. RPA not only stabilizes a fully open repair complex, but also facilitate its creation. Furthermore, RPA is essential for coordinating the NER nucleases and the interactions for the correct positioning of endonuclease incisions (reviewed in de Laat *et al.*, 1999).

TCR recognition

DNA damages that induce poor helix distortion but block transcription

elongation are preferentially repaired by TCR. In both *S. cerevisiae* and human cells, it is proposed that when elongating RNA polymerase is blocked by DNA lesions in the transcribed strand, it becomes an efficient damage sensor for TCR. In humans the transcription bubble that is present at the lesion can serve as a substrate for XPC-hHR23B-independent repair (Hanawalt and Mellon, 1993; Friedberg, 1996; Mu and Sancar, 1997). CPDs which arrest transcription were reported to be resistant to repair by DNA photolyase, indicating the arrested transcription complex was stably bound at sites of base damage and that it shielded the damage from this repair enzyme. TFIIS, a component of RNA polymerase II promoted transcript cleavage in this system (Donahue *et al.*, 1994).

Lesions that efficiently block transcription may also be efficiently recognized by GGR, due to local disruption of base pairing at the site of the lesion (Hess *et al.*, 1997). Thus, the GGR pathway and TCR may compete for lesions (Van Hoffen *et al.*, 1995). One hypothesis for TCR is that the stalled RNA polymerase can attract NER components through direct interaction or by modifying local chromatin structure to generate optimal conditions for repair. Moreover, it is observed that the repair rate of structurally different lesions by TCR is very similar suggesting that, in contrast to GGR, the structure of the lesion is less important for damage recognition in TCR (Van Hoffen *et al.*, 1995, 2003).

DNA unwinding and open complex formation

The sequential steps following the initial recognition of DNA damages by GGR

and TCR are similar: Rad3p and Rad25p are subunits of the basal transcription factor TFIIH protein complex which exhibit DNA dependent ATPase and helicase function. These unwind the DNA duplex over the damage containing region from the 5'-3' and 3'-5' direction respectively. Then the unwound region is stabilized by the binding of Rad14p to the damaged strand and RPA to the opposite undamaged strand to form an open repair complex. Here the TFIIH complex is recruited to the damaged site either by Rad4p-Rad23p in GGR or as a part of the transcriptional factors associating with the RNA polymerase II complex (de Laat *et al.*, 1999; Prakash and Prakash, 2000).

Dual incision and excision of damaged DNA

Incision of a DNA lesion by NER in *S. cerevisiae* requires the Rad1p- Rad10p complex and Rad2p. These single-strand DNA endonucleases act in a structure specific manner and cleave single stranded DNA at its junction with the duplex DNA. Respectively, Rad1p-Rad10p and Rad2p incise DNA on the 5' and 3' side of the damage (Tomkinson *et al.*, 1993; Bardwell *et al.*, 1994; Harrington and Lieber, 1994; Prakash and Prakash, 2000).

The distance between these incision sites for DNA damage is about 30 nucleotides. However, this can vary for different types of damage. However, the 3' incision always operates closer to the damaged base than does the 5' incision.

Then the incised oligonucleotide fragment is excised from the DNA. The precise mechanism of this excision step is not understood. For GGR, Rad16p has been proposed as enabling this step (Yu *et al.*, 2004). However, it is clear that the

formation of large single-stranded gaps which may be attacked by nucleases and cause genome severance is avoided during oligonucleotide excision. Unlike other pre-incision NER proteins which may have left at this stage, RPA remains bound to the undamaged single stranded DNA to protect it from possible nuclease attack and to facilitate the repair synthesis for filling the gap (de Laat *et al.*, 1999; Prakash and Prakash, 2000; Friedberg, 2001).

Repair synthesis and gap ligation

Following DNA damage excision the next step is to restore the 27–30 nucleotide gap by repair synthesis. This is undertaken by a similar protein complex used for normal DNA replication and it uses the opposite undamaged strand as a template. DNA polymerases δ or ε, as well as the accessory replication proteins PCNA, RPA and RFC are required for repair synthesis. RPA can stimulate the DNA polymerases δ or ε needed for repair synthesis and which initiates at the 5' incision site. Finally, DNA ligase I restores the covalent integrity of the previously damaged strand (Friedberg, 2001).

1.3.2.2 NER in humans

NER in humans is illustrated in Fig.1.5. In recent years, considerable detail of the human NER process has been obtained by protein purification and *in vitro* reconstituted repair systems. These studies show that NER in humans at least requires protein factors such as: XPC-hHR23B, XPA, CSA, CSB, RPA, TFIIH, XPG and ERCC1-XPF. The human proteins required for NER assemble in an ordered, stepwise

fashion at damage which is a substrate for NER. I will next discuss the specific function of these proteins (Wood, 1997; Friedberg, 2001). In GGR, the damage recognition, protein binding potency and the repair efficiency are considered to be decided by the characteristics of helix distortion induced through the formation of DNA damage and the DNA context in which the lesion resides (Seeberg and Fuchs, 1990).

XPC-hHR23B (human homologue of Rad4p-Rad23p) and DDB (DNA damage binding protein, which has no homologue in *S. cerevisiae*) act in the human GGR damage recognition step, and cells with defective XPC genes do not perform GGR, yet TCR is operational (Venema *et al.*, 1991; Mu and Sancar, 1997; Wood, 1999; van Hoffen *et al.*, 2003).

Like Rad4p-Rad23p, the XPC-hHR23B complex has strong affinity for DNA lesions and can bind lesions directly. However, with CPDs this affinity is reduced, possibly because CPDs cause only a subtle DNA helix distortion that is not easily sensed by XPC-hHR23B (Kusumoto *et al.*, 2001). Ng *et al.* (2003) have found that hHR23 proteins function in NER by governing XPC stability via partial protection against proteasomal degradation. Interestingly, NER-type DNA damage further stabilizes XPC and thereby enhances repair.XPC-hHR23B was also reported to bind to a bubble structure without a DNA lesion *in vitro*, yet it can only initiate repair when there is a lesion in the bubble (Sugasawa *et al.*, 2001). Thus local unwinding and the presence of DNA damage are both essential for NER to start.

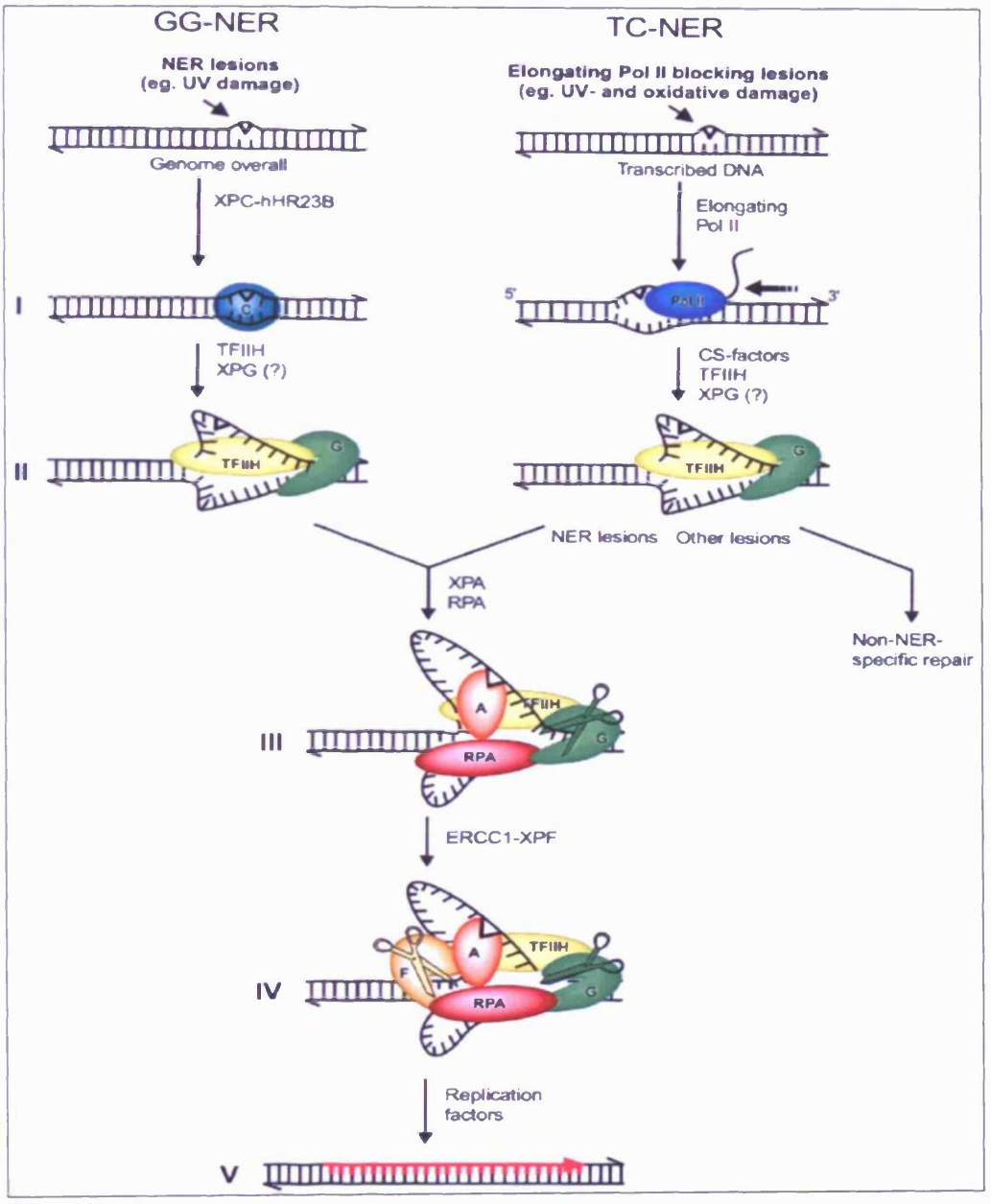

Figure 1.5 *Model for mechanism of GGR and TCR in human cells.* (Adapted from Reed and Waters, 2003)

DNA lesions that can cause local unwinding of a few DNA bases may create a structure variation facilitating further unwinding by repair proteins, and are good substrates for GGR. This observation suggests that NER proteins might detect a transcription bubble with a RNA polymerase stalled at a DNA lesion without the

requirement of XPC-hHR23B (Mu and Sancar, 1997). This is in accord with the essential function of XPC-hHR23B, together with the helicase complex TFIIH, needed to initiate the opening of < 10 nucleotides and form an open complex around the lesion (de Laat *et al.*, 1999).

The DDB complex consists of a heterodimer of two XPE proteins, p48 and p127. DDB is a repair complex specifically needed for human NER, especially for the repair of moderately helix distorting lesions such as CPDs. DDB facilitates the stability and lesion sensing of XPC-hHR23B, and also it may be involved in histone acetylation because it is related to the histone acetylase p300 (Chu and Chang, 1988; Datta *et al.*, 2001; van Hoffen *et al.*, 2003). Recently, Sugasawa et al. (2005) has reported that XPC undergoes reversible ubiquitylation upon UV irradiation of cells and that this depends on the presence of functional DDB activity. XPC and DDB were demonstrated to interact physically and both are polyubiquitylated by the recombinant UV-DDB-ubiquitin ligase complex. Their data suggested that ubiquitylation plays a critical role in the transfer of the UV induced damage from UV-DDB to XPC. XPA and RPA are thought to bind to DNA after the binding of XPC–hHRAD23B.

Similarly to *S. cerevisiae*, human TCR is proposed to perform damage recognition by the arrested RNA polymerase transcription machinery at the DNA lesions. This does not require the XPC-hHR23B complex (Mu and Sancar, 1997), but depends on the TCR-specific CSA (homologue of Rad28p) and CSB (homologue of Rad26p) proteins (Venema *et al.*, 1990), these, although not components of the normal transcriptional machinery, are recruited to the damaged sites where the

transcription stops. Mutation of the genes encoding these proteins leads to a hereditary recessive disease called Cockayne Syndrome (CS), which still has normal GGR (Venema *et al.*, 1990; van Hoffen *et al.*, 1993; Hanawalt, 2000). CSA and CSB are also thought to be able to displace the stalled polymerase to render the damage accessible for repair (reviewed in Svejstrup, 2002).

The subsequent steps of human TCR and GGR are similar. The XPB (homolog of yeast Rad25p) and XPD helicases (homolog of Rad3p) of the transcription factor TFIIH open about 30 base pairs of DNA around the lesion. The XPA (homolog of Rad14p) may confirm the presence of damage by probing for an abnormal backbone structure. The single-stranded-binding protein RPA binds to the undamaged strand to stabilize the open structure. XPG (homolog of Rad2p) and ERCC1/XPF (homologs of Rad10p/Rad1p), the NER endonucleases, respectively cleave 3' and 5' end of the borders of the opened structure only in the damaged strand, generating a 24-32 oligonucleotide containing the lesion. Then the regular DNA replication machinery finishes the whole repair process by DNA ligase I filling the gap (reviewed in Hoeijmakers, 2001).

Human diseases associated with NER defects

Xeroderma pigmentosum (XP), Cockayne syndrome (CS), trichothiodystrophy (TTD) cerebro-oculofacio-skeletal syndrome (COFS), and XP with DeSanctis-Cacchione syndrome (XP-DSC) are syndromes associated with inborn defects in human NER (Andressoo and Hoeijmakers, 2005). Their common character is extreme sensitivity to sunlight. XP shows a dramatic more than 1000-fold incidence

of skin cancer. The disorder arises from mutations in one of seven NER-involved genes *XPA* to *XPG*, and a mutation in the *XPV* gene that disturbs how DNA replication copes with a damaged template (Cordonnier *et al.*, 1999). Mutation in the *CSA* or *CSB* genes causes a TCR-specific disease that is distinct to XP. However, no predisposition to cancer is observed in CS patients, but patients are UV sensitive. This might be explained by the fact that the TCR defect causes CS cells to be particularly sensitive to damage-induced apoptosis, thereby protecting patients from cancers (reviewed in Spivak, 2005). Impaired physical and neurological developments are found in CS too. As well as in XP, CS suffers also can exhibit features of premature ageing. TTD is a condition sharing many symptoms with CS, but with the additional features of brittle hair, nails and scaly skin. Unlike in CS and TTD patients, defects in neuronal migration and innervation in COFS start during development in utero. Rapid postnatal degeneration of both the glial and neuronal compartment in COFS and severe failure to thrive leads to death during the first few years of life (Del Bigio *et al.*, 1997; Graham Jr. *et al.*, 2001). Notably, the severe form of CS (CS type II), COFS and infantile XPCS complex are one of the most severe dwarfing illnesses known (Rapin *et al.*, 2000). *XPD* or *XPB* mutants can give rise to all these diseases. This can be explained as subunits of TFIIH, XPB and XPD have dual functions: NER and transcription initiation. Mutations may affect both NER and transcription, causing developmental delay and reduced expression of the matrix proteins that causes brittle hair and scaly skin (Vermeulen *et al.*, 2001). Thus the phenotype of sufferers will depend on precisely where the mutations are and how they influence these processes

(reviewed in Andressoo and Hoeijmakers, 2005).

1.3.3. Transcription and NER

In 1985, Hanawalt and colleagues observed that the rate of CPD repair in the transcriptionally active *DHFR* gene was about 5-fold faster than in the whole genome of Chinese hamster ovary (CHO) cells (Bohr *et al.*, 1985). This faster repair is often reported to be specifically restricted to the transcribed strand (TS) of the active gene, while the non-transcribed strand (NTS) of the same gene is repaired with a rate similar to the non-transcribed regions of the genome overall. However, exceptions to this occur and transcription activation can enhance NTS repair as well in some cells and genes. TCR operates for several types of DNA damage in both prokaryotic and eukaryotic cells (Bohr *et al.*, 1985, 1987, 1991; Mellon *et al.*, 1989; Leadon *et al.*, 1991, 1992; Smerdon and Thoma, 1990; Li and Waters, 1996; Teng *et al.*, 1997, 1998; Teng and Waters, 2000). However, even for the *DHFR* gene, the extent of TCR is not comparable when it is inserted in different chromosomal locations despite it has been equally transcribed at the various locations (Hu *et al.*, 2002; Feng *et al.*, 2003).

Holo-TFIIH is a nine subunit protein complex (Winkler *et al.*, 1998), most of which are indispensable for NER (Hanawalt *et al.*, 1994; Svejstrup *et al.*, 1995; de Laat *et al.*, 1999). In yeast, TFIIH was reported to exist in two different forms: (1) a form that is active in transcription, holo-TFIIH, which consists of core-TFIIH and TFIIK, the (C-terminal domain) CTD kinase complex, and; (2) a form uniquely active in DNA repair that lacks TFIIK. The yeast core TFIIH consists of Rad3p, Rad25p,

Ssl1p, Tfb1p, Tfb2p, Tfb3p, Tfb4p, the human homologs of which are XPD, XPB, GTF2H2 (p44), GTF2H1 (p62),GTF2H4 (p52), MAT1, GTF2H3 (p34) (Bhatia *et al.*, 1996; Wood, 1999). In transcription, TFIIK, a protein complex of Ccl1 (homologue of human cyclin H) and Kin28 (homologue of human Cdk7) has protein kinase activity directed toward the C-terminal domain of Rpb1, the largest subunit of RNA polymerase II. However, no role for TFIIK in NER has been demonstrated (Feaver *et al.*, 1994, 1999). Identification of the *XPB* gene encoding the 89kDa subunit of human TFIIH revealed a direct link between DNA transcription and NER (Schaeffer *et al.*, 1993).

It is proposed that when transcription elongation complexes arrest at sites of DNA damage in the TS, the TFIIH complex promotes rapid assembly of the NER machinery at such sites, thus facilitating strand specific repair. During initiation of transcription the obligatory loading of TFIIH onto the gene promoter site facilitates the direct coupling of RNA polymerase II transcription with NER at the damage sites in the TS (Friedberg *et al.*, 1995; Sancar, 1996; Wood, 1996). However, some observations suggested that TFIIH dissociates from the transcription complex soon after promoter clearance and is not normally associated with the RNA polymerase II elongation complex (Dvir *et al.*, 1997; Goodrich and Tjian, 1994). Another explanation for the dual roles of TFIIH in transcription and NER comes from the observation that two of the TFIIH subunits, Rad3p and Rad25p in yeast (XPD and XPB in humans), are DNA helicases with opposite polarity (Guzder *et al.*, 1994a, 1994b; Sung *et al.*, 1987, 1996). As discussed in section 1.3.3.2, these ATP-dependent

helicases may melt and maintain the open complex (bubble structure) in the DNA duplex. The borders of such bubbles comprise junctions between duplex and single-stranded DNA which are recognized by the NER endonucleases.

Evidence in support of a TFIIH-mediated unwinding of regions of the DNA duplex during NER has been provided with an *in vitro* system reconstituted from purified human proteins (Evans *et al.*, 1997; You *et al.*, 1998). In an *in vitro* NER system entirely consisting of purified proteins, neither a TFIIH mutant (lacking Rad3p and Rad25p) nor purified Rad3p or Rad25p proteins alone were active in NER, but the combination of them promoted the incision of UV-damaged DNA. These results provided the first evidence for a direct requirement of Rad3p, Rad25p, and of one or more other subunits of the TFIIH in the incision step of NER (Sung *et al.*, 1996). Mutations in the ATP binding site of Rad25p/XPB caused defects in both transcription and NER, while similar mutations in Rad3 only affect NER (Feaver *et al.*, 1993; Guzder *et al.*, 1994a, 1994b). Evidence also suggests other subunits in TFIIH are required both for transcription and NER (Schaeffer *et al.*, 1994; van Vuuren *et al.*, 1994; Wang *et al.*, 1995; Feaver *et al.*, 1999, 2000; de Laat *et al.*, 1999; Teng and Waters, 2000). Data in yeast are now emerging that question whether the elongating polymerase alone is the only trigger for TCR (Li and Smerdon, 2004) and it is possible TCR is driven not only by the polymerase stalling, but also by specific chromatin structural changes that accompany transcription.

1.4 Chromatin structure and DNA repair

Eukaryotic DNA in the cell nucleus is organized and compacted into chromatin, a condensed structure which inhibits the interaction between proteins and DNA. Chromatin folding is quite dynamic, and the degree of folding directly influences the activity of DNA in transcription, replication, and recombination. As a result it is important to know how critical factors in these metabolic processes gain access to their target sequences in the context of chromatin. There are several levels of structural organization in chromatin which could contribute to modulate accessibility of binding sites for factors. The first level of compaction of DNA in chromatin is the nucleosome. This consists of an octamer of core histones, a tetramer of histones H3 and H4 and two dimers of histones H2A and H2B, with 146 base pairs of DNA wrapped around them in 1.75 left-handed superhelical turns. A linker histone H1 directs the path of DNA between the adjacent nucleosomes that make up the chromatin fiber (Wolffe, 1998). In *S. cerevisiae* there are some H1-like Hho1p histones (Landsman, 1996). However, disruption of *HHO1* results in no significant changes in the phenotypes examined. Downs *et al.* (2003) have showed that Hho1p is inhibitory to DNA repair by homologous recombination (HR). They also reported that Hho1p is abundant and associated with the genome in yeast, consistent with a global affect on DNA repair. They also showed that Hho1p is inhibitory to the recombination-dependent mechanism of telomere maintenance. Recently, the researches suggested that linker histones appear to affect only the transcription of a

small subset of genes, and, in fact, act to activate as well as repress transcription (reviewed in Harvey and Downs, 2004).

Nucleosomes have been found, in many promoter and enhancer regions, to be positioned so as they are located over defined regions of DNA (Simpson, 1991; Thoma, 1992; Wolffe, 1994, 1998; Pruss *et al.*, 1996; Beato and Eisfeld, 1997). Studies showed chromatin affects the transcription process at many levels; nucleosomes can prevent the binding of certain transcriptional regulatory proteins and initiation factors, and they can also impede elongation by RNA polymerase II. In order for transcription to occur, repressive chromatin must be remodeled (Workman *et al.*, 1992). Therefore, as in transcription, replication and recombination, the precise regulation of chromatin structure is likely essential for DNA damage to be accessible to NER proteins.

Chromatin is not an inert repressive structure, contrarily, it is a living vibrant entity with continual remodeling. The nucleosome and chromatin fibre are in a continual state of flux (Urnov and Wolffe, 2001). These diverse processes are correlated with specific covalent modifications of histone tails or on the core of histone proteins, and chromatin remodeling mediated by the SWI/SNF family of enzymes (Struhl, 1998; Peterson and Workman, 2000; Waterborg, 2000; Roth *et al.*, 2001, Wolffe, 2001; Bonenfant *et al.*, 2005). Among the histone covalent modifications, are phosphorylation (Nowak and Corces, 2004), methylation (Fitzpatrick and Wilson, 2003; Weissmann and Lyko, 2003), acetylation (Datta *et al.*, 2001; Bird *et al.*, 2002; Teng *et al.*, 2002; Katan-khaykovich and Struhl, 2002) and

ubiquitination (Hochstrasser, 1996; Sweder and Madura, 2002). Phosphorylation and demethylation may be required prior to acetylation, and recently, methylases and deacetylases are also thought to be able to open chromatin structure and activate transcription (Nusinzon and Horvath, 2005; reviewed in Martin and Zhang, 2005). For this thesis, I will discuss further histone acetylation and deacetylation.

1.4.1 Acetylation and deacetylation

Histone acetylation renders chromatin accessible to DNA binding proteins by destabilizing the nucleosome and the chromatin fibre (Lee *et al.*, 1993; Tse *et al.*, 1998). Histones consist of a core domain and a highly charged tail domain. The core histones, involved in histone–histone interactions and in wrapping DNA into nucleosomes, have a key role in transcriptional regulation; the tail domains, lying on the outside of the nucleosome, provide an attractive signaling platform and can interact with other important regulatory proteins including acetylases and deacetylases (Grunstein *et al.*, 1995; Wolffe, 1996; Cheung *et al.*, 2000, Henikoff and Ahmad, 2005).

Acetylation of lysines in the histone amino-termini neutralizes their positive charge, decreasing interactions with DNA and histone-histone interactions between neighboring nucleosomes (Luger, 1997; Deckert and Struhl, 2001). This may displace the termini from nucleosomes leading to their unfolding and a more open or permissive chromatin environment for transcription (See Fig. 1.6). Therefore, chromatin enriched in acetylated histones is more enficiently transcribed (Ura *et al.*, 1997; Nightingale *et al.*, 1998). The tails of histones H3 and H4 are important for the

transcriptional regulation of many genes, and mutations in these histone tails can cause derepression or diminished activation (Durrin *et al.*, 1991; Mann and Grunstein, 1992; Deckert and Struhl, 2001). Acetylation can act on a few nucleosomes or become general to much of the chromatin at particular stages of the cell cycle (Hebbes *et al.*, 1988; Wolffe and Hayes, 1999).

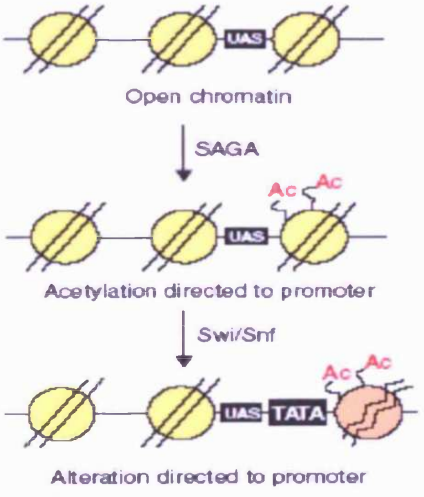

Figure 1.6 *Histone acetylation and transcription* (Adapted from,Berger, 2002)

Histone acetylases

Histone acetyltransferase activities (HATs) were grouped into two general classes based on their suspected cellular origin and functions. Cytoplasmic B-type HATs catalyze acetylation linked to the transport of newly synthesized histones from the cytoplasm to the cell nucleus, while nuclear A-type HATs catalyze transcription-related acetylation events which is the topic of interest here (Brownell and Allis, 1996; Brownell *et al.*, 1996; Grunstein, 1997; Struhl, 1998). Histone

acetylase, TAF (TBP-associated factor) 130/250 is a subunit of the TFIID complex, which is a basic component of the RNA Polymerase II transcription machinery in all eukaryotic cells. It was suggested that there is an important role of HATs in transcription. This led to the idea that TFIID itself comes equipped to modify the core histones and facilitate access of the other basal transcription factors to promoters packaged into chromatin (Mizzen *et al.*, 1996). The yeast Gcn5p which was a previously characterized component of the transcriptional machinery is the first A-type histone acetylase to be identified (Brownell *et al.*, 1996). This supported the suggestion that there is a direct relationship between histone acetylation and transcription activity, and that the modification of histones is a general function of the transcriptional machinery. In yeast, Gcn5p is not essential for cell growth, but it is important for the expression of a subset of genes. Mutation of the Gcn5p catalytic domain results in eliminating or dramatically reducing the transcription and the acetylation of histones (Georgakopoulos and Thireos, 1992; Brownell *et al.*, 1996; Kuo *et al.*, 1998). Gcn5p is found in two distinct multiprotein complexes, ADA and SAGA (Grant *et al.*, 1997), both of which contain Ada proteins. The SAGA complex also contains Spt proteins, including Spt3 which interacts with the TATA-binding protein (TBP) (Eisenmann *et al.*, 1992). More recently it has been identified in a third SAGA-like (SLIK) complex (Pray-Grant, 2002; Workman et al., 2002; Daniel *et al.*, 2004). These studies on Gcn5p resulted in a general model for HAT recruitment to specific promoters by DNA-bound activating proteins (Brownell and Allis, 1996; Wolffe and Pruss, 1996). Several other transcription adaptor/coactivator proteins also

have intrinsic HAT activity. These proteins include mammalian Gcn5p (Yang *et al.*, 1996; Wang *et al.*, 1997; Xu *et al.*, 2000) and its orthologue, PCAF (Yang et al., 1996), CREB-binding protein (CBP) (Ogryzko *et al.*, 1996; Bannister and Kouzarides, 1996), p300 (Ogryzko *et al.*, 1996), and human $TAF_{II}250$ with its yeast homologue $TAF_{II}130$ (Mizzen *et al.*, 1996; Dunphy *et al.*, 2000). All these HAT activities are connected to transcription, and indicate histone acetylation plays an important role in this process (Kornberg and Lorch, 1999). It was possible that HATs may facilitate DNA repair as well as transcription. The chromatin regulation via A-type HATs (particular Gcn5p) on NER will be discussed later.

Histone deacetylases

In contrast to HATs which facilitate gene transcription through chromatin remodelling, histone deacetylases (HDACs) can cause gene repression. These two conserved types of chromatin modification proteins control the acetylation level together (Struhl, 1998). Human HDAC1 protein and its yeast homolog, Rpd3p, are members of the best described HDACs family (Taunton *et al.* 1996; Rundlett *et al.* 1996). HDAC/Rpd3p homologues have been found in a wide variety of eukaryotes and in each organism there are typically multiple family members which are presumed to have histone deacetylase activity. Both *HDA1* and *RPD3* deletions increase *in vivo* acetylation levels at all researched sites in both the H3 and H4 histones. *RPD3* deletion causes a greater impact at lysines 5 and 12 of histone H4 (Rundlett *et al.*, 1996, 1998). HDAC1 and Rpd3p generate large complexes with the Sin3 corepressor and other proteins (Pazin and Kadonaga 1997). These HDAC/Rpd3p

complexes associate with DNA-binding repressors such as Mad (Hassig *et al.*, 1997; Laherty *et al.*, 1997), Ume6 (Kadosh and Struhl 1997), or with transcriptional corepressors for nuclear receptors such as SMRT (Nagy *et al.* 1997) and NCoR (Alland *et al.*, 1997; Heinzel *et al.*, 1997), and these phenomena are in accord with the functions of HDAC/Rpd3 as a repressor protein.

Histone acetylation patterns are very complicated, and individual histone acetylases and deacetylases display distinct specificities. Some HATs and HDACs act on their targets randomly, whereas others are quite specific in the individual lysine residues and particular histones they affect. For example, Gcn5p preferentially acetylates lysine 14 of histone H3 (Kuo *et al.*, 1996; Grant *et al.*, 1998), and HDAC/Rpd3p preferentially deacetylates lysines 5 and 12 of histone H4 (Rundlett *et al.*, 1996; Taunton *et al.*, 1996). Moreover, the HATs have different acetylating abilities on nucleosomal or free histones, therefore, the recombinant form of HATs can differ dramatically from the normal *in vivo* histone acetylase complex. It is reported that the recombinant Gcn5p can only acetylate free histones, whereas endogenous Gcn5p in the ADA and SAGA complexes can acetylate nucleosomes (Grant *et al.*, 1997). This suggests that the Ada or Spt proteins are required for Gcn5p to act on nucleosomal substrates.

1.4.2 Other chromatin remodeling factors

In addition to the covalent chromatin modifications mentioned before, other chromatin-remodeling complexes can also carry out key enzymatic activities, changing chromatin structure by altering the contact pattern of DNA–histones within

a nucleosome. These complexes can be divided into three classes on the basis of the similarities of their ATPase subunits to the Swi2/Snf2, Isw1, and Mi-2 proteins (Martens and Winston, 2003). Swi/Snf complexes comprise nine or more proteins, including both conserved core and nonconserved components. Studies have shown that Swi2/ Snf2 proteins possess both ATPase and remodeling activities. In *S. cerevisiae*, most other Swi/Snf and RSC (remodeling structure of chromatin, a Swi/Snf-like chromatin remodeling complex in yeast) subunits are also required for chromatin remodeling activity *in vivo* (Winston and Carlson, 1992; Moggs and Almouzni, 1999; Whitehouse et al., 1999; Tsukiyama *et al.*, 2002; Martens and Winston, 2002). Previously Swi/Snf complexes have been characterized as transcriptional activators. However, researchers have also shown that Swi/Snf represses transcription, although it is uncertain whether it does this directly or not (Sudarsanam and Winston, 2000; Narlikar *et al.*, 2002). New studies strongly suggest that Swi/Snf directly represses transcription and that the Swi/Snf subunits involved in repression are different from those in activation; only Swi2/Snf2 is reported to be required for repression of *SER3*, whereas most subunits are required for transcriptional activation (Winston and Carlson, 1992; Martens and Winston, 2002). Results obtained via chromatin immunoprecipitation (ChIP) showed the presence of both Swi2/Snf2 and Snf5, the latter not being required for repression at the *SER3* promoter. This, in combination with studies that detected changes in the chromatin structure over the *SER3* promoter in a *⊿snf2* mutant, strongly suggests a direct role for Swi/Snf in repression of this gene (Martens and Winston, 2002, 2003). Therefore,

differential use of the same complex may occur at promoters that are activated or repressed by Swi/Snf, and Swi/Snf repression may occur by multiple mechanisms.

Swi2/Snf2 proteins are members of the SF2 family of DNA helicases, although Swi2/Snf2 proteins do not function as helicases. Research on the mechanism of Swi/Snf remodeling shows that Swi2/Snf2, as well as other remodeling enzymes, is capable of generating superhelical torsion, a state that can be achieved by either translocation or twisting of nucleosomal DNA in an ATP-dependent manner (Havas *et al.*, 2000)

It should be mentioned here that the Rad16 protein, which with Rad7p and Abf1p is part of the *S. cerevisiae* GGR specific essential complex, is a member of the Swi/Snf family; Rad16p contains conserved motifs with related ATPase activity, the complex displaying a DNA-dependent ATPase function (Guzder *et al.*, 1997). There are indications that Rad7p and Rad16p may act in perturbations of chromatin structure,, and it has been suggested that these proteins may have a role in chromatin remodeling. However, it should also be mentioned that Rad16p and its complex can create torsion in DNA to facilitate the excision of an incised CPD, so its role may also extend this to stage of the GGR process (Yu *et al.*, 2004).

ISW1 and ISW2, two subunits of the ISW family also have been identified in *S. cerevisiae* (Tsukiyama *et al.*, 1999). This study demonstrated that the activities of ATP-dependent chromatin remodeling are essential for functions of ISW1 and ISW2 *in vivo*. Moreover, all the other identified chromatin remodeling factors, including members of RSC, ACF, RSF, NURF and Mi-2 families, have the putative ATPase

subunit that belongs to the Swi/Snf superfamily (Eisen *et al.*, 1995).

1.5 *MFA2* as a model gene

The *MFA2* gene in *S. cerevisiae* was employed as a model gene for research on NER in this thesis.

S. cerevisiae haploid cells exhibit **a**- or α- type cellular phenotypes. These cell types are specialized in mating and are distinguished from one another by the production of mating-type specific proteins. *MFA2* is an **a**-mating type specific gene encoding the **a**-factor precursor consisting of 38 amino acids and it is located on the left arm of chromosome XIV (Michaelis *et al.*, 1992). The regulation of this gene is shown in Fig. 1.7. In **a**-mating type cells, transcription of the **a**-specific gene (eg. *MFA2*) is stimulated by binding the transcriptional activator protein Mcm1p to the α2 operator in the upstream region of gene promoter (Acton *et al.*, 1997; 2000). The role of the Mcm1p in transcriptional activation of **a**-specific genes is unclear, however, deletion of the α2 operator in the *MFA2* promoter results in the loss of *MFA2* expression. In α-cells, co-binding of Mcm1p with α2 factor represses **a**-specific genes (Wahi and Johnson, 1995).

In addition to α2p and Mcm1p, full repression of *MFA2* in α-cells also requires the function of the Tup1p-Ssn6p general repressor, since deletion of *TUP1* leads to the derepression of *MFA2* in α-cells (see Chapter 3). The Tup1p repression domain was reported to overlap a region that interacts directly with histone H3 and H4 N-terminal tails *in vitro*, and interacts physically with at least three histone deacetylases

(Edmondson *et al.*, 1996; Watson *et al.*, 2000; Wu *et al.*, 2001). Another model has been proposed for the mechanism of repression by Tup1p-Ssn6p by involving its direct action on the RNA Polymerase II machinery. Tup1p-Ssn6p weakly represses transcription *in vitro* on purified DNA templates, and mutations in components of RNA Polymerase II holoenzyme have been found to partially alleviate repression by Tup1p-Ssn6p (Herschbach *et al.* 1994; Redd *et al.* 1997; Lee *et al.*, 2000).

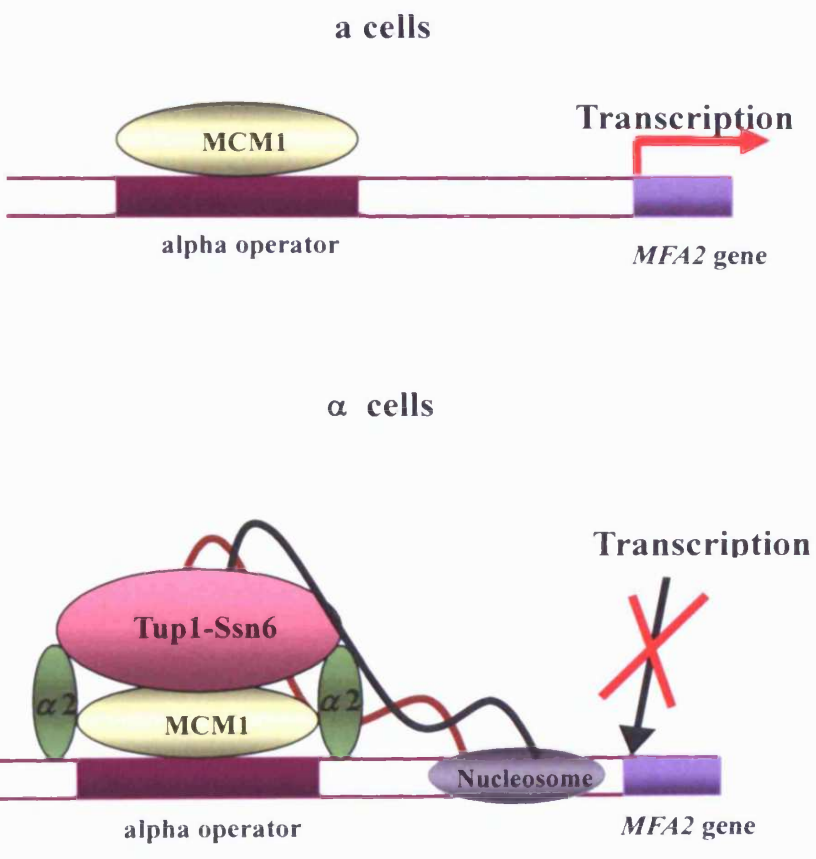

Figure 1.7 *Models for regulation of MFA2 gene in* **a**- *and* α-*mating type cells.* In **a**-cells, **a**-specific genes are activated by the binding of Mcm1p to the upstream promoter sequence, accompanied with local nucleosome disruption by histone acetylases, including Gcn5p. In α-cells, α2 factor cooperatively binds with Mcm1p to the α2 operator and recruits the Tup1p-Ssn6p general repressor. Tup1p-Ssn6p represses *MFA2* expression through the fixed positioning of nucleosome, a reduced level of histone acetylation accomplished via histone deacetylases.

There are a number of advantages to using *MFA2* gene as a model gene for studying DNA repair:

1) This gene is well characterized. Fig. 1.8 shows the sequence of the *HaeIII* restriction fragment from *MFA2* which includes 83 bp of the *MFA2* transcribed sequence and its 517 bp upstream promoter region. The Mcm1p/α2p binding site and the putative TATA box are located in the upstream region -221 to -251 and -119 to -125 respectively.

2) The regulation of the gene is relatively well understood, as described above. As it is a mating type specific gene, the transcription of *MFA2* can be easily controlled by selecting **a-** or α-mating type cells. Thus the influence of *MFA2* transcriptional activity on DNA repair can be examined by comparing CPD repair at *MFA2* between **a-** and α-cells.

3) *MFA2* is a small gene and its coding sequence and transcribed sequence are only 117 bp and 328 bp, respectively. Hence, the examination of CPDs in the fragment generated by a restriction enzyme (eg. *RsaI*) can provide detailed information about repair of CPDs for the transcribed, upstream and downstream regions on a single sequencing gel. Other restriction enzymes can be used to create smaller fragments focusing on specific regions. For example, *HaeIII* generates a fragment including the promoter region and the first part of the transcribed region of *MFA2*.

4) The chromatin structure around the *MFA2* gene has been well defined. MNase mapping suggested the presence of four positioned nucleosomes in the control and coding region of *MFA2* in α- cells where the gene is repressed. However, fixed

nucleosomes are undetectable in **a**-cells where *MFA2* is transcribed (Teng *et al.*, 2001, 2006).

Figure 1.8 The *MFA2* sequence digested by *HaeIII*. Base pairs are numbered in relation to the first "A" of the "ATG" start codon. The restriction fragment contains part of the *MFA2* coding region (+1 to +83) and its upstream region (-1 to -517). The Mcm1p binding site (printed in orange) and TATA box (printed in blue) are indicated at -221 to -251 and -119 to -125 respectively. Underlined are the potential CPD sites.

5) Regulation of *MFA2* transcription is in part achieved by the histone acetylase Gcn5, through remodelling chromatin structure in its promoter region (Teng *et al.*, 2002). The deletion of *GCN5* markedly reduced the GGR and TCR of CPDs in the transcriptionally active *MFA2*, whereas no detectable defect was seen for repair of the genome overall (Teng *et al.*, 2002). In *⊿gcn5*, the *MFA2* transcription level is reduced by fourfold. These changes in transcription correlate with the changes in NER found in the *⊿gcn5* mutant. However, the NER defect is not solely due to reduced TCR, GGR in the *MFA2* regulatory region is also reduced.
6) There is reduced NER at *MFA2* in the *⊿gcn5* mutant, yet NER for most of the yeast genome is unperturbed. As a result, histone acetylation likely allows efficient access of the repair machinery to DNA damage either indirectly via influencing transcription or directly via modifying chromatin structure irrespective of transcription via action at specific chromatin domains.

Finally, our research group had previously developed the technology to examine CPD induction and repair at the resolution of individual dipyrimidine, and we have accrued much information on the kinetics of CPD repair at *MFA2*, including the role of Rad16p, it was logical to build on this research.

1.6 The present study

Elucidating the relationship between DNA transcription, repair and chromatin remodeling has become critical for us to understand the precise way in which cells

respond to DNA damage in the various chromatin structures throughout the genome.

MFA2 gene is derepressed via the histone acetyltransferase Gcn5p in **a** cells. Here I have investigated the effect of deletion of *TUP1* or *GCN5* or both on CPD repair and gene expression (Chapters 3 and 5, respectively). As mentioned earlier, the Rad7p-Rad16p-Abf1p complex is essential for GGR in non-transcribed sequence of the entire genome including upstream regulating regions and the NTS of active genes. Research was also carried out on the role of Rad16p in repair at *MFA2*, both with or without an additional deletion of the *TUP1* gene.

Here I have employed the previously mentioned technology to examine the role of repair of induced CPDs in the various mutants and I have selected events to strains where transcription of *MFA2* is functional or not.

Chapter 2

Materials and Methods

The methods described in this chapter are related to the growth and storage conditions of yeast strains, and the techniques applied in this study which include UV treatment of cells, purification of DNA, gel electrophoresis and other methods for analyzing DNA repair at the nucleotide resolution.

2.1 Yeast strains

The haploid *S. cerevisiae* strains used in this study are:

PSY316 (*MATα ade2-101 ura 3-52 leu 2-3,112 Δhis 3-200 lys2 trp1*)

Δtup1 (*MATα ade2-101 ura 3-52 leu 2-3,112 HIS::TUP1 lys2 trp1*)

Δgcn5 (*MATα ade2-101 ura 3-52 leu 2-3,112 Δhis 3-200 lys2 trp1*)

Δtup1gcn5 (*MATα ade2-101 ura 3-52 leu 2-3,112 HIS::TUP1 lys2 trp1*)

Δ rad16 (*MATα ade2-101 URA::RAD16 leu 2-3,112 Δhis 3-200 lys2 trp1*)

Δ tup1rad16 (*MATα ade2-101 URA::RAD16 leu 2-3,112 HIS::TUP1 lys2 trp1*)

Δtup1mfa2^{TATA} (*MATα mfa2*^{TATA}, *ade2-101 ura 3-52 leu 2-3,112 HIS::TUP1 lys2 trp1*)

PSY316 (*MAT***a** *ade2-101 ura 3-52 leu 2-3,112 Δhis 3-200 lys2 trp1*)

Δgcn5 (*MAT***a** *ade2-101 ura 3-52 leu 2-3,112 Δhis 3-200 lys2 trp1*)

Δtup1 (*MAT***a** *ade2-101 ura 3-52 leu 2-3,112 HIS::TUP1 lys2 trp1*)

Δtup1gcn5 (*MAT***a** *ade2-101 ura 3-52 leu 2-3,112 HIS::TUP1Δhis 3-200 lys2 trp1*)

2.2 Storage and growth conditions

All the strains in use were stored and grown in yeast complete medium (YC, see Appendix).

For long period storage, yeast cells in exponential phase were frozen in YC medium containing 30% glycerol and kept at -70° C. Storage of YC slopes at 4 °C was used when inocula were often needed. Before use of strains for every experiment, fresh preculture was made from the stock by inoculating 25 ml of medium. This culture was then incubated at 28°C with shaking, allowing it to reach stationary phase and subsequently stored at 4°C. Large scale cultures required for repair experiments were obtained by inoculating fresh medium overnight with this stationary phase liquid culture, also at 28°C and under continue shaking. The amount of preculture used was empirically calibrated so as to achieve a cell density of $2\sim4\times10^7$ cells/ml the next morning.

The growth media, all the glassware and other containers for storage or growth of the yeast cells were autoclaved. Moreover, all manipulations were carried out under standard aseptic conditions.

2.3 The UV treatment of yeast cells

An aliquot of 50ml of yeast cells in pre-chilled phosphate buffered saline (PBS, see Appendix) at a density of 2×10^7 cells/ml were exposed to 254 nm UV light. The

UV lamp was switched on at least half an hour before irradiation to ensure a stable emission. Except when they were being treated by UV, all the cells were kept on ice and stored in the dark to avoid additional visible light during the treatment. Then cells were collected by using a Beckman Avanti J-25 centrifuge at 4°C. After centrifugation, cells were resuspended in fresh YC, and allowed to repair for various times in the dark at 28° C on a shaker prior to the isolation of DNA. The details of the procedure were as follows:

1) Yeast cells at a density of $2\sim4\times10^7$ cells/ml were collected by centrifugation at 4,000 rpm for 5 min using a Beckman Avanti J-25 centrifuge and a Beckman JA-10 rotor.
2) Cells were washed and then resuspended in 400ml chilled 1xPBS. Brief sonication was applied to disperse clumps of cells if necessary. Cell density was checked by using a haemocytometer to count cells and the suspension was adjusted to 2×10^7 cells/ml by the addition of chilled PBS.
3) Prior to UV irradiation, a 250ml sample was removed from the cell suspension and kept on ice, providing an untreated (**U**) control sample.
4) A batch of 50ml of cell suspension was placed in a Pyrex dish (Φ=14 cm) such that the depth of cell suspension was about 0.3 cm. The dish was gently shaken to ensure a uniform dose to all cells while the cell suspension was irradiated under a VL-215G UV lamp (Vilber Lourmat, France) at a dose rate of 10 $J/m^2 \cdot s$. This irradiation was repeated until all the cell suspension had been treated.

5) 250ml of cell suspension after irradiation was collected by centrifugation at 4,000 rpm for 5 min and kept on ice to serve as a sample (**0**) with no repair time. The remainder of the UV-treated cells was collected as above, then resuspended in 300 ml/400ml of fresh YC and incubated at 28°C in the dark on a shaker for DNA repair. At each repair time (1, 2, 3 or 4 hours) the same fraction of cells were taken from the culture. All samples were centrifuged as above and the cell pellets were resuspended in 40 ml of chilled PBS in the dark to prevent photoreactivition.

2.4 Preparation of yeast genomic DNA

A protocol for the isolation of genomic DNA from yeast cells was described in Teng *et al.* (1997), which is suitable for extraction of genomic DNA from as many as 1×10^{10} cells per sample. The details of the procedure are:

1) Cells suspended in 40ml chilled PBS from each sample above were collected by centrifugation at 4,000 rpm for 5 min using Beckman JA-10 rotor. Following removal of the supernatant, the cells were resuspended in 5ml of sorbitol-TE solution (see Appendix I).

2) 0.5ml of zymolyase 20T (10 mg/ml in Sorbitol solution, ICN Biochemicals, Inc.) and 0.5ml of 0.28M β-mercaptoethanol (Sigma) were added to each sample, and mixed well by shaking. Cells were incubated either at 37°C for 1 hour in a shaking incubator, or at 4°C overnight in the dark. The production of spheroplasts was monitored under a light microscope.

3) Spheroplasts were gently centrifuged at 3,000 rpm for 5 min with a Beckman

JA20 rotor and incubated in 5ml of 1:1(v/v) lysis buffer/1xPBS solution (see Appendix I). 0.2ml RNase A (pancreatic RNAse, Sigma. 10mg/ml in TE buffer) was added to each sample. All samples were incubated at 37°C for 1 hour with occasional shaking. Following RNaseA treatment, 0.5ml of proteinase K solution (Amresco, freshly made in 5mg/ml in TE buffer) was added. The samples were incubated at 65°C for 2 hours with shaking at regular intervals.

4) An equal volume (about 6ml) of phenol:chloroform:isoamyl alcohol (25:24:1 in volume, Sigma) was added. The tubes were shaken vigorously and then centrifuged at 10,000 rpm for 10 minutes using a JA-20 rotor. The aqueous upper phase containing DNA was then transferred to a fresh 24ml disposable polypropylene tube using a 3ml plastic Pasteur Pipette. Care was taken to not to disturb the interface and the phenol/chloroform phase.

5) To ensure complete deproteinization, a second extraction with phenol/chloroform/isoamyl alcohol was performed as above, and then a third extraction with chloroform:isoamyl alcohol (24:1 in volume, Sigma). The aqueous phase was transferred to a fresh tube.

6) 2 volumes (12ml) of pre-chilled 100% ethanol (-20°C) were added to each sample. After being mixed gently by inversion, the samples were kept at -20°C overnight to precipitate the DNA.

7) DNA pellets were collected by centrifugation at 4,000 rpm for 15 minutes with a Beckman JS 4.2 rotor in a Beckman J6B centrifuge. The pellets were allowed to air dry, and then dissolved in 1 ml of TE. After being completely dissolved, the

DNA was reprecipitated by addition of an equal volumn of pre-chilled (-20°C) isopropanol. The samples were left at room temperature for 20 minutes. The DNA pellets were carefully removed with Gilson pipette tips into new eppendorfs. Finally, the DNA was resuspended in 1ml of TE.

8) The quality of the DNA samples was checked by both non-denaturing agarose gel electrophoresis (see 2.5) and UV spectrophotometery (Beckman DU-530). Samples with clean DNA should give a sharp bright band on an EtBr stained agarose gel upon a UV transilluminator and a ratio of optical absorbance at 260nm to that at 280nm of around 1.8. The DNA samples were stored at -20° C until further research.

2.5 DNA electrophoresis

DNA electrophoresis on agarose or polyacrylamide gels was routinely used for checking DNA quality, monitoring DNA manipulation and sequencing DNA fragments. Because normally DNA is negatively charged, DNA fragments move from the cathode to the anode of the gel. The electrophoretic mobility of DNA fragments is dependent on their size, the shorter fragments move quicker. The agarose and polyacrylamide gels used in this study are described here.

2.5.1 Non-denaturing agarose gel electrophoresis

1 % non-denaturing agarose gels were used to check double-stranded DNA routinely, for DNA quality, restriction efficiency, *etc.*

1. 1.5 g of agarose powder was rendered molten in 150 ml 1 × TAE buffer by using a microwave oven. Then 1 μl of 10 mg/ml EtBr was added and mixed well.

2. The molten agarose was left to cool down to ~60°C, and then poured into a gel tray (11 × 14 cm, in a horizontal electrophoretic tank). A comb was quickly put in the molten agarose to form the sample wells. The gel was set for about 1 hr at room temperature. Then 1 × TAE was added as running buffer.

3. After removing the comb, the DNA samples (2 μl of DNA preparation mixed with 8 μl of H_2O and 3 μl of non-denaturing loading buffer) were carefully loaded onto the gel wells. Electrophoresis was carried out at a constant voltage of 80V for 40 min using a Sigma powerpack. The gel was visualised by UV transillumination.

Genomic DNA ran as a discrete high molecular weight band visible with the UV transilluminator. To check the efficiency of yeast DNA digestion, 5 μl of restricted DNA dissolved in TE buffer was routinely examined by non-denaturing agarose gel as described above. Here, the efficiently digested genomic DNA migrates on the gel as a smear.

2.5.2 Denaturing polyacrylamide gel electrophoresis

In this study, a 0.4 mm denaturing polyacrylamide gel was used for DNA sequencing, analysis of nucleosome positions and for examining DNA repair at the level of the nucleotide.

1. Two glass plates (20 × 60 cm and 20 × 62 cm) were cleaned with detergent and

washed thoroughly with water, then wiped with ethanol carefully to remove grease, finger-prints *etc.* Next the shorter plate was siliconised with dimethyldichlorosilane solution on its inner surface. The two plates were separated with 0.4 mm side spacer strips and firmly sealed with vinyl insulation tape.

2. 80 ml of 6 % acrylamide EASI gel (acrylamide:bis-acrylamide = 19:1, 7 M urea, 1×TBE, ScottLab) was degassed under vacuum conditions in a flask for 10 min, and then 650 µl of 10 % APS and 35 µl of TEMED were added and mixed with gentle shaking. The gel mixture was then poured slowly into the gel mould. A comb was inserted into the top part of the gel immediately for setting the sample wells. The gel was set at room temperature for 1 hour.

3. A GIBCO electrophoresis system (Model SA) and a Pharmacia powerpack (EPS 3500) were used for running the sequencing gel. Pre-running of the gel in 1×TBE buffer was carried out at 70 W for 30 min, with loading buffer added to check sample wells.

4. DNA samples were loaded carefully into the gel wells. Electrophoresis was carried out under the same conditions as gel pre-running for the desired time that depended on the size of DNA fragment. When electrophoresis had finished, the plates were separated carefully. The gel was covered with a piece of Watman filter paper (3 MM) carefully to make sure the whole gel contacted the paper. The gel was carefully taken off with the filter paper from the glass plate, and covered with

cling film.

5. Then the gel was dried in a Bio-Rad gel dryer under vacuum at 80 °C for 2 hrs. The dried gel was exposed to a phosphorimager screen in a cassette for enough time dependent on the labeling efficiency. The phosphorimager screen was then scanned with a phosphorimager screen scanner (Molecular Dynamics) for further analysis.

2.6 Northern blotting

Northern blotting was used to examine the relative transcription levels of genes on different backgrounds. It is very similar to Southern blotting except that it targets RNA rather than DNA. Extra care was taken when dealing with RNA as all the glassware, tips and solutions *etc.* were pre-treated according to the standard requirement of working with RNA. The procedure is described here.

2.6.1 Isolation of total RNA

The yeast total RNA was extracted by using the hot phenol method (Schmitt and Tipper, 1990). 3×10^8 cells (at a density of $2\sim4\times10^7$ cells/ml) were collected by centrifugation. After washed with sterile H_2O, the cells were transferred to a 1.5 ml eppendorf tube. 0.5 ml of RNA lysis buffer (10 mM Tris, pH 7.5; 10mM EDTA, pH 8.0; 0.5% SDS) and an equal volume of phenol (pH 4.3±0.2, Sigma) were added, after which the tube was incubated at 65°C for at least 30 min with regular vigorous

vortexing before cooling down rapidly on ice for 10 min. Following centrifugation at maximum speed in a microfuge for 5 min, the top aqueous layer was transferred to a fresh tube where a normal phenol/chloroform extraction (once with phenol/chloroform and once with chloroform, see section 2.4) was performed to complete the RNA extraction. The RNA was then precipitated by the addition of 2.5 volumes of absolute ethanol at -20°C overnight. The RNA pellets were collected, washed and redissolved in 80µl of sterile H_2O plus 20µl of 5x RNA loading buffer (see Appendix I) and thereafter kept at -80°C until further use.

2.6.2 Separation of RNA under formaldehyde-agarose (FA) gel electrophoresis

Formaldehyde-agarose (FA) gel electrophoresis was routinely used with RNA fragments. 1.2~1.5% of agarose (depending on the size of the RNA fragments to be resolved) was melted in 200ml of 1x FA gel buffer. After the gel mixture was cooled down to 65°C in a water bath, 1µl of EtBr (10mg/ml) and 3.6ml of 37% formaldehyde were added, and then the gel mixture was poured into a gel mould with a comb plugged in, and left to completely set (more than 30min at room temperature). The gel was mounted in the electrophoresis tank filled with 1x FA gel running buffer. The gel was maintained at equilibrium with the running buffer for 30 to 45 min before RNA samples were loaded. About 10µl of each RNA sample (the amount of loading was adjusted among samples to give an equal signal of the internal control gene after hybridisation) was loaded into the well, and finally the gel was run at 10V/cm for 2-3 hours.

2.6.3 Northern hybridisation

Transferring DNA from the gel to the membrane, and the subsequent hybridisation with radioactive probes was similar to Southern blotting except for the buffers for transfer and hybridization.

RNA was transferred to a nylon-based membrane (GeneScreen Plus, PerkinElmer Life Sciences, Inc., USA) under 20 times diluted 1M phosphate buffer (see Appendix I) using a Pressure Blotter (Stratagene Ltd., UK) with a pressure of 80 psi for 2 hours. Phosphate buffer gives a better signal-noise ratio for transferring and hybridisation. Because of its low salt concentration, it took about 5 hours to complete the transfer process.

The membrane carrying the transferred RNA was rinsed with distilled water and rolled inside a glass tube containing hybridisation solution (0.5M phosphate buffer, 7% SDS, 1% BSA, 1mM EDTA) at 60°C for 1 hour on the rotating spindle in a Hybaid Oven. 100µl of radioactive strand specific probe (see section 2.7) was added to the tube. The tube was placed back into the Hybaid Oven and kept at 60°C overnight under constant rotation. After hybridisation, the membrane was washed twice with phosphate washing buffer (40mM phosphate buffer, 4% SDS, 1mM EDTA) on the shaking platform at 60°C for 15 minutes.

Following the washing step, the membrane was covered by cling film and placed in a cassette against a phosphorimager screen (Molecular Dynamics, Inc.). Exposure was overnight at room temperature. The image was generated by scanning

the phosphorimager screen using a scanner (Storm 860, Molecular Dynamics, Inc.) and quantified using ImageQuant software (Molecular Dynamics, Inc.) The analysis of image data will be described in section 2.8.

In this research, all experiments involving radioactive isotopes were performed according to the safety guideline.

2.7 Preparation of specific probes

In this study all DNA or RNA probes synthesised for hybridisation were strand specific so they can detect the TS and NTS or transcripts separately. The base of this approach is to employ a 5' biotinylated primer and Dynabeads so as single stranded DNA can be retrieved. The synthesis began from PCR amplification of the DNA sequence of interest by using genomic DNA as a template. PCR primers were designed using the computer Oligo software. Normally PCR utilized one biotinylated and one non-biotinylated primer (Oswel, UK). Once PCR had finished, the product was loaded onto a 1% non-denaturing agarose gel and visualized by UV transillumination. PCR conditions were optimized in order to obtain unique PCR of the sequence desired. The required PCR product was isolated by using Dynabeads and a magnetic particle concentrator (MPC). Dynabeads are streptavidin coated superparamagnetic spheres which are able to bind tightly to 5' biotinylated residue on one strand of the PCR product and then be separated from the rest of PCR mixture in a magnetic field provided by a MPC. The bound double stranded PCR product was then denatured by incubation in a NaOH solution. Once again, by placing the mixture

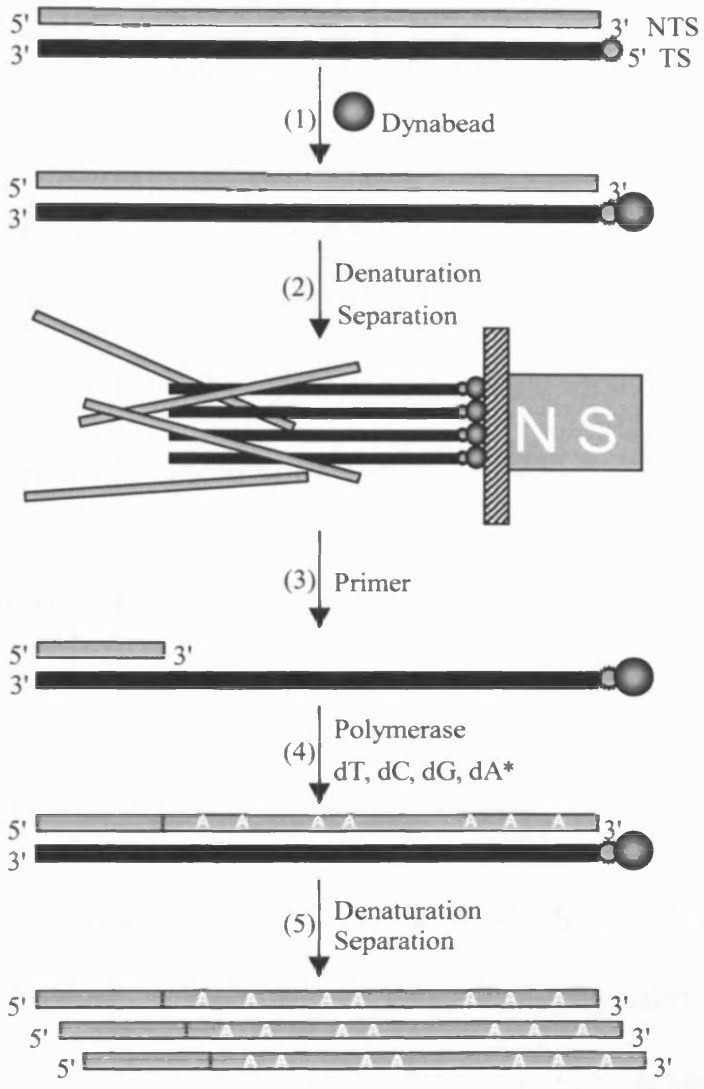

Figure 2.1 *Schematic representation of the procedure for probe synthesis.* (1) Dynabeads bind to the biotin (✪) end to enrich appropriate PCR products (2) Double stranded DNA is denatured in 0.1 M NaOH. The beads with associated single stranded DNA are kept on the Eppendorf wall in a MPC. The supernatant is removed. (3) The second primer annealed to the 3' end of the single stranded DNA. (4) [α^{32}P]dATP (dA*) and the other three dNTPs are recruited for the primer extension reaction by DNA polymerase. (5) The newly synthesized probe is separated from the template in a MPC. (Adapted from Teng, PhD thesis, 2000)

in the MPC the biotin labelled strand was separated from the non-biotinylated strand by collecting the beads and removing the supernatant with a pipette. The probe was synthesised upon this biotinylated single stranded DNA template by primer extension using Sequenase Version 2.0 T7 DNA Polymerase (Amersham Pharmacia Biotech) and a α-[^{32}P] dATP (6000 Ci/mmol, Amersham) containing dNTP mixture. The [^{32}P] incorporated probe was collected with a pipette as a supernatant when directly placing the mixture after heating to a denaturing temperature in the MPC.

2.7.1 PCR amplification of the sequence of interest

A pair comprising one biotinylated primer and one non-biotinylated primer was designed for standard PCR amplifications as described below:

1μl of each primer (20μM), 1.75μl of dNTPs(10mM), 5μl of 10×Taq buffer (Promega), 4.5μl of $MgCl_2$ (25 mM), 10 μl of 100x diluted untreated (U) DNA template, and 1.25 units of Taq polymerase (Promega) were mixed up and supplemented with RNA-free water to a final volume of 50μl.

PCR was carried out in an OmniGene thermal cycler (Hybaid) and the program was run as: (1) denaturation at 95°C for 4 min; (2) 28-30 cycles of: 30 seconds of denaturation at 95°C; 30 seconds of annealing (55°C); 1 min of extension at 68°C, and (3) finally, at 72°C for 10 min to complete the DNA synthesis.

2.7.2 Synthesis of the radioactive probe by primer extension

1) 20µl of washed Dynabeads in 2×BW (binding and washing) buffer (see Appendix I) were added to 20µl of PCR product to bind to the biotin end of the PCR products. This was undertaken at room temperature for 15 minutes, with occasional mixture by pipette. The MPC was used to collect the beads associated with the PCR product and the supernatant discarded.
2) After two washes with H_2O, the beads were resuspended in 30µl of 0.1M NaOH at room temperature for 10 minutes to denature the dsDNA. The MPC was used to keep the biotinylated strand associated with the beads on the Eppendorf wall, while the supernatant containing the other strand was discarded.
3) The beads were washed twice with H_2O and resuspended in 20µl of 1xBW. 1µl of the appropriate non-biotinylated primer (20 µM) was added. The solution was mixed thoroughly by pipette. After the tube was incubated at 65°C for 2 min, it was allowed to cool down slowly to room temperature over a period of about 30 minutes. Using a MPC, beads and bound fragments were separated from the supernatant, and then washed twice with 60µl H_2O.
4) The beads were resuspended in 10µl of water. 8 µl of 5 × Sequenase reaction buffer (Amersham), 4µl of dATP buffer (0.1 mM dTTP, dGTP and dCTP), 3µl of α-[^{32}P] dATP (6000 Ci/mmol, Amersham), 1µl of Sequenase (in 5µl sequenase dilution buffer, Amersham), 2.8µl of DTT (0.1M) were added. The solution was mixed thoroughly by pipette and incubated at 37°C for 10 minutes. The beads with

the associated dsDNA fragment were collected using the MPC and the supernatant was discarded.

5) After washing twice with 60µl H_2O, the beads were resuspended in 100µl TE buffer. Immediately after incubation at 95°C for 3 minutes to denature the DNA fragments, the supernatant containing the newly synthesised radioactive probe was transferred to a fresh tube on ice while the beads and the biotinylated ssDNA were immobilized by the magnet in an MPC. This probe is ready for use as in the following section to detect the complementary sequence on the membrane for Northern blotting, or if required, for DNA analysis via Southern blotting.

2.8 Examining DNA repair at nucleotide level

Investigation of DNA damage and repair at the gene level are carried out by Southern blotting. However, this cannot give subtle information concerning repair rate at specific nucleotide positions, and which may be influenced by local chromatin structure. An end-labelling high resolution method was developed in our group to examine DNA damage and repair at nucleotide resolution. It has been used to detect the inducing and repair of CPDs and oxidative damage in budding yeast and *E. coli* (Teng *et al.*, 1997, 1998; Li and Waters, 1996, 1997; Meniel and Waters, 1999; Teng and Waters, 2000; Yu *et al.*, 2001; Teng *et al.*, 2002). DNA is incubated with specific DNA glycosylases that cut at the site of DNA damage (e.g. *T4* or *ML* CPD glycosylase as used in this thesis). The end-labelling method involves a biotin modification of the primer, which was termed a probe, and Dynabeads (Fig. 2.2).

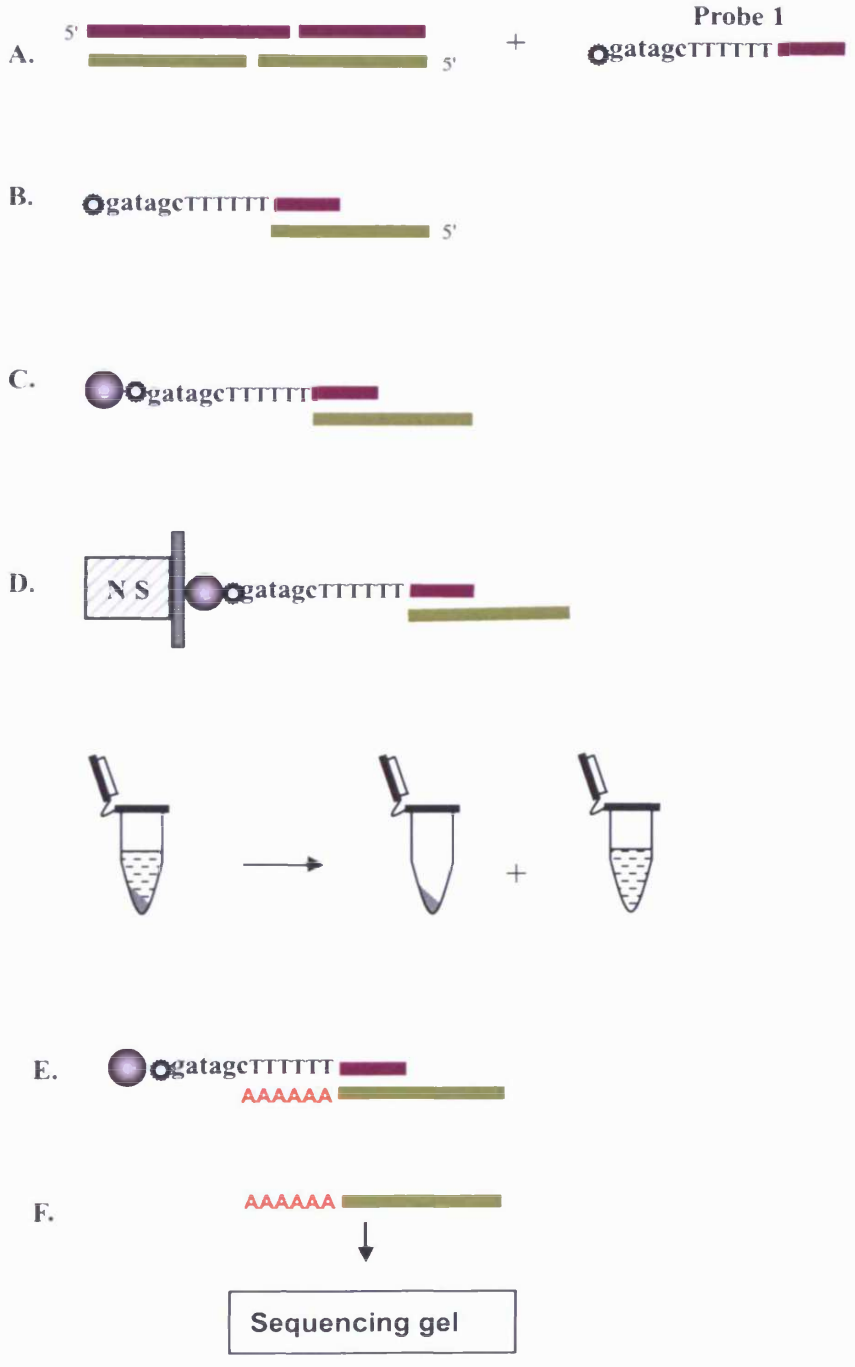

Figure 2.2 *Purification and end-labelling of DNA fragments.* **A.** Probe 1 was added to the restricted and CPD cut DNA. **B.** The Probe annealed to the complementary TS sequences at 3' end. **C.** Dynabeads ◯ were added to bind the biotin ✪ at the 5' end of the probe. **D.** Dynabeads and the associated DNA fragments were isolated, and the supernatant was saved for purification of the NTS strand. **E.** purified DNA was radioactively labelled at 3' end. **F.** After denaturing, end-labelled DNA was loaded onto a sequencing gel.

Genomic DNA was digested by appropriate restriction enzymes to generate an interested DNA fragment, followed by specific damage recognition endonuclease incision. The released ssDNA with different lengths generated from denaturation was isolated via a biotinylated primer together with Dynabeads, and the purified DNA fragments are while they still attach Dynabeads. Finally, each single stranded DNA fragment was end-labelled with radioactive dATPs and separated by electrophoresis. In this study, this technique was used to analyse UV induced CPDs in the *S. cerevisiae* *MFA2* gene.

2.8.1 Creating probes for high resolution analyses

In this study, probes for high resolution sequencing gel were created for *MFA2* gene and other tested genes. Probe 1 is complementary to, and anneals to the TS, whereas Probe 2 is complementary to, and anneals to the NTS. These probes were designed so that they had an overhang of six dTs followed by 5'-biotin-NNNNNN3' with no thymine residues at the N3' end (Fig. 2.3). The dTs overhang serve as a template for the polymerization of radioactive dATPs at the 3' end of the complementary to the 3' ends of the restriction fragments containing the *MFA2* complementary DNA fragment. The 5'-biotin binds to Dynabeads, hence the beads and the associated DNA fragments can be separated from the solution with MPC and simply removing the supernatant. The overhanging sequence of six dNs (gatagc) was designed to prevent folding back of the probe itself, and it was inserted between six dTs and biotin to keep the relatively large Dynabeads at a distance from the dTs. This

design ensures the complete polymerisation of six dAs without steric hindrance from the Dynabeads.

The HaeIII-HaeIII restriction fragment

The *HaeIII* restriction fragment is 599 bp in length; it contains the part of *MFA2* coding region and the upstream promoter region.

Probe 1:
5'Biotin-gatagctttttttCCCTCATCTATTTTCTCGGAAAACTTGGTG3'
Tm= 64.4 °C (0.1 M Na^+).

Probe 2:
5'Biotin-gatagctttttttCCCTTGATTATATAGATTGTCTTTCTTTTCAGAGGAT3'
Tm= 63.7 °C (0.1 M Na^+).

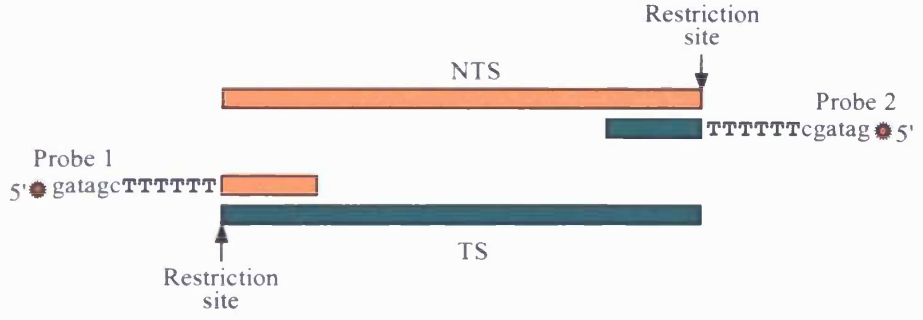

Figure 2.3 *The probe creation for the restriction fragment.* The Probes are designed and consist of two parts: the complementary sequence and the modification sequence. The complementary sequence is a 20~30 mer oligonucleotide which is complementary to the 3′ end of the *MFA2* restriction fragment. ●**gatagcTTTTTT** is the 5′ biotinylated modification sequence which is added to the 5′ end of the complementary sequence. Probe 1 anneals to the TS whereas Probe 2 anneals to the NTS (Adapted from Yu, PhD thesis, 2001)

2.8.2 Digestion and purification of single-stranded fragments

1. 50 μg of genomic DNA (about 100μl volume) was digested by restriction endonucleases at 37 °C for 90 min at the recommended working condition in a reaction volume of 200 μl.
2. The restricted DNA fragments were extracted by 1 volume (200 μl) of phenol/chloroform/iso-amyl alcohol (24:24:1) and followed by 1 volume (200 μl) of chloroform/iso-amyl alcohol (24:1). The upper phase containing restricted DNA fragments was carefully removed to a fresh tube without disturbing the interface.
3. 1/10 volume (20 μl) of 3 M NaOAc was added to each tube. The DNA was then precipitated by the addition of 1 volume (220 μl) of pre-chilled iso-proponol (-20 °C) with gentle inverting. After precipitation at –70 °C for 10 min, the DNA pellets were collected by centrifugation at 10,000 rpm using a bench-top microfuge.
4. The DNA was dissolved completely in 110 μl of TE buffer, and then 10 μl of *ML* CPD endonuclease was added to cut the DNA at CPD sites. Incubation was carried out at 37 °C for 60 min.
5. 120 μl of phenol/chloroform/iso-amyl alcohol (24:24:1) followed by 120 μl of chloroform/iso-amyl alcohol (24:1) were used for protein extraction as described in step 2. The upper phase containing DNA fragments was transferred to a fresh 0.5 ml Eppendorf tube.

6. 30 µl of 5 M NaCl and 2 µl of Probe 1 (1 µM) were added to each sample and mixed by vortexing. After brief spinning, samples were heated at 95 °C for 5 min to denature the dsDNA and then incubated at the annealing temperature for 15 min, allowing the probes to anneal to the complementary *MFA2* TS.
7. 10 µl of washed Dynabeads (10 mg/ml in 1 × BW buffer) was added to each tube to bind the 5' biotin at room temperature for 15 min with occasional inverting. The beads associated with DNA fragments were collected by a MPC. The supernatant was then transferred to a fresh tube for the NTS purification (step 8). The Dynabeads associated with the restricted fragments were resuspended in 60 µl of 1 × B&W buffer for step 9.
8. 2 µl of Probe 2 (1 µM) was added to the supernatant for the purification of the NTS as described in steps 6 and 7. The beads associated with the NTS were resuspended in 60 µl of 1 × B&W buffer.
9. 60 µl of bead suspension in 1 × B&W buffer was heated at annealing temperature for 5 min to eliminate non-specific annealing. The beads with associated DNA fragments were collected with an MPC and the supernatant was removed. Two washes were carried out with 60 µl of water at room temperature.

2.8.3 Labelling the fragments

1. Resuspended Dynabeads with associated restricted DNA fragments in 5 µl of H_2O, and then 2 µl of 5 × Sequenase Reaction Buffer (200 mM Tris.HCl, pH 7.5, 100 mM $MgCl_2$, 250 mM NaCl), 0.7 µl of 0.1 M DTT, 0.5 units of T7 DNA

polymerase and 1 μl (5 μCi) of [α^{32}P] dATP (6000 Ci/mmol Amersham) were added. The solution was mixed by pipette and incubated at 37 °C for 10 min for the polymerization of radioactive dATP.

2. The Dynabeads associated with radioactive labelled DNA fragments were immobilized on the Eppendorf wall by an MPC, and washed twice with 40 μl of TE buffer at room temperature.
3. Following the removal of the 2nd TE wash, 3 μl of loading buffer (95 % Formamide, 20 mM EDTA, 0.05 % Bromophenol Blue) was added and mixed thoroughly by pipette. The mixture was left at room temperature for 5 min. The labelled DNA fragments were eluted from the Dynabead-probe.
4. The MPC was used to immobilize the Dynabead-probe, and the loading buffer containing the labelled fragments was loaded onto a 6 % denaturing polyacrylamide gel for electrophoresis as described in section 2.5.2.

2.8.4 Sequencing the *MFA2* containing fragments

To indicate the precise position of CPDs within the DNA sequence investigated, a sequencing ladder for *MFA2* containing fragment was run alongside the UV treated DNA samples during electrophoresis. The procedure for sequencing the *MFA2* fragment is described here.

The sequencing ladder was synthesised by using T7 Sequenase Version 2.0 DNA sequencing kit (Amersham Pharmacia Biotech) according to the manufacturer's instructions. Because the single stranded DNA fragments were purified with a probe

complementary to their 3' ends (see Figure 2.2) and DNA synthesis can only proceeds from the 5' end to the 3' end, it is required to load the sequencing ladder reflecting the sequence of the opposite strand to indicate the actual position of a DNA lesion in a specific DNA strand. The probe used to generate sequencing ladders was modified as well, but in some different from that served to isolate single stranded DNA after damage incision. Six random nucleotides were added to the primer at the 5' end before the complementary sequence to compensate in the length of the ladder in the same way as the single stranded DNA samples are labelled with six radioactive dATPs. This allows a direct reference from the running positions of the sequencing ladder to that of the DNA damage ladder.

The fragments of interest were amplified via PCR using the primers indicated below. Primer 1 and Primer 2 are the same sequence as the biotinylated Probe 1 and Probe 2, respectively. Primers 3 and 4 are the modified versions of Primer 2 and Primer 1, respectively. The modification involves removal of the 12 bp overhang of Primers 1 and 2 and replacement with a random hexanucleotide. The purpose of the random hexanucleotide added to the 5' end of Primers 3 and 4 is to allow the sequencing ladder to run alongside the DNA damage ladder at the same position, since the DNA damage ladder is end-labelled with 6 dAs residues.

HaeIH-HaeIII fragment

Primer1: 5'Biotin-gatagctttttt CCCTCATCTATTTTCTCGGAAAACTTGGTG3'

Primer2: 5'Biotin-gatagctttttttCCCTTGATTATATAGATTGTCTTTCTTTTCAGAGGAT3'

Primer3: 5'gatagcAAGAGGCCCTTGATTATATAGATTGTCTTTCTTTT3'

Primer4: 5'gatagcAACAGGCCCTCATCTATTTTCTCGGA3'

1. 1 μl (20 μM) of Primers 1 and 3 for TS (or Primer 2 and 4 for NTS), 8 μl of dNTP mixture (1.25 mM of each dATP, dCTP, dGTP, and dTTP), 5 μl of Thermophilic DNA polymerase 10 × Buffer, 1 unit of Taq DNA polymerase (Promega), 1 ng of DNA templates were mixed in a tube in a final volume of 50 μl.

2. The tube was incubated at 95°C for 2 min and then 30 PCR cycles were carried out: denaturation at 95°C for 30 s, primer annealing at 57°C for 30 s and primer extension at 72°C for 30 s. Finally the tube was incubated at 72°C for 4 min to complete the primer extension.

3. 20 μl of Dynabeads (in 2 × B&W) were added to 20 μl of the PCR product to bind to the biotin at the 5' end of the extended Primer 1 at r.t. for 10 min, mixing occasionally with a pipette. The beads associated with the PCR product were collected using an MPC and the supernatant was discarded.

4. The beads with associated DNA fragments were resuspended in 30 μl of 0.1 M NaOH at r.t. for 10 min to denature the DNA. The supernatant was removed, and the beads were washed twice with 30 μl of H_2O, and then the beads were resuspended in 20 μl of 1 × B&W.

5. 1 μl of Primer 3 (20 μM) were added to the bead suspension and the tube was incubated at 65 °C for 2 min., then allowed to cool slowly to r.t. After a brief spin

in a microfuge, the beads were washed twice with 40 µl of H_2O, and resuspended in 8 µl of H_2O and 2 µl of 5 × sequenase reaction buffer.

6. 5.5 µl of reaction mixture containing 2 µl of 8 times diluted Labelling Mix (dGTP) (7.5 µM dGTP, 7.5 µM dCTP, 7.5 µM dTTP), 0.5 µl of [^{35}S] dATP (10 µCi/ml at >1000 Ci /mmol), 2 µl of Sequenase (8 times dilution, 1.6 U/µl) and 1 µl 0.1 M DTT were added and the tube was incubated at room temperature for 2 min.

7. 4 fresh tubes each contains 2.5 µl of one of the four termination mixtures (ddATP, ddGTP, ddCTP, ddTTP) were incubated at 37 °C. 3.5 µl of the reaction mixture (step 6) was added to each termination tube and the tubes were incubated at 37 °C for 5 min.

8. The beads with associated DNA fragments were washed twice with 40 µl of TE buffer, and resuspended in 20 µl of stop solution (95 % formamide, 20 µM EDTA, 0.05 % bromophenol blue, 0.05 % xylene cyanol FF).

Because the analysis was of cyclobutane pyrimidine dimers, a mixture of ddCTP and ddTTP termination reactions was loaded to one lane and a mixture of ddGTP and ddATP termination reactions to another.

2.8.5 Damage quantification and repair analysis

The sequencing gel data was analysed by using ImageQuant software version 5.0. The intensity of each band, which reflects the frequency of DNA damage at a specific site, was measured as collective pixel values. To avoid a false judgement

about repair resulting from a slightly varied loading of DNA samples in each lane, an adjustment was made as the total signal from individual lanes were multiplied by a factor to give equal values, and then the signal of each band was accordingly multiplied. The value from non-irradiated DNA was subtracted as a non-specific background. The damage remaining after particular repair times was presented as a percentile with respect to the initial damage (0 lane, 100% CPD damage).

$$\% \text{ (CPD remaining)} = \frac{[\text{CPD}]_t}{[\text{CPD}]_0} \text{ X100}$$

Here t represents a particular repair time and 0 represents when the repair starts (no repair time). % (repaired CPD) can be used for expressing the result alternatively as follows:

% (repaired CPD) = 100% - % (CPD remaining)

To generate repair curves, the data points representing % damage at defined sites at each repair time were fitted to an exponential curve. Finally the time, where 50% of the damage was removed ($T_{50\%}$ value), was calculated to compare repair rates of individual damages.

Chapter 3

TUP1 deletion derepresses *MFA2* in *S. cerevisiae* alpha cells and accelerates NER in the control region of *MFA2*

3.1 Introduction

In the yeast *S. cerevisiae* there exists three different cell types; **a**- or α- haploid cells and **a**/α diploid cells. The haploid cells are regulated by the expression of genes at *MAT*, the active mating type locus. Haploid **a**- and α- cells can mate to form an **a**/α diploid cell. In *MAT*α cells, products of *MAT*α are the α1 and α2 proteins. α1 is an activator for the transcription of α-specific genes, whereas α2 is a part of the repressor for **a**-specific genes in α-cells (Herskowitz, 1989; Dranginis, 1990, Murphy *et al.*, 1993). Without the non-cell type specific protein Mcm1p binding to DNA sequences upstream of target genes, α1 or α2 factor alone is not sufficient for the cell type specific gene regulation. The Mcm1p has been identified as the transcription factor, which can bind to the Mcm1p binding site, the P box (Hwang-shum *et al.*, 1991; Christ and Tye, 1991; Mead *et al.*, 1996). In *S. cerevisiae*, a 31bp α2 operator sequence has been found located about 200 bp upstream of the transcription start point at **a**-specific genes and which includes the *MFA2* gene (Wilson and Herskowitz, 1986). In α-cells, Mcm1p and α2 factors cooperatively bind to the α2 operators, with

Mcm1p binding to the centre of the operator and α2 to the ends of the operator, in the control region of **a**-specific genes to repress them. Binding of the α2/Mcm1p complex to the operator establishes a repressive chromatin structure, in which nucleosomes are precisely positioned over essential promoter elements of **a**-specific genes. These nucleosomes are destabilized in the presence of amino terminal mutations in histone H4, resulting in a partial derepression of **a**-specific gene expression (Sauer *et al.*, 1988; Shimizu *et al.*, 1991; Roth *et al.*, 1992; Watson *et al.*, 2000). Studies also show that repression of *MFA2* additionally requires a protein complex of Tup1p-Ssn6p, which has been identified as a general transcription repressor complex in yeast (Keleher *et al.*, 1992; Redd *et al.*, 1997; Smith and Johnson, 2000; Li and Reese, 2001).

Tup1p and Ssn6p proteins are evolutionarily conserved from yeast to mammals. Repression by the Tup1p-Ssn6p complex has several distinguishing features. Firstly, it is exceedingly efficient, causing more than 1000-fold repression for some target genes. Secondly, Tup1p-Ssn6p regulates more than 3% of the genes in *S. cerevisiae*; about 180 genes participating in different pathways. Finally, it has versatility with respect to the nature and number of activators it can repress (Smith and Johnson, 2000). Some genes that can be repressed efficiently by Tup1p–Ssn6p are activated by several different activator proteins working together. Although Tup1p-Ssn6p does not bind to DNA directly, this complex can cause strong repression when a specific DNA-binding protein, such as α2/Mcm1p (for an **a**-specific gene), Mig1p (for a glucose-specific gene), or Crt1p (for a DNA-damage-inducible gene), *etc.*, which attract it to DNA so as it is located at a variety of positions along the upstream control

region, and which are dependent on its target gene (Nehlin *et al.*, 1991; Herschbach and Johnson, 1993; Tzamarias and Struhl, 1995; Huang *et al.*, 1998). In particular, the DNA-binding protein need not overlap with the upstream activating sequence (UAS), which are the binding sites for activators, the TATA box or the starting points of transcription. Thus, Tup1p-Ssn6p mediated repression appears to be independent of the number and identity of the activator proteins responsible for directing transcription of the target gene. Tup1p shows a preferred interaction with hypoacetylated histone tails *in vitro* (Edmondson *et al.*, 1996). If it behaves *in vivo* in the same manner, this would then contribute to generating a fixed repressed state, as suggested by Davie *et al.* (2002). It has also been shown that Tup1p inhibits the binding of TBP at the *SUC2* promoter (Kuras and Struhl, 1999), and this could be why on derepression Tup1p moves away from nucleosome 4 at the *SUC2* promoter region (Boukaba *et al.*, 2004).

There are three general models to explain how Tup1p–Ssn6p may repress transcription. The first model suggests the complex has a direct interference with the activator. In principle, Tup1p-Ssn6p could contact the activator once it is bound to DNA and compromise its ability to activate transcription. However, with the *GAL4* gene Tup1p-Ssn6p can exert tight transcriptional repression, while still allowing occupancy of the UAS by the activator (Redd *et al.*, 1996). This fact suggests that the primary mechanism of Tup1p-Ssn6p is not in preventing the activator from binding to DNA. Thus, it remains a possible mechanism which needs further direct experimental data to support it.

The second model for gene repression by Tup1p-Ssn6p is through the interaction with the general transcription machinery. Mutations in several components of the RNA polymerase II holoenzyme, including Srb10/11 (Kuchin and Carlson, 1998), Med3p (Papamichos-Chronakis *et al.*, 2000), and Srb7p (Gromoller and Lehming, 2000), can decrease Tup1p-Ssn6p repression. Moreover, direct physical interactions between Tup1p- Ssn6p and Med3p, Srb7p, and Srb10p/11p (Zaman *et al.*, 2001) have also been observed in experiments. In addition, a modest amount of repression can be established on a nonnucleosomal template in vitro (Redd *et al.*, 1997), suggesting that Tup1p-Ssn6p may directly target multiple aspects of the transcription machinery for repression.

The third model for Tup1p-Ssn6p to repress genes is by altering the local chromatin structure and positioning nucleosomes around target genes such as for the repression of **a**-mating type specific genes (e.g. *MFA2* gene) in α-cells. The chromatin structures of two other **a**-specific genes, *STE6* and *BAR1*, were analysed and nucleosomes were found to be precisely positioned upstream of those genes in α-cells but not in **a**-cells, and these nucleosomes are in a position to occlude the binding of proteins to DNA around the TATA box and the transcription initiation site (Shimizu *et al.*, 1991; Patterton and Simpson, 1994). At the *STE6* gene, Tup1p was shown to cross-link throughout the entire gene, and two Tup1p molecules per nucleosome were incorporated into the repressive chromatin structure of a minichromosome (Ducker and Simpson, 2000). These results suggest a relationship between the organization of chromatin and the repression of the **a**-specific genes in α-cells. Deletion of *TUP1*

results in the derepression of the **a**-specific genes and disruption of the positioned nucleosomes adjacent to the α2 operator (Cooper *et al.*, 1994; Gavin *et al.*, 2000). A similar phenomenon also has been found at the *MFA2* gene (see data in this chapter). Moreover, the repressing domain of Tup1p was found to interact *in vitro* directly with the N-terminal tails of hypoacetylated histones H3 and H4 (Edmondson *et al.*, 1996). Deletion or mutation of these histone tails, under some conditions, partially relieves Tup1p–Ssn6p-mediated repression *in vivo* (Edmondson *et al.*, 1996, 1998). Three types of multi-protein complexes found for chromatin remodeling can acetylate nucleosomes (such as ADA or SAGA), deacetylate nucleosomes (such as HAD), or alter nucleosome structure in an ATP-dependent manner (such as SWI/SNF). Tup1p-Ssn6p interacts physically with at least three histone deacetylases, and a combination of mutations in the deacetylase genes *RPD3*, *HOS1*, and *HOS2* derepresses all Tup1p-Ssn6p-regulated genes examined (Watson *et al.*, 2000; Wu *et al.*, 2001). These results suggest that the repressor complex alters histone modification states to facilitate interactions with histones and that these interactions are required to maintain a stable repressive state. Tup1p has been shown to spread along the length of a repressed **a** cell-specific gene *STE6*; this indicates that the corepressor may serve an structural function (Ducker and Simpson 2000). The interactions of Tup1p with the histone tails might also sterically limit reacetylation of H3 and H4, stabilizing the underacetylated, repressed state. However, other evidence also shows that Tup1p-Ssn6p is not simply a corepressor with histone deacetylases but also that it is involved in recruiting SWI/SNF and SAGA during the transcriptional induction

process (Proft and Struhl, 2002). Therefore, at some regulated genes Tup1p-Ssn6p can bring the HATs for histone acetylation to the same promoter that it recruits the HDACs to for deacetylation.

Recently, Zhang and Reese (2004) also report that redundant mechanisms, including nucleosome positioning, histone deacetylation, and mediator interference, are used by Tup1p-Ssn6p to repress the DNA damage-inducible *RNR3* gene. At the *RNR3* locus, Tup1p-Ssn6p requires the ISW2 chromatin remodeling complex to establish nucleosome positioning *in vivo* to disrupt chromatin structure without affecting other Tup1p repressing functions. Deleting *ISW2*, the histone deacetylase gene *HDA1*, or genes encoding mediator subunits individually only induce slight or no derepression of *RNR3* and *HUG1*. However, enhanced transcription was observed when Mediator mutations were combined with *Δisw2* or *Δhda1* mutations, and the strongest level of derepression occurred in triple *Δisw2/Δhda1*/Mediator mutants. The increased transcription in the mutants was not due to the loss of Tup1p at the promoter and correlated with increased TBP cross-linking to promoters. Thus, Tup1p utilizes multiple redundant mechanisms to repress transcription of native genes, and these may be important for it to act as a global corepressor at a wide variety of promoters.

MFA2 is one of the **a**-mating type specific genes and encodes an **a**-factor precursor (Michaelis and Herskowitz, 1988). The upstream control region of *MFA2* contains a TATA box and a α2 operator located at the position –119 and –251 respectively. Because the regulation of *MFA2* is easily controlled by mating type

selection and the size of this gene is small (the transcribed region is only 328 bp), it has been used as a model gene for DNA repair investigations by our group (Teng *et al.*, 1997; 1998; Meniel and Waters, 1999; Teng and Waters, 2000, Yu *et al.*, 2001; Teng *et al.*, 2002; Yu *et al.*, 2005). To analyze the effect of *TUP1* deletion on transcription, chromatin structure and DNA repair at *MFA2*, here, I applied Northern blotting to detect the *MFA2* gene expression in wild type and mutants, and the high resolution technique (Teng *et al.*, 1997) to investigate CPD repair at the nucleotide level. In addition to a *Δtup1* mutant, I also used the *Δtup1mfa2*^{TATA} mutant which has site specific mutations at the TATA box in the *Δtup1* strain which abolishes transcription, and determined how this impinges on NER.

3.2 Material and methods

3.2.1 Yeast strains

PSY316 (*MATα ade2-101 ura 3-52 leu 2-3,112 Δhis 3-200 lys2 trp1*)

Δtup1 (*MATα ade2-101 ura 3-52 leu 2-3,112 HIS::TUP1 lys2 trp1*)

Δtup1mfa2^{TATA} (*MATα mfa2*^{TATA}, *ade2-101 ura 3-52 leu 2-3,112 HIS::TUP1 lys2 trp1*)

PSY316 (*MAT***a** *ade2-101 ura 3-52 leu 2-3,112 Δhis 3-200 lys2 trp1*)

Δtup1 (*MAT***a** *ade2-101 ura 3-52 leu 2-3,112 HIS::TUP1 lys2 trp1*)

3.2.2 DNA extraction of strains

This was undertaken as described in Chapeter 2.

3.2.3 Detection of the mRNA level of *MFA2*

This was undertaken as described in Chapter 2. To prepare the *MFA2* RNA probe, primer A 5'-biotin-CTATCATCTTCATACAACAATAACTACCA3' and Primer B, 5'CTAATGATGAGAGAATTGGAATAAATTAG3' were used; for the *ACT1* RNA probe, Primer A, 5'-biotin-GCCGGTTTTGCCGGTGACG3' and Primer B, 5'CCGGCAGATTCCAAACCCAAAA 3' were used. PCR was carried out using Primer A and B to amplify the sequences of interest. The RNA specific probes were synthesised by Primer B extension using the biotinylated strand as a template.

3.2.4 Detection of CPD repair at *MFA2*

This was undertaken also as described in Chapter 2.

3.3 Results

3.3.1 The comparison of UV sensitivity

UV sensitivity of a strain with a gene specific mutation can indicate a role of that gene in a DNA repair pathway. I examined the UV sensitivities in both **a**- and α- cells of the wild-type and *Δtup1* mutant (Figure 3.1). As shown in this figure, the *Δtup1* **a**- and *Δtup1* α-cells are only marginally UV sensitivity compared with the wild-type strains. These results suggest that Tup1p may only play a minor role in DNA repair, but its effect on survival is less than that of Gcn5p (see Chapter 5) or Rad16p (see Chapter 4). The former is a prominent histone acetylase regulating 5% of yeast genes, while the latter is essential for repair of almost all the non-transcribed regions of the whole genome.

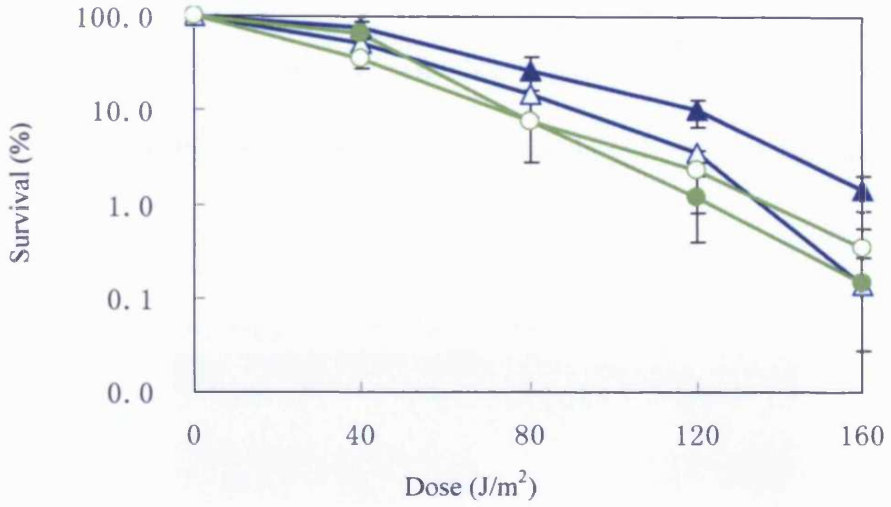

Figure 3.1 *The UV sensitivity of the strains studied.* (▲)PSY316**a**, (△)PSY316α, (●) *Δtup1***a**, (○) *Δtup1*α.

3.3.2 The mRNA levels of *MFA2*

In wild type **a**-cells, the protein Mcm1p binds to the promoter region of *MFA2* (an **a**-mating type specific gene) to activate transcription. In α cells, *MFA2* is repressed by the yeast general repressor complex Tup1p-Ssn6p (Ducker and Simpson, 2000; Gavin *et al.*, 2000). In my research, Northern blotting was used to examine the *MFA2* mRNA level in wild type and *Δtup1* strains so as to determine the influence of the deletion of Tup1p on *MFA2* transcription (Fig.3.2). Here, the *ACT1* gene was used as an internal control to adjust the loading of samples, since it is active in all the strains employed and Tup1p does not have a role in its regulation. As *MFA2* is an **a**-specific gene, it was transcribed in wild type PSY316 **a**-cells and no *MFA2* transcription was detected in PSY316α cells. In *Δtup1***a**-cells, *MFA2* was active with a transcription level similar

to that in wild-type PSY316 **a**-cells. Moreover, *MFA2*, repressed in PSY316α cells, was also active in *Δtup1*α cells with levels as in wild type PSY316 **a**-cells and *Δtup1***a** mutant cells. Thus Tup1p plays an essential role in the repression of *MFA2* in α cells.

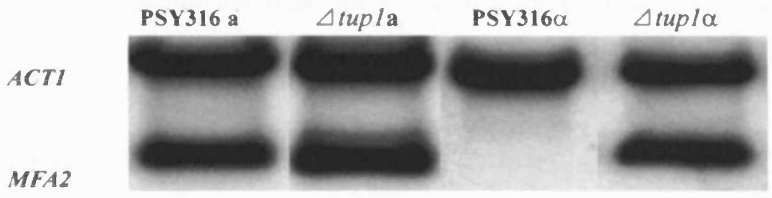

Figure 3.2 *The transcription of MFA2 as detected by Northern blotting.* 10μl of total RNA from each sample was run on 1.2% agarose gel (containing 6.7% formaldehyde) and blotted on to a nitrocellulose membrane. Radioactive dATP labeled *MFA2* gene TS fragments were used as probes to detect *MFA2* mRNA levels in both **a** and α of wild type PSY316 and mutant strains, and *ACT1* was used as an internal control to standardize the loading of total RNA in the quantification.

3.3.3 Nucleotide excision repair at *MFA2* in wild type, *Δtup1* and *Δtup1mfa2*^{TATA} strains

To investigate whether CPD repair at the nucleotide level is affected by deletion of *TUP1*, experiments were undertaken as described in Chapter 2. Figures 3.3~3.4 provide typical gel images for detecting CPDs in the TS and the NTS of the *HaeIII* restriction fragment containing the upstream control region of *MFA2* in wild type PSY316 and *Δtup1* cells irradiated with 150 J/m^2 UV light. Figure 3.6 are typical gel images used for analysis of CPD repair at *MFA2* in *Δtup1*α and *Δtup1mfa2*^{TATA}

α-cells irradiated with 150 J/m^2 UV light. Figure 3.8 depicts gel images for CPD repair analysis at *MFA2* in wild type and *⊿tup1* cells irradiated with 70 J/m^2 UV light. In all the sequencing gels, the numbers on the left denote the nucleotide positions in the control region of *MFA2*. The time allowed for CPD repair was up to 3 hours and the data are expressed as the time for removing 50% of CPDs ($t_{50\%}$) at the damage sites (Fig.3.5, 3.7, 3.9). The intensity of the detectable bands was quantified after phosphorimaging with ImageQuant software (Molecular Dynamics, CA, USA). Then Microsoft Excel software was applied to create graphs (repair % vs repair time) to estimate the $t_{50\%}$. If less than 3 hours, the $t_{50\%}$ was directly read from the graphs; while if more than 3 hours, the $t_{50\%}$ was obtained by extrapolation. For sites with very slow repair, the estimation of $t_{50\%}$ by extrapolation may not be accurate, therefore, any $t_{50\%}$ of more than 6 hours were normally set as 6 hours. The repair of a group of closely linked CPDs, all of which show a similar repair rate, is represented as a single point.

Repair of CPDs in wild type and ⊿tup1 at the nucleotide level after 150J/m^2 of UV treatment

From Fig.3.5, it was very clear that deletion of *TUP1* enhanced CPD repair significantly both in the TS and NTS of *MFA2* in wild type α-cells. There is little difference in repair rates between wild type and *TUP1* deleted **a**-cells. In wild type **a**-cells, the average repair time for 50% repair of CPDs in the examined fragment is 2.20±0.14h for the TS strand, and 3.05±0.07h for the NTS. In the *⊿tup1* **a**-cells, the

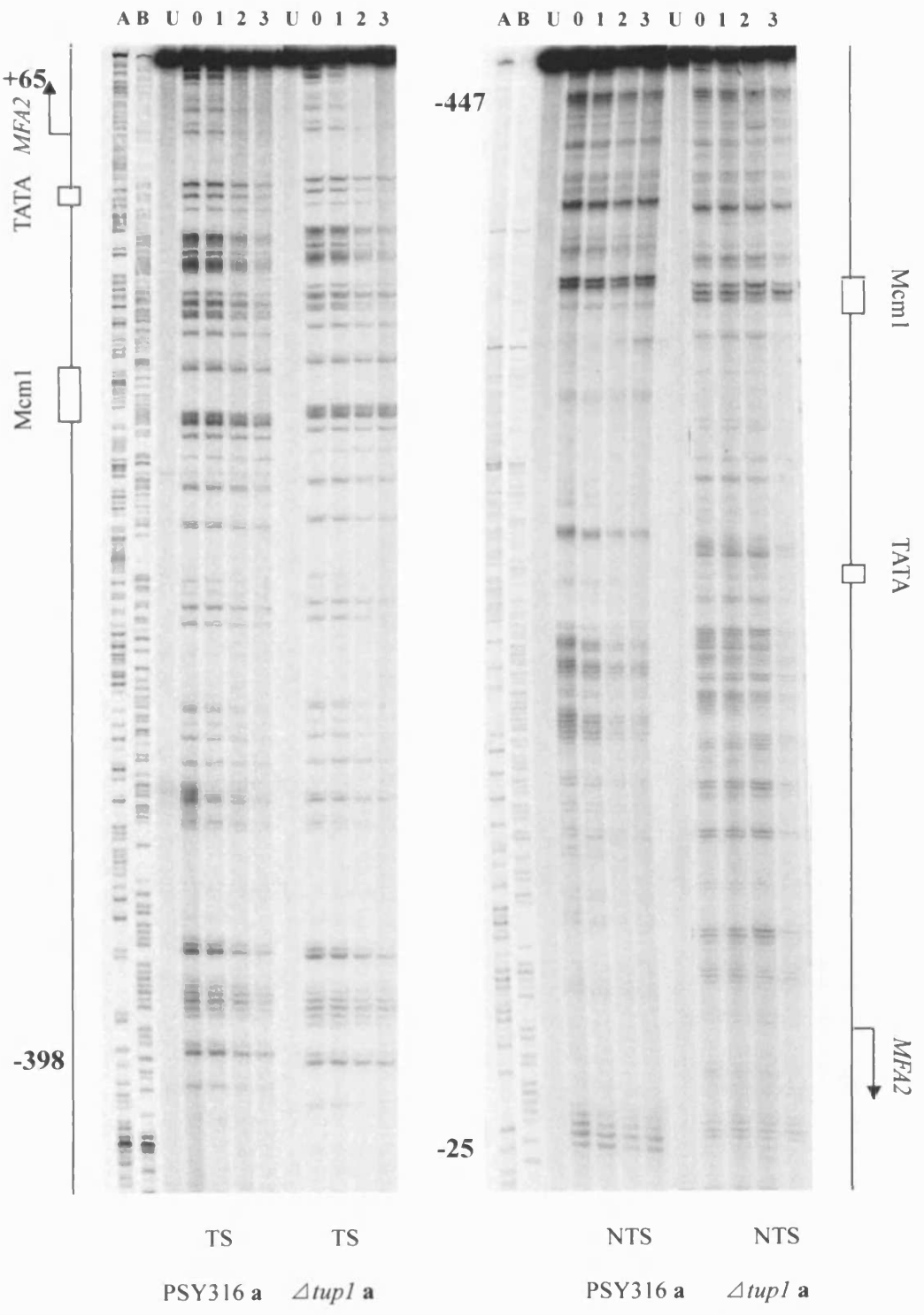

Figure 3.3 *Typical autoradiographs detecting CPDs repair at TS and NTS of MFA2 in PSY316* **a** *and ⊿tup1* **a** *strains at nucleotide level. (150J/m^2)*

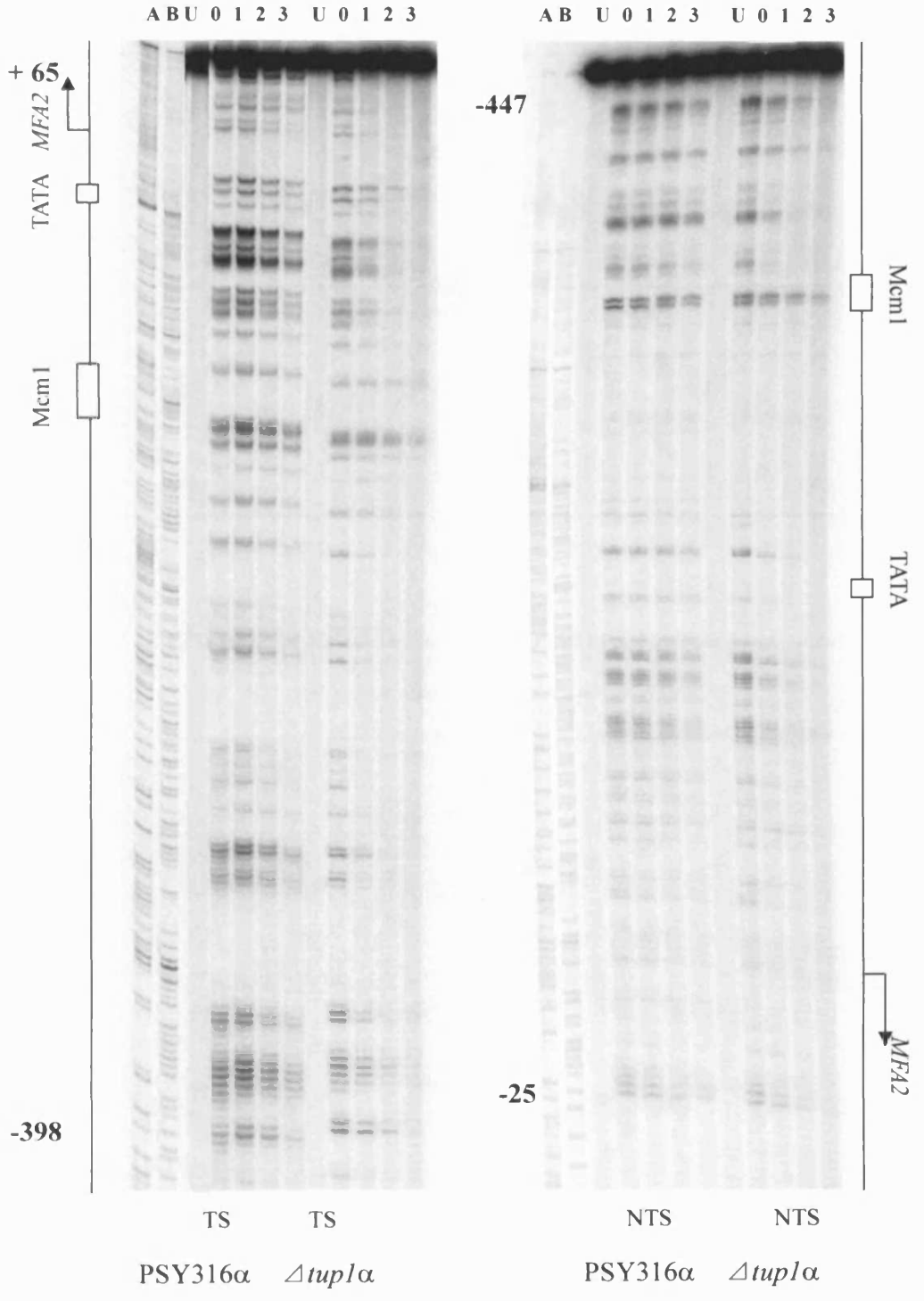

Figure 3.4 *Typical autoradiographs detecting CPDs repair at TS and NTS of MFA2 in PSY316 α and Δtup1 α strains at nucleotide level (150J/m^2).*

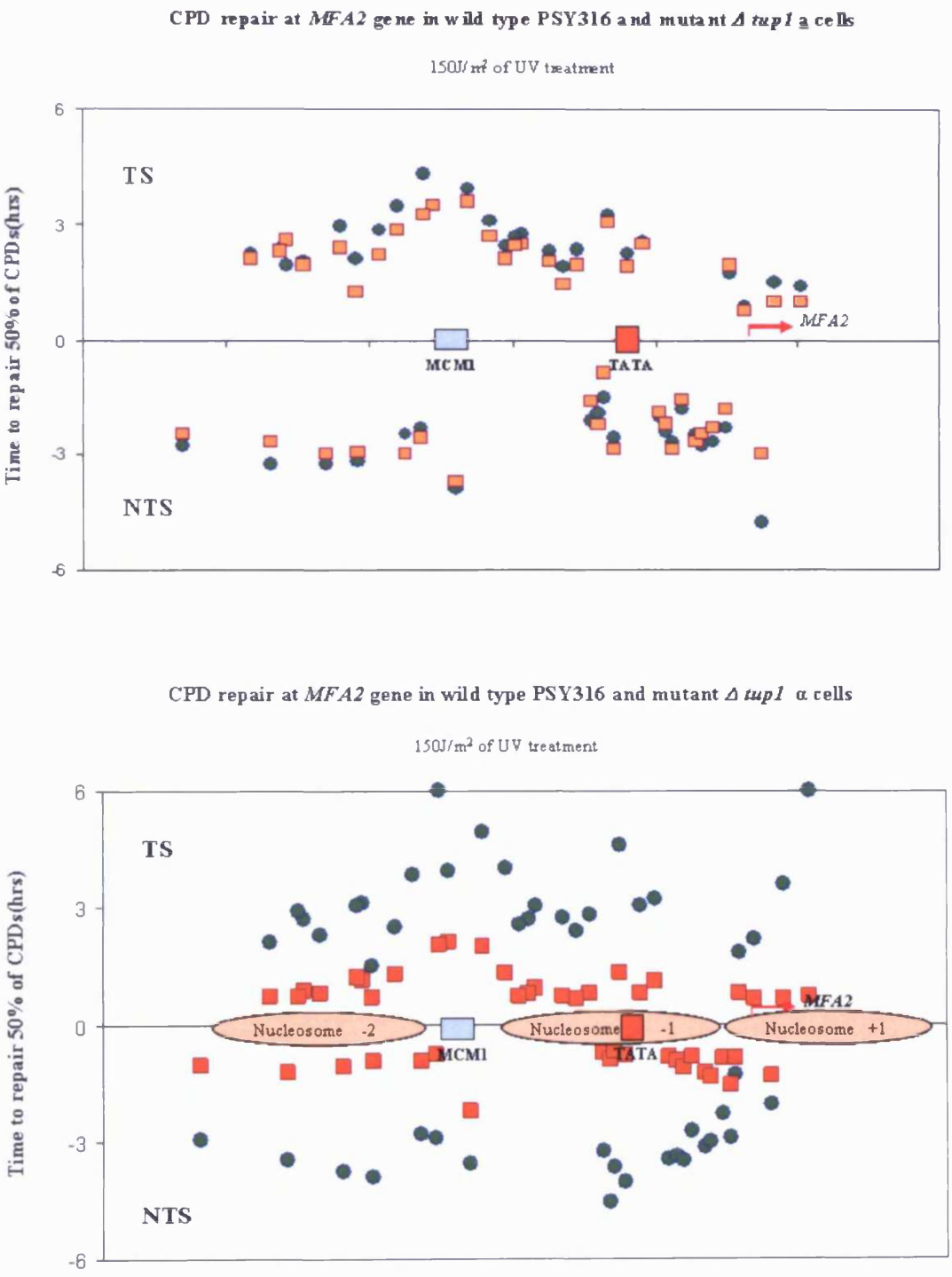

Figure.3.5 *Quantitative result of CPD repair at MFA2 in wild type PSY316 and mutant ⊿tup1 cells (150J/m²).* The time to repair 50% CPDs (t_{50}%) at a given site was calculated or extrapolated. The $t_{50}\% \geq 6$ hours was shown at the same repair level on the graph. The green circles (●) represent CPDs in wild type PSY316 cells, and the yellow squares (■) represent the CPDs in *⊿tup1* cells.

average time for 50% repair of CPDs in this region is 2.21±0.07h for the TS and 2.80±0.14h for the NTS. This shows deletion of *TUP1* in wild type **a**-cells does not obviously increase the repair rate in either the transcribed strand or non-transcribed strand of *MFA2*. However, in the absence of Tup1p, repair of CPDs of both the TS and NTS has been significantly enhanced in α-cells. In wild type α-cells, the average repair rate for 50% repair of CPDs is 2.60±0.14h for the TS and 3.18±0.05h for the NTS. In *⊿tup1*α-cells, 50% of CPDs are repaired in 1.00±0.05h for the TS and 1.10±0.16h for the NTS. The deletion of *TUP1* can derepress *MFA2* and change the chromatin structure around *MFA2* so as to result in no positioned nucleosomes in α-cells (Teng *et al.*, 2006). Conceivably, both the transcriptional status and the chromatin conformation could account for the accelerated repair in the control region of *MFA2* in *⊿tup1*α-cells. It must also be noted that repair in *⊿tup1*α-cells is even faster than in *⊿tup1***a** or wild type **a**-cells, although the extents of *MFA2* transcription are similar. Hence, *⊿tup1*α-cells are not similar to *⊿tup1***a** or wild type **a**-cells with respect to roles of NER.

In wild type α-cells (Fig.3.5) in the strand that becomes the TS in **a**-cells, the repair rate for CPDs increases from nucleotide -292 to -384, becomes slower around the Mcm1p binding site at -221 to -251, and then repair increases until at the TATA box where CPDs are repaired more slowly. In the lower strand CPDs around the Mcm1p binding site are repaired very slowly at an average rate of about 4h for 50% repair. In *⊿tup1*α-cells, repair of all CPDs is much enhanced, although the CPDs

around Mcm1p binding site in the upper strand are still repaired slower compared with CPDs at other sites.

Repair of CPDs at MFA2 in $\Delta tup1mfa2^{TATA}$ at the nucleotide level after 150J/m^2 UV treatment

The effects of deleting *TUP1* on *MFA2* are changing its transcription status and the chromatin structure around this gene, both of which could account for the accelerated repair in $\Delta tup1\alpha$-cells. To clarify how the *MFA2* transcription initiated by deletion of *TUP1* influences the enhanced repair in α-cells, I compared the CPD repair in the control region of *MFA2* in $\Delta tup1\alpha$-cells and $\Delta tup1mfa2^{TATA}\alpha$-cells after 150J/m^2 UV treatment. The TATA box in this latter strain had been changed by site specific mutation so as TBP binding is inefficient (see reference of Myslinski *et al.*, 1993). This sequence now has changed from TATATA to GCGCGC.

Typical sequencing gels for CPD repair in $\Delta tup1\alpha$-cells and $\Delta tup1mfa2^{TATA}$ α-cells are shown in Fig. 3.6. From the quantitative data in Fig.3.7, it is clear that the repair of CPDs in both strands of *MFA2* in $\Delta tup1mfa2^{TATA}$ α-cells is slower than in $\Delta tup1\alpha$-cells yet still faster than in wild type α-cells. The average repair time for 50% of the CPD is 1.55±0.06h for the upper strand and 1.70±0.08h for the lower strand. Similar to the trend for CPD repair in wild type and $\Delta tup1\alpha$-cells, the CPDs between nucleotides from -221 to -251 (the Mcm1p binding site) and from -119 to -125 (TATA box) in $\Delta tup1mfa2^{TATA}$ α-cells are repaired more slowly compared to

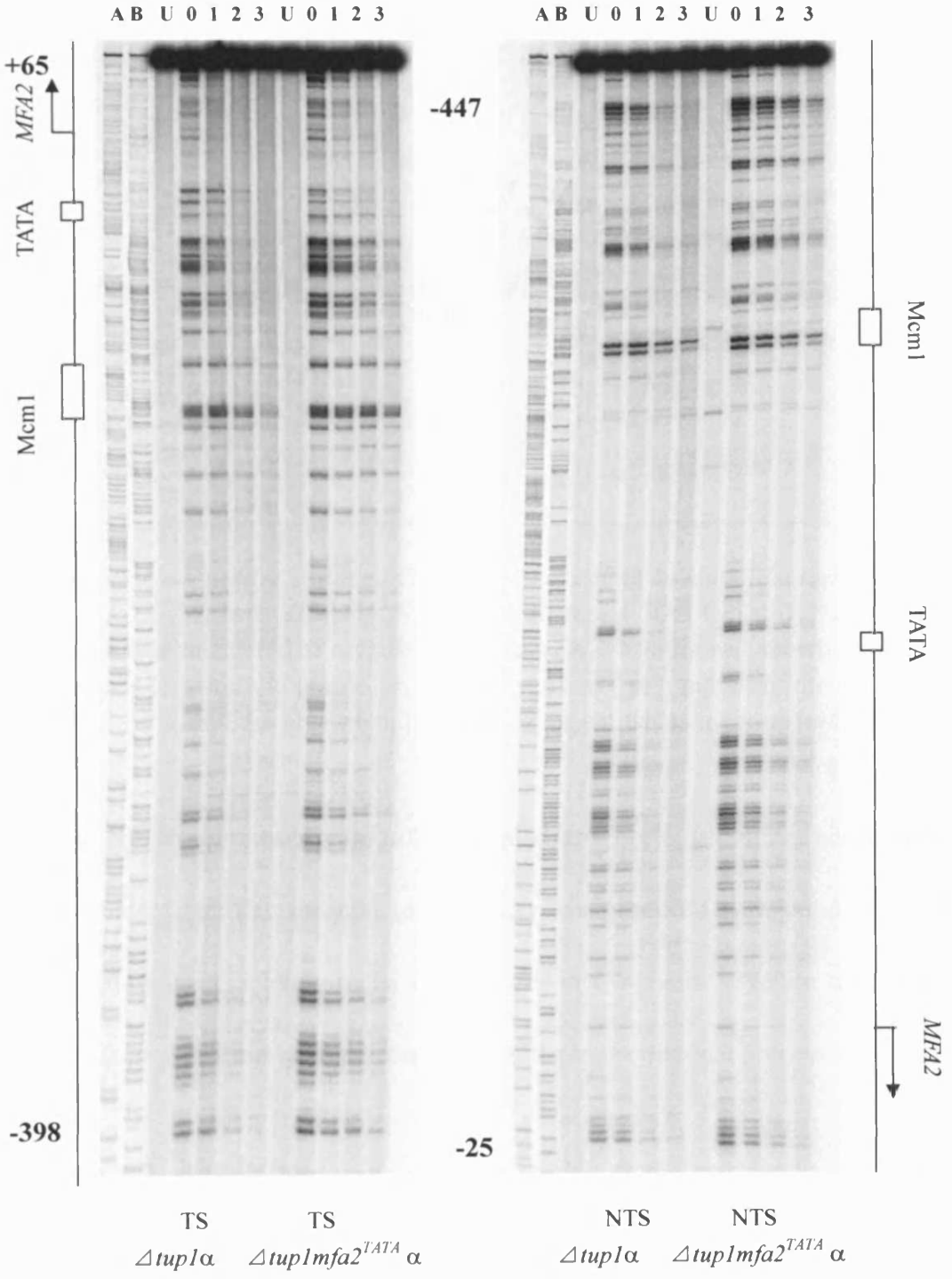

Figure 3.6 *Typical autoradiographs detecting CPDs repair at TS and NTS of MFA2 in Δtup1 α and Δtup1mfa2^{TATA} α strains at nucleotide level (150J/m^2).*

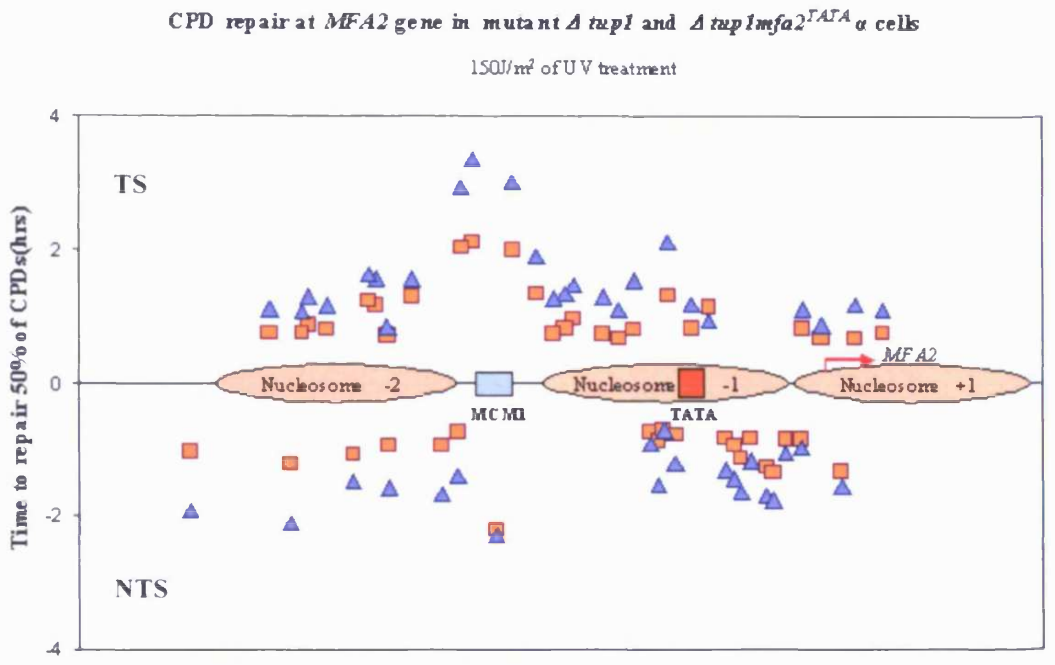

Figure 3.7 *Quantitative result of CPD repair at MFA2 in mutant ⊿tup1 and ⊿tup1mfa2^{TATA} α-cells (150J/m^2).* The time to repair 50% CPDs (t_{50}%) at a given site was calculated or extrapolated. The $t_{50}\% \geq 4$ hours was shown at the same repair level on the graph. The yellow squares (■) represent the CPDs in *⊿tup1* cells, and the blue triangles (▲) represent CPDs in *⊿tup1mfa2^{TATA}* cells.

other sites. Therefore, transcription of *MFA2* in *⊿tup1*α-cells is a minor contributor, but not the only, factor that accounts for the faster repair induced by deletion of *TUP1*. The other component is likely to be the changes in chromatin structure due to the absence of Tup1p, and this occurs irrespective of the transcriptional process.

Repair of CPDs in wild type and ⊿tup1 α strains at the nucleotide level after 70J/m^2 of UV treatment

To determine whether the enhanced NER occurs at *MFA2* in *⊿tup1* α-cells is UV dose dependent, I treated the cells with 70J/m^2 UV light. From Fig. 3.9, it is clear that

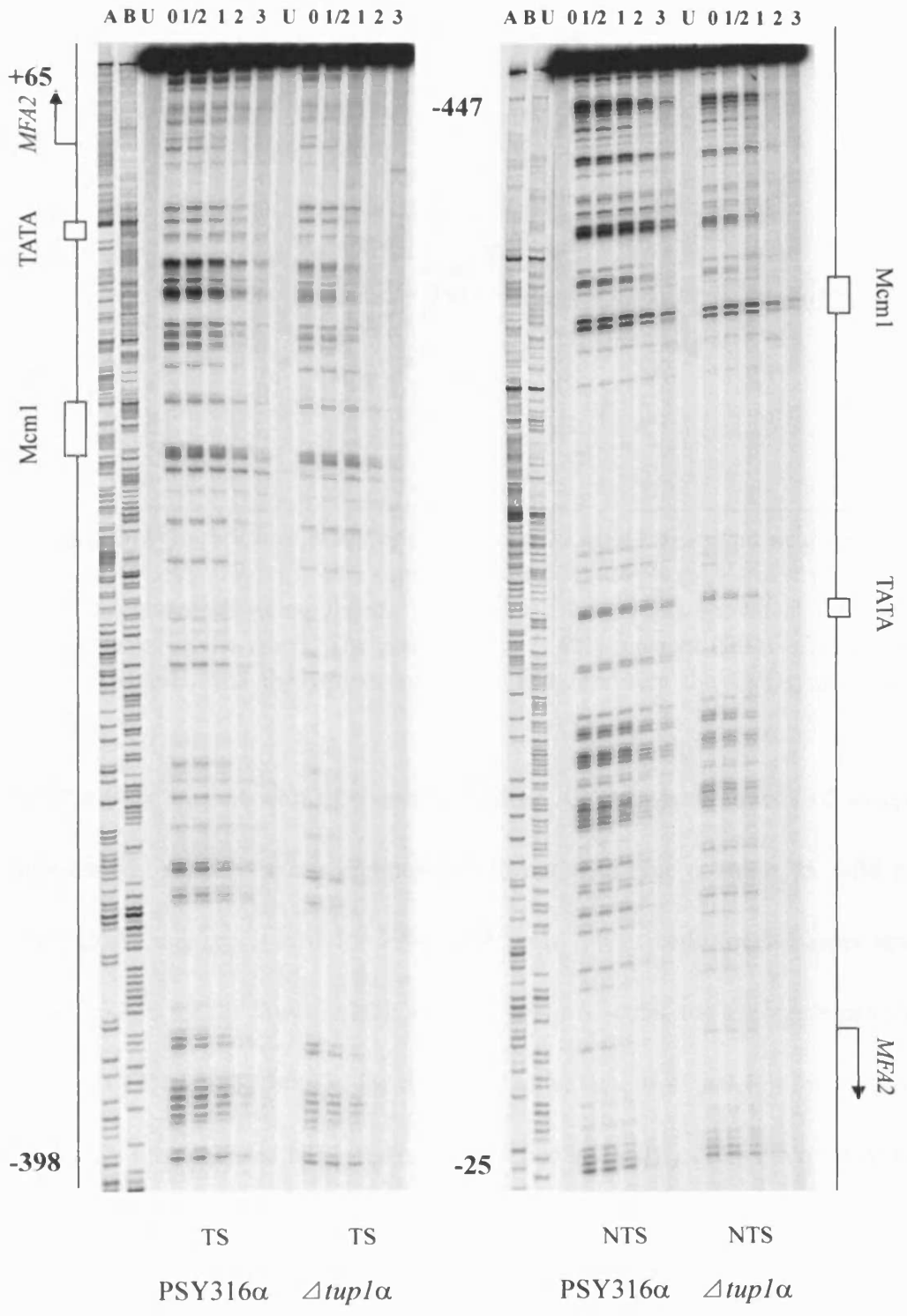

Fig. 3.8 *Typical autoradiographs detecting CPDs repair of MFA2 at TS and NTS of PSY316 α and ⊿tup1 α strains at nucleotide level (70J/m^2).*

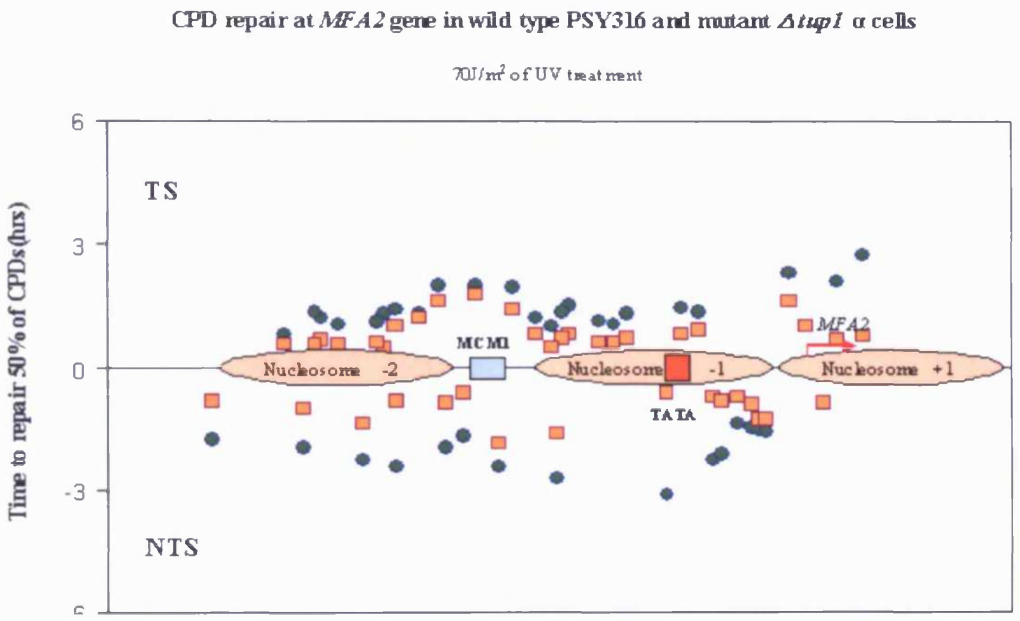

Figure 3.9 *Quantitative result of CPD repair at MFA2 in mutant wild type and Δtup1 α-cells (70J/m²).* The time to repair 50% CPDs (t_{50}%) at a given site was calculated or extrapolated. The $t_{50}\% \geq 6$ hours was shown at the same repair level on the graph. The green circles (●) represent CPDs in wild type PSY316 cells, and the yellow squares (■) represent the CPDs in *Δtup1* cells.

when cells were treated with this lower UV dose, CPD in both strands of *Δtup1*α strain were still repaired faster compared with the wild type α strain. In wild type α-cells, the average repair time for 50% of CPDs is 1.40±0.14h for the upper strand and 2.00±0.14h for the lower strand; while in *Δtup1*α-cells, the average repair time for 50% of CPDs is 0.85±0.07h for the upper strand and 0.95±0.21h for the lower strand. Hence the enhanced NER due to the absence of Tup1p occurs over a relatively broad UV dose range.

3.3.4 Repair of CPDs in the control region of the *RPB2* gene is not enhanced in *⊿tup1* α-cells at the nucleotide level

The deletion of *TUP1* in α-cells can result in enhanced repair for CPDs in both strands of **a**-mating type specific genes, including *MFA2*, *STE2*, *STE6*, and other Tup1p regulated genes, such as *RNR3*, *DRK2*, *etc.* (Teng *et al.*, 2006). To ensure this effect is not due to a general upregulation of NER and that it is specific to only Tup1p regulated genes, I studied CPDs repair of the *RPB2* gene after 70J/m^2 UV treatment in wild type and *⊿tup1* α-cells at the nucleotide level.

The *RPB2* gene encodes the second largest subunit of RNA polymerase II, it is active in both **a**- and α-cells and it is not regulated by Tup1p. Fig. 3.10 is the high resolution gels for CPD repair of *RPB2* in wild type and *⊿tup1* α-cells. The quantitative results in Fig. 3.11 shows that repair of CPDs in the TS of *RPB2* is virtually identical at most nucleotide sites while in the NTS repair shows some differences between in wild type and *⊿tup1* α-cells. The average repair time for 50% of CPDs is 0.65±0.07h for the TS and 2.35±0.07h for NTS of *RPB2* in wild type α-cells. In *⊿tup1* α-cells, the average repair time for 50% of CPDs is 0.55±0.07h for the TS and 1.75±0.07h for NTS of *RPB2*. The difference in repair rates for CPDs in the NTS of the *RPB2* gene between wild type and *⊿tup1* α strains is much small than that for *MFA2*, which increased from 2.00±0.14h in wild type to 0.95±0.21h in the *⊿tup1* α strain. Therefore, the deletion of *TUP1* only shows a limited effect on NER at *RPB2*. Further research on other genes where Tup1p does not regulate

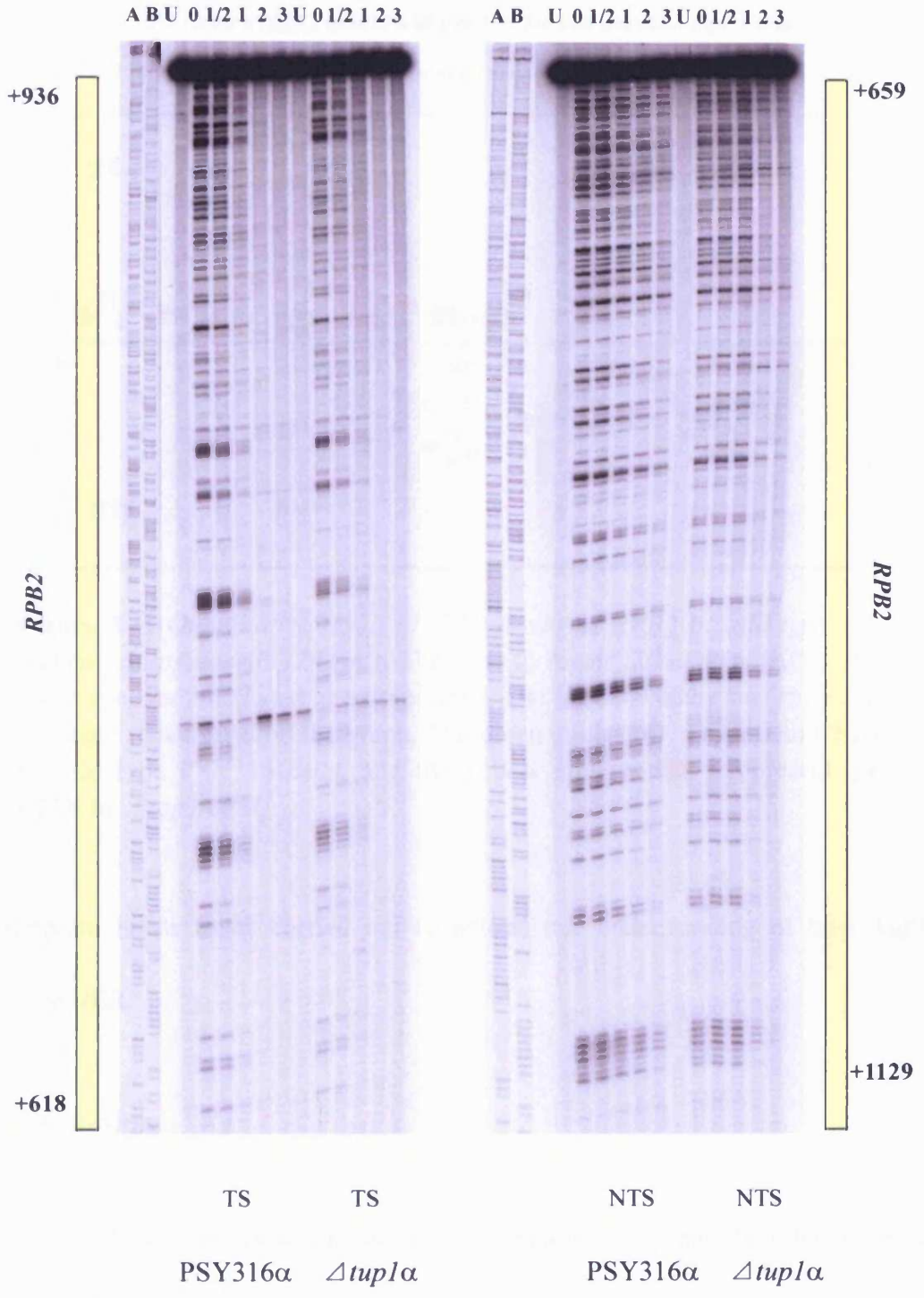

Figure 3.10 *Typical autoradiographs detecting CPDs repair of RPB2 at TS and NTS of PSY316 α and Δtup1α strains at nucleotide level (70J/m^2).*

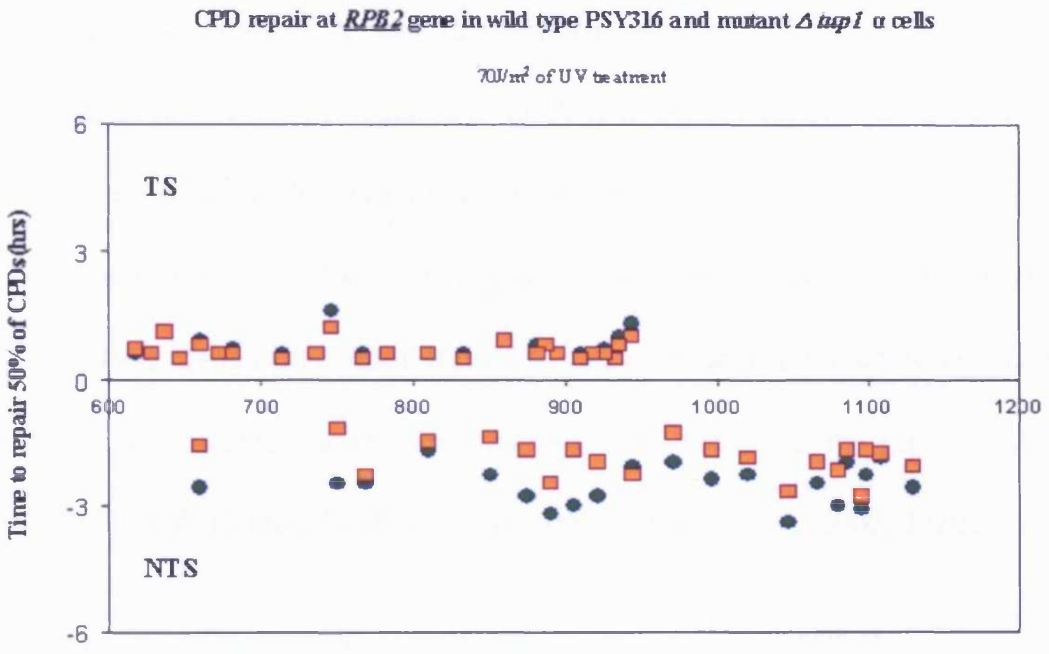

Figure 3.11 *Quantitative result of CPD repair at RPB2 in wild type and mutant Δtup1 α-cells (70J/m²).* The time to repair 50% CPDs (t_{50}%) at a given site was calculated or extrapolated. The $t_{50}\% \geq 6$ hours was shown at the same repair level on the graph. The green circles (●) represent CPDs in wild type PSY316 cells, and the yellow squares (■) represent the CPDs in *Δtup1* cells.

transcription needs to be carried out to extend our understanding of how Tup1p influence NER.

3.4 Discussion

In this chapter, the experiments were designed to investigate the effect of *TUP1* deletion on NER at the regulatory region of *MFA2*. NER is a multistep repair system which can repair various DNA lesions including CPDs. Since packaging DNA into a nucleosome (the basic structure) of chromatin has a influence on DNA transactions, including transcription, replication and repair. These processes require a flexible

chromatin structure is required for the accessibility of DNA for the proteins to complete their function. It was reported that *in vitro* a DNA lesion within the mononucleosome core was repaired 5- to 10-fold less efficiently than those in naked DNA (Hara *et al.*, 2000). The results of nucleosome mapping *in vivo* also provide clear evidence on how NER is modulated by nucleosomes (Livingstone-Zatchej and Thoma, 1999; Teng *et al.*, 2006). However, such modulation does not occur equally at all genes and exhibits variety with transcriptional status and the gene in question (Wellinger and Thoma, 1997; Li *et al.*, 1999; Morse *et al.*, 2002; Ferreiro *et al.*, 2004).

The remodeling events operating on chromatin structure normally are classified into two groups: those that are ATP-dependent and those that are ATP-independent. Histone acetylation is a part of the latter group, which also includes the methylation and phosphorylation of histones. As the data showed in Chapter 5 and in Teng *et al.* (2002), Gcn5p, a histone acetylase, can relax the chromatin structure by modifying the histone tails to facilitate efficient NER in the control region of the *MFA2* mating type specific gene.

In **a**-cells, activator Mcm1p binds to the control region of *MFA2* to activate transcription. In α-cells, Mcm1p and α2 factors cooperatively bind to the α2 operator in the control region of *MFA2* and the general repressor complex Tup1p-Ssn6p is also recruited to this site for the repression of *MFA2*. When comparing NER at *MFA2* in different mating types, I found that TCR occurred in the TS of active *MFA2* in **a**-cells. The slower GGR governs repair of the NTS of the active *MFA2* and both strands of

the repressed *MFA2* gene; this pathway is dependent on Rad16p (also see Chapter 4). Around the Mcm1p binding sites, slower repair has been observed both in **a**- and α-cells. Previously, deletion of *TUP1* was reported to derepress the **a**-specific genes *STE2* and *STE6* in α-cells and this disrupted the nucleosomes at these regions (Ducker and Simpson, 2000). In this chapter, my data shows that *MFA2* also becomes active in α-cells in the absence of Tup1p. There is substantially enhanced repair of CPDs in the *MFA2* control region of both the TS and NTS in the *⊿tup1*α strain. Teng *et al.* (2006) also has observed a similar enhanced NER at other mating type specific genes, including *RNR3*, *DRK2*, *TIR2*, *etc.* and where Tup1p governs transcription.

Teng *et al.* (2006) mapped the nucleosome positions at the *MFA2* gene in wild type and *⊿tup1*α-cells at low resolution (Fig.3.12). In wild type α-cells, four nucleosomes were mapped according to MNase sensitivity at *MFA2*; in *⊿tup1*α-cells, all four positioned nucleosomes are disrupted. By comparing the MNase digestion pattern between wild type α-cells, *⊿tup1*α-cells and naked DNA, it can be seen that the MNase digestion pattern at *MFA2* in *⊿tup1*α-cells is identical to that in naked DNA. Thus in this strain there is an altered chromatin structure that is more accessible for enzymes. The pattern in wild type α-cells is completely different due to the protection afforded by the positioned nucleosomes. The results from other assays detecting restriction site accessibility also confirmed that chromatin in the control region of *MFA2* is more accessible in *⊿tup1*α-cells than in wild type α-cells (Teng *et al.*, 2006).

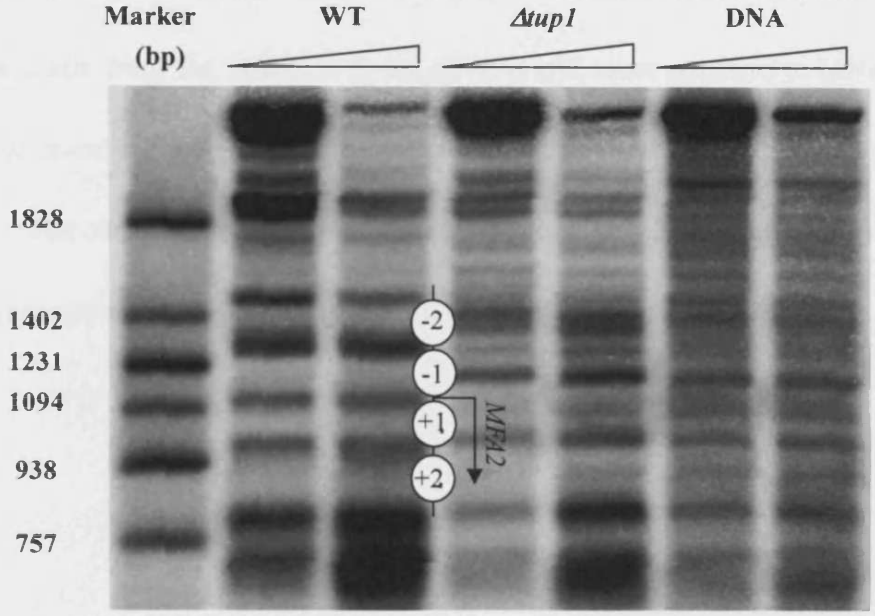

Figure 3.12 *Low resolution nucleosome positioning.* The amounts of MNase used are indicated at the top of each lane. The numbers to the left of the markers show the size of the bands. The positioned nucleosomes at *MFA2* in wild type α-cells are shown as circles numbered with -2, -1, +1, +2. (Adapted from Teng *et al.*, 2006)

These data show that the deletion of *TUP1* in α-cells activates *MFA2* transcription and results in changing the chromatin structure at *MFA2*, and a faster CPD repair in both the TS and NTS strands. The *Δtup1mfa2*^{TATA} α mutant with site specific mutations at the TATA box abolished transcription that was induced by *TUP1* deletion. CPDs in these cells were repaired more slowly than *Δtup1* without TATA box for both strands, but still faster than in wild type α-cells. Since TCR could not operate in both *Δtup1mfa2*^{TATA} and wild type α-cells, this indicates that Tup1p modulated local chromatin structure so as to affect NER in the absence of transcription. We needed to know whether this TATA box mutant has changed the chromatin structure around the promoter at *MFA2*. Extensive digestion with MNase does reveal a difference at *MFA2* between *Δtup1* single α-cells and *Δtup1mfa2*^{TATA}

α-cells. The chromatin from the *Δtup1mfa2*^{TATA} strain is more resistant to MNase than chromatin from the *Δtup1* α-strain, yet it is still more sensitive to MNase than in wild type α-cells (Teng, personal communication). Therefore, this provides further evidence that chromatin structure modulates NER at *MFA2* and Tup1p plays a role in NER irrespective of whether transcription operates.

Chapter 4

The absence of Tup1p partially suppresses the requirement for Rad16p in GGR at the control region of the *MFA2*

4.1 Introduction

In *S. cerevisiae* α-cells, transcription of the *MFA2* gene is repressed by a complex of Tup1p-Ssn6p with cooperative binding of Mcm1p and α2 factors. There are two α2 operator sequences in the control region of *MFA2*- see Chapter1 Figure 1.7 (Nehlin *et al.*, 1991; Smith and Johnson, 2000). The DNA-binding protein α2/Mcm1p need not overlap with the upstream activating sequence (UAS), where the activators binds, or with the TATA box, or the starting points of transcription (Edmondson *et al.*, 1996). As a result, Tup1p-Ssn6p mediated repression is not dependent on the number and identity of the activator proteins responsible for the transcription of the target gene. Nucleosomes are found to be precisely positioned over the promoter of *MFA2* in α-cells. This occurs with many repressed genes and is in accord with the hypothesis that a compacted chromatin structure is required for gene repression (Teng *et al.*, 2001). Furthermore, Tup1p binds preferentially to hypoacetylated histone tails H3 and H4 *in vitro* (Edmondson *et al.*, 1996), and interacts with three histone deacetylases at *MFA2* (Watson *et al.*, 2000; Wu *et al.*,

2001). In strains with mutated histone tails or deacetylases Tup1p regulated genes can be derepressed including *MFA2* (Edmondson *et al.*, 1996; Watson *et al.*, 2000). Histone acetylation is one of the important chromatin remodeling events for gene activation (Berger, 2002). In Chapter 5, I will discuss how the absence of the acetylase Gcn5p effects transcription and NER at *MFA2*. Here, I examined the effect of a *TUP1* deletion on the requisite for Rad16p in GGR at regulatory region of *MFA2*.

Rad16p and Rad7p form a stable complex which is only essential for GGR in *S. cerevisiae* (Terleth *et al.*, 1990; Bang *et al.*, 1992, Verhage *et al.*, 1994). Rad16p is required for the removal of CPDs from repressed genes, e.g. *HMLα*, and from the non-transcribed strand of transcribed genes, e.g. the NTS of *MFA2* and *RPB2*, and other transcriptionally silenced regions (Bang *et al.*, 1992; Mueller and Smerdon, 1995; Teng *et al.*, 1997). Later, Reed *et al.* (1999) found that autonomously replicating sequence binding factor 1 (Abf1p) is a component of the Rad7p/Rad16p NER subcomplex. Specific *abf1* mutants are UV sensitive and defective in the removal of photoproducts. It appears the Rad7p/Rad16p/Abf1p may play a central and specialized role in uniquely in GGR. Yu *et al.* (2004) reported Rad7p/Rad16p/Abf1p complex generates DNA superhelical torsion in postincision step of GGR. Recently, Ramsey *et al.* (2004) also discovered that Elc1, the yeast homologue of a mammalian E3 subunit, is a novel component of Rad7p/Rad16p complex (see later).

In α-cells, the mating type locus *MATα* is actively transcribed and the *HMLα* locus is repressed in a closed heterochromatin-like structure (Nasmyth and Shore, 1987). In the *Δrad16* mutant, *HMLα* is not repaired while *MATα* is repaired but at a

slower rate compared with its repair in wild type cells. It was proposed that Rad16p is involved in the function of unraveling the DNA structure to facilitate the binding of other NER proteins. Verhage *et al.* (1994) showed the Rad7p and Rad16p are required for the repair of the NTS at the transcriptionally active gene *RPB2*, where the chromatin structure is thought to be unfolded. Teng *et al.* (1997) also reported Rad16p is needed to repair all of the NTS of *MFA2* in **a**- and α- cells, while surprisingly there was only a partial requisite for Rad16p in repairing the *MFA2* control region.

Rad16p is a member of the Snf2p/Swi2p ATPase family (Prakash *et al.*, 1993; Eisen *et al.*, 1995), which functions as a DNA-stimulated ATPase (Guzder *et al.*, 1997). The *RAD16* gene has been cloned and its open reading frame (ORF) contains putative helicases motifs that are present in a wide variety of eukaryotic proteins including Snf2p (Peterson and Herskowitz, 1992; Winston and Carlson, 1992). Except for Snf2p, a number of other proteins in this Snf2p/Swi2p ATPase family also have been found to remodel chromatin structure (Vignali *et al.*, 2000), this suggests that the Rad16p/Rad7p/Abf1p complex might also function to open the chromatin structure around the damaged DNA to allow access of the NER machinery (Thoma, 1999; Prakash and Prakash, 2000).

However, Reed *et al.* (1998) reported that in contrast to the defective *incision* of damaged DNA observed in extracts of most yeast NER mutant strains, *rad7* and *rad16* mutants are proficient in the incision of damaged DNA both *in vitro* and *in vivo*, but are defective at the oligonucleotide excision stage and repair synthesis stages of the NER pathway. They concluded that the Rad7p/Rad16p/Abf1p complex facilitates the

excision of oligonucleotides containing damage and the subsequent repair synthesis during the NER of transcriptionally silent DNA in yeast.

Recently, Yu *et al.* (2004) reported that this protein complex generates superhelicity in DNA through the catalytic activity of the Rad16p component in postincision events in NER. The torsion generated in the DNA by this Rad7p/Rad16p/Abf1p complex is necessary to remove the damage-containing oligonucleotide during NER. They concluded that in yeast the molecular mechanism of NER includes the generation of superhelical torsion in DNA. This observation extends the list of SF2 family (see later) members that share the ability to generate superhelicity in DNA (Havas *et al.*, 2000). Furthermore, these experiments revealed that the mechanical energy generated by the SWI/SNF-like ATPase motor of Rad16p during DNA supercoil formation, can be utilized to facilitate structural changes in the DNA during NER.

Proteins in the large family of Swi2p/Snf2p ATPases can be organized into two large subfamilies. Snf2p falls into the SF2 subgroup (Gorbalenya *et al.*, 1989), which includes a number of demonstrated and putative complexes with functions as disparate as RNA splicing, recombination and DNA repair. Rad16p protein is a member of this group and is most closely related to a smaller subset of SF2 proteins characterized by the presence of a RING finger motif. Rad16p also contains this zinc finger-binding domain, embedded within its ATPase domains (Prakash *et al.*, 1993; Eisen *et al.*, 1995; Saurin *et al.*, 1996). RING proteins can interact with ubiquitin-conjugating enzymes (Ubcs or E2s), and many of these can function as

ubiquitin-protein ligases (E3s) (Lorick *et al.*, 1999; Joazeiro and Weissman, 2000; Aravind *et al.*, 2003). The presence of these motifs suggested that Rad16p functions as both an ATPase and an E3 ubiquitin ligase. The Rad16p ATPase is important for the functioning of the complex *in vivo*, and genetic analysis uncovered new interactions between this complex and Rad23p, a repair factor that links repair to proteasome function. Elc1p is the yeast homologue of a mammalian E3 subunit, and recently it was found to be a novel component of Rad7p/Rad16p complex (Ramsey *et al.*, 2004), and a physical interaction between Rad7p and Elc1p was reported by Ho *et al.* (2002). The Rad4p-Rad23p complex recognizes UV-damaged DNA and Rad4p protein has been reported to interact with Rad7p (Wang *et al.*, 1997). These suggested that Rad4p could be a substrate for the inferred E3 activity of the Rad7p/Rad16p/Abf1p complex.

As mentioned in Chapter 3, one model for how Tup1p-Ssn6p represses genes is by altering the local chromatin structure and positioning nucleosomes around target genes. Deletion of *TUP1* results in the derepression of the **a**-specific genes and disruption of the positioned nucleosomes adjacent to the α2 operator (Cooper *et al.*, 1994; Gavin *et al.*, 2000). A similar phenomenon has been found at the *MFA2* gene (see the data in Chapter 3).

One proposed function of the Rad16p/Rad7p/Abf1p complex is that it influences the chromatin structure around the damaged DNA to allow NER. As a structural variation in chromatin structure is induced by *TUP1* deletion, I wished to analyze the effect of *TUP1* deletion on the Rad16p requisite for NER at *MFA2*. I employed the

high resolution approach (Teng *et al.*, 1997) to investigate CPD repair at the nucleotide level in a number of mutants, including *⊿rad16* and *⊿tup1rad16* α-cells.

4.2 Material and methods

4.2.1 Yeast strains

⊿rad16 (*MATα ade2-101 URA::RAD16 leu 2-3,112 Δhis3-200 lys2 trp1*)

⊿tup1rad16 (*MATα ade2-101 URA::RAD16 leu 2-3,112 HIS::TUP1 lys2 trp1*)

4.2.2 DNA extraction

This was undertaken as described in Chapter 2.

4.2.3 Detection of CPDs repair at *MFA2*

This was undertaken also as described in Chapter 2.

4.3 Results

4.3.1 The comparison of UV sensitivity

UV sensitivity of a strain harbouring a mutation in a specific gene indicates a role of that gene in DNA repair. Hence, I examined the UV sensitivities in α-cells of the *⊿rad16* and *⊿tup1rad16* mutant (Figure 4.1). As shown in this figure, the *⊿rad16* and *⊿tup1rad16* α are more UV sensitive compared with the wild type PSY316 α strain. The fact that the additional presence of the *⊿tup1* in the *⊿rad16* strain does not increase UV sensitivity indicates that Tup1p has no appreciable role in

influencing overall cell survival after UV irradiation.

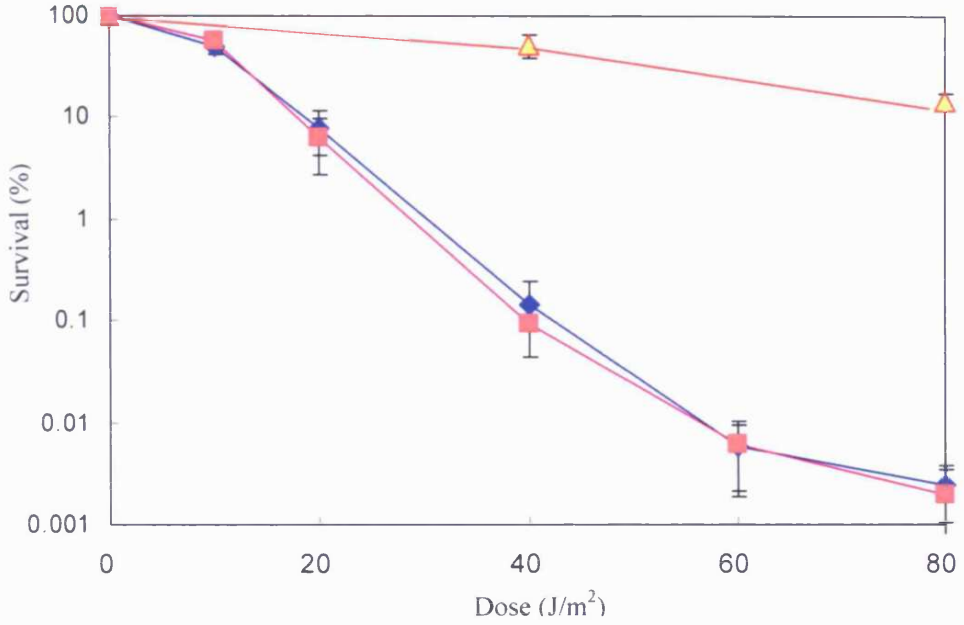

Figure 4.1 *The UV sensitivity of the strains studied.* (△) wild type PSY316α, (◆) *⊿rad16α*, (■) *⊿tup1rad16α*.

4.3.2 Nucleotide excision repair at *MFA2* in *⊿rad16* and *⊿tup1rad16* strains

To investigate whether CPD repair at the nucleotide level in *MFA2* is affected by deletion of *TUP1* in the background of a *RAD16* mutant, experiments were undertaken as described in Chapter 2. Figure 4.2 provides typical gel images for detecting CPDs in the TS and the NTS of the *HaeIII* restriction fragment containing the upstream control region of *MFA2*; *⊿rad16α* and *⊿tup1rad16α* cells were irradiated with 150 J/m^2 of UV light. Figure 4.4 depicts gel images for CPD repair analysis at *RPB2* in *⊿rad16α* and *⊿tup1rad16α* cells irradiated with 70 J/m^2 UV light. In all the sequencing gels in Figure 4.2, the numbers on the left denote the nucleotide positions in the control region of *MFA2*. The time allowed for CPD repair

was up to 3 hours and the data are expressed as the time for removing 50% of CPDs ($t_{50\%}$) at the damage sites (Fig.4.3, 4.5). The intensity of the detectable bands was quantified after phosphorimaging with ImageQuant software (Molecular Dynamics, CA, USA). Then Microsoft Excel software was applied to create graphs (repair % vs repair time) to estimate the $t_{50\%}$. If less than 3 hours, the $t_{50\%}$ was directly read from the graphs; while if more than 3 hours, the $t_{50\%}$ was obtained by extrapolation. As for sites with very slow repair, the estimation of $t_{50\%}$ by extrapolation may not be accurate, therefore, any $t_{50\%}$ of more than 6 hours were set as 6 hours. It should be noted that if $t_{50\%}$ are at the 6hr point I can not distinguish between slow repair and no repair. The repairing of groups of closely linked CPDs, all of which show a similar repair rate, is represented as a single point.

The results presented in Figure 4.3 show that in *⊿rad16α*-cells, no CPD repair can be detected for the strand which would be the TS and NTS in active *MFA2*; this result is accord with the crucial role of Rad16p in GGR at non-transcribed region. However deletion of *TUP1* enhances CPD repair both in the TS and NTS of the control region at *MFA2* in *⊿tup1rad16α*-cells. In *⊿tup1rad16α*-cells, 50% of CPDs are repaired in 2.30±0.07h for the TS and 3.30±0.28h for the NTS. Here, the repair of many CPDs in the control region NTS at *MFA2* was a surprise as it has

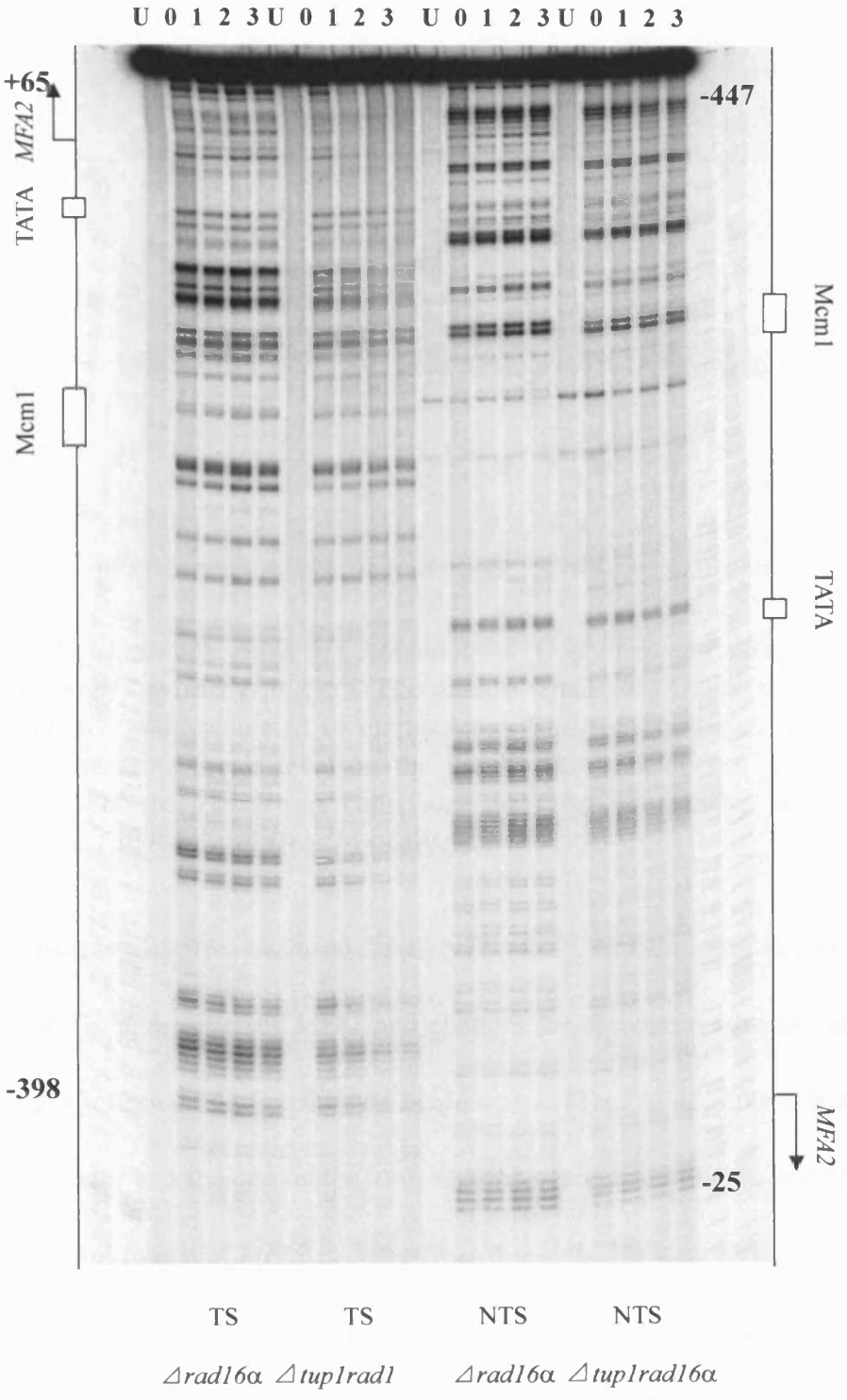

Figure 4.2 *Typical autoradiographs detecting CPDs repair at TS and NTS of MFA2 in Δrad16α and Δtup1rad16α strains at nucleotide level (150J/m^2).*

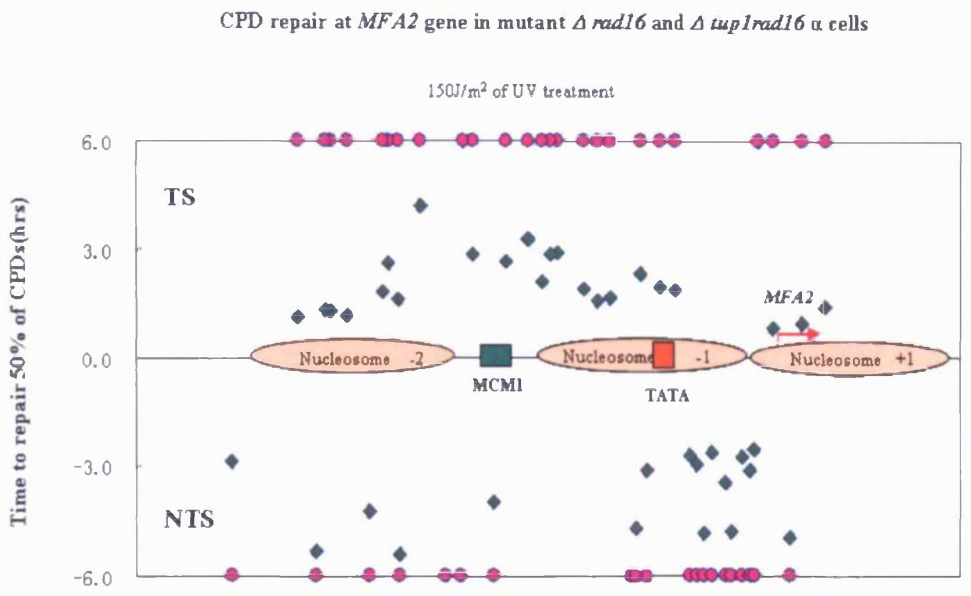

Figure 4.3 *Quantitative result of CPD repair at MFA2 in mutant ⊿rad16 and ⊿tup1rad16 α-cells (150J/m²).* The time to repair 50% CPDs (t_{50}%) at a given site was calculated or extrapolated. The $t_{50}\% \geq 6$ hours was shown at the same repair level on the graph. The pink circles (●) represent CPDs in *⊿rad16* α cells, and the green diamonds (◆) represent the CPDs in *⊿tup1rad16* αcells.

always been assumed Rad16p was need for all NTS repair. As mentioned in Chapter3, the deletion of *TUP1* derepresses *MFA2* and changes the chromatin structure around *MFA2* in α-cells resulting in no positioned nucleosomes (Teng *et al.*, 2006). Both the transcriptional status and the chromatin conformation can account for the accelerated repair in the control region of *MFA2* in *⊿tup1rad16* α-cells. Hence, deletion of *TUP1* can partly suppress the absolute requisite of Rad16p in GGR at the *MFA2* gene.

In *⊿tup1rad16* α-cells (Fig.4.3), repair of CPDs in the TS increases from nucleotide -384 to -309, becomes slower around the Mcm1p binding site at -221 to -251, and then repair increases again until at the TATA box where CPDs are repaired more slowly. Moreover, from the transcription start site, CPDs in TS are repaired

faster again (the time for repairing 50% CPDs is about 1.2h). In the lower strand, CPDs are repaired very slowly in *⊿tup1rad16* α-cells and no repair in *⊿rad16*α-cells. At nucleotide sites -447~-415, and a longer sequence from -138 to -25, the repair rate for CPDs in NTS of the *⊿tup1rad16*α-cells increases to about 3h while in *⊿rad16*α-cells these CPDs still could not be repaired. Hence, in *⊿tup1rad16*α-cells, repair of most CPDs is much enhanced compared to those in *⊿rad16*α-cells, although the CPDs around Mcm1p binding site in the upper and down strands are still repair slower compared with CPDs at other sites.

4.3.3 Nucleotide excision repair at *RPB2* gene in *⊿rad16* and *⊿tup1rad16* strains

The deletion of *TUP1* in *⊿rad16*α-cells results in enhanced repair for CPDs at *MFA2* and partly complements the absolute requirement of Rad16p in GGR at *MFA2*. To ensure this effect is not due to a general upregulation of NER and that it is specific to only Tup1p regulated genes, I studied CPDs repair at the *RPB2* gene after 70J/m^2 of UV in *⊿rad16* and *⊿tup1rad16* α-cells at the nucleotide level (there is no known involvement of Tup1p in the transcriptional regulation of *RPB2*, nor is it a mating type specific gene).

Fig. 4.4 presents the high resolution gels for CPD repair of *RPB2* in *⊿rad16* and *⊿tup1rad16* α-cells. The quantitative results in Fig. 4.5 shows that repair of CPDs in both the TS and NTS of *RPB2* are identical at all nucleotide sites in *⊿rad16* and *⊿tup1rad16* α-cells. The average repair time for 50% of CPDs is 0.65±0.07h for the

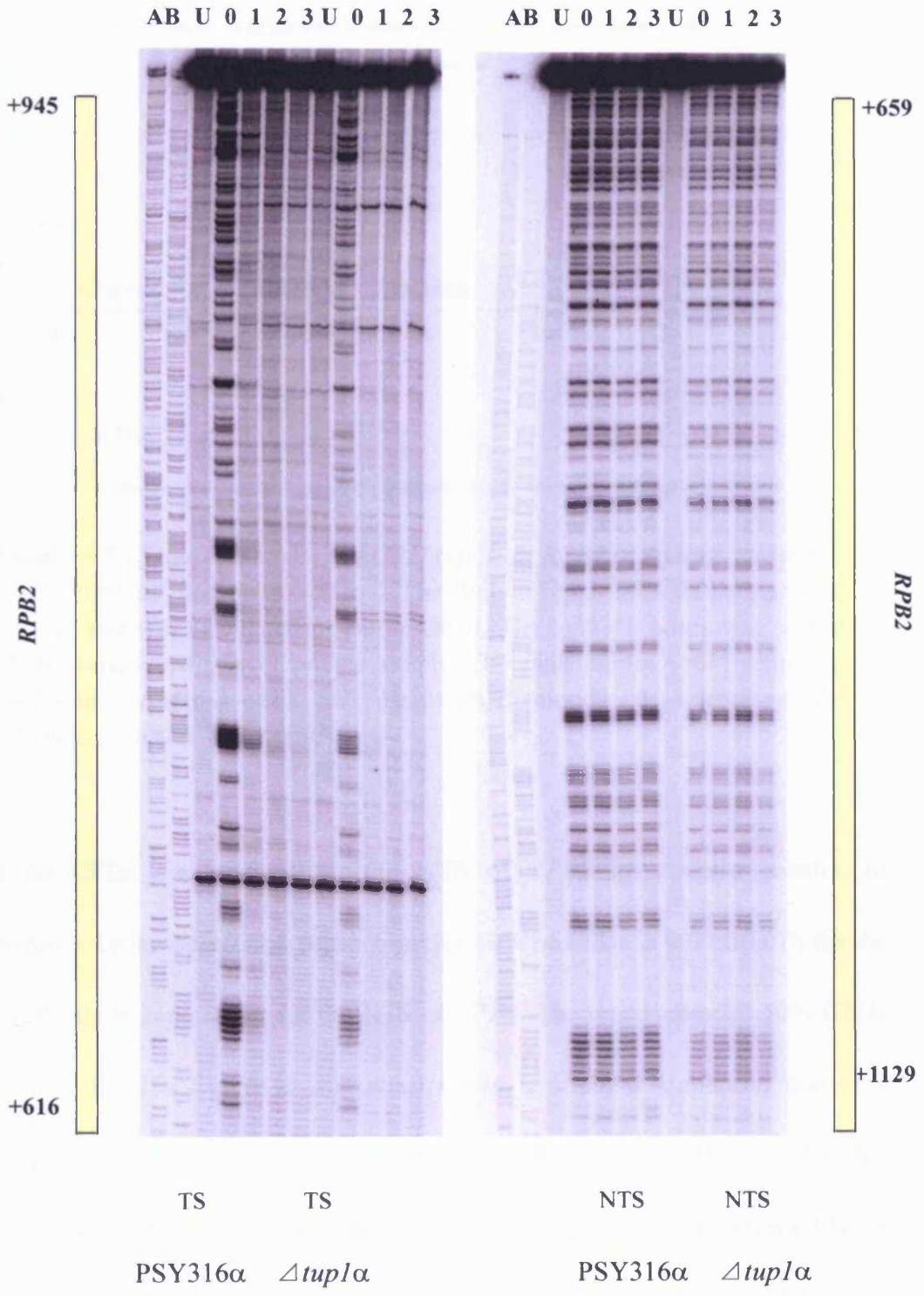

Figure 4.4 *Typical autoradiographs detecting CPDs repair of RPB2 at TS and NTS of Δrad16α and Δtup1rad16α strains at nucleotide level (70J/m^2).*

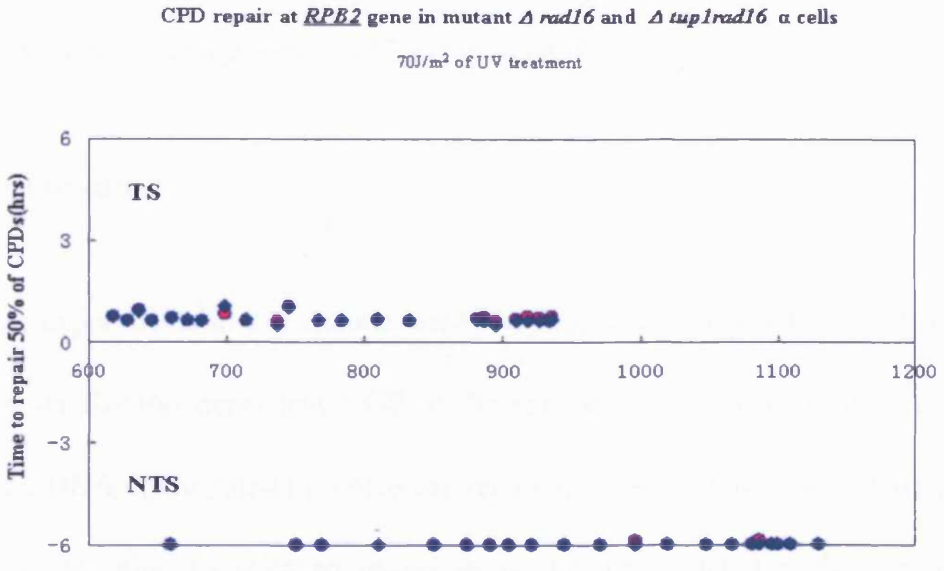

Figure 4.5 *Quantitative result of CPD repair at RPB2 in mutant ⊿rad16 α and ⊿tup1rad16 α-cells (70J/m²).* The time to repair 50% CPDs (t_{50}%) at a given site was calculated or extrapolated. The $t_{50}\% \geq 6$ hours was shown at the same repair level on the graph. The pink circles (●) represent CPDs in *⊿rad16* α-cells, and the green diamonds (◆) represent the CPDs in *⊿tup1rad16* α-cells.

TS and no CPDs are repaired for the NTS of *RPB2* in *⊿rad16* α-cells. In *⊿tup1rad16* α-cells, the average repair time for 50% of CPDs is 0.60±0.07h for the TS and again there is no repair for the NTS of *RPB2*. The repair rates for 50% CPDs in the TS of the *RPB2* gene in the *⊿tup1rad16* α strain is similar to that in a *⊿rad16α*, which indicates as expected that the Rad16p does not affect TCR at the active *RPB2* gene. Moreover, in both the *⊿rad16* and *⊿tup1rad16* α strains CPDs in the NTS of *RPB2* could not be repaired in 6h. Therefore, the deletion of *TUP1* does not show any enhancement of GGR at *RPB2* in the absence of Rad16p. This indicates that the observation at *MFA2* in the *⊿tup1rad16* α strain may be specific only to Tup1p regulated genes. Research on other genes where Tup1p does or does not

regulate transcription needs to be carried out to extend our understanding of how Tup1p influence the requirement of Rad16p in GGR.

4.4 Discussion

The experiments in this chapter were designed to investigate the effect of *TUP1* deletion on Rad16p dependent GGR at the regulatory region of *MFA2* and *RPB2*. GGR is a DNA repair pathway which can repair various DNA lesions including CPDs in the transcriptionally silenced sequences of the whole genome. Since positioned nucleosomes over a non-transcribed region of the genome are thought to be a strong negative influence on GGR, a more flexible chromatin structure is needed for the accessibility of GGR proteins to the damage sites. Rad16p has been considered to be a member of the SWI/SNF ATPase family which changes the chromatin structure in ATP-dependent way (Bang *et al.*, 1992). Reed *et al.* (1998) also considered that the Rad7p/Rad16p/Abf1p complex of proteins facilitate the excision of oligonucleotides containing sites of base damage and the repair synthesis during GGR in yeast. Yu *et al.* (2004) reported that this protein complex generates superhelicity in DNA through the catalytic activity of the Rad16p component in postincision events in GGR. This observation extends the list of SF2 family members that share the ability to generate superhelicity in DNA and these data also revealed that the mechanical energy generated by the SWI/SNF-like ATPase motor of Rad16p during DNA supercoil formation, can be utilized to facilitate structural changes in the DNA during GGR.

In this chapter, I find that the deletion of *TUP1* in α-cells can partially suppress

the requirement for Rad16p in GGR at the *MFA2* regulatory region. The possibility that a Tup1p non-regulated gene could be affected indirectly due to the deletion of *TUP1* and complement the absolute requisite of Rad16p in GGR for whole genome has been investigated. The results show that repair in the NTS of *RPB2* is still Rad16p dependent in a background of *TUP1* deletion. Research by Teng (personal communication) has shown other Tup1p regulated genes, such as the **a**-mating type specific genes *STE2* and *BAR1*, also undergo partial suppression of the requirement for Rad16p in GGR at some sites in *Δtup1* α cells, as at *MFA2*. At another type Tup1p regulated gene, *RNR3*, GGR is still dependent on Rad16p (Teng, personal communication). One difference between *STE2* and *BAR1* compared to *RNR3* is that the latter does not possess a Mcm1p binding site. These results indicate that the suppression of the requisite of Rad16p for GGR due to deleting *TUP1* is a local effect and possibly linked to the chromatin remodeling due to the presence of a Mcm1p binding sites. Results from other assays detecting restriction site accessibility have also confirmed that chromatin in the control region of *MFA2* is more accessible in *Δtup1*α-cells than in wild type α-cells (Teng *et al.*, 2006)

If the proposal of Yu *et al.* (2004) and as mentioned earlier is considered, it is possible that the changes chromatin structure created by the *TUP1* deletion may form a specific DNA structure so as GGR can operate without the involvement of Rad16p. Thus the excision of CPDs occurs via the local action of other proteins at *MFA2*. The microarrays results of genes involved in NER in a *Δtup1* α strain shows that the transcription level of these genes are not obviously changed (Teng, personal

communication). It is possible that there may be a number of remodeling factors which affect NER in specific regions of the genome, especially the regulatory region of genes where various chromatin remodeling factors act to regulate gene expression. Further research on the role of Tup1p in the suppression of the requisite for Rad16p in GGR, may give us insight into the relationship between chromatin structure remodeling, transcription and NER. Here, one likely avenue would be to examine NER in chromatin *in vitro* in extracts from the various strains and to examine the proteins recruited by ChIP, along with any change in chromatin structure. Reed (Personal communication) has now achieved NER of CPDs in chromatin *in vitro*, so this is more feasible than previously envisaged.

Chapter 5

Absence of the histone acetylase Gcn5p does not affect the enhanced NER caused by absence of Tup1p in the control region of *MFA2* gene

5.1 Introduction

In eukaryotes, the packaging of DNA into chromatin prevents the access of machineries necessary to regulate DNA metabolism, including gene expression and DNA repair (Thoma, 1999; Smerdon and Conconi, 1999; Becker and Horz, 2002). Chromatin is a progressively higher-order structure composed of compacted nucleosomes. Each nucleosome consists of an octamer of histone proteins with two turns of 146 bp DNA wrapped around its exterior (Wolffe, 1998). Chromatin remodeling, including alterations in the levels, sites, and types of posttranslational histone modifications, is now recognized as a central component of gene regulation (Strahl and Allis, 2000). Complexes of chromatin-remodeling carry out key enzymatic activities, changing chromatin structure by altering DNA–histone contacts (See review of Berger, 2002; Khorasanizadeh, 2004).

Histone acetyltransferases (HATs) and deacetylases (HDACs) are chromatin re-modelers. The mechanisms for them to affect transcription and DNA repair are

thought to involve a number of events. First, histone acetylation may modulate the accessibility of DNA through structural changes of the chromatin fiber. Second, the lysine residues and their modifications also provide specific binding surfaces for the recruitment of repressors and activators of gene activity (Kurdistani *et al.*, 2004). A bromodomain protein module has been shown to bind acetylated lysines *in vitro* (Dhalluin *et al.*, 1999; Jacobson *et al.*, 2000; Hassan *et al.*, 2002), and these domains are found in several eukaryotic transcription factors including Gcn5p and TFII250 (the largest subunit of the TFIID transcription initiation complex), as well as in chromatin-remodeling complexes such as Snf2p of the yeast SWI/SNF complex. Third, findings indicating that acetylation of different lysine residues have distinct roles in gene activity at the level of single genes and/or the whole genome have led to the proposal that histone acetylation and other modifications act as "histone codes" effecting downstream events such as transcription and repair (Strahl and Allis, 2000; Jenuwein and Allis, 2001, reviewed in de la Cruz *et al.*, 2005). For example, studies utilizing mammalian cells identified H4K8 and H3K14 as required acetylation sites for recruitment of transcription-related activation complexes specifically for the human *IFN*-β gene (Agalioti *et al.*, 2002).

Once recruited to chromatin, HATs and HDACs generate a localized domain of modified histones, resulting in activation or repression, respectively, of their target genes (Struhl 1999; Wu and Grunstein, 2000; Berger, 2002). Reversible acetylation of core histones by HATs can alleviate the repression, which is caused by the interaction between positively charged histone amino tails and negatively charged DNA, to

provide direct access for the transcription machinery to the target genes. Increased histone acetylation is associated with increased transcription, whereas decreased acetylation is associated with gene repression (Kuo and Allis, 1998; Struhl, 1998; Wolffe and Hayes, 1999; Krebs and Peterson, 2000). Gcn5p, one of the HATs in *S. cerevisiae*, acts as a catalytic subunit in the ADA and SAGA nucleosomal HAT complexes that are specific for histones H3/H2B (Grant, 1997; Rojas *et al.*, 1999; Trievel *et al.*, 1999; Clements *et al.*, 2003). It is also a member of a SAGA-like complex (SLIK) identified by Grant and colleagues (Pray-Grant *et. al*, 2002). The yeast SAGA complex containing Gcn5p is targeted to promoters positioned in natural or ectopic locations by activators, such as Gcn4p and Swi5p, thereby creating local domains of histone H3 hyperacetylation and subsequent transcriptional activation (Kuo *et al.*, 1998, 2000; Cosma *et al.*, 1999; Krebs *et al.*, 1999). However, a significant portion of the Gcn4-targeted histone acetylation by Gcn5p is independent of transcriptional activity. These observations provide strong evidence for promoter-selective, targeted histone acetylation by Gcn5p that facilitates transcription in a causal fashion. In addition, Gcn5p also functions in an untargeted manner to acetylate H3 on a more genome-wide scale (Kuo *et al.*, 2000). In an analogous mechanism leading to transcriptional repression, the Rpd3 HDAC is targeted to yeast promoters by the DNA-bound repressor Ume6, and it deacetylates histones H3 and H4 (Kadosh and Struhl 1997, 1998; Rundlett *et al.*, 1998).

As mentioned in Chapter 3, repression of the *MFA2* gene in α-cells also requires a general transcription repressor complex Tup1p-Ssn6p, *via* interactions with histones

H3 and H4 (Watson *et al.*, 2000). This repression mediated by the Tup1p-Ssn6p complex clearly has a chromatin component. Tup1p-histone interactions are important to Tup1p–Ssn6p repression *in vivo*. Moreover, a number of other factors such as Sin4p, Srb10p, Srb11p, Srb8p and Med3p, all members of sub-complexes associated with RNA polymerase II (Kuchin and Carlson, 1998), are required for Tup1p–Ssn6p functions. This suggests that Tup1p–Ssn6p may effect repression by interacting with specific transcription proteins. Hence, Tup1p–Ssn6p is a multifunctional protein complex, which can interact with transcription proteins to halt transcription and interact with histones to maintain the repressed state.

In Chapter 3, I investigated the effect of *TUP1* deletion on DNA repair at the *MFA2* and *RPB2* genes. The data show that the *MFA2* gene is derepressed in a *⊿tup1* strain and the repair of CPDs on both the TS and NTS of *MFA2* is faster than in wild type strain, while less enhanced repair occurred at *RPB2*. In this chapter, to clarify whether histone acetylation affects NER as well as affecting the derepression of *MFA2* or whether the two effects can be divorced after *TUP1* deletion, I have undertaken DNA repair studies *in vivo* with *GCN5* deleted *S. cerevisiae* strains in different genetic backgrounds. Here, I describe experiments investigating the roles of Gcn5p in NER at nucleotide resolution in the *MFA2* control region.

5.2 Material and methods

5.2.1 Yeast strains

PSY316 (*MAT***a** *ade2-101 ura 3-52 leu 2-3,112 Δhis 3-200 lys2 trp1*)

Δgcn5 (*MAT***a** *ade2-101 ura 3-52 leu 2-3,112 Δhis 3-200 lys2 trp1*)

Δtup1gcn5 (*MAT***a** *ade2-101 ura 3-52 leu 2-3,112 HIS::TUP1Δhis 3-200 lys2 trp1*)

PSY316 (*MATα ade2-101 ura 3-52 leu 2-3,112 Δhis 3-200 lys2 trp1*)

Δgcn5 (*MATα ade2-101 ura 3-52 leu 2-3,112 Δhis 3-200 lys2 trp1*)

Δtup1gcn5 (*MATα ade2-101 ura 3-52 leu 2-3,112 HIS::TUP1 lys2 trp1*)

5.2.2 DNA extraction of strains

This was undertaken as described in Chapter 2.

5.2.3 Detection of the mRNA level of *MFA2*

This was undertaken as described in Chapter 2. To prepare the *MFA2* RNA probe, primer A 5'-biotin-CTATCATCTTCATACAACAATAACTACCA3' and Primer B, 5'CTAATGATGAGAGAATTGGAATAAATTAG3' were used; for the *ACT1* RNA probe, Primer A, 5'-biotin-GCCGGTTTTGCCGGTGACG3' and Primer B, 5'CCGGCAGATTCCAAACCCAAAA 3' were used. PCR was carried out using Primer A and B to amplify the sequences of interest. The RNA specific probes were synthesised by Primer B extension using the biotinylated strand as a template.

5.2.4 Detection of CPDs repair at *MFA2*

This was undertaken also as described in Chapter 2.

5.3 Results

5.3.1 The comparison of UV sensitivity

UV sensitivity of a strain with a gene specific mutation can indicate a role of that gene in a DNA repair pathway. I examined the UV sensitivities of the wild-type, the *⊿gcn5* mutant and the double-mutant strain *⊿tup1gcn5* (Figure 5.1). The *⊿gcn5* and *⊿tup1gcn5* mutant exhibited a mild UV sensitivity compared with the wild-type strain. These results suggest that the *GCN5* may play roles in DNA repair but that its role is less significant than that of *RAD16* (see Chapter 4), which is essential for repair of almost all the non-transcribed regions of the whole genome.

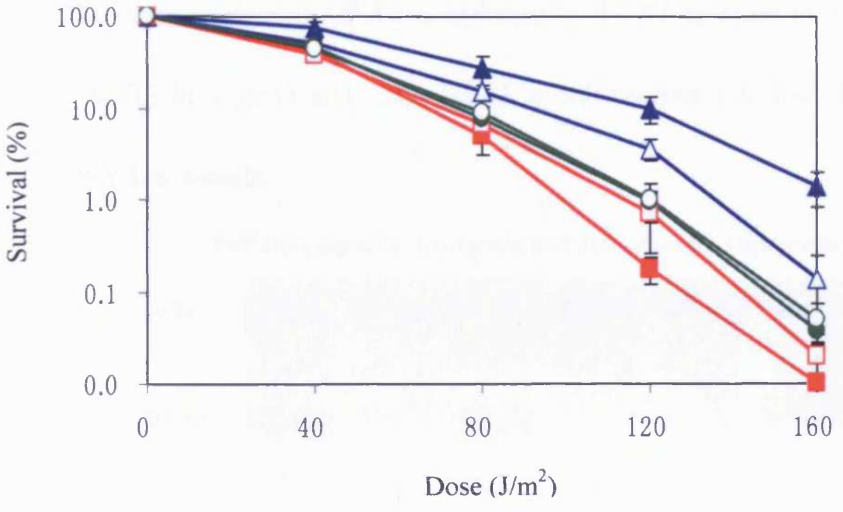

Figure 5.1 *The UV sensitivity of the strains studied.* (▲)PSY316**a**, (△)PSY316α, (■) *⊿gcn5*a, (□) *⊿gcn5*α, (●) *⊿tup1gcn5*a, (○) *⊿tup1gcn5*α.

5.3.2 The mRNA levels of *MFA2*

MFA2 is a mating type specific gene—in wild type **a**-cells, the protein Mcm1p

binds to the promoter region of *MFA2* to activate transcription; while in alpha cells, it is repressed by the yeast general repressor complex Tup1p-Ssn6p which indirectly binds to the Mcm1p binding site *via* interacting with two α2 factors in the upstream region of *MFA2*. In this research, Northern Blotting was used to examine *MFA2* mRNA level in wild type, *⊿gcn5* and *⊿tup1gcn5* strains to determine the influence of the acetylase Gcn5p on *MFA2* transcription (Fig.5.2). The *ACT1* gene was used as a control to adjust the loading of samples, since it is active in all the strains employed and neither Gcn5p nor Tup1p have a role in its regulation. No *MFA2* transcription was detected in PSY316α and *Δgcn5α*, however, *MFA2* was active in *⊿tup1gcn5* cells with levels similar to as in *⊿tup1* mutant cells. Thus Gcn5p does not play an obvious role in the derepression of *MFA2* as induced by *TUP1* deletion in α cells. The mRNA level of *MFA2* in *⊿gcn5* and *⊿tup1gcn5* **a**-cells shows a 4- fold decrease compared that in PSY316 **a**-cells.

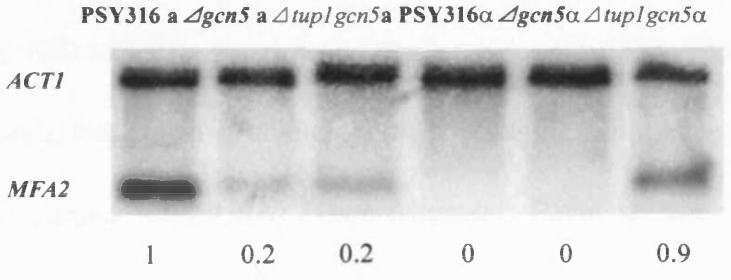

Figure 5.2 *The transcription of MFA2 as detected by Northern blotting.* 10μl of total RNA from each sample was run on 1.2% agarose gel (containing 6.7% formaldehyde) and blotted on to a nitrocellulose membrane. Radioactive dATP labeled *MFA2* gene TS fragments were used as probes to detect *MFA2* mRNA levels in both **a** and α of wild type PSY316 and mutant strains, and *ACT1* was used as an internal control to standardize the loading of total RNA in the quantification.

5.3.3 Repair of CPDs in the control region of MFA2 at the nucleotide level

Teng *et al.* (2002) in our group have used slot blotting with a CPD specific antibody to investigate whether deletion of *GCN5* affects repair in overall genomic DNA. Their data indicated that the NER of CPDs from the whole genome proceeded at an indistinguishable rate in *⊿gcn5* compared with that in the wild-type cells. Thus the NER enzymatic activity is not globally impaired due to the deletion of *GCN5*.

To investigate whether CPD repair at the nucleotide level is affected by deletion of *GCN5*, experiments were undertaken as described in Chapter 2. Figure 5.3~5.6 provide typical gel images for detecting CPDs in the TS and the NTS of the *HaeIII* restriction fragment containing the upstream control region of *MFA2* in PSY316, *⊿gcn5* and *⊿tup1gcn5* cells irradiated with 150 J/m^2 UV light. In all the sequencing gels, the numbers on the left denote the nucleotide positions in the control region of *MFA2*. Time of CPD repair was up to 3 hours and the data are expressed as the time for removing 50% of CPDs ($t_{50\%}$) at the damage sites (Fig.5.7). The intensity of the detectable bands was quantified after phosphorimaging with ImageQuant software (Molecular Dynamics, CA, USA). Then Microsoft Excel software was applied to create graphs (repair % vs repair time) to estimate the $t_{50\%}$. If less than 3 hours, the $t_{50\%}$ was directly read from the graphs; while if more than 3 hours, $t_{50\%}$ was obtained by extrapolation. As for sites with very slow repair, the estimation of $t_{50\%}$ by extrapolation may not be accurate, therefore, any $t_{50\%}$ more than 6 hours were set as 6 hours. As in Chapters 3 and 4, the repair of groups of closely linked CPDs, all of which show a similar repair rate, are represented as a single point.

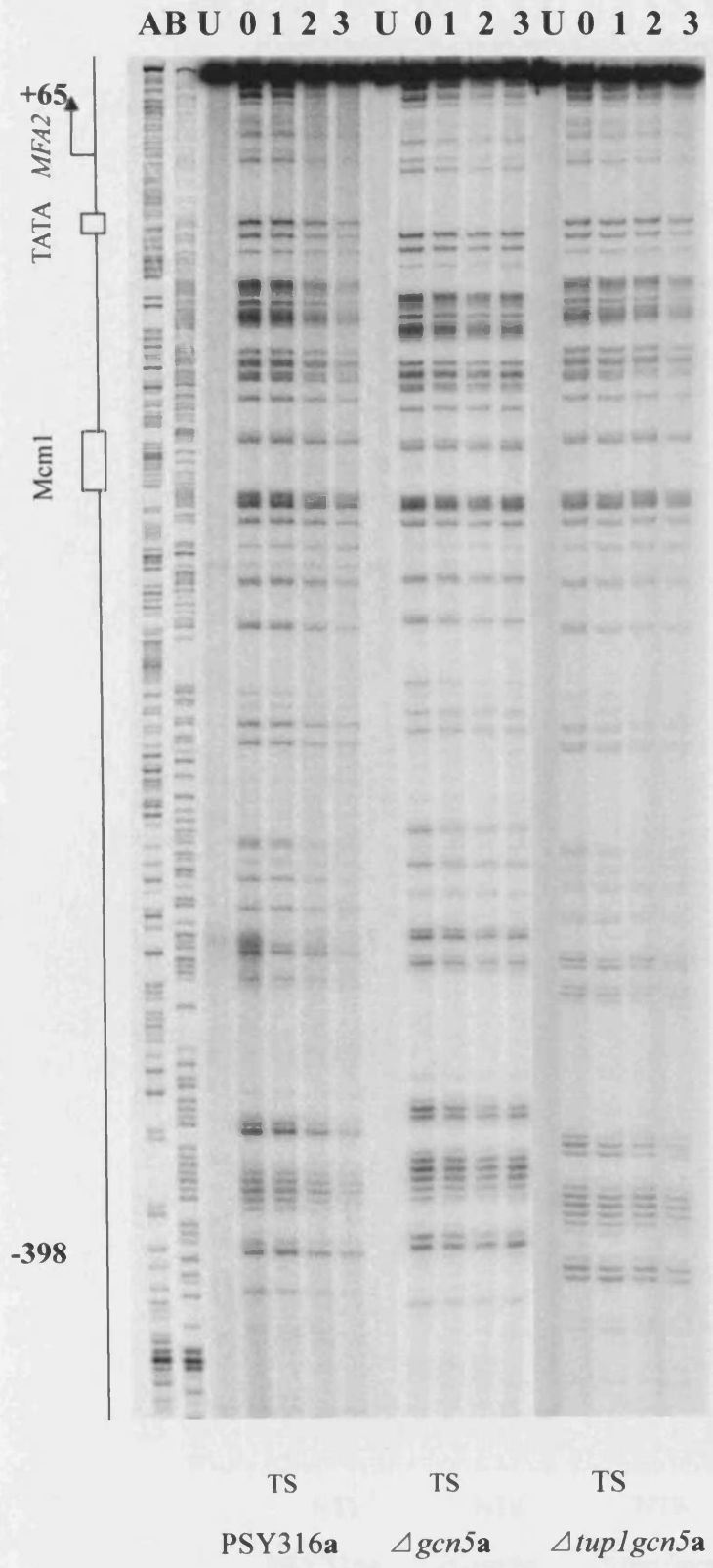

Figure 5.3 *Typical autoradiographs detecting CPDs repair at TS of PSY316a, ⊿gcn5a and ⊿tup1gcn5a strains at nucleotide level.*

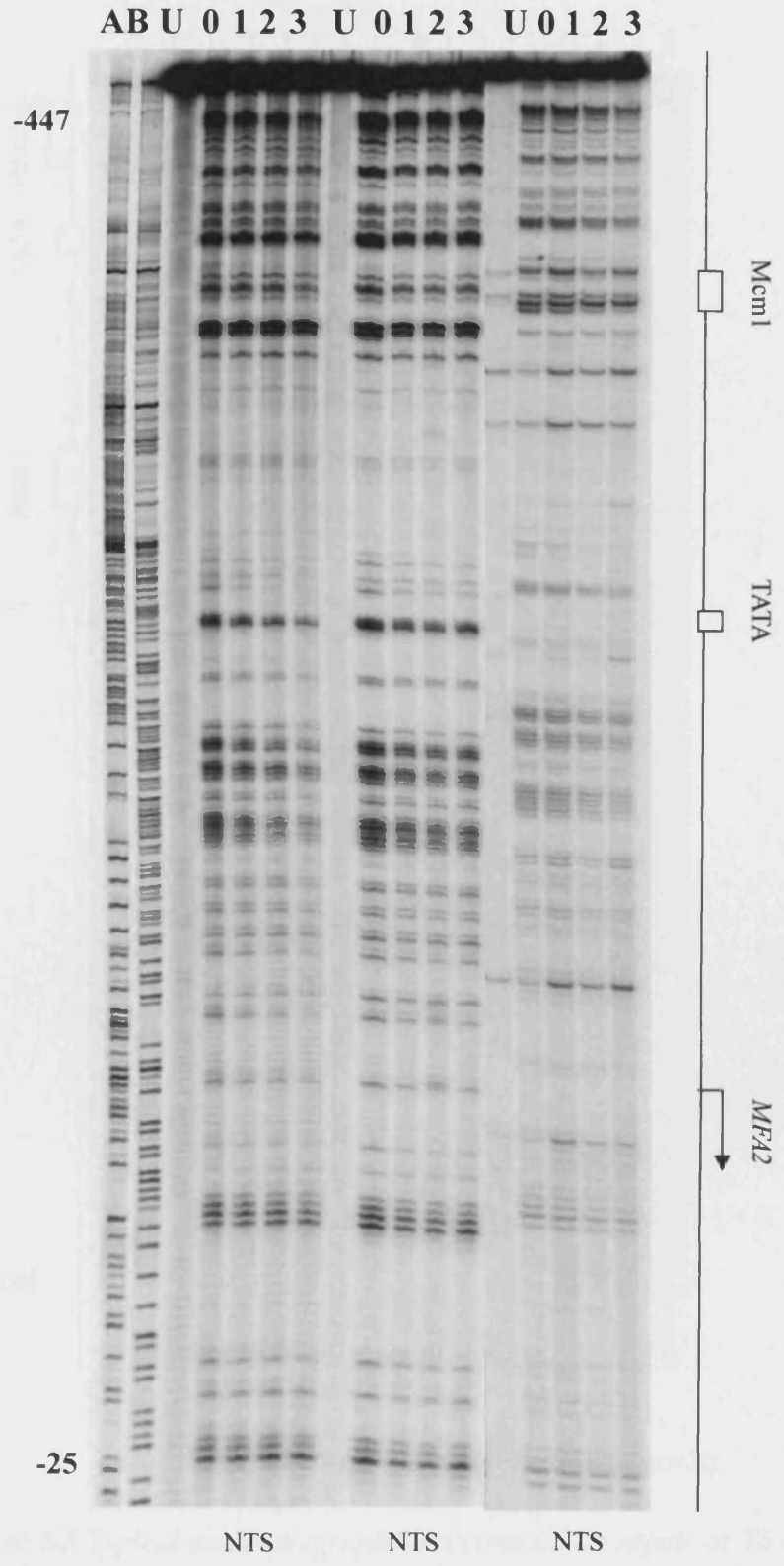

Figure 5.4 *Typical autoradiographs detecting CPDs repair at NTS of MFA2 in PSY316a, ⊿gcn5a and ⊿tup1gcn5a strains at nucleotide level (150J/m^2).*

Figure 5.5 *Typical autoradiographs detecting CPDs repair at TS of MFA2 in PSY316α, Δgcn5α and Δtup1gcn5α strains at nucleotide level (150J/m²).*

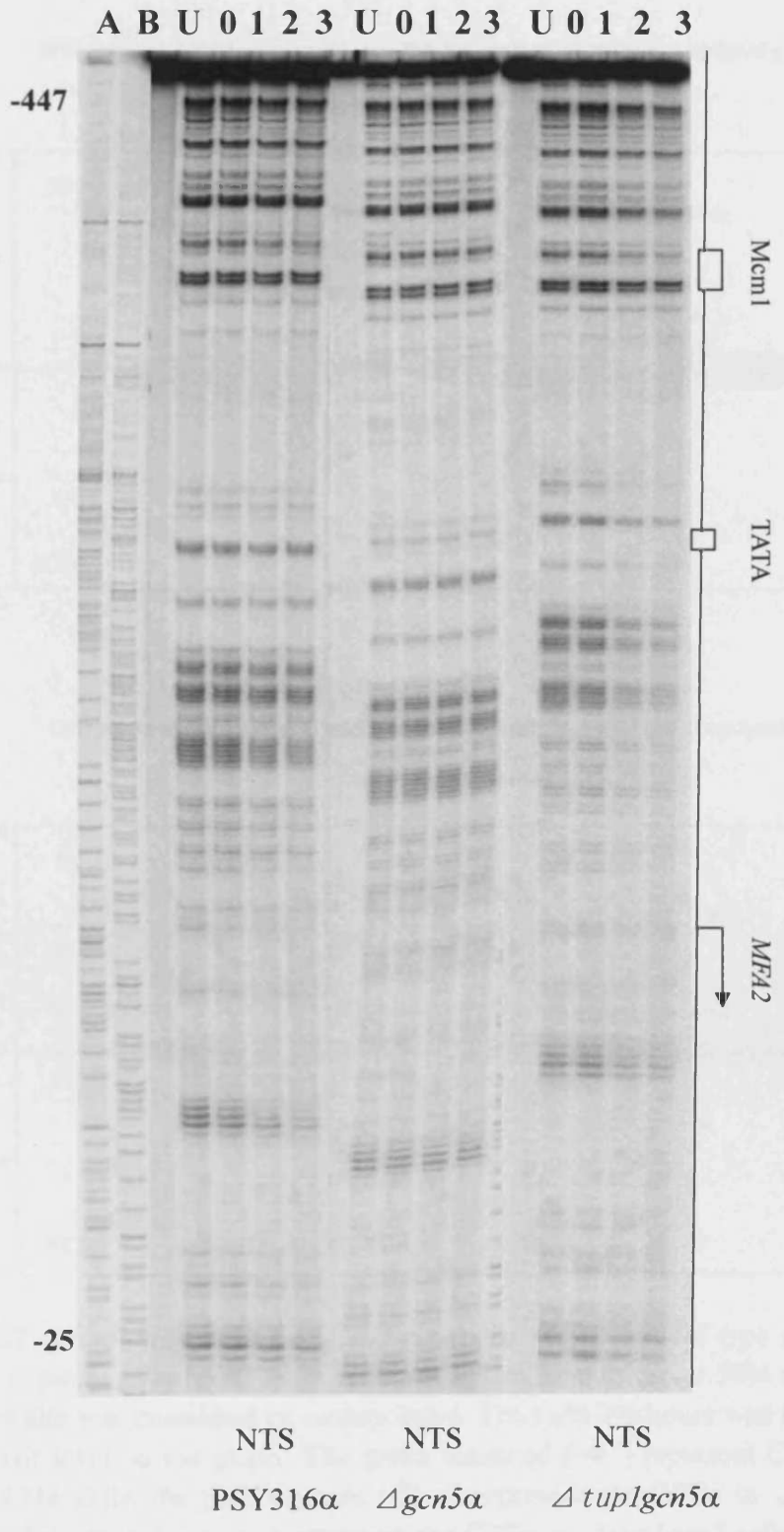

Figure 5.6 *Typical autoradiographs detecting CPDs repair at NTS of MFA2 in PSY316α, Δgcn5α and Δtup1gcn5α strains at nucleotide level (150J/m²).*

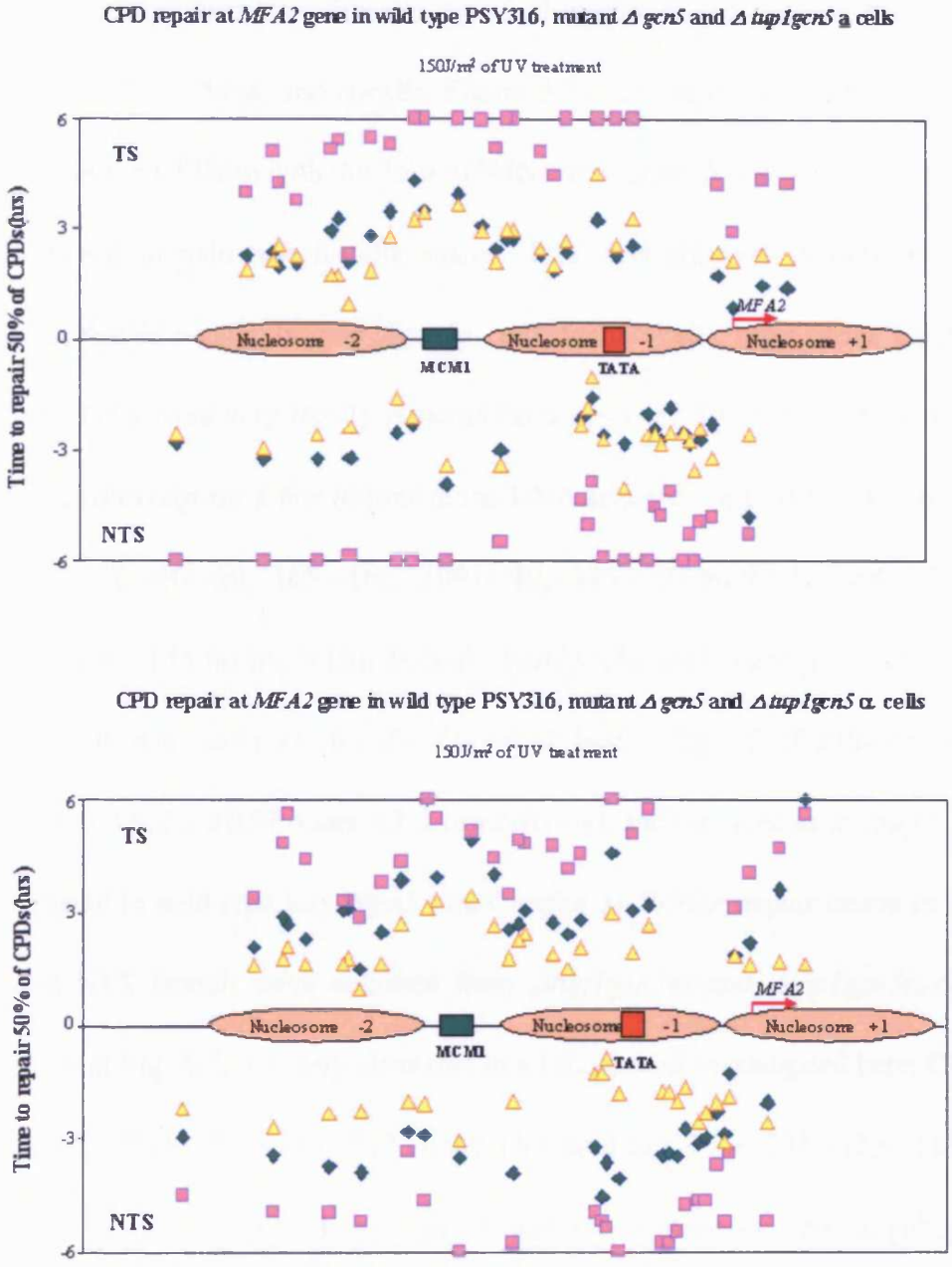

Figure.5.7 *Quantitative result of CPD repair at MFA2 in wild type PSY316 and mutants ⊿gcn5, ⊿tup1gcn5 cells (150J/m²).* The time to repair 50% CPDs (t_{50}%) at a given site was calculated or extrapolated. The $t_{50}\% \geq 6$ hours was shown at the same repair level on the graph. The green diamond (◆) represent CPDs in wild type PSY316 cells, the pink squares (■) represent the CPDs in *⊿gcn5* cells, and the yellow triangles (△) represent the CPDs in *⊿tup1gcn5* cells.

When treated with a UV dose of 150J/m^2, the CPDs at *MFA2* in wild type PSY316 are repaired faster than those in *Δgcn5*. However, they are slower than repair in *Δtup1gcn5* in both the **a**- and α-cells. Figure 5.7 shows that, in wild type **a**-cells, the majority of the CPDs in both the TS and NTS were repaired at a $t_{50\%}$ of less than 3 hours. However, in wild type α-cells, many CPDs were relatively slowly repaired compared to that in **a**-cells. In both *Δgcn5***a**- and *Δgcn5*α-cells, most of the CPDs in both TS and NTS were very slowly repaired (at a $t_{50\%}$ over 5 hours) or not repaired ($t_{50\%} \geq 6$ hours) except for a few lesions in the DNA sequence (e.g. -13~-14, -16~-17, -19~-20, -36~-38, -46~-50, -163~-166, -309~-310, -346~-347 on the TS, and -78~-85, -137~-138, -145~-146 on the NTS). In both *Δtup1gcn5***a**- and *Δtup1gcn5*α-cells, the repair of CPDs was faster (at a t_{50}% 2.6±0.12 hours TS; 2.8±0.21hours NTS; 2.2±0.24 hours TS, 2.3 ±0.07 hours NTS, respectively), and the same as in *Δtup1* cells when compared to wild type and *Δgcn5* (see Chapter 3). Similar repair trends in both the TS and NTS strands were obtained from *Δtup1gcn5***a**- and *Δtup1gcn5*α-cells. Moreover, from Fig. 5.7, it is very clear that in all the strains investigated here, CPDs in the region of -280~-215, -133~-119 on the TS strand and -275~-202, -129~-114 on the NTS strand are repaired much slower compared to those in their neighboring region. These sites are in the region of the Mcm1p (-221~-251) binding site and the TATA box (-119~-125), where it appears that CPD repair is dramatically reduced, possibly due to the binding of proteins.

5.4 Discussion

HATs, which function enzymatically by transferring an acetyl group to the particular lysine side chains within a core histone's basic N-terminal tail region, are now known to play a major role in chromatin regulation which is highly conserved from yeast to mammals. Lysine acetylation is postulated to weaken interactions between histone and DNA or nucleosome-nucleosome interactions, thereby destabilizing nucleosome structure or arrangement to give other factors more access to certain genetic loci. By altering protein-DNA interactions, histone acetyltransferases and deacetylases can not only activate or repress genes, but they may also influence in DNA damage formation and repair (Smerdon and Conconi, 1999; Sterner and Berger, 2000; Roth *et al.*, 2001; Khorasanizadeh, 2004). The results obtained in this chapter indicate that as previously reported in **a**-mating type cells deletion of *GCN5* affects the transcription of *MFA2* and the DNA repair in the promoter region of *MFA2* gene. Here, I have shown the partial defect in NER in *Δgcn5* **a** strains also extends to events in α cells, and I have determined how the presence of Tup1p influences these events.

5.4.1 Gcn5p is important for *MFA2* transcription

MFA2 is an **a**-mating type specific gene, which is transcriptionally active in **a**-cells and repressed in the α-cells by the Tup1p-Ssn6p complex. Since the transcription of *MFA2* is severely impaired in *Δgcn5* cells (decreased to 20% of that in wild type), Gcn5p plays an important role in its regulation.

Gcn5p is found to regulate the expression of 5% of the whole yeast genome

(Holstege *et al.*, 1998). It is one of the subunits in the HAT complexes ADA and SAGA that specifically acetylates nucleosomal histones (Grant *et al.*, 1997, 1999; Zhang *et al.*, 1998). Because hyperacetylation of N-terminal tails of core histones correlates with the activity of certain genes, the Gcn5p HAT activity suggests a close link between histone acetylation and transcription activation (Wolffe and Pruss, 1996; Wang *et al.*, 1997; Filetici *et al.*, 1998; Berger, 2002). Gcn5p was also shown to affect the chromatin organization of a chromosomal gene directly during its transcriptional activation (Filetici *et al.*, 1998). In *Δgcn5***a** mutant cells, *MFA2* transcription is reduced to 20% of that in wild type **a**-cells. Gcn5p acetylation is known to facilitate the binding of other activators or transcription factors such as TBP efficiently to a nucleosomal binding site and, with the Swi/Snf complex and Nhp6p, stimulate the formation of the TBP-TFIIA-DNA complex on the promoter region during the activation of a gene (Imbalzano *et al.*, 1994; Biswas *et al.*, 2004). In the absence of Gcn5p, other histone acetyltransferases or chromatin remodeling factors like members in Swi/Snf superfamily may partially complement the HAT activity of Gcn5p and that may account for the remaining 20 % transcription of *MFA2*. Snf2p was reported to have a partially redundant role with Gcn5p in the control of the *SUC2* gene expression (Sudarsanam *et al.*, 1999). In *Δgcn5*α cells, the deletion of *GCN5* has no effect on the repression of *MFA2*, indicating that this HAT has no role in repression of *MFA2*.

As mentioned in Chapter3, deletion of *TUP1* derepresses the *MFA2* gene in α-cells. In the genetic background of *Δgcn5*, *MFA2* gene still becomes transcriptionally active because of the absence of Tup1p. The transcription level is

similar to that in wild type **a**-cells and *Δtup1* α-cells, and much higher than that in *Δgcn5* **a**-cells. The Tup1p-Ssn6p repressor complex can alter histone modification states (with cooperation of the deacetylases) to facilitate interactions with histones (underacetylated) which are required to maintain a stable repressive state. Here, the result indicates that the absence of the repressor Tup1p probably dramatically changes the chromatin structure at the *MFA2* gene, and facilitates the access of transcription factors to complete their function, and that this can occur irrespective of the presence of Gcn5p. This may or may not function by increasing acetylation level at H3 at *MFA2*. This could be examined by ChIP in the relevant strains, as by Yu *et al.* (2005).

5.4.2 Gcn5p plays a role in NER in the promoter region of *MFA2*

The UV survival results in this study indicate that the *Δgcn5* mutant shows a mild UV sensitivity compared to the wild type strain, but it is not as sensitive as the *rad16* mutant strain (see Chapter 4). Mutants occupying defective essential NER gene are hypersensitive to UV, whereas mutations in the *RAD7*, *RAD16* and *RAD23* confer moderate sensitivity to UV light. The weak UV sensitivity of the *Δgcn5* strain rules out a significant role of Gcn5 in global NER.

Teng *et al.* (2002) examined CPD repair at the level of the nucleotide at the *MFA2* transcribed region. Here I obtained a similar result where in the promoter region of *MFA2*, a considerable reduction in the repair rate occurred for both the NTS and the TS of the transcribed region in the Δ*gcn5* strain compared to wild-type cells. Since the transcription level of *MFA2* in the Δ*gcn5* **a** strain dropped to 20% of the

normal level, this may account for the decrease in TCR of the TS of the transcribed region. However, it could not explain the decrease in NER in the NTS of *MFA2* in **a**-cells and the non-transcribed region in α-cells where it is governed by the GGR pathway. From the results of this chapter and Teng *et al.* (2006), the repair of the *MFA2* NTS does not differ markedly irrespective of whether the gene is transcriptionally active in **a**-cells or inactive in α-cells. Hence Gcn5p has a clear role in the NER of the non-transcribed *MFA2*. However, these results cannot identify the exact role of Gcn5p in NER.

Gcn5p, a subunit of the ADA or SAGA complexes, was first thought to physically bridge the activation domain to the basal transcription machinery and then was found to perform as HAT activity since gene activity is correlated with histone acetylation (Guarente, 1995; Sterner *et al.*, 1999). Gcn5p plays a role in controlling the expression of 5% of the yeast genome, yet 20% of the genome is under-acetylated in the mutant, thus the effect on DNA repair at *MFA2* but not on much of the genome, is in keeping with a role limited to a smaller fraction of the genome.

It is speculated that Gcn5p functions prior to, or during the DNA repair process such that it might be recruited to the upstream damage area by some factor that can detect damage, and hence allow the efficient access of the repair machinery. This issue was addressed through chromatin immunoprecipitations (ChIP) by Yu *et al.* (2005). This study shows that, in α-cells, Lys9 and/or Lys14 of histone H3, but not the relevant sites of histone H4 in two nucleosomes at the repressed *MFA2* promoter are hyperacetylated ten fold by Gcn5p following UV. This level of histone

hyperacetylation diminishes gradually as repair proceeds. Accompanying this, chromatin in the promoter becomes more accessible to restriction enzymes following UV and returns to the pre-UV state gradually. UV-related histone hyperacetylation and chromatin remodelling in the *MFA2* promoter are dependent on Gcn5p and partially on Swi2p respectively. Deletion of *GCN5*, but not of *SWI2* impairs the repair of DNA damage in the *MFA2* promoter. The post-UV histone modifications and chromatin remodelling at the repressed *MFA2* promoter do not activate *MFA2* transcription, nor do they require damage recognition by Rad4p or Rad14p. Hence, Gcn5p can acetylate histone H3 before the start of DNA repair at *MFA2*. Moreover, Gcn5p is only responsible for the histone hyperacetylation in some domains (e.g. *MFA2*) in response to UV, similar to its pattern in transcription activation, and other HATs must be responsible for the genome-wide post-UV histone acetylation in the Δ*gcn5* mutant.

It is also feasible that Gcn5p might be required to keep nucleosomes mobile at *MFA2* while the repair process is occurring. Brand *et al.* found a link between DNA damage recognition and chromatin modification through hGcn5 containing TFTC (TBP-free TAFII complex). The Δ*gcn5* mutation in **a**-cells leads to reduced repair rates in *MFA2* and to a five fold reduction of mRNA levels. Here it is possible that the repair effect is also a consequence of transcription or transcription-related chromatin remodelling influencing the repair mechanisms. Thus, function of Gcn5p in NER would only be indirectly via its HAT activity on transcription. However, because there are effects in α-cells in the absence of transcription, it is likely that the deletion of GCN5p disturbs the balance between histone acetylation and deacetylation at

MFA2 and it results in a local chromatin change that can directly affect DNA repair irrespective of transcription. Results in this chapter and Yu *et al.* have clarified this issue. From Fig. 5.7, CPDs in Δ*gcn5* α-cells are repaired slower than that in wild type α-cells. This indicates that in addition to its role in transcription, Gcn5p also has a role in NER at *MFA2*. Yu *et al.* (2005) found that during the post-UV period, a rapid increase of histone H3 acetylation was detected at 10 minutes (5.1 ± 1.0 fold) and reached its peak level (9.9 ± 0.4 fold) at 30 minutes in wild type cells. As repair progresses, the levels of histone H3 acetylation decreased gradually to: 8.6 ± 0.7 fold at 1 hour, 6.9 ± 1.3 fold at 2 hours and 5.1 ± 0.7 fold at 3 hours. This UV-stimulated histone H3 acetylation is primarily Gcn5p dependent, as in the Δ*gcn5* mutant histone H3 acetylation was only stimulated to 2.4 ± 0.4 fold at a maximum by 30 minutes after UV. Therefore, Gcn5p may be required to keep chromatin accessible for repair enzymes at *MFA2* during the repair process, and this function is independent of its role in transcription activation. With respect to its influencing nucleosome mobility it is worthy to note that UV induced accessibility of restriction sites at nucleosome cores in the *MFA2* regulation region is normal in a Δ*gcn5* strain. This may suggest Gcn5p has a role at a different level of chromatin organization.

In summary, the histone acetyltransferase Gcn5p plays a role in efficient NER at both the transcriptionally active and repressed *MFA2* loci. Whether other HAT complexes such as NuA3, NuA4 or Elp3 have roles in DNA repair can be also examined. Since histone acetylation is balanced by the action of both histone acetylases and deacetylases, the role of deacetylases in DNA repair should also be

determined.

5.4.3 The deletion of *TUP1* accelerates the NER at *MFA2* gene

Tup1p-Ssn6p is the complex that represses *MFA2* in α-cells. It binds to the promoter region of *MFA2* and interacts with the underacetylated histone H3 and H4 tails, altering the local chromatin structure around target genes to abolish transcription activation. The result of Chapter3 shows that deletion of *TUP1* in α-cells activates *MFA2*, with the transcription level as in wild type a-cells. Here, I have also shown that the *MFA2* gene becomes active in Δ*tup1gcn5* α-cells with the same transcription level in Δ*tup1*, while it is inactive in Δ*gcn5* α-cells. This indicates that the absence of Tup1p will completely disturb the repression mechanism of *MFA2* and facilitate the transcription initiation irrespective of Gcn5p. However, since Tup1p does not act as a repressor at *MFA2* in **a**-mating type strains, in Δ*tup1gcn5* **a**-cells the deletion of *TUP1* has no effect on the transcription level of *MFA2*, which is still only 20% of that in wild type **a**-cells.

The repair of CPDs both at the TS and NTS in the promoter region of *MFA2* is accelerated by the deletion of Tup1p in the genetic background of Δ*gcn5* **a**- and α-cells, and is even faster than in wild type at most damage sites investigated. I can speculate from these phenomena as follows: the changes of chromatin structure induced by deletion of *TUP1* in α-cells may be much more significant than those caused by acetylation of Gcn5p and this gives a better accessibility for repair proteins at *MFA2*, even more than in the wild type cells; or the transcription of *MFA2* caused

by deletion of *TUP1* also influences the enhanced repair in Δ*tup1gcn5* α-cells; or in both a- and α-cells, the absence of Tup1p can lead to the recruitment of some proteins, which have a role in a damage signalling pathway or the repair process and which is normally absent in the presence of Tup1p at the *MFA2* gene.

New results from Teng *et al.* (personal communication) show that the deletion of *TUP1* results in the flexibility of nucleosomes at upstream sequences in those genes it regulates in α-cells. The MNase mapping pattern is similar to that of naked DNA, and one assumes it facilitates the binding of proteins for transcription or repair to the DNA substrates around the Mcm1p site, the TATA box and the transcription initiation site. Further research will be carried out to investigate the binding of TBP to the *MFA2* promoter through ChIP. From the data in Chapter 3, the repair of CPDs in Δ*tup1mfa2*^{TATA} α-cells is not abolished and not much slower than in Δ*tup1*. This suggests that the transcription of *MFA2* induced by deletion of *TUP1* only plays a minor role in the faster repair that occurs in Δ*tup1gcn5* α-cells. To address the third possibility we need to first screen genes via microarrays to examine the spectrum of loci which Tup1p has a role and to identify loci where repair can be examined in relation to its activity. This will clarify whether the effects we see are specific to *MFA2* or whether they pertain to other part of the genome. Preliminary data of Teng indicate that other loci do indeed have changes in repair and interestingly these appear not to be all of those regulated by Tup1p, but a subset where Mcm1p also has a role.

Chapter 6

General discussion and future experiments

The works presented in this thesis focuses on the effects of transcription and chromatin remodelling on NER. The repair experiments were designed to investigate how the deletion of the yeast general repressor gene *TUP1* influenced the NER of UV induced CPDs at *MFA2*. I then determined how the Rad16p dependent GGR sub-pathway at *MFA2* is affected by Tup1p, and examined the role of the histone acetylase Gcn5p in NER at *MFA2*.

6.1 Enhanced NER induced by *TUP1* deletion at *MFA2* gene

In Chapter 3, the influence of deleting *TUP1* on the removal of CPDs by NER from the both TS and NTS of the **a**-mating type specific gene *MFA2* was studied at the nucleotide level. Compared with wild type PSY316 **a**- and α-cells, the CPDs were repaired faster in both *Δtup1* **a**- and α-cells, especially in *Δtup1* α-cells. Teng *et al.* (2006) has observed a similar enhanced NER at other mating type specific genes, including *RNR3*, *DRK2*, *TIR2*, *etc.*, where Tup1p also governs transcription. For the *RPB2* gene, which is not regulated by Tup1p, the deletion of *TUP1* had a very limited effect on NER (Chapter 3). Moreover, *MFA2* which is silenced in wild type α-cells becomes derepressed in *Δtup1*α-cells, with a similar transcription level as in wild type **a**-cells. Previously, Ducker and Simpson (2000) also have reported that deletion of

TUP1 can derepress the **a**-specific genes *STE2* and *STE6* in α-cells and this disrupted the nucleosomes at these regions.

TCR would operate on the TS of *MFA2* in *Δtup1*α-cells and result in preferential repair of this strand, but the change of chromatin structure likely accounts for the enhanced GGR at *MFA2* in *Δtup1*α-cells. The results of nucleosome mapping *in vivo* provide evidence as to how NER may be modulated by nucleosomes. It should be mentioned that such modulation does not occur equally at all genes and shows variation with transcriptional status and the gene in question (Li *et al.*, 1999; Morse *et al.*, 2002; Ferreiro *et al.*, 2004). Teng *et al.* (2006) found that the four nucleosomes at *MFA2* which are positioned in wild type α-cells were disrupted in *Δtup1*α-cells. The MNase digestion pattern at *MFA2* in *⊿tup1*α-cells is identical to that in naked DNA. Hara *et al.* (2000) reported that *in vitro* a DNA lesion within the mononucleosomes core was repaired 5- to 10-fold less efficiently than those in naked DNA. Teng *et al.* (2006) also used other assays to detect restriction site accessibility and confirmed that chromatin in the control region of *MFA2* is more accessible in *⊿tup1*α-cells than in wild type α-cells. Therefore, the changes of chromatin structure at *MFA2* induced by Tup1p deletion account for the enhanced repair in the non-transcribed region of *MFA2*.

To clarify the effect of transcription induced by Tup1p absence on enhanced NER at *MFA2*, I also investigate the repair in *Δtup1mfa2*^{TATA} α-cells. Those results showed that the repair of CPDs in both strands of *MFA2* in *Δtup1mfa2*^{TATA} α-cells was still faster than in wild type α-cells although slower than in *Δtup1*α-cells. This

indicates that the transcription of *MFA2* in *Δtup1α*-cells is one, but not the only reason, for the faster repair induced by the deletion of *TUP1*. Therefore, chromatin structure modulates NER at *MFA2* and Tup1p plays a role in influencing NER irrespective of whether transcription operates.

This result further supports the idea that factors which alter chromatin states can influence NER irrespective of whether the genes are transcriptionally active (Yu *et al.*, 2005; Reed, 2005)

6.2 Deletion of *TUP1* partially suppresses the absolute requisite of Rad16p in GGR at *MFA2* gene

In chapter 4, I investigated the effect of *TUP1* deletion on the Rad16p dependent GGR at the regulatory region of *MFA2* and at the *RPB2* gene. GGR is the pathway to repair CPDs in the transcriptionally silent sequences of the genome. It has been proposed a more flexible chromatin structure is required for the DNA damage to be accessible by GGR proteins (de Laat *et al.*, 1998; wood, 1999; van Hoffen *et al.*, 2003; Teng *et al.*, 2005(review); Reed, 2005). Rad16p is a member of SWI/SNF ATPase family, and it was proposed that it changes the chromatin structure in an ATP-dependent way (Bang *et al.*, 1992). The complex of Rad7p/Rad16p/Abf1p is also considered to facilitate the excision of DNA fragments containing damage during GGR in yeast (Reed *et al.*, 1998). Recently this protein complex has also been shown to generate superhelicity in DNA through the catalytic activity of the Rad16p component in postincision events in GGR (Yu *et al.*, 2004). These results suggested that the

mechanical energy, which produced by the SWI/SNF-like ATPase motor of Rad16p during formation of DNA supercoils, can be used to facilitate changes in DNA structure during GGR. How this impinges on chromatin structure is not yet known.

In Chapter 4, I surprisingly found that in α-cells the deletion of *TUP1* can partially suppress the requirement for Rad16p in GGR at the *MFA2* regulatory region. This is a local effects because I investigated repair at a Tup1p non-regulated gene and in total genomic DNA-here in the former there was an absolute requisite for Rad16p in GGR and no detectable reduction was seen in the genome overall. Furthermore, Teng (personal communication) has applied microarrays to investigate changes of transcription level for NER genes in a *⊿tup1* α strain; there were no obvious changes of transcription level of these genes. Deletion of *TUP1* in α-cells can also partially release the requirement for Rad16p in GGR at other **a**-mating type specific genes such as *STE2* and *BAR1*, but not at other type Tup1p regulated genes, such as *RNR3*, where Rad16p is still required for GGR (Teng, personal communication). These results suggest that the suppression of the requisite of Rad16p for GGR due to deleting *TUP1* is a local effect and are linked to the observations shown in Chapter 3 where deletion of *TUP1* active *MFA2* transcription and chromatin remodeling. It would appear that the presence of the Mcm1p sequence is necessary and experiments to mutate this and then examine NER are needed.

Given the suggestions above from Yu *et al.* (2004), then there is a possibility that chromatin structure remodeling is induced by the *TUP1* deletion and it may form a specific DNA structure so as GGR can operate without Rad16p. Thus the excision of

CPDs may occur by other proteins *via* the local action at *MFA2*. There may be a number of remodeling factors which affect NER in specific regions of the genome, especially the regulatory region of genes where various chromatin remodeling factors act to regulate gene expression. Further research needs to be carried on for the role of Tup1p in the suppression of the requisite for Rad16p in GGR and this should provide insight into the relationship between chromatin structure remodeling, transcription and NER, and determine if any of the above suggested modes of action apply.

6.3 Gcn5p plays roles in transcription, chromatin remodeling and NER at *MFA2* gene

NER is a multistep repair system which can repair various DNA lesions including CPDs. Compacting DNA into nucleosomes is considered to be a negative regulation for DNA repair. Histone acetylases acts as part of the chromatin remodeling actions which are required for DNA repair. One histone acetylase is Gcn5p. This can relax the chromatin structure by modifying the histone tails to facilitate efficient NER in the control region of the *MFA2*. Yu *et al.* (2005) has reported that Gcn5p can increase the acetylation level at H3.

In Chapter 5, the results indicated that deletion of *GCN5* affects the transcription of *MFA2* and the DNA repair in the promoter region of *MFA2* gene in both **a**- and α-cells, and I have examined how the presence of Tup1p influences these events.

First, the transcription of *MFA2* is severely impaired in *Δgcn5* **a**-cells with a drop to 20% of that in wild type **a**-cells. Therefore, Gcn5p is important in its transcriptional

regulation. However, in *Δgcn5* α-cells, the deletion of *GCN5* has no effect on the repression of *MFA2*, indicating that this HAT has no role in repression of *MFA2*.

Gcn5p is a subunit of the HAT complexes ADA, SAGA and SLIK, that specifically acetylate nucleosomal histones (Grant *et al.*, 1997, 1999; Zhang *et al.*, 1998). Since hyperacetylation of histones tails is directly related with the transcription of certain genes, the HAT activity of Gcn5p indicates a close link between histone acetylation and transcription activation (Berger, 2002). Gcn5p also affects the chromatin organization of a chromosomal gene directly during its transcriptional activation (Filetici *et al.*, 1998) and Gcn5p acetylation is known to facilitate the binding of other activators or transcription factors such as TBP. These then bind efficiently to a nucleosomal binding site and stimulate the formation of the TBP-TFIIA-DNA complex in the promoter region during the activation of gene. This is undertaken with the cooperation of a Swi/Snf complex and Nhp6p (Imbalzano *et al.*, 1994; Biswas *et al.*, 2004). As for the remaining 20% transcription of *MFA2,* there is a possibility that other histone acetyltransferases, phosphorylases and methylases or chromatin remodeling factors such as members of the Swi/Snf superfamily may facilitate some transcription in the absence of Gcn5p. For example, Sudarsanam *et al.* (1999) has reported that Snf2p has a partially redundant role with Gcn5p in the control of *SUC2* gene expression.

I found that in *Δtup1gcn5*α-cells, the *MFA2* gene is transcribed with a transcription level similar to that in wild type **a**-cells and *Δtup1* α-cells. This is much higher than that in *Δgcn5* **a**-cells. Thus there is no role for Gcn5p in facilitating the

transcription there. However, the transcription level of *MFA2* in *Δtup1gcn5* **a**-cells is still similar to that in *Δgcn5* **a**-cells, i.e. at 20% of that in wild type **a**-cells. Hence Gcn5p does have a role. This result suggests that the absence of the repressor Tup1p probably dramatically changes the chromatin structure at the *MFA2* gene in *Δtup1gcn5*α-cells, and facilitates the access of transcription factors to complete their function. This can occur irrespective of the presence of Gcn5p.

In Chapter 5, it was reported that slower repair occurs in the promoter region of *MFA2* for both the NTS and the TS of the promoter region in the Δ*gcn5* strain compared to wild-type cells. The drop of transcription level of *MFA2* in the Δ*gcn5* **a** strain to 20% of the normal level may account for the decrease in TCR of the TS of the transcribed region. However, it is not the reason for the decrease in the region where GGR operates. The results of this chapter and Teng *et al.* (2002) suggested that the repair of the NTS of *MFA2* does not differ markedly irrespective of whether the gene is active in **a**-cells or inactive in α-cells. Thus Gcn5p is involved in the GGR of the non-transcribed region of *MFA2*. However, these results do not provide a clear answer for the precise function of Gcn5p in NER.

Yu *et al.* (2005) applied ChIP to address the topic. Their study showed that, Lys9 and/or Lys14 of histone H3 in α-cells are hyperacetylated ten fold by Gcn5p following UV. This level of histone hyperacetylation diminishes gradually as repair proceeds. At the same time, chromatin in the promoter becomes more accessible to restriction enzymes following UV and returns to the pre-UV state gradually. Hence, Gcn5p can acetylate histone H3 before the start of DNA repair at *MFA2*. Moreover,

Gcn5p is only responsible for the histone hyperacetylation in some domains (e.g. *MFA2*) in response to UV, similar to its pattern in transcription activation, and other HATs must be responsible for the genome-wide post-UV histone acetylation in the *Δgcn5* mutant.

There were two other important results in this study of Yu *et al.* (2005). First, Gcn5p did not influence the accessibility of restriction sites at the nucleosomes cores of the two nucleosomes in the *MFA2* regulating region. This suggests Gcn5p may influence a higher order of chromatin remodeling here, but that it does not have a role in nucleosome mobility after UV.

Second, the action of Gcn5p is not dependent on functional NER but the return of the chromatin to its pre-UV status is dependent on NER. This suggests local DNA damage is detected by components other than the Rad14/Rad4 proteins which are considered to be amongst the first proteins to bind to CPDs in naked DNA.

It was originally possible that the repair effect of Gcn5p was a consequence of transcription or transcription-related chromatin remodelling influencing the repair mechanisms as the paper of Teng *et al.* (2002) examined events in **a**-cells only. Thus, the function of Gcn5p in NER would only be indirectly via its HAT activity in transcription. Another possibility was that the deletion of *GCN5* disturbs the balance between histone acetylation and deacetylation at *MFA2* and results in a local chromatin change that can directly affect DNA repair irrespective of transcription. Results in this chapter and Yu *et al.* (2005) indicate that since CPDs in Δ*gcn5* α-cells are repaired slower than that in wild type α-cells, Gcn5p also has a role in NER at the

repressed *MFA2* gene. Thus, Gcn5p may be required to keep chromatin accessible for repair enzymes at *MFA2* during the repair process and this is definitely independent of its role in transcription activation; *MFA2* remains repressed after UV in these cells.

The result of Chapter 3 shows that deletion of *TUP1* in α-cells activates *MFA2*, and enhances NER at *MFA2*. In this chapter, CPDs were also repaired faster in Δ*tup1gcn5* **a**- and α-cells; even faster than in wild type at most damage sites investigated. The changes of chromatin structure induced by deletion of *TUP1* in α-cells thus are more significant than those caused by acetylation of Gcn5p, and likely provide a better accessibility for repair or damage signalling at *MFA2* even more than in the wild type cells; or the transcription of *MFA2* caused by deletion of *TUP1* also effects the enhanced repair in Δ*tup1gcn5* α-cells. However there are few changes if the TATA box is mutated, so this is not a major event.

6.4 Further experiments

In Chapter 3, the enhanced NER at *MFA2* induced by deletion of *TUP1* is a very interesting phenomenon and needs to be investigated in other Tup1p regulated genes. This has now been done by Teng for *BAR1*, *RNR3*, *etc.* so as to determine how many different genes are affected by this Tup1p absence. It may be that the Mcm1sequence is crucial here, so mutating it may provide some insight. Second, it is now worthwhile using ChIP to determine which proteins are involved in transcription or NER in Δ*tup1*and Δ*tup1mfa2*^{TATA}. Teng *et al.* (2006) has found that the deletion of *TUP1* results in the flexibility of nucleosomes at upstream sequences in those genes it

regulates in α-cells. Further research could investigate the binding of TBP to the *MFA2* promoter through ChIP in these instances and to see how it, along with transcriptional components are recruited compared to when the genes are normally active.

As for the results which have showed Tup1p absence can partly suppress the requirement of Rad16p in GGR, further experiments can be carried out on CPD repair in a $\Delta tup1rad16mfa^{TATA}$ strain to find how this phenomenon is related to the transcription induced by *TUP1* deletion in $\Delta tup1rad16$ α-cells. Here again, ChIP can give us more clues.

In Chapter 5, the histone acetylase Gcn5p was found to play a role in efficient NER at both the transcriptionally active and repressed *MFA2* loci. In the future, it is worth examining whether other HAT complexes such as NuA3, NuA4 or Elp3 have roles in DNA repair at *MFA2*. This is because, even in the absence of Gcn5p, there is both some transcription in **a**-cells and some NER in α-cells.

Both histone acetylases and deacetylases are essential for the balance of histone acetylation level in cells. Thus, it is also important to investigate the role of deacetylases in DNA repair.

Finally, if possible, we could also undertake some *in vitro* experiments to provide even further insight into this topic. Here chromatin containing CPDs can be examined to see what remodelling factors influences NER and how they work.

Appendix I

Growth media and solution

AI.1 Growth media

All media used in this thesis had been autoclaved for 20-30min at 15psi.

Yeast Complete (YC)

16g Glucose; 20ml YC Stock solution. Made up to 400ml with H_2O. YC slopes and plates were obtained by supplementing this medium with 8 Bacto-Agar [Difco Laboratories, USA]

YC Stock solution

240g Mycological peptone; 400g Yeast extract; 40g Casein hydrolysate; 1g F-inositol; 200mg Nicotinic acid; 200mg Riboflavin; 200mg Calcium pantothenate; 200mg Aneurin hydrochloride; 100mg Para-amino benzoic acid; 16 mg Pyridoxine; 0.5mg Biotin; 100ml Chloroform. Made up to 5000ml with H_2O.

YPD medium

2g Yeast extract; 1g Bacto-Peptone and 4g Glucose. Made up to 200ml with H2O. YPD slopes and plates were obtained by added with 4g Bacto-Agar.

AI. 2 Stock Solutions

0.5M EDTA (pH0.8)

EDTA • Na_2 • $2H_2O$	186.1g
H_2O	800ml

Stir vigorously on a magnetic stirrer. Adjust the pH to 8.0 with NaOH (~20g of NaOH pellets). Add H_2O to make 1 litre.

1M Tris

Tris base	121.1g
H_2O	800ml

Adjust the pH to the desired value by adding concentrated HCl. Add H_2O to make 1 litre.

pH	HCl
7.4	70ml
7.6	60ml
8.0	42ml

TE Buffer

Tris-HCl, pH7.5	10mM
EDTA, pH8.0	1mM

3M Sodium acetate (pH5.2)

Sodium acetate • $3H_2O$	408.1g
H_2O	800ml

Adjusted the pH to 5.2 with glacial acetic acid. Add H2O to make 1 litre.

5M NaCl

NaCl	292.2g
H_2O	up to 1 litre

10% SDS (Sodium dodecyl sulphate)

SDS (electrophoresis grade)	100g
H2O	900ml

Heat to 68°C to assist dissolution. Adjust the pH to 7.2 by adding a few drops of concentrated HCl. Make up the volume to 1 litre with H_2O.

20× SSC

NaCl (3 M)	175.3 g
Sodium citrate dihydrate (0.3 M)	88.2 g
H_2O	800 ml

Adjust the pH to 7.0 with HCl. Make up the volume to 1 litre with H_2O.

1M Phosphate solution

Na_2HPO_4	71 g
H_3PO_4 (85%)	4 ml
H_2O	up to 1000 ml.

Phosphate Buffered Saline (PBS)

NaCl	8 g
KCl	0.2 g
Na_2HPO_4	1.44 g
KH_2PO_4	0.24 g
H_2O	800 ml

Adjust the pH to 7.4 with 5 M NaOH. Add H_2O to 1 litre.

1 M DTT (Dithiothreitol)

DTT	3.09 g

Dissolved in 20 ml of 0.01 M sodium acetate (pH 5.2). Sterilise by filtration. Do not autoclave DTT or solution containing DTT.

Solutions for DNA and RNA extraction

SEC Buffer

Sorbitol	1.0 M
EDTA	100 mM

Citrate Phosphate buffer (pH 5.8)	10 mM

Sorbitol solution

Sorbitol	0.9 M
Tris·HCl (pH 8.0)	100 mM
EDTA	100 mM

DNA Lysis Buffer

Urea	4 M
NaCl	200 mM
Tris-HCl (pH 8.0)	100 mM
CDTA	10 mM
n-Lauroyl Sarcosine	0.5% (w/v)

RNA Lysis Buffer

Tris-HCl (pH 7.5)	10 mM
EDTA (pH 8.0)	10mM
SDS	0.5%

AI.5. Solutions for electrophoresis

50× TAE

2 M Tris base	242 g
1 M Sodium Acetate·$3H_2O$	136 g
50 mM EDTA·Na_2·$2H_2O$	19 g

Adjust to pH7.2 with glacial acetic acid. Add H_2O to make 1 litre.

10× TBE

Tris base	108 g
Boric acid	55 g
$Na_2EDTA·2H_2O$	9.3 g

Add H_2O to 1 litre.

Denaturing running buffer

NaOH	36 mM
EDTA	1 mM.

Non denaturing loading buffer

Ficoll	10%
SDS	0.5%
Bromophenol Blue	0.06%

Made up in 1× TAE.

Denaturing loading buffer

NaOH	50 mM
EDTA	1 mM
Ficoll	2.5%
Bromocresol Green	0.025%

Sequencing gel-loading buffer

Deionized formamide	95%
EDTA (pH 8.0)	20 mM
Xylene cyanol FF	0.05%
Bromophenol blue	0.05%

Neutralising gel washing buffer

Tris-HCl (pH7.5)	1 M
NaCl	1.5 M

Fixative solution for sequencing gel

Methanol (15%)	600 ml
Acetic acid (5%)	200 ml

Add H_2O to make 4 litres.

Solutions for Northern Blotting

10× FA gel buffer

3-[N-Morpholino]propanesulfonic acid (MOPS) (free acid)	200 mM
Sodium acetete	50 mM
EDTA	10 mM

Adjust pH to 7.0 with NaOH.

1× FA gel running buffer

10× FA gel buffer	100 ml
37% (12.3) Formaldehyde	20 ml
RNase-free water	880 ml

5× RNA loading buffer

Saturated aqueous bromophenol blue	16 µl
0.5 M EDTA, pH 8.0	80 µl
37% (12.3) formaldehyde	720 µl
formamide	3 ml
10× FA gel buffer	4 ml

Add RNase-free water to 10 ml

10× MOPS buffer

Morpholinopropanesulphonic acid (0.4 M) 83.7 g
Sodium Acetate·H_2O (0.1 M) 13.6 g
EDTA·Na_2·$2H_2O$ (10 mM) 1.87 g
Adjust pH to 7.2 with NaOH. Add H_2O to make to 1 litre.

(Pre)hybridisation solution for RNA

Phosphate solution (1M)	5 ml
SDS (20%)	3.5 ml
BSA	0.25 mg
EDTA (0.5M, pH 8.0)	20 µl
H_2O	up to 10 ml.

Probe stripping solution

SSC (20x)	2.5 ml
SDS (10%)	50 ml
H_2O	up to 500 ml

Appendix II

Cell survival as a function of UV dose

AII.1 Cell survival in Chapter 3

PSY316 a-cells

UV dose (J/m^2)	Dilution	Number of colonies (% Survival)			Mean survival (%)	Standard deviation (%)
		Experiment 1	Experiment 2	Experiment 3		
0	10^{-4}	89/90(100)	116/126(100)	176/185(100)	100	0
40	10^{-4}	66/67(74)	81/86(69)	153/158(86)	76.5	8.7
80	10^{-4}	32/33(36.3)	34/32(27.3)	27/30(15.8)	26.5	10.3
120	10^{-3}	110/114(12.5)	125/137(10.8)	124/106(6.4)	9.9	3.2
160	10^{-2}	201/173(2.1)	149/120(1.1)	188/193(1.1)	1.42	0.6

***Δtup1* a-cells**

UV dose (J/m^2)	Dilution	Number of colonies (% Survival)			Mean survival (%)	Standard deviation (%)
		Experiment 1	Experiment 2	Experiment 3		
0	10^{-4}	115/115(100)	251/257(100)	201/204(100)	100	0
40	10^{-4}	76/80(68)	138/141(55)	142/133(68)	63.6	7.5
80	10^{-3}	87/83(7.4)	190/187(7.4)	168/167(8.3)	7.7	0.5
120	10^{-3}	6/6(0.5)	51/53(2.1)	18/21(1.0)	1.2	0.8
160	10^{-2}	11/13(0.1)	79/64(0.3)	12/10(0.1)	0.15	0.1

PSY316 α-cells

UV dose (J/m^2)	Dilution	Number of colonies (% Survival)			Mean survival (%)	Standard deviation (%)
		Experiment 1	Experiment 2	Experiment 3		
0	10^{-4}	113/113(100)	109/93(100)	73/78(100)	100	0
40	10^{-4}	54/46(44)	36/52(44)	49/50(66)	51.1	12.5
80	10^{-3}	146/127(12)	157/180(17)	107/127(16)	14.8	2.4
120	10^{-3}	28/29 (2.6)	36/39(3.7)	41/25(4.4)	3.6	0.9
160	10^{-2}	6/6(0.05)	10/10(0.1)	10/10(0.1)	0.1	0.04

Δtupl α-cells

UV dose (J/m^2)	Dilution	Number of colonies (% Survival)			Mean survival (%)	Standard deviation (%)
		Experiment 1	Experiment 2	Experiment 3		
0	10^{-4}	244/251(100)	116/114(100)	119/116(100)	100	0
40	10^{-4}	104/98(41)	39/43(36)	32/30(26)	34.3	7.3
80	10^{-3}	233/232(9.4)	132/131(11.4)	26/27(2.3)	7.7	4.8
120	10^{-3}	84/84(3.4)	32/34(2.9)	5/9(0.6)	2.3	1.5
160	10^{-2}	78/83(0.33)	64/64(0.56)	30/30(0.3)	0.4	0.16

AII.2 Cell survival in Chapter 4

Δrad16 α-cells

UV dose (J/m^2)	Dilution	Number of colonies (% Survival)			Mean survival (%)	Standard deviation (%)
		Experiment 1	Experiment 2	Experiment 3		
0	10^{-4}	155/153(100)	155/157(100)	161/153(100)	100	0
10	10^{-4}	94/92(57)	77/73(48)	73/62(43.0)	49.4	7.2
20	10^{-4}	26/11(12.2)	12/11(6.1)	8/9 (5.5)	7.95	3.7
40	10^{-2}	27/51(0.26)	12/8(0.06)	17/18(0.11)	0.14	0.1
60	10^{-2}	6/19(0.007)	16/15(0.009)	2/3(0.001)	0.006	0.004
80	10^{-1}	5/2(0.002)	5/7(0.004)	3/1(0.001)	0.002	0.001

Δtuplrad16 α-cells

UV dose (J/m^2)	Dilution	Number of colonies (% Survival)			Mean survival (%)	Standard deviation (%)
		Experiment 1	Experiment 2	Experiment 3		
0	10^{-4}	263/263(100)	162/157(100)	267/271(100)	100	0
10	10^{-4}	162/173(64)	94/93(59)	118/121(44)	55.7	10.1
20	10^{-4}	33/17(9.5)	4/4(2.5)	11/25(6.8)	6.3	3.52
40	10^{-2}	32/35(0.13)	15/21(0.11)	12/9(0.04)	0.093	0.048
60	10^{-2}	29/22(0.01)	12/9(0.007)	5/5(0.002)	0.006	0.004
80	10^{-1}	9/10(0.004)	2/2(0.001)	3/3(0.001)	0.002	0.001

AII.3 Cell survival in Chapter 5

Δgcn5 **a-cells**

UV dose (J/m^2)	Dilution	Number of colonies (% Survival)			Mean survival (%)	Standard deviation (%)
		Experiment 1	Experiment 2	Experiment 3		
0	10^{-4}	97/99(100)	107/102(100)	286/295(100)	100	0
40	10^{-4}	38/39(39)	43/43(41)	135/134(46)	42.2	3.6
80	10^{-3}	40/48(4.5)	52/65(5.6)	149/123(4.7)	4.9	0.6
120	10^{-3}	2/1(0.15)	2/3(0.24)	4/4(0.14)	0.18	0.06
160	10^{-2}	1/1(0.01)	1/3(0.02)	0/0(0)	0.01	0.01

Δtup1gcn5 **a-cells**

UV dose (J/m^2)	Dilution	Number of colonies (% Survival)			Mean survival (%)	Standard deviation (%)
		Experiment 1	Experiment 2	Experiment 3		
0	10^{-4}	151/165(100)	137/141(100)	121/133(100)	100	0
40	10^{-4}	53/58(35)	68/53(44)	71/72(56)	45.0	10.7
80	10^{-3}	67/77(4.6)	89/88(6.4)	157/153(12.2)	7.7	4.0
120	10^{-3}	8/13(0.66)	17/13(1.08)	14/15(1.14)	0.96	0.26
160	10^{-2}	8/5(0.04)	4/6(0.04)	4/4(0.03)	0.04	0.01

Δgcn5 **α-cells**

UV dose (J/m^2)	Dilution	Number of colonies (% Survival)			Mean survival (%)	Standard deviation (%)
		Experiment 1	Experiment 2	Experiment 3		
0	10^{-4}	149/156(100)	262/241(100)	99/105(100)	100	0
40	10^{-4}	62/68(43)	81/83(33)	37/42(39)	38	5.1
80	10^{-3}	105/107(7)	237/265(10)	42/18(3)	6.6	3.5
120	10^{-3}	13/15(0.9)	28/22(1)	3/1(0.2)	0.7	0.44
160	10^{-2}	3/2(0.02)	7/7(0.03)	0/0(0)	0.01	0.01

Δtup1gcn5 **α-cells**

UV dose (J/m^2)	Dilution	Number of colonies (% Survival)			Mean survival (%)	Standard deviation (%)
		Experiment 1	Experiment 2	Experiment 3		
0	10^{-4}	107/111(100)	198/198(100)	132/127(100)	100	0
40	10^{-4}	52/34(39)	101/98(50)	58/48(41)	43.5	5.9
80	10^{-3}	115/104(10)	252/265(13)	57/46(4)	9.0	4.6
120	10^{-3}	14/12(1.2)	27/25(1.3)	7/6(0.5)	1.0	0.44
160	10^{-2}	7/2(0.04)	6/7(0.03)	20/10(0.1)	0.1	0.05

Appendix III

Data from experiments for CPD repair in the *MFA2* at nucleotide level

AIII.1 CPD repair in the *MFA2* in Chapter 3

Table AIII.1-1 CPD repair in the *MFA2* TS in the wild type PSY316 a strain

CPDs position	Experiment 1				Experiment 2			
	Repair time(hours)				Repair time (hours)			
	0	1	2	3	0	1	2	3
Top band	67056	77156	66084	65045	622353	795190	346756	996236
2	316	257	83	56	2211	925	668	778
-16	418	344	171	91	4075	2497	520	1231
-37	181	88	33	10	1760	710	288	353
-48	408	327	145	92	4199	3409	691	1648
-108	1122	1015	493	277	8635	9580	3884	4598
-119	717	572	272	167	6981	7144	2995	2400
-133	241	228	133	97	2128	3122	1650	1765
-155	2338	2008	830	333	25687	28403	10396	12188
-164	905	684	274	71	11318	9851	3422	3526
-174	3131	2611	1129	435	32620	34662	12835	14570
-193	509	450	249	115	3639	4630	1830	2291
-198	1167	1143	576	282	11821	12963	5546	6882
-205	1160	1043	455	290	8596	8671	3491	4448
-215	460	465	253	162	4391	5272	2126	3364
-231	741	781	455	359				
-255	879	878	591	402	19292	24087	13270	23334
-262	1380	1443	857	679				
-293	602	512	302	207	5005	5032	2217	3204
-309	141	108	52	46	1016	831	320	468
-316	407	378	225	142	3055	3863	1997	2825
-320	373	319	194	130	3620	3978	1891	2552
-346	313	263	129	51	3525	3249	1322	1485
-358					9114	9806	4375	5689
-362	291	288	107	86	4407	4143	1836	2199
-382	1447	1206	524	249	17763	17143	7145	9625
Sum	86704	94567	74615	69876	817216	999161	431473	1107659
Ratio	1.00	1.09	0.86	0.81	1.00	1.22	0.53	1.36

Table AIII.1-1 Adjusted CPD repair in the *MFA2* TS in the wild type PSY316 **a** strain

CPDs position	Experiment 1				Experiment 2			
	Repair time (hours)				Repair time (hours)			
	0	1	2	3	0	1	2	3
2	316	236	97	69	2211	757	1266	574
-16	418	315	199	113	4075	2042	986	908
-37	181	81	38	13	1760	580	545	261
-48	408	300	169	114	4199	2788	1309	1216
-108	1122	930	572	344	8635	7836	7356	3392
-119	717	525	316	207	6981	5843	5673	1770
-133	241	209	155	121	2128	2553	3125	1302
-155	2338	1841	965	413	25687	23231	19691	8992
-164	905	627	318	88	11318	8057	6481	2601
-174	3131	2394	1312	540	32620	28350	24310	10750
-193	509	412	289	143	3639	3787	3466	1690
-198	1167	1048	669	350	11821	10603	10505	5078
-205	1160	956	528	360	8596	7092	6612	3282
-215	460	426	294	201	4391	4312	4027	2482
-231	741	716	529	446				
-255	879	805	687	498	19292	19701	25133	17215
-262	1380	1323	996	843				
-293	602	469	351	257	5005	4115	4200	2364
-309	141	99	60	57	1016	679	607	345
-316	407	346	262	176	3055	3160	3782	2084
-320	373	293	226	161	3620	3254	3582	1882
-346	313	241	150	63	3525	2658	2503	1096
-358					9114	8020	8286	4198
-362	291	264	125	107	4407	3389	3477	1622
-382	1447	1106	609	309	17763	14021	13533	7101

Table AIII.1-1 CPD repair in the *MFA2* TS in the wild type PSY316 **a** strain

CPDs position	Experiment 1					Experiment 2				
	Repair time (hours)				$T_{50\%}$	Repair time (hours)				$T_{50\%}$
	0	1	2	3		0	1	2	3	
2	100	76	31	22	1.6	100	34	57	26	1.4
-16	100	77	48	28	2.0	100	50	24	22	1.0
-37	100	45	21	7	1.0	100	33	31	15	0.9
-48	100	75	42	29	1.8	100	66	31	29	1.4
-108	100	84	52	31	2.2	100	91	85	39	2.7
-119	100	74	45	29	1.9	100	84	81	25	2.4
-133	100	88	65	51	3.0	100	100	100	61	3.2
-155	100	80	42	18	1.8	100	90	76	35	2.6
-164	100	70	36	10	1.6	100	71	57	23	2.0
-174	100	78	43	18	1.8	100	87	74	33	2.4
-193	100	82	58	29	2.2	100	100	95	47	2.8
-198	100	91	58	31	2.4	100	90	88	43	2.8
-205	100	84	46	32	2.1	100	83	77	38	2.6
-215	100	94	65	44	2.7	100	98	91	57	3.2
-231	100	98	73	61	3.4					
-255	100	93	79	58	3.3	100	100	100	89	5.3
-262	100	97	73	62	3.5					
-293	100	79	59	44	2.6	100	82	84	47	2.8
-309	100	72	43	41	1.8	100	67	59	34	1.8
-316	100	86	65	44	2.7	100	100	100	68	3.5
-320	100	80	61	44	2.6	100	90	98	52	3.0
-346	100	78	49	21	2.0	100	75	71	31	2.2
-358						100	88	90	46	2.8
-362	100	92	44	38	2.2	100	77	79	37	2.6
-382	100	78	43	22	1.8	100	79	76	40	2.4

Table AIII.1-2 CPD repair in the *MFA2* NTS in the wild type PSY316 **a** strain

CPDs position	Experiment 1				Experiment 2			
	Repair time (hours)				Repair time (hours)			
	0	1	2	3	0	1	2	3
Top band	76793	73523	64455	43641	895050	694159	466252	983690
-431	3732	3289	1886	823	29608	21314	13047	10735
-369	872	793	523	247	7900	5232	3453	4059
-330	742	656	379	216	6052	4608	2749	2692
-308	3043	2785	1762	869	29628	23207	15023	16927
-275	682	394	274	102	2656	1917	1295	1356
-264	1294	843	501	207	10554	6756	3949	3803
-240	2909	2655	1923	990	29925	23396	17088	22486
-140	229	165	83	42	1670	874	426	504
-137	165	109	59	25	1874	856	241	281
-129	919	775	463	182	12015	7620	3846	4105
-98	1324	1050	469	234	12154	7038	3205	3195
-93	1511	1255	669	284	19511	12309	5656	5690
-88	449	389	203	92	4769	3108	1522	2131
-82	2105	1694	730	272	29008	16281	6289	6013
-72	402	357	172	70	3906	3210	1545	1670
-68	329	279	182	68	2833	2147	1092	1162
-60	202	194	125	48	2108	1322	717	593
-54	266	251	198	106	1399	1078	558	652
-51	398	209	159	65	2533	1480	817	672
-25	1679	1497	1050	590	14333	10860	7306	9769
Sum	100045	93159	76267	49172	1119486	848773	556076	1082186
Ratio	1.00	0.93	0.76	0.49	1.00	0.76	0.50	0.97

Table AIII.1-2 Adjusted CPD repair in the *MFA2* NTS in the wild type PSY316 **a** strain

CPDs position	Experiment 1				Experiment 2			
	Repair time (hours)				Repair time (hours)			
	0	1	2	3	0	1	2	3
-431	3732	3532	2473	1675	29608	28113	26266	11105
-369	872	851	686	502	7900	6900	6952	4199
-330	742	704	497	440	6052	6078	5534	2785
-308	3043	2990	2311	1768	29628	30609	30244	17510
-275	682	423	360	208	2656	2528	2608	1402
-264	1294	905	658	422	10554	8910	7950	3934
-240	2909	2851	2522	2015	29925	30858	34401	23261
-140	229	177	109	86	1670	1153	857	522
-137	165	117	78	50	1874	1129	485	291
-129	919	832	608	369	12015	10051	7743	4247
-98	1324	1128	615	475	12154	9283	6451	3305
-93	1511	1348	878	577	19511	16235	11387	5886
-88	449	418	266	188	4769	4099	3063	2204
-82	2105	1819	957	553	29008	21473	12661	6220
-72	402	383	226	142	3906	4234	3110	1728
-68	329	299	238	138	2833	2832	2198	1202
-60	202	208	164	98	2108	1743	1444	614
-54	266	269	260	216	1399	1422	1124	675
-51	398	224	209	133	2533	1951	1645	695
-25	1679	1608	1378	1199	14333	14324	14708	10106

Table AIII.1-2 signal remaining (%)

CPDs position	Experiment 1					Experiment 2				
	Repair time (hours)				$T_{50\%}$	Repair time (hours)				$T_{50\%}$
	0	1	2	3		0	1	2	3	
-431	100	95	66	45	2.8	100	95	89	38	2.8
-369	100	98	79	58	3.2	100	87	88	53	3.2
-330	100	95	67	59	2.4	100	100	91	46	2.9
-308	100	98	76	58	3.2	100	100	100	59	3.2
-275	100	62	53	31	3.2	100	95	98	53	3.0
-264	100	70	51	33	2.0	100	84	75	37	2.6
-240	100	98	87	69	3.8	100	100	100	78	4.0
-140	100	77	47	37	2.0	100	69	51	31	1.9
-137	100	71	47	30	1.9	100	60	26	16	1.3
-129	100	91	66	40	2.6	100	84	64	35	2.5
-98	100	85	46	36	1.9	100	76	53	27	2.1
-93	100	89	58	38	2.2	100	83	58	30	2.3
-88	100	93	59	42	2.2	100	86	64	46	2.7
-82	100	86	45	26	1.9	100	74	44	21	1.9
-72	100	95	56	35	2.1	100	100	80	44	2.8
-68	100	91	73	42	2.7	100	100	78	42	2.8
-60	100	100	81	48	2.9	100	83	68	29	2.4
-54	100	100	98	81	4.3	100	100	80	48	3.0
-51	100	56	53	33	1.6	100	77	65	27	2.1
-25	100	96	82	71	4.2	100	100	103	71	3.7

Table AIII.1-3 CPD repair in the *MFA2* TS in the wild type PSY316 alpha strain

CPDs position	Experiment 1				Experiment 2			
	Repair time (hours)				Repair time (hours)			
	0	1	2	3	0	1	2	3
Top band	181941	180110	124105	222032	216766	355950	268800	288472
2	542	698	593	731	629	1162	1036	746
-16	936	1075	720	678	1229	2099	1490	806
-37	586	527	220	185	869	967	456	148
-48	1189	958	369	280	1873	1738	895	309
-108	2034	2069	1571	1286	3131	4628	2741	1446
-119	1518	1710	1162	914	2264	3222	1871	955
-133	467	612	624	585	910	1509	999	493
-155	10796	10301	6260	5374	15256	18938	10327	5720
-164	3967	3442	1784	1531	5697	6714	3046	1561
-174	11250	10644	6702	5435	18018	22136	11778	6280
-193	2010	2025	1337	1102	2905	4136	2445	1271
-198	3160	3063	1753	1314	4640	6515	3179	1509
-205	2281	1957	1317	1109	5566	6059	3036	1596
-215	808	821	700	704	1682	2431	1421	808
-231					2633	4173	2781	1927
-255	4820	4984	3963	3831	8569	12526	8133	5816
-262	2056	2219	1910	2060	4011	5443	4057	3291
-293	1396	1130	744	605	2417	2501	1371	851
-309	849	554	222	172	990	882	387	212
-316	729	730	525	427	1266	2060	1227	583
-320	1312	1230	954	818	3248	4057	2157	1330
-346	1453	1215	615	475	2351	2531	1312	718
-358	5358	4912	2674	2076	8035	9808	5378	3087
-362	2963	2737	1772	1525	5778	7028	4020	2526
-382	4783	3558	2108	1588	8844	8826	4250	2202
Sum	249203	243279	164705	256837	329577	498039	348594	334665
Ratio	1.00	0.98	0.66	1.03	1.00	1.51	1.06	1.02

Table AIII.1-3 Adjusted CPD repair in the *MFA2* TS in the wild type PSY316 alpha strain

CPDs position	Experiment 1				Experiment 2			
	Repair time (hours)				Repair time (hours)			
	0	1	2	3	0	1	2	3
2	542	715	897	709	629	769	979	735
-16	936	1102	1090	658	1229	1389	1409	794
-37	586	539	334	180	869	640	431	146
-48	1189	982	558	272	1873	1150	847	304
-108	2034	2120	2378	1248	3131	3063	2591	1424
-119	1518	1751	1758	887	2264	2132	1769	941
-133	467	627	944	568	910	999	945	485
-155	10796	10552	9472	5214	15256	12532	9763	5633
-164	3967	3526	2699	1486	5697	4443	2880	1537
-174	11250	10903	10141	5274	18018	14648	11136	6184
-193	2010	2074	2024	1069	2905	2737	2312	1251
-198	3160	3137	2652	1275	4640	4312	3005	1487
-205	2281	2004	1992	1076	5566	4010	2871	1572
-215	808	841	1059	683	1682	1609	1344	796
-231					2633	2761	2629	1898
-255	4820	5105	5996	3717	8569	8289	7689	5728
-262	2056	2273	2889	1999	4011	3602	3836	3241
-293	1396	1157	1125	587	2417	1655	1297	838
-309	849	568	336	167	990	584	366	209
-316	729	748	794	414	1266	1363	1160	574
-320	1312	1260	1444	794	3248	2685	2039	1310
-346	1453	1245	930	460	2351	1675	1241	707
-358	5358	5031	4047	2015	8035	6490	5085	3040
-362	2963	2804	2681	1480	5778	4651	3800	2488
-382	4783	3644	3190	1541	8844	5840	4018	2169

Table AIII.1-3 Signal remaining (%)

CPDs position	Experiment 1					Experiment 2				
	Repair time (hours)				$T_{50\%}$	Repair time (hours)				$T_{50\%}$
	0	1	2	3		0	1	2	3	
2	100	100	100	100	6.0	100	100	100	100	6.0
-16	100	100	100	70	3.6	100	100	100	65	3.4
-37	100	92	57	31	2.4	100	74	50	17	2.0
-48	100	82	47	23	2.0	100	61	45	16	1.6
-108	100	100	100	61	3.3	100	98	83	45	2.9
-119	100	100	100	58	3.2	100	94	78	42	2.8
-133	100	100	100	100	6.0	100	100	100	53	3.1
-155	100	98	88	48	3.0	100	82	64	37	2.6
-164	100	89	68	37	2.6	100	78	51	27	2.1
-174	100	97	90	47	2.9	100	81	62	34	2.5
-193	100	100	100	53	3.1	100	94	80	43	2.9
-198	100	99	84	40	2.8	100	93	65	32	2.5
-205	100	88	87	47	2.9	100	72	52	28	2.1
-215	100	100	100	85	4.6	100	96	80	47	3.0
-231						100	100	100	72	3.8
-255	100	100	100	77	4.0	100	97	90	67	3.6
-262	100	100	100	97	6.0	100	90	96	81	5.8
-293	100	83	80	42	2.6	100	68	54	35	2.1
-309	100	67	40	20	1.6	100	59	37	21	1.4
-316	100	100	100	57	3.2	100	100	92	45	2.9
-320	100	96	100	61	3.4	100	83	63	40	2.6
-346	100	86	64	32	2.4	100	71	53	30	2.0
-358	100	94	75	38	2.7	100	81	63	38	2.5
-362	100	95	90	50	3.0	100	81	66	43	2.7
-382	100	76	67	32	2.4	100	66	45	25	1.8

Table AIII.1-4 CPD repair in the *MFA2* NTS in the wild type PSY316 alpha strain

CPDs position	Experiment 1				Experiment 2			
	Repair time (hours)				Repair time (hours)			
	0	1	2	3	0	1	2	3
Top band	699630	655033	609804	842720	519291	467914	463188	449416
-431	38193	35468	25835	18899	29726	26707	17094	10396
-369	13219	12845	10748	9339	9322	9567	6596	4332
-330	4400	4100	3431	3025	3048	3037	2267	1704
-308	33707	33333	27425	24921	22323	21909	18323	13537
-275	2047	1783	1278	772	1405	1380	901	493
-264	10357	9979	6600	5121	6591	5737	3445	2285
-240	24694	23055	18879	16823	15080	13549	11238	7654
-140	1609	1817	1508	1409	1149	1249	828	680
-137	815	909	746	572	571	531	483	324
-129	8906	8706	7099	7094	6029	5420	4578	3450
-98	12019	12095	9102	7984	9327	8549	5972	4418
-93	19181	18747	14727	13392	12974	11893	8475	5849
-88	3357	4114	3268	2549	2927	2791	1908	1311
-82	25518	23587	16711	11858	18294	15913	9352	5514
-72	4785	4621	3709	2838	2903	2911	1764	1171
-68	4195	4324	2862	2173	2598	2426	1627	1014
-60	2590	2233	1106	760	1559	1351	671	366
-54	1812	1689	1250	1010	1255	1172	589	435
-51	2196	1139	566	445	1572	960	373	296
-25	15399	11798	6809	4619	9279	7157	3098	1962
Sum	928631	871374	773463	978324	677222	612125	562770	516606
Ratio	1.00	0.94	0.83	1.05	1.00	0.90	0.83	0.76

Table AIII.1-4 Adjusted CPD repair in the *MFA2* NTS in the wild type PSY316 alpha strain

CPDs position	Experiment 1				Experiment 2			
	Repair time (hours)				Repair time (hours)			
	0	1	2	3	0	1	2	3
-431	38193	37798	31018	17939	29726	29548	20570	13628
-369	13219	13689	12904	8864	9322	10585	7937	5679
-330	4400	4369	4119	2871	3048	3360	2727	2234
-308	33707	35523	32927	23656	22323	24239	22050	17746
-275	2047	1900	1534	733	1405	1527	1084	647
-264	10357	10634	7924	4861	6591	6348	4146	2995
-240	24694	24570	22667	15969	15080	14990	13524	10034
-140	1609	1936	1810	1337	1149	1382	996	891
-137	815	969	896	543	571	587	582	425
-129	8906	9278	8523	6734	6029	5996	5509	4522
-98	12019	12890	10928	7579	9327	9458	7186	5792
-93	19181	19979	17682	12712	12974	13157	10198	7667
-88	3357	4384	3923	2420	2927	3088	2296	1718
-82	25518	25137	20063	11256	18294	17606	11254	7228
-72	4785	4925	4454	2694	2903	3220	2123	1535
-68	4195	4608	3436	2062	2598	2684	1958	1330
-60	2590	2380	1328	721	1559	1494	807	479
-54	1812	1800	1500	959	1255	1297	709	570
-51	2196	1214	680	423	1572	1062	449	388
-25	15399	12574	8175	4384	9279	7918	3729	2571

Table AIII.1-4 Signal remaining (%)

CPDs position	Experiment 1					Experiment 2				
	Repair time (hours)				$T_{50\%}$	Repair time (hours)				$T_{50\%}$
	0	1	2	3		0	1	2	3	
-431	100	99	81	47	2.9	100	99	69	46	2.8
-369	100	100	98	67	3.5	100	100	85	61	3.3
-330	100	99	94	65	3.5	100	100	89	73	3.9
-308	100	100	98	70	3.6	100	100	99	79	4.1
-275	100	93	75	36	2.7	100	100	77	46	2.9
-264	100	100	77	47	2.9	100	96	63	45	2.8
-240	100	99	92	65	3.4	100	99	90	67	3.5
-140	100	100	100	83	4.4	100	100	87	78	4.4
-137	100	100	100	67	3.5	100	100	100	74	3.8
-129	100	100	96	76	3.9	100	99	91	75	4.0
-98	100	100	91	63	3.4	100	100	77	62	3.4
-93	100	100	92	66	3.5	100	100	79	59	3.3
-88	100	100	100	72	3.7	100	100	78	59	3.3
-82	100	99	79	44	2.9	100	96	62	40	2.6
-72	100	100	93	56	3.2	100	100	73	53	3.1
-68	100	100	82	49	3.0	100	100	75	51	3.0
-60	100	92	51	28	2.3	100	96	52	31	2.3
-54	100	99	83	53	3.1	100	100	57	45	2.7
-51	100	55	31	19	1.2	100	68	29	25	1.3
-25	100	82	53	28	2.2	100	85	40	28	2.0

Table AIII.1-5 CPD repair in the *MFA2* TS in the *Δtup1* **a** strain

CPDs position	Experiment 1				Experiment 2			
	Repair time (hours)				Repair time (hours)			
	0	1	2	3	0	1	2	3
Top band	95931	74351	76494	130623	282720	289443	263601	420842
2	599	234	60	61	1079	488	100	177
-16	785	287	120	93	1782	881	265	289
-37	281	67	38	43	789	244	62	91
-48	751	432	241	208	1849	1348	614	547
-108	1759	1047	766	753	4022	3561	1861	1461
-119	1296	751	392	299	2980	2328	834	508
-133	436	302	241	237	926	1025	669	540
-155	4403	2587	1415	1080	10744	8546	3253	1974
-164	1993	965	425	278	4403	2792	993	623
-174	5737	3491	1963	1430	12998	10910	4133	2095
-193	481	372	265	208	1754	1526	704	478
-198	2181	1295	933	867	5197	4359	2356	1847
-205	2111	1307	748	655	3944	3377	1540	775
-215	982	639	450	466	2276	2083	1172	966
-231	1496	1060	881	1079	3191	3299	2485	2397
-255	4383	3234	2681	3400	10230	9701	7411	7646
-262	1025	666	559	637	2267	1913	1291	1323
-293	1022	592	383	387	2551	1969	1009	878
-309	238	115	49	42	760	454	147	168
-316	780	557	352	334	1546	1535	867	572
-320	895	629	348	328	1557	1514	766	482
-346	697	388	245	171	1327	995	420	318
-358	1567	971	867	868				
-362	787	476	406	381	1621	1146	370	401
-382	3351	2028	1227	1049	7479	5688	2667	2085
Sum	135965	98842	92549	145978	369994	361126	299590	449483
Ratio	1.00	0.73	0.68	1.07	1.00	0.98	0.81	1.21

Table AIII.1-5 Adjusted CPD repair in the *MFA2* TS in the *Δtup1* **a** strain

CPDs position	Experiment 1				Experiment 2			
	Repair time (hours)				Repair time (hours)			
	0	1	2	3	0	1	2	3
2	599	321	88	57	1079	500	124	146
-16	785	394	177	86	1782	902	328	238
-37	281	93	55	40	789	250	77	75
-48	751	595	354	193	1849	1381	758	450
-108	1759	1440	1126	702	4022	3648	2298	1202
-119	1296	1033	576	278	2980	2385	1029	419
-133	436	415	354	220	926	1050	826	445
-155	4403	3558	2079	1006	10744	8756	4017	1625
-164	1993	1327	625	259	4403	2861	1227	513
-174	5737	4802	2883	1332	12998	11178	5104	1724
-193	481	512	389	194	1754	1564	870	393
-198	2181	1781	1370	808	5197	4466	2910	1520
-205	2111	1798	1099	610	3944	3460	1902	638
-215	982	879	661	434	2276	2134	1447	795
-231	1496	1458	1295	1005	3191	3380	3069	1973
-255	4383	4449	3938	3167	10230	9939	9152	6294
-262	1025	916	821	593	2267	1960	1594	1089
-293	1022	815	563	361	2551	2017	1246	723
-309	238	158	72	39	760	465	182	138
-316	780	767	517	311	1546	1573	1071	471
-320	895	865	511	305	1557	1551	946	397
-346	697	534	361	159	1327	1019	519	262
-358	1567	1336	1273	809				
-362	787	655	597	355	1621	1174	457	330
-382	3351	2790	1803	977	7479	5828	3294	1716

Table AIII.1-5 Signal remaining (%)

CPDs position	Experiment 1					Experiment 2				
	Repair time (hours)				$T_{50\%}$	Repair time (hours)				$T_{50\%}$
	0	1	2	3		0	1	2	3	
2	100	54	15	10	1.0	100	46	12	14	0.9
-16	100	50	23	11	1.0	100	51	18	13	1.0
-37	100	33	20	14	0.8	100	32	10	10	0.7
-48	100	79	47	26	2.0	100	75	41	24	1.8
-108	100	82	64	40	2.6	100	91	57	30	2.4
-119	100	80	44	21	1.9	100	80	35	14	1.8
-133	100	95	81	51	3.0	100	100	90	48	3.0
-155	100	81	47	23	2.0	100	82	38	15	1.8
-164	100	67	31	13	1.4	100	65	28	12	1.4
-174	100	84	50	23	2.1	100	86	39	13	1.9
-193	100	100	81	40	2.8	100	89	50	23	2.2
-198	100	82	63	37	2.5	100	86	56	29	2.4
-205	100	85	52	29	2.2	100	88	48	16	2.1
-215	100	90	67	44	2.8	100	94	64	35	2.6
-231	100	97	87	67	3.6	100	100	97	62	3.4
-255	100	100	90	72	3.8	100	97	90	62	3.4
-262	100	89	80	58	3.4	100	87	71	48	3.0
-293	100	80	55	35	2.3	100	79	49	29	2.1
-309	100	66	30	16	1.4	100	61	24	18	1.2
-316	100	98	66	40	2.6	100	100	70	31	2.6
-320	100	97	57	34	2.4	100	100	61	26	2.4
-346	100	77	52	23	2.0	100	77	39	20	1.8
-358	100	85	81	52	3.1					
-362	100	83	76	45	2.8	100	73	28	20	1.6
-382	100	83	54	29	2.2	100	78	44	23	2.0

Table AIII.1-6 CPD repair in the *MFA2* NTS in the *Δtup1* **a** strain

CPDs position	Experiment 1				Experiment 2			
	Repair time (hours)				Repair time (hours)			
	0	1	2	3	0	1	2	3
Top band	314254	249769	170154	439773	54713	48755	45958	73222
-431	17359	12305	5143	4926	4113	3055	2110	1609
-369	3602	2441	1084	1265	850	594	423	418
-330	3627	2712	1359	2037	699	600	383	354
-308	14027	10467	4944	6131	3325	2731	1913	1899
-275	1275	1007	488	684	343	266	212	238
-264	6440	4265	2258	2370	1305	904	648	488
-240	14308	11357	6438	9839	3449	2619	2085	2498
-140	692	472	148	413	263	174	65	50
-137	694	218	69	223	196	85	31	36
-129	4699	2966	1564	2994	879	579	325	360
-98	9825	6958	2258	3195	1629	969	419	441
-93	6312	4145	1426	1305	1587	1109	641	481
-88	1943	1166	648	1167	272	204	118	72
-82	9346	5465	1495	1160	2079	1239	564	404
-72					359	265	193	143
-68	1839	1349	589	847	267	206	111	82
-60	2235	1570	699	1115	240	156	75	72
-54					239	177	106	154
-51	1051	620	232	319	280	173	88	129
-25	4731	3852	2018	1999	1128	1047	677	682
Sum	418259	323104	203013	481761	78217	65909	57144	83833
Ratio	1.00	0.77	0.49	1.15	1.00	0.84	0.73	1.07

Table AIII.1-6 Adjusted CPD repair in the *MFA2* NTS in the *Δtup1* **a** strain

CPDs position	Experiment 1				Experiment 2			
	Repair time (hours)				Repair time (hours)			
	0	1	2	3	0	1	2	3
-431	17359	15928	10595	4276	4113	3626	2888	1501
-369	3602	3160	2234	1098	850	705	579	390
-330	3627	3511	2799	1769	699	712	524	331
-308	14027	13549	10186	5322	3325	3240	2618	1772
-275	1275	1303	1005	593	343	315	290	222
-264	6440	5522	4651	2058	1305	1073	886	456
-240	14308	14701	13263	8542	3449	3108	2854	2331
-140	692	610	305	358	263	207	89	47
-137	694	282	141	194	196	101	43	34
-129	4699	3839	3223	2600	879	687	445	335
-98	9825	9007	4652	2774	1629	1150	574	412
-93	6312	5366	2938	1133	1587	1316	877	449
-88	1943	1509	1334	1013	272	242	162	67
-82	9346	7075	3080	1007	2079	1471	771	377
-72					359	315	264	133
-68	1839	1746	1214	735	267	245	152	77
-60	2235	2032	1440	968	240	185	103	67
-54					239	210	145	144
-51	1051	803	479	277	280	205	120	120
-25	4731	4987	4158	1736	1128	1242	926	636

Table AIII.1-6 Signal remaining (%)

CPDs Position	Experiment 1					Experiment 2				
	Repair time (hours)				$T_{50\%}$	Repair time (hours)				$T_{50\%}$
	0	1	2	3		0	1	2	3	
-431	100	92	61	25	2.4	100	88	70	36	2.6
-369	100	88	62	30	2.4	100	83	68	46	2.8
-330	100	97	77	49	2.9	100	100	75	47	2.9
-308	100	97	73	38	2.7	100	97	79	53	3.0
-275	100	100	79	47	2.9	100	92	85	65	3.7
-264	100	86	72	32	2.6	100	82	68	35	2.5
-240	100	100	93	60	3.2	100	90	83	68	4.1
-140	100	88	44	52	1.9	100	79	34	18	1.7
-137	100	41	20	28	0.8	100	52	22	17	1.0
-129	100	82	69	55	3.5	100	78	51	38	2.1
-98	100	92	47	28	2.2	100	71	35	25	1.6
-93	100	85	47	18	2.0	100	83	55	28	2.2
-88	100	78	69	52	3.3	100	89	60	25	2.3
-82	100	76	33	11	1.6	100	71	37	18	1.6
-72						100	88	73	37	2.6
-68	100	95	66	40	2.7	100	92	57	29	2.4
-60	100	91	64	43	2.7	100	77	43	28	1.9
-54						100	88	61	60	3.3
-51	100	76	46	26	1.9	100	73	43	43	1.8
-25	100	100	88	37	2.8	100	100	82	56	3.1

Table AIII.1-7 CPD repair in the *MFA2* TS in the *Δtup1* alpha strain

CPDs position	Experiment 1				Experiment 2			
	Repair time (hours)				Repair time (hours)			
	0	1	2	3	0	1	2	3
Top band	203625	211777	264891	242152	872029	1225450	1221802	1103937
2	528	138	102	128	6300	2747	1162	434
-16	704	112	90	78	4968	1547	717	586
-37	464	92	121	149	2775	1051	779	1282
-48	924	176	219	170	5337	2456	780	894
-108	2208	1007	418	453	9282	6278	1933	1838
-119	1622	468	82	159	7319	3359	1170	591
-133	508	228	36	117	4936	2848	1314	633
-155	5411	1456	313	189	22059	10608	2938	1790
-164	2309	473	230	193	8883	3491	1485	1040
-174	6519	1559	322	243	30780	12536	3096	2309
-193	1134	356	125	80	8430	5303	3001	2137
-198	2819	810	194	131	13739	7804	2755	1899
-205	1543	363	180	112	8995	3303	1327	1002
-215	892	565	470	417	6516	4355	2819	3164
-231	1460	1135	830	482	8540	7988	4016	2228
-255	4791	3659	2217	1329	20409	25251	14334	6568
-262	1207	865	622	481	4468	4452	2456	1094
-293	1412	520	600	670	4976	4365	2963	2860
-309	467	114	191	115	1696	686	474	577
-316	629	188	172	199	2907	2598	1311	613
-320	631	244	138	119	4568	3393	2537	1373
-346	625	248	281	235	2730	780	683	569
-358	2275	690	289	192	9519	5945	2905	2410
-362	1710	454	205	242	6959	2382	870	950
-382	3365	873	503	281	15590	6867	2794	2515
Sum	249782	228570	273838	249116	1094712	1357842	1282422	1145292
Ratio	1.00	0.92	1.10	1.00	1.00	1.24	1.17	1.05

Table AIII.1-7 Adjusted CPD repair in the *MFA2* TS in the *Δtup1* alpha strain

CPDs position	Experiment 1				Experiment 2			
	Repair time (hours)				Repair time (hours)			
	0	1	2	3	0	1	2	3
2	528	151	93	129	6300	2214	992	415
-16	704	122	82	78	4968	1247	612	560
-37	464	101	111	149	2775	847	665	1225
-48	924	192	199	170	5337	1980	666	855
-108	2208	1100	381	454	9282	5062	1650	1757
-119	1622	512	74	160	7319	2708	999	565
-133	508	249	33	117	4936	2296	1122	605
-155	5411	1591	285	189	22059	8553	2508	1711
-164	2309	517	210	193	8883	2814	1267	994
-174	6519	1703	293	244	30780	10107	2643	2207
-193	1134	389	114	80	8430	4275	2562	2042
-198	2819	885	177	131	13739	6291	2352	1815
-205	1543	397	164	112	8995	2663	1133	958
-215	892	617	429	418	6516	3511	2406	3025
-231	1460	1240	757	483	8540	6440	3428	2129
-255	4791	3999	2022	1333	20409	20358	12236	6278
-262	1207	945	567	483	4468	3589	2096	1046
-293	1412	568	547	672	4976	3519	2529	2733
-309	467	125	174	115	1696	553	405	551
-316	629	206	157	199	2907	2094	1119	586
-320	631	267	126	120	4568	2736	2165	1312
-346	625	271	256	235	2730	629	583	544
-358	2275	754	263	193	9519	4793	2480	2304
-362	1710	497	187	242	6959	1921	743	908
-382	3365	954	459	281	15590	5536	2385	2404

Table AIII.1-7 Signal remaining (%)

CPDs Position	Experiment 1					Experiment 2				
	Repair time (hours)				$T_{50\%}$	Repair time (hours)				$T_{50\%}$
	0	1	2	3		0	1	2	3	
2	100	29	18	24	0.7	100	35	16	7	0.8
-16	100	17	12	11	0.5	100	25	12	11	0.7
-37	100	22	24	32	0.6	100	31	24	44	0.7
-48	100	21	22	18	0.6	100	37	12	16	0.8
-108	100	50	17	21	1.1	100	55	18	19	1.1
-119	100	32	5	10	0.7	100	37	14	8	0.8
-133	100	49	7	23	1	100	47	23	12	1
-155	100	29	5	3	0.7	100	39	11	8	0.8
-164	100	22	9	8	0.6	100	32	14	11	0.7
-174	100	26	4	4	0.6	100	33	9	7	0.7
-193	100	34	10	7	0.8	100	51	30	24	1.1
-198	100	31	6	5	0.7	100	46	17	13	0.9
-205	100	26	11	7	0.6	100	30	13	11	0.7
-215	100	69	48	47	2	100	54	37	46	1.4
-231	100	85	52	33	2.2	100	75	40	25	1.8
-255	100	83	42	28	1.9	100	100	60	31	2.4
-262	100	78	47	40	2	100	80	47	23	2.1
-293	100	40	39	48	1.7	100	71	51	55	2.2
-309	100	27	37	25	0.6	100	33	24	33	0.8
-316	100	33	25	32	1.4	100	72	38	20	1.7
-320	100	42	20	19	1.4	100	60	47	29	1.8
-346	100	43	41	38	0.9	100	23	21	20	0.7
-358	100	33	12	8	0.8	100	50	26	24	1
-362	100	29	11	14	0.7	100	28	11	13	0.8
-382	100	28	14	8	0.7	100	36	15	15	0.8

Table AIII.1-8 CPD repair in the *MFA2* NTS in the *Δtup1* alpha strain

CPDs position	Experiment 1				Experiment 2			
	Repair time (hours)				Repair time (hours)			
	0	1	2	3	0	1	2	3
Top band	316413	297962	329370	379473	679185	926436	957147	1015311
-431	12705	4319	830	600	60453	35857	10176	6638
-369	3606	1455	452	290	15016	10961	4027	2564
-330	2002	672	295	161	5913	4332	2112	2291
-308	9371	3132	749	557	36295	20432	5961	4286
-275	885	285	188	337	2741	1564	834	1189
-264	2974	793	143	80	10682	3941	1135	1175
-240	8853	6175	2886	2192	28604	32129	19473	13743
-140	352	89	96	129	1739	773	540	853
-137	482	114	106	84	1974	563	557	736
-129	2681	686	144	167	9557	3948	1034	533
-98	3272	889	235	202	13936	5282	1728	1051
-93	4596	1503	392	420	18346	9253	2976	1928
-88	846	338	127	178	3718	2206	1076	1092
-82	6884	1686	474	413	24309	10221	2980	2171
-72	976	598	150	147	4528	2901	1073	882
-68	708	311	168	152	2794	2015	1116	1203
-60	686	231	107	76	1900	1147	409	323
-54	724	515	93	226	2314	1916	974	905
-51	755	222	120	124	1390	646	356	289
-25	4187	2091	795	729	16354	11561	4843	3119
Sum	383957	324066	337919	386736	941750	1088083	1020527	1062283
Ratio	1.00	0.84	0.88	1.01	1.00	1.16	1.08	1.13

Table AIII.1-8 Adjusted CPD repair in the *MFA2* NTS in the *Δtup1* alpha strain

CPDs position	Experiment 1				Experiment 2			
	Repair time (hours)				Repair time (hours)			
	0	1	2	3	0	1	2	3
-431	12705	5117	943	596	60453	31035	9391	5885
-369	3606	1723	514	288	15016	9487	3716	2273
-330	2002	796	335	160	5913	3749	1949	2031
-308	9371	3711	850	553	36295	17684	5501	3800
-275	885	337	214	335	2741	1354	770	1054
-264	2974	939	163	79	10682	3411	1048	1041
-240	8853	7317	3280	2176	28604	27808	17970	12184
-140	352	105	109	128	1739	669	498	756
-137	482	135	120	84	1974	487	514	652
-129	2681	813	164	166	9557	3417	954	473
-98	3272	1053	267	200	13936	4572	1595	932
-93	4596	1781	446	417	18346	8009	2746	1709
-88	846	401	144	177	3718	1909	993	968
-82	6884	1998	538	410	24309	8846	2750	1925
-72	976	708	171	146	4528	2511	990	782
-68	708	369	191	151	2794	1744	1030	1067
-60	686	273	122	75	1900	992	377	287
-54	724	610	106	225	2314	1658	899	802
-51	755	263	136	123	1390	559	328	256
-25	4187	2477	903	723	16354	10006	4469	2765

Table AIII.1-8 Signal remaining (%)

CPDs position	Experiment 1					Experiment 2				
	Repair time (hours)				$T_{50\%}$	Repair time (hours)				$T_{50\%}$
	0	1	2	3		0	1	2	3	
-431	100	40	7	5	0.8	100	51	16	10	1.0
-369	100	48	14	8	1.0	100	63	25	15	1.2
-330	100	40	17	8	0.8	100	63	33	34	1.3
-308	100	40	9	6	0.8	100	49	15	10	1.0
-275	100	38	24	38	0.8	100	49	28	38	1.0
-264	100	32	5	3	0.7	100	32	10	10	0.7
-240	100	83	37	25	2.0	100	97	63	43	2.6
-140	100	30	31	36	0.6	100	38	29	43	0.8
-137	100	28	25	17	0.6	100	25	26	33	0.7
-129	100	30	6	6	0.7	100	36	10	5	0.8
-98	100	32	8	6	0.7	100	33	11	7	0.7
-93	100	39	10	9	0.8	100	44	15	9	0.9
-88	100	47	17	21	1.0	100	51	27	26	1.0
-82	100	29	8	6	0.7	100	36	11	8	0.8
-72	100	73	18	15	1.4	100	55	22	17	1.1
-68	100	52	27	21	1.1	100	62	37	38	1.4
-60	100	40	18	11	0.6	100	52	20	15	1.0
-54	100	84	15	31	1.6	100	72	39	35	1.7
-51	100	35	18	16	0.7	100	40	24	18	0.9
-25	100	59	22	17	1.3	100	61	27	17	1.2

Table AIII.1-9 CPD repair in the *MFA2* TS in the *Δtup1mfa2*^{TATA} alpha strain

CPDs position	Experiment 1				Experiment 2			
	Repair time (hours)				Repair time (hours)			
	0	1	2	3	0	1	2	3
Top band	238941	254664	278464	351233	1092330	862806	1048805	1045568
2	677	315	98	130	10895	5531	1930	993
-16	931	450	168	151	6190	3002	1024	392
-37	842	296	124	81	3689	1390	431	286
-48	1483	686	357	318	8541	4028	1818	1098
-108	1908	768	288	342	8272	2587	1068	408
-119	1126	598	289	181	4463	1776	798	202
-133	500	461	314	257	9714	5121	2456	936
-155	7907	5150	2009	1088	38605	19524	9195	3272
-164	3517	1769	542	320	16950	6454	2602	1118
-174	9701	5756	1650	851	52870	24811	9227	3660
-193	2114	1278	487	288	13973	7294	3338	1700
-198	4433	2700	992	647	23245	11001	4982	2051
-205	2335	1252	477	290	15470	6531	2506	1013
-215	1438	1262	639	689	9957	5559	2817	1642
-231	2259	2331	1524	1187	14296	8450	6711	4274
-255	7004	6705	4946	4915	33105	22847	21850	13148
-262	1858	1787	1298	1100	7613	5110	4204	1706
-293	1767	1328	778	910	8767	3539	2276	1497
-309	656	300	95	80	3544	1055	439	329
-316	610	570	195	284	4749	2224	1231	620
-320	768	658	303	329	7399	3353	2337	1765
-346	539	312	202	396	5794	2193	907	355
-358	3870	2141	860	661	16320	7515	4389	2322
-362	2591	1307	448	553	11754	4499	1948	1167
-382	5398	2796	1105	790	25754	9724	4983	2227
Sum	305175	297640	298653	368073	1454261	1037924	1144272	1093748
Ratio	1.00	0.98	0.98	1.21	1.00	0.71	0.79	0.75

Table AIII.1-9 Adjusted CPD repair in the *MFA2* TS in the *Δtup1mfa2*^{TATA} alpha strain

CPDs position	Experiment 1				Experiment 2			
	Repair time (hours)				Repair time (hours)			
	0	1	2	3	0	1	2	3
2	677	323	100	108	10895	7750	2453	1320
-16	931	461	172	126	6190	4207	1301	521
-37	842	303	126	67	3689	1947	548	380
-48	1483	704	365	264	8541	5643	2310	1460
-108	1908	788	294	284	8272	3625	1357	543
-119	1126	614	295	150	4463	2488	1014	269
-133	500	473	321	213	9714	7175	3121	1244
-155	7907	5280	2053	902	38605	27356	11686	4351
-164	3517	1814	554	265	16950	9043	3307	1486
-174	9701	5901	1686	705	52870	34763	11726	4866
-193	2114	1311	498	239	13973	10220	4242	2260
-198	4433	2768	1014	537	23245	15413	6332	2727
-205	2335	1283	487	241	15470	9151	3185	1347
-215	1438	1294	653	572	9957	7789	3580	2183
-231	2259	2390	1557	984	14296	11839	8529	5683
-255	7004	6875	5054	4075	33105	32012	27769	17482
-262	1858	1832	1327	912	7613	7160	5343	2269
-293	1767	1361	795	755	8767	4959	2893	1990
-309	656	308	97	67	3544	1478	558	437
-316	610	585	200	235	4749	3115	1565	824
-320	768	674	310	272	7399	4698	2970	2347
-346	539	320	207	328	5794	3073	1153	472
-358	3870	2195	878	548	16320	10529	5578	3087
-362	2591	1340	457	459	11754	6304	2475	1552
-382	5398	2867	1129	655	25754	13625	6333	2961

Table AIII.1-9 Signal remaining (%)

CPDs position	Experiment 1					Experiment 2				
	Repair time (hours)				$T_{50\%}$	Repair time (hours)				$T_{50\%}$
	0	1	2	3		0	1	2	3	
2	100	48	15	16	0.9	100	71	23	12	1.3
-16	100	50	18	13	1.0	100	68	21	8	1.3
-37	100	36	15	8	0.8	100	53	15	10	1.0
-48	100	47	25	18	1.0	100	66	27	17	1.3
-108	100	41	15	15	0.8	100	44	16	7	0.9
-119	100	55	26	13	1.1	100	56	23	6	1.1
-133	100	95	64	43	2.7	100	74	32	13	1.6
-155	100	67	26	11	1.3	100	71	30	11	1.5
-164	100	52	16	8	1.0	100	53	20	9	1.0
-174	100	61	17	7	1.1	100	66	22	9	1.2
-193	100	62	24	11	1.2	100	73	30	16	1.5
-198	100	62	23	12	1.2	100	66	27	12	1.3
-205	100	55	21	10	1.1	100	59	21	9	1.1
-215	100	90	45	40	2.0	100	78	36	22	1.8
-231	100	100	69	44	2.8	100	83	60	40	2.5
-255	100	98	72	58	3.2	100	97	84	53	3.1
-262	100	99	71	49	2.9	100	94	70	30	2.6
-293	100	77	45	43	1.8	100	57	33	23	1.3
-309	100	47	15	10	0.9	100	42	16	12	0.8
-316	100	96	33	39	1.8	100	66	33	17	1.4
-320	100	88	40	35	1.9	100	63	40	32	1.6
-346	100	59	38	61	1.2	100	53	20	8	1.1
-358	100	57	23	14	1.1	100	65	34	19	1.4
-362	100	52	18	18	1.0	100	54	21	13	1.0
-382	100	53	21	12	1.1	100	53	25	11	1.1

Table AIII.1-10 CPD repair in the *MFA2* NTS in the *Δtup1mfa2*^{TATA} alpha strain

CPDs position	Experiment 1				Experiment 2			
	Repair time (hours)				Repair time (hours)			
	0	1	2	3	0	1	2	3
Top band	366315	368106	392806	404687	884824	707475	833294	853640
-431	14721	13083	6251	3105	100374	58858	35202	14520
-369	4267	3609	2061	1263	25180	14819	10085	4643
-330	2290	1750	614	427	11090	5828	2766	1615
-308	11771	8675	3259	1713	62332	35680	16768	7370
-275	1054	858	406	302	4679	2595	1362	773
-264	3593	2349	874	475	16308	8940	4221	1868
-240	11034	9519	5107	3714	46197	29813	21003	12201
-140	355	314	195	275	2719	1516	680	714
-137	656	188	104	224	3467	1001	366	483
-129	3854	2169	666	366	15186	7542	3042	1343
-98	4460	2749	952	479	20843	9963	4362	1883
-93	6655	4646	1597	943	28925	15136	6771	2982
-88	1321	922	382	289	5787	3141	1546	883
-82	10201	5547	1531	941	41020	16906	6482	2703
-72	893	819	385	346	6206	3158	1572	810
-68	721	657	305	348	4391	2144	1223	705
-60	855	433	182	185	2811	1035	466	238
-54	918	670	432	404	3457	1891	1071	712
-51	971	367	176	98	2038	502	241	165
-25	6329	4379	1885	1201	24589	12735	6608	3225
Sum	453233	431809	420172	421784	1312422	940679	959132	913476
Ratio	1.00	0.95	0.93	0.93	1.00	0.72	0.73	0.70

Table AIII.1-10 Adjusted CPD repair in the *MFA2* NTS in the *Δtup1mfa2*^{TATA} alpha strain

CPDs position	Experiment 1				Experiment 2			
	Repair time (hours)				Repair time (hours)			
	0	1	2	3	0	1	2	3
-431	14721	13733	6743	3336	100374	82118	48169	20862
-369	4267	3788	2223	1357	25180	20675	13800	6671
-330	2290	1837	662	458	11090	8131	3784	2321
-308	11771	9105	3515	1841	62332	49781	22945	10589
-275	1054	900	437	324	4679	3620	1863	1110
-264	3593	2465	943	510	16308	12472	5776	2685
-240	11034	9991	5509	3991	46197	41595	28739	17530
-140	355	330	211	296	2719	2116	930	1026
-137	656	198	112	241	3467	1397	500	693
-129	3854	2276	718	393	15186	10523	4163	1930
-98	4460	2885	1027	515	20843	13901	5969	2705
-93	6655	4876	1722	1014	28925	21117	9265	4284
-88	1321	968	412	310	5787	4382	2116	1269
-82	10201	5823	1651	1011	41020	23587	8870	3883
-72	893	860	415	372	6206	4406	2151	1163
-68	721	690	329	374	4391	2991	1674	1013
-60	855	454	197	199	2811	1444	637	342
-54	918	703	466	434	3457	2639	1466	1023
-51	971	385	190	105	2038	700	330	237
-25	6329	4596	2034	1291	24589	17767	9042	4633

Table AIII.1-10 Signal remaining (%)

CPDs position	Experiment 1					Experiment 2				
	Repair time (hours)				$T_{50\%}$	Repair time (hours)				$T_{50\%}$
	0	1	2	3		0	1	2	3	
-431	100	93	46	23	2.1	100	82	48	21	2
-369	100	89	52	32	2.2	100	82	55	26	2.2
-330	100	80	29	20	1.6	100	73	34	21	1.6
-308	100	77	30	16	1.6	100	80	37	17	1.8
-275	100	85	42	31	2.0	100	77	40	24	1.8
-264	100	69	26	14	1.4	100	76	35	16	1.7
-240	100	91	50	36	2.0	100	90	62	38	2.5
-140	100	93	59	83	2.2	100	78	34	38	1.8
-137	100	30	17	37	0.7	100	40	14	20	0.8
-129	100	59	19	10	1.1	100	69	27	13	1.4
-98	100	65	23	12	1.3	100	67	29	13	1.4
-93	100	73	26	15	1.4	100	73	32	15	1.6
-88	100	73	31	23	1.6	100	76	37	22	1.7
-82	100	57	16	10	1.1	100	58	22	9	1.1
-72	100	96	47	42	2.0	100	71	35	19	1.6
-68	100	96	46	52	2.0	100	68	38	23	1.6
-60	100	53	23	23	1.1	100	51	23	12	1
-54	100	77	51	47	2.0	100	76	42	30	1.9
-51	100	40	20	11	0.8	100	34	16	12	0.8
-25	100	73	32	20	1.6	100	72	37	19	1.6

Table AIII.1-11 CPD repair in the *MFA2* TS in the wild type PSY316 alpha strain (70J/m^2)

CPDs position	Experiment 1					Experiment 2				
	Repair time (hours)					Repair time (hours)				
	0	0.5	1	2	3	0	0.5	1	2	3
Top band	1659915	1675877	1617953	1692241	1749976	287048	299071	278248	369304	362047
2	8426	8857	8247	5551	2657	941	1041	1031	767	392
-16	6767	6457	5466	2773	906	1092	1156	1019	505	224
-37	10296	7629	4002	1595	798					
-48	2375	2060	1433	1678	12					
-108	11327	10410	7192	2505	1116	2886	2698	1685	601	210
-119	8825	8446	5950	2337	950	2056	1781	1233	422	148
-133	7221	7596	5773	3477	1549	1026	844	626	213	167
-155	56540	50940	30439	12074	4321	12864	11539	6962	2922	935
-164	18341	15873	9058	2535	784	4755	3743	1883	599	204
-174	66366	59327	34847	11453	3226	15644	13202	7507	2604	700
-193	11864	11684	8666	3373	2084	3127	2955	1970	693	194
-198	16550	16075	10422	2999	630	3439	3198	1976	567	127
-205	17158	15048	7927	1615	721	4832	4068	2021	450	167
-215	5925	5883	3542	1112	1151	1514	1309	745	288	214
-231	9412	9039	7140	3842	2130	2390	2427	1632	807	241
-255	26031	24852	20088	10750	4519	6519	6549	4614	2835	1053
-262	9718	9127	8365	6301	3226	2078	2137	1691	1510	718
-293	6002	4948	3730	1369	877	1326	1141	697	242	147
-309	3405	2794	1929	975	594					
-316	3352	3299	2259	579	260	1403	1200	701	225	77
-320	6687	6405	4252	2037	1419	2500	2163	1259	423	181
-346	4745	3793	2431	672	209	1297	976	615	245	135
-358	18729	15489	9863	3258	1373	4768	4189	2428	831	355
-362	11634	9939	7123	2694	1323	3680	3234	2001	849	417
-382	19252	12893	6557	1932	1105	4162	3031	1429	410	235
Sum	2026862	2004740	1834654	1781724	1787917	371347	373650	323973	388313	369286
Ratio	1.00	0.99	0.91	0.88	0.88	1.00	1.01	0.87	1.05	0.99

Table AIII.1-11 Adjusted CPD repair in the *MFA2* TS in the wild type PSY316 alpha strain (70J/m^2)

CPDs position	Experiment 1					Experiment 2				
	Repair time (hours)					Repair time (hours)				
	0	0.5	1	2	3	0	0.5	1	2	3
2	8426	8955	9111	6314	3012	941	1034	1181	733	394
-16	6767	6528	6038	3155	1027	1092	1149	1168	483	225
-37	10296	7713	4422	1814	905	0	0	0	0	0
-48	2375	2083	1583	1908	14	0	0	0	0	0
-108	11327	10525	7946	2849	1265	2886	2681	1931	575	211
-119	8825	8539	6573	2658	1077	2056	1770	1414	403	149
-133	7221	7680	6378	3956	1756	1026	838	717	203	168
-155	56540	51502	33628	13735	4899	12864	11468	7980	2794	940
-164	18341	16048	10007	2884	889	4755	3720	2158	573	205
-174	66366	59982	38498	13028	3657	15644	13121	8604	2491	704
-193	11864	11813	9574	3837	2363	3127	2937	2258	662	195
-198	16550	16253	11514	3411	714	3439	3178	2265	543	128
-205	17158	15215	8757	1838	817	4832	4043	2316	430	168
-215	5925	5948	3913	1265	1305	1514	1301	854	275	215
-231	9412	9139	7889	4370	2415	2390	2412	1871	772	243
-255	26031	25126	22192	12229	5123	6519	6509	5289	2711	1059
-262	9718	9228	9241	7168	3658	2078	2124	1938	1444	722
-293	6002	5003	4121	1557	994	1326	1134	799	231	148
-309	3405	2824	2132	1110	673	0	0	0	0	0
-316	3352	3335	2496	658	295	1403	1193	804	215	77
-320	6687	6476	4698	2317	1608	2500	2150	1444	405	182
-346	4745	3835	2686	765	237	1297	970	705	234	135
-358	18729	15660	10896	3706	1557	4768	4163	2783	795	357
-362	11634	10048	7869	3064	1500	3680	3214	2294	812	419
-382	19252	13036	7243	2198	1253	4162	3012	1638	392	236

Table AIII.1-11 Signal remaining (%)

CPDs position	Experiment 1						Experiment 2					
	Repair time (hours)					$T_{50\%}$	Repair time (hours)					$T_{50\%}$
	0	0.5	1	2	3		0	0.5	1	2	3	
2	100	100	100	75	36	2.7	100	100	100	78	42	2.8
-16	100	96	89	47	15	2.1	100	100	100	44	21	2.2
-37	100	75	43	18	9	0.9						
-48	100	88	67	80	1	2.2						
-108	100	93	70	25	11	1.4	100	93	67	20	7	1.3
-119	100	97	74	30	12	1.6	100	86	69	20	7	1.4
-133	100	100	88	55	24	2.2	100	82	70	20	16	1.3
-155	100	91	59	24	9	1.3	100	89	62	22	7	1.3
-164	100	87	55	16	5	1.1	100	78	45	12	4	1.0
-174	100	90	58	20	6	1.2	100	84	55	16	5	1.1
-193	100	100	81	32	20	1.6	100	94	72	21	6	1.4
-198	100	98	70	21	4	1.4	100	92	66	16	4	1.3
-205	100	89	51	11	5	1.0	100	84	48	9	3	1.0
-215	100	100	66	21	22	1.4	100	86	56	18	14	1.1
-231	100	97	84	46	26	2.1	100	100	78	32	10	1.8
-255	100	97	85	47	20	2.1	100	100	81	42	16	1.9
-262	100	95	95	74	38	2.6	100	100	93	70	35	2.6
-293	100	83	69	26	17	1.4	100	85	60	17	11	1.2
-309	100	83	63	33	20	1.4						
-316	100	99	74	20	9	1.5	100	85	57	15	6	1.1
-320	100	97	70	35	24	1.7	100	86	58	16	7	1.2
-346	100	81	57	16	5	1.1	100	75	54	18	10	1.0
-358	100	84	58	20	8	1.2	100	87	58	17	7	1.2
-362	100	86	68	26	13	1.4	100	87	62	22	11	1.3
-382	100	68	38	11	7	0.8	100	72	39	9	6	0.8

Table AIII.1-12 CPD repair in the *MFA2* NTS in the wild type PSY316 alpha strain (70J/m^2)

CPDs position	Experiment 1					Experiment 2				
	Repair time (hours)					Repair time (hours)				
	0	0.5	1	2	3	0	0.5	1	2	3
Top band	1354465	1313082	1342808	1394795	1409901	531331	497552	503858	522027	601278
-431	82002	76264	63269	30597	11820	26253	21487	17174	7464	2495
-369	24789	23399	21665	11608	4033	8293	6989	5885	2836	1183
-330	7956	7627	7827	4698	2555	2415	2123	1880	943	599
-308	62760	61314	58237	40476	20192	19869	16650	14915	9758	5040
-275	3887	3675	2990	1387	912					
-264	20567	18804	15937	6296	1717	7345	6701	5204	1662	316
-240	40073	38164	34747	23582	12344	10684	9359	8363	5352	2727
-140	2026	2094	2022	1296	872					
-137	1211	993	798	419	420					
-129	12143	11344	9961	7653	5082	3515	3069	2930	2467	1909
-98	15970	15098	13152	7967	3721	7683	6636	5642	3397	1918
-93	28056	26138	22933	13057	6079	9604	8442	7430	4037	1971
-88	4306	4231	3914	1941	983	1782	1686	1422	687	426
-82	36713	33446	23778	6368	2149	11651	10077	7426	1913	767
-72	6271	5798	4445	1267	632	3306	2724	2078	539	275
-68	5270	4475	3615	1128	645	1576	1427	1001	375	272
-60	3002	2553	1588	331	236					
-54						1812	1190	841	302	363
-51	1865	1337	603	490	1045					
-25	21244	15651	9268	2432	1520	5552	3779	2128	551	445
Sum	1734576	1665487	1643558	1557787	1486857	652672	599894	588177	564311	621984
Ratio	1.00	0.96	0.95	0.90	0.86	1.00	0.92	0.90	0.86	0.95

Table AIII.1-12 Adjusted CPD repair in the *MFA2* NTS in the wild type PSY316 alpha strain ($70J/m^2$)

CPDs position	Experiment 1					Experiment 2				
	Repair time (hours)					Repair time (hours)				
	0	0.5	1	2	3	0	0.5	1	2	3
-431	82002	79427	66772	34070	13789	26253	23378	19057	8633	2618
-369	24789	24369	22865	12926	4705	8293	7604	6530	3280	1242
-330	7956	7943	8260	5232	2981	2415	2310	2087	1091	629
-308	62760	63858	61462	45069	23556	19869	18115	16551	11286	5288
-275	3887	3828	3156	1544	1064	0	0	0	0	0
-264	20567	19584	16820	7010	2003	7345	7291	5774	1922	331
-240	40073	39747	36671	26258	14401	10684	10183	9280	6190	2862
-140	2026	2181	2134	1443	1017	0	0	0	0	0
-137	1211	1035	842	467	490	0	0	0	0	0
-129	12143	11814	10512	8521	5929	3515	3339	3251	2853	2003
-98	15970	15724	13880	8871	4341	7683	7220	6261	3929	2013
-93	28056	27222	24203	14538	7091	9604	9184	8244	4669	2068
-88	4306	4407	4131	2161	1147	1782	1834	1578	794	447
-82	36713	34834	25095	7091	2507	11651	10964	8240	2213	805
-72	6271	6039	4692	1410	738	3306	2964	2306	624	289
-68	5270	4661	3815	1256	752	1576	1553	1111	434	285
-60	3002	2659	1676	369	276	0	0	0	0	0
-54						1812	1295	933	350	381
-51	1865	1392	637	546	1219	0	0	0	0	0
-25	21244	16300	9782	2708	1773	5552	4112	2362	637	467

Table AIII.1-12 Signal remaining (%)

CPDs position	Experiment 1						Experiment 2					
	Repair time (hours)					$T_{50\%}$	Repair time (hours)					$T_{50\%}$
	0	0.5	1	2	3		0	0.5	1	2	3	
-431	100	97	81	42	17	1.9	100	89	73	33	10	1.6
-369	100	98	92	52	19	2.2	100	92	79	40	15	1.8
-330	100	100	100	66	38	2.6	100	96	86	45	26	2.1
-308	100	100	98	72	38	2.6	100	91	83	57	27	2.2
-275	100	98	81	40	27	2.0						
-264	100	95	82	34	10	1.8	100	99	79	26	5	1.6
-240	100	99	92	66	36	2.6	100	95	87	58	27	2.4
-140	100	100	100	71	50	3.0						
-137	100	85	70	39	41	1.6						
-129	100	97	87	70	49	3.0	100	95	92	81	57	3.2
-98	100	98	87	56	27	2.2	100	94	81	51	26	2.1
-93	100	97	86	52	25	2.2	100	96	86	49	22	2.2
-88	100	100	96	50	27	2.3	100	100	89	45	25	2.2
-82	100	95	68	19	7	1.4	100	94	71	19	7	1.4
-72	100	96	75	23	12	1.5	100	90	70	19	9	1.4
-68	100	88	72	24	14	1.4	100	99	70	28	18	1.6
-60	100	89	56	12	9	1.1						
-54	100						100	71	51	19	21	1.0
-51	100	75	34	29	65	0.8						
-25	100	77	46	13	8	0.9	100	74	43	11	8	0.9

Table AIII.1-13 CPD repair in the *MFA2* TS in the *Δtup1*alpha strain (70J/m^2)

CPDs position	Experiment 1					Experiment 2				
	Repair time (hours)					Repair time (hours)				
	0	0.5	1	2	3	0	0.5	1	2	3
Top band	1117898	1283818	1601394	1546952	1496676	263125	281611	331723	333215	318192
2	4796	3942	2172	1219	806	841	391	98	134	49
-16	3042	2399	1033	714	694	958	539	200	173	159
-37	4217	4078	2252	932	341					
-48	1080	1274	968	391	2404					
-108	7537	6464	4345	1555	881	2641	2019	1107	370	167
-119	5517	4258	2592	644	648	1899	1300	661	267	88
-133	3165	2723	1856	565	591	776	565	418	160	130
-155	14421	11604	5817	1296	1238	5487	3560	1494	256	182
-164	4976	3390	1426	428	1021	1687	1088	401	105	81
-174	17787	13101	4724	1065	495	6841	4091	1335	246	302
-193	4750	3772	3152	1321	945	1853	1114	486	116	119
-198	7836	5773	2854	605	763	2319	1592	647	83	109
-205	4269	2528	819	327	1145	2125	1095	377	93	113
-215	3952	2889	2743	667	858	1463	935	621	146	295
-231	4672	5080	4473	1714	1240	1984	1845	1325	431	205
-255	12181	14479	14985	5562	2195	4995	5177	3963	1528	492
-262	2228	3327	3893	1540	809	673	1050	907	362	191
-293	2326	2258	2057	912	1309	735	608	358	129	114
-309	1074	698	761	335	279					
-316	1688	848	418	111	133	949	400	147	80	88
-320	2166	1467	1793	1336	1422	1294	609	312	181	199
-346	1773	917	466	183	122	674	319	117	89	88
-358	5441	3529	2468	1045	1142	2237	1224	542	178	143
-362	4257	2792	1849	662	1062	2406	1209	495	278	312
-382	8854	5233	2877	931	988	3384	1511	610	288	295
Sum	1251900	1392640	1674188	1573012	1520209	311347	313852	348346	338909	322113
Ratio	1.00	1.11	1.34	1.26	1.21	1.00	1.01	1.12	1.09	1.03

Table AIII.1-13 Adjusted CPD repair in the *MFA2* TS in the *Δtup1*alpha strain (70J/m^2)

CPDs position	Experiment 1					Experiment 2				
	Repair time (hours)					Repair time (hours)				
	0	0.5	1	2	3	0	0.5	1	2	3
2	4796	3544	1624	970	664	841	388	88	123	48
-16	3042	2156	773	568	571	958	534	179	159	153
-37	4217	3666	1684	741	281	0	0	0	0	0
-48	1080	1146	724	312	1980	0	0	0	0	0
-108	7537	5810	3249	1238	726	2641	2003	989	340	162
-119	5517	3828	1938	512	533	1899	1290	591	245	85
-133	3165	2447	1388	450	487	776	561	374	147	125
-155	14421	10432	4350	1031	1019	5487	3531	1335	236	176
-164	4976	3047	1066	341	841	1687	1080	358	96	78
-174	17787	11777	3532	847	407	6841	4058	1193	226	292
-193	4750	3391	2357	1051	778	1853	1105	435	107	115
-198	7836	5189	2134	481	628	2319	1580	579	76	105
-205	4269	2273	613	261	943	2125	1086	337	86	109
-215	3952	2597	2051	531	706	1463	927	555	135	285
-231	4672	4566	3345	1364	1021	1984	1831	1185	396	198
-255	12181	13016	11206	4427	1808	4995	5136	3542	1403	476
-262	2228	2991	2911	1225	666	673	1042	811	333	184
-293	2326	2030	1538	726	1078	735	603	320	118	110
-309	1074	627	569	267	230	0	0	0	0	0
-316	1688	762	312	88	110	949	397	131	74	85
-320	2166	1318	1341	1064	1171	1294	604	279	166	193
-346	1773	825	349	145	101	674	316	104	82	85
-358	5441	3172	1845	832	940	2237	1214	485	163	138
-362	4257	2510	1383	527	874	2406	1199	443	255	301
-382	8854	4704	2152	741	813	3384	1498	545	265	285

Table AIII.1-13 Signal remaining (%)

CPDs position	Experiment 1						Experiment 2					
	Repair time (hours)					$T_{50\%}$	Repair time (hours)					$T_{50\%}$
	0	0.5	1	2	3		0	0.5	1	2	3	
2	100	74	34	20	14	0.8	100	46	10	15	6	0.7
-16	100	71	25	19	19	0.8	100	56	19	17	16	0.6
-37	100	87	40	18	7	1.0						
-48	100	100	67	29	100	1.6						
-108	100	77	43	16	10	0.9	100	76	37	13	6	0.9
-119	100	69	35	9	10	0.8	100	68	31	13	4	0.8
-133	100	77	44	14	15	0.9	100	72	48	19	16	1
-155	100	72	30	7	7	0.7	100	64	24	4	3	0.7
-164	100	61	21	7	17	0.6	100	64	21	6	5	0.6
-174	100	66	20	5	2	0.6	100	59	17	3	4	0.6
-193	100	71	50	22	16	1.0	100	60	23	6	6	0.6
-198	100	66	27	6	8	0.7	100	68	25	3	5	0.7
-205	100	53	14	6	22	0.6	100	51	16	4	5	0.5
-215	100	66	52	13	18	0.9	100	63	38	9	19	0.7
-231	100	98	72	29	22	1.6	100	92	60	20	10	1.2
-255	100	100	92	36	15	2.0	100	100	71	28	10	1.6
-262	100	100	100	55	30	2.5	100	100	120	50	27	2.0
-293	100	87	66	31	46	1.4	100	82	44	16	15	1.0
-309	100	58	53	25	21	1.0						
-316	100	45	18	5	7	0.6	100	42	14	8	9	0.5
-320	100	61	62	49	54	1.6	100	47	22	13	15	0.6
-346	100	47	20	8	6	0.6	100	47	15	12	13	0.5
-358	100	58	34	15	17	0.7	100	54	22	7	6	0.6
-362	100	59	32	12	21	0.7	100	50	18	11	13	0.5
-382	100	53	24	8	9	0.6	100	44	16	8	8	0.5

Table AIII.1-14 CPD repair in the *MFA2* NTS in the *Δtup1*alpha strain (70J/m^2)

CPDs position	Experiment 1					Experiment 2				
	Repair time (hours)					Repair time (hours)				
	0	0.5	1	2	3	0	0.5	1	2	3
Top band	990239	1052447	1288630	1238922	1194267	450393	500633	530213	529605	423648
-431	43359	35591	24659	4709	2014	20081	14943	7684	861	348
-369	10279	9655	7838	1467	849	4590	3779	2263	465	161
-330	3305	3371	3446	1062	915	1243	1303	773	186	223
-308	21707	17425	11197	2475	2054	8293	6466	3151	531	622
-275	1731	1315	2735	374	599					
-264	6273	4124	2178	1366	2088	3125	1970	702	244	233
-240	20484	22272	24090	10822	6332	7497	7402	6405	2771	1101
-140	966	516	732	417	415					
-137	1368	598	1362	783	1329	1752	717	402	237	276
-129	6826	4954	2752	622	685	3502	2037	1037	256	255
-98	8081	6271	3320	836	373	6008	3972	1843	497	196
-93	11036	9038	5778	1268	676	5404	4256	2030	485	146
-88	2368	2341	1821	666	560	1524	1267	597	200	145
-82	15983	12129	6877	1220	695	7188	5211	2176	349	65
-72	2829	2377	1859	519	502	1973	1596	815	245	161
-68	2035	1682	1783	654	573	962	980	460	193	84
-60	1272	1009	693	217	177					
-54	2088	1945	2468	1112	1166	1269	1083	566	196	115
-51	1212	1201	1055	700	502					
-25	10636	9613	7000	2252	2168	3337	2709	1463	298	210
Sum	1164076	1199874	1402273	1272463	1218940	528139	560325	562580	537620	427988
Ratio	1.00	1.03	1.20	1.09	1.05	1.00	1.06	1.07	1.02	0.81

Table AIII.1-14 Adjusted CPD repair in the *MFA2* NTS in the *Δtup1*alpha strain (70J/m^2)

CPDs position	Experiment 1					Experiment 2				
	Repair time (hours)					Repair time (hours)				
	0	0.5	1	2	3	0	0.5	1	2	3
-431	43359	34529	20470	4307	1924	20081	14084	7214	846	430
-369	10279	9367	6507	1342	811	4590	3562	2124	457	198
-330	3305	3270	2861	972	874	1243	1228	725	183	275
-308	21707	16905	9295	2264	1961	8293	6095	2958	521	768
-275	1731	1276	2270	342	572	0	0	0	0	0
-264	6273	4001	1808	1250	1994	3125	1857	659	239	287
-240	20484	21608	19998	9901	6047	7497	6977	6013	2722	1359
-140	966	501	607	382	396	0	0	0	0	0
-137	1368	580	1131	716	1269	1752	676	377	233	340
-129	6826	4806	2285	569	655	3502	1920	973	251	314
-98	8081	6084	2756	765	357	6008	3744	1730	489	242
-93	11036	8769	4797	1160	645	5404	4012	1906	476	180
-88	2368	2271	1511	610	535	1524	1194	560	196	178
-82	15983	11767	5709	1116	663	7188	4912	2043	343	81
-72	2829	2306	1543	475	479	1973	1505	765	241	198
-68	2035	1631	1480	598	548	962	924	432	189	104
-60	1272	979	576	198	169					
-54	2088	1887	2049	1017	1113	1269	1021	531	193	142
-51	1212	1165	876	640	479					
-25	10636	9326	5811	2060	2071	3337	2554	1374	292	259

Table AIII.1-14 Signal remaining (%)

CPDs position	Experiment 1						Experiment 2					
	Repair time (hours)					$T_{50\%}$	Repair time (hours)					$T_{50\%}$
	0	0.5	1	2	3		0	0.5	1	2	3	
-431	100	80	47	10	4	1.0	100	70	36	4	2	0.7
-369	100	91	63	13	8	1.3	100	78	46	10	4	0.9
-330	100	99	87	29	26	1.8	100	99	58	15	22	1.2
-308	100	78	43	10	9	0.9	100	73	36	6	9	0.8
-275	100	74	131	20	33	2.2						0.7
-264	100	64	29	20	32	0.7	100	59	21	8	9	0.6
-240	100	105	98	48	30	2.4	100	93	80	36	18	1.8
-140	100	52	63	40	41	1.2						0.6
-137	100	42	83	52	93	2.1	100	39	22	13	19	0.5
-129	100	70	33	8	10	0.8	100	55	28	7	9	0.6
-98	100	75	34	9	4	0.8	100	62	29	8	4	0.7
-93	100	79	43	11	6	0.9	100	74	35	9	3	0.8
-88	100	96	64	26	23	1.4	100	78	37	13	12	0.8
-82	100	74	36	7	4	0.8	100	68	28	5	1	0.7
-72	100	82	55	17	17	1.1	100	76	39	12	10	0.8
-68	100	80	73	29	27	1.5	100	96	45	20	11	1.1
-60	100	77	45	16	13	0.9						
-54	100	90	98	49	53	2.0	100	80	42	15	11	1.1
-51	100	96	72	53	40	2.3						
-25	100	88	55	19	19	1.2	100	77	41	9	8	0.8

Table AIII.1-15 CPD repair in the *RPB2* TS in the wild type PSY316 alpha strain ($70J/m^2$)

CPDs position	Experiment 1				Experiment 2			
	Repair time (hours)				Repair time (hours)			
	0	1	2	3	0	1	2	3
Top band	1296520	1291672	1360070	1342293	1279848	1418805	1459070	1524191
944	5650	2253	2277	1996				
936	8906	3356	249	447	12518	3419	1327	813
934	29083	3629	1014	76	42194	6145	1470	934
926	77535	17420	3512	2390	98575	24060	5452	3804
918	15572	3024	1047	1806	17115	3516	2149	1618
910	10073	1404	433	1174	13386	3375	2299	3024
895	29485	3519	1739	926	36814	5639	1088	1872
887	17786	4705	2396	1101	24349	7913	2038	1877
882	6091	837	1806	477	9115	1645	1830	1587
860	4404	1054	850	294	6577	2363	2618	2985
833	8655	873	698	199	11956	1534	867	1538
810	18180	2460	1407	540	23181	3132	1557	1924
784	10257	1527	1155	971	12239	1864	1111	954
767	7095	1087	353	388	9507	1829	1391	1473
746	4305	1952	1649	1050	4297	2185	1552	1542
737	26708	4005	1468	908	31422	5545	1544	1956
714	17590	2539	1030	2298	22682	5126	3130	2596
699	2570	685	395	367	2275	852	663	797
682	39216	8779	1581	1303	45474	11624	2763	2020
672	3501	420	96	238	4284	681	259	473
660	7092	1946	932	948	6432	1859	794	1066
646	5944	531	300	380	8690	1689	1165	1179
636	3525	1456	758	662	3392	1411	707	1011
628	33328	5257	1653	1171	38734	6864	1446	1430
618	5978	1133	681	641	5179	1272	922	1062
Sum	1695049	1367523	1389549	1365044	1770232	1524344	1499208	1563725
Ratio	1.00	0.81	0.82	0.81	1.00	0.86	0.85	0.88

Table AIII.1-15 Adjusted CPD repair in the *RPB2* TS in the wild type PSY316 alpha strain (70J/m^2)

CPDs position	Experiment 1				Experiment 2			
	Repair time (hours)				Repair time (hours)			
	0	1	2	3	0	1	2	3
944	5650	2793	2777	2479				
936	8906	4159	303	556	12518	3971	1566	921
934	29083	4499	1237	94	42194	7136	1736	1058
926	77535	21592	4285	2968	98575	27941	6438	4307
918	15572	3748	1277	2243	17115	4083	2538	1832
910	10073	1741	528	1458	13386	3920	2715	3424
895	29485	4361	2121	1149	36814	6549	1284	2120
887	17786	5832	2923	1367	24349	9189	2406	2124
882	6091	1037	2204	592	9115	1910	2160	1797
860	4404	1306	1037	365	6577	2744	3091	3379
833	8655	1082	852	247	11956	1781	1024	1741
810	18180	3049	1717	671	23181	3637	1838	2178
784	10257	1893	1409	1205	12239	2164	1312	1080
767	7095	1347	430	482	9507	2124	1643	1668
746	4305	2419	2012	1304	4297	2538	1832	1746
737	26708	4965	1791	1127	31422	6439	1823	2214
714	17590	3147	1256	2854	22682	5952	3696	2938
699	2570	849	482	456	2275	989	782	902
682	39216	10881	1928	1618	45474	13499	3263	2287
672	3501	521	117	296	4284	790	306	535
660	7092	2413	1137	1177	6432	2159	937	1207
646	5944	658	366	472	8690	1961	1375	1334
636	3525	1805	925	822	3392	1639	835	1145
628	33328	6516	2017	1455	38734	7972	1707	1619
618	5978	1404	831	796	5179	1477	1088	1202

Table AIII.1-15 Signal remaining (%)

CPDs position	Experiment 1					Experiment 2				
	Repair time (hours)				$T_{50\%}$	Repair time (hours)				$T_{50\%}$
	0	1	2	3		0	1	2	3	
944	100	49	49	44	1.0					
936	100	47	3	6	0.9	100	32	13	7	0.7
934	100	15	4	0	0.6	100	17	4	3	0.6
926	100	28	6	4	0.7	100	28	7	4	0.7
918	100	24	8	14	0.6	100	24	15	11	0.6
910	100	17	5	14	0.6	100	29	20	26	0.7
895	100	15	7	4	0.6	100	18	3	6	0.6
887	100	33	16	8	0.8	100	38	10	9	0.8
882	100	17	36	10	0.6	100	21	24	20	0.6
860	100	30	24	8	0.7	100	42	47	51	0.9
833	100	13	10	3	0.6	100	15	9	15	0.6
810	100	17	9	4	0.6	100	16	8	9	0.6
784	100	18	14	12	0.6	100	18	11	9	0.6
767	100	19	6	7	0.6	100	22	17	18	0.6
746	100	56	47	30	1.6	100	59	43	41	1.5
737	100	19	7	4	0.6	100	20	6	7	0.6
714	100	18	7	16	0.6	100	26	16	13	0.7
699	100	33	19	18	0.7	100	43	34	40	0.9
682	100	28	5	4	0.7	100	30	7	5	0.7
672	100	15	3	8	0.6	100	18	7	12	0.6
660	100	34	16	17	0.8	100	34	15	19	0.7
646	100	11	6	8	0.6	100	23	16	15	0.6
636	100	51	26	23	1.0	100	48	25	34	1.0
628	100	20	6	4	0.6	100	21	4	4	0.6
618	100	23	14	13	0.7	100	29	21	23	0.7

Table AIII.1-16 CPD repair in the *RPB2* NTS in the wild type PSY316 alpha strain (70J/m^2)

CPDs position	Experiment 1				Experiment 2			
	Repair time (hours)				Repair time (hours)			
	0	1	2	3	0	1	2	3
Top band	1227109	971692	1018042	1061926	1502259	1231334	1345811	1439646
659	27807	19157	12759	6919				
751	36472	24764	16708	7995	38567	20321	18284	11393
770	47176	30401	20117	12593	30796	19183	15977	11117
810	20978	12348	4878	1903	18598	9184	4691	2028
851	38454	25679	16771	6876	39480	24114	16374	8372
875	10016	6951	5487	2948	9537	6458	5047	3177
891	17042	12305	10996	6700	14656	10703	9633	7416
905	5389	3968	3031	1855	3838	4085	3294	2165
921	2201	1426	1099	681	2538	1359	862	603
945	18346	11487	6053	2860	22606	14936	9613	5553
971	20098	11452	6801	2640	21425	12880	7280	3295
996	29136	16888	12741	7272	26162	16288	11436	6686
1019	13973	9310	5294	3239	15775	9240	5251	3221
1047	6982	4900	3910	2993	7380	5009	4081	3234
1066	28260	19599	13290	6614	31299	19448	12470	7844
1080	12377	9194	7505	4250	12386	9271	6728	4309
1086	11162	6619	3967	1520	9485	5879	3268	1407
1095	4474	3782	3066	1629	3249	3040	2589	1597
1099	5685	4081	2208	1001	4684	3409	1982	894
1109	4122	2285	1331	826	9098	5240	2990	1355
1129	35841	23791	17678	9144	28196	18629	12803	7157
Sum	1623101	1232078	1193734	1154384	1852013	1450012	1500463	1532468
Ratio	1.00	0.76	0.74	0.71	1.00	0.78	0.81	0.83

Table AIII.1-16 Adjusted CPD repair in the *RPB2* NTS in the wild type PSY316 alpha strain ($70J/m^2$)

CPDs position	Experiment 1				Experiment 2			
	Repair time (hours)				Repair time (hours)			
	0	1	2	3	0	1	2	3
659	27807	25237	17349	9728				
751	36472	32623	22718	11242	38567	25955	22568	13768
770	47176	40049	27352	17707	30796	24502	19720	13435
810	20978	16267	6633	2675	18598	11730	5790	2450
851	38454	33829	22803	9668	39480	30799	20210	10117
875	10016	9157	7461	4145	9537	8249	6230	3839
891	17042	16210	14951	9420	14656	13670	11889	8962
905	5389	5228	4121	2608	3838	5217	4066	2617
921	2201	1879	1495	957	2538	1736	1064	729
945	18346	15132	8231	4021	22606	19077	11865	6711
971	20098	15087	9247	3712	21425	16451	8986	3982
996	29136	22248	17324	10225	26162	20804	14115	8080
1019	13973	12265	7198	4554	15775	11802	6481	3892
1047	6982	6456	5317	4209	7380	6398	5037	3908
1066	28260	25819	18071	9300	31299	24840	15392	9480
1080	12377	12111	10205	5975	12386	11841	8305	5207
1086	11162	8720	5393	2138	9485	7509	4033	1700
1095	4474	4983	4169	2290	3249	3882	3195	1931
1099	5685	5376	3002	1407	4684	4354	2446	1080
1109	4122	3010	1810	1162	9098	6693	3690	1638
1129	35841	31342	24037	12857	28196	23794	15803	8650

Table AIII.1-16 Signal remaining (%)

CPDs position	Experiment 1					Experiment 2				
	Repair time (hours)				$T_{50\%}$	Repair time (hours)				$T_{50\%}$
	0	1	2	3		0	1	2	3	
659	100	91	62	35	2.5					
751	100	89	62	31	2.4	100	67	59	36	2.2
770	100	85	58	38	2.4	100	80	64	44	2.6
810	100	78	32	13	1.6	100	63	31	13	1.4
851	100	88	59	25	2.3	100	78	51	26	2.1
875	100	91	74	41	2.7	100	86	65	40	2.6
891	100	95	88	55	3.1	100	93	81	61	3.4
905	100	97	76	48	2.9	100	100	100	68	3.5
921	100	85	68	43	2.7	100	68	42	29	1.7
945	100	82	45	22	1.9	100	84	52	30	2.2
971	100	75	46	18	1.8	100	77	42	19	1.8
996	100	76	59	35	2.3	100	80	54	31	2.2
1019	100	88	52	33	2.1	100	75	41	25	1.8
1047	100	92	76	60	3.5	100	87	68	53	3.1
1066	100	91	64	33	2.3	100	79	49	30	2.0
1080	100	98	82	48	2.9	100	96	67	42	2.6
1086	100	78	48	19	2.0	100	79	43	18	1.8
1095	100	100	93	51	3.0	100	100	98	59	3.2
1099	100	95	53	25	2.1	100	93	52	23	2.2
1109	100	73	44	28	1.8	100	74	41	18	1.7
1129	100	87	67	36	2.5	100	84	56	31	2.3

Table AIII.1-17 CPD repair in the *RPB2* TS in the *Δtup1* alpha strain (70J/m^2)

CPDs position	Experiment 1				Experiment 2			
	Repair time (hours)				Repair time (hours)			
	0	1	2	3	0	1	2	3
Top band	990381	1345456	1308991	1268352	1257284	1369946	1333564	1291959
936	4320	2121	340	747	6634	1440	1564	1064
934	13700	1912	1653	899	23472	2450	664	1298
926	41872	9099	1754	2786	67910	12183	2264	4140
918	5939	1432	928	737	10544	2028	1616	1452
910	4793	656	553	913	9784	1794	2073	1777
895	14999	2538	1305	1253	23584	2474	1169	1456
887	10040	3484	2815	2732	17260	4433	1624	2088
882	3734	1142	656	1337	5763	1305	1094	1213
860	2552	1502	816	937	4082	1555	1771	1655
833	5133	1035	625	1184	7677	1871	1401	1090
810	8707	1875	962	1275	12816	3111	1709	1254
784	5696	1011	960	1416	8225	1897	645	737
767	3754	240	391	456	6196	1063	701	454
746	2404	1570	781	674	4070	1916	1208	1142
737	18567	3457	1405	1018	29059	4626	1248	1014
714	11901	1875	1026	1279	22341	3292	2264	1768
699					1353	704	438	511
682	14114	3934	1250	969	20236	4418	1457	1008
672	2166	299	580	533	2974	563	563	473
660	3551	1587	548	601	4462	1588	774	1108
646	3725	670	391	487	7474	1475	1011	1166
636	1834	1028	631	685	2535	1161	709	909
628	15421	3159	1317	1372	22823	3922	1572	1270
618	4033	1136	946	979	5518	1771	1120	1278
Sum	1193336	1392217	1331624	1293621	1584074	1432986	1364224	1323284
Ratio	1.00	1.17	1.12	1.08	1.00	0.90	0.86	0.84

Table AIII.1-17 Adjusted CPD repair in the *RPB2* TS in the*Δtup1* alpha strain (70J/m^2)

CPDs position	Experiment 1				Experiment 2			
	Repair time (hours)				Repair time (hours)			
	0	1	2	3	0	1	2	3
936	4320	1818	305	689	6634	1591	1816	1274
934	13700	1639	1481	829	23472	2709	772	1554
926	41872	7799	1572	2570	67910	13468	2629	4955
918	5939	1227	831	679	10544	2241	1876	1738
910	4793	563	495	842	9784	1983	2407	2127
895	14999	2175	1169	1156	23584	2735	1358	1743
887	10040	2987	2523	2520	17260	4900	1885	2500
882	3734	979	588	1233	5763	1443	1270	1453
860	2552	1287	731	864	4082	1719	2057	1982
833	5133	887	560	1092	7677	2068	1627	1304
810	8707	1608	862	1177	12816	3439	1984	1501
784	5696	866	860	1307	8225	2097	749	882
767	3754	205	351	421	6196	1175	814	544
746	2404	1346	700	622	4070	2118	1403	1368
737	18567	2964	1259	939	29059	5114	1449	1214
714	11901	1607	919	1180	22341	3639	2629	2116
699					1353	778	509	611
682	14114	3372	1120	894	20236	4884	1691	1207
672	2166	256	520	491	2974	622	654	567
660	3551	1360	492	554	4462	1755	899	1326
646	3725	574	350	449	7474	1631	1174	1396
636	1834	882	565	632	2535	1283	823	1088
628	15421	2707	1180	1266	22823	4336	1825	1520
618	4033	973	847	903	5518	1958	1300	1529

Table AIII.1-17 Signal remaining (%)

CPDs position	Experiment 1					Experiment 2				
	Repair time (hours)				$T_{50\%}$	Repair time (hours)				$T_{50\%}$
	0	1	2	3		0	1	2	3	
936	100	42	7	16	0.9	100	24	27	19	0.7
934	100	12	11	6	0.5	100	12	3	7	0.6
926	100	19	4	6	0.6	100	20	4	7	0.6
918	100	21	14	11	0.6	100	21	18	16	0.6
910	100	12	10	18	0.5	100	20	25	22	0.6
895	100	15	8	8	0.6	100	12	6	7	0.6
887	100	30	25	25	0.8	100	28	11	14	0.6
882	100	26	16	33	0.6	100	25	22	25	0.6
860	100	51	29	34	0.9	100	42	50	49	1.0
833	100	17	11	21	0.6	100	27	21	17	0.7
810	100	18	10	14	0.6	100	27	15	12	0.7
784	100	15	15	23	0.6	100	25	9	11	0.6
767	100	5	9	11	0.5	100	19	13	9	0.6
746	100	56	29	26	1.2	100	52	34	34	1.0
737	100	16	7	5	0.6	100	18	5	4	0.6
714	100	14	8	10	0.5	100	16	12	9	0.6
699						100	58	38	45	1.1
682	100	24	8	6	0.6	100	24	8	6	0.6
672	100	12	24	23	0.6	100	21	22	19	0.6
660	100	38	14	16	0.8	100	39	20	30	0.7
646	100	15	9	12	0.6	100	22	16	19	0.6
636	100	48	31	34	1.0	100	51	32	43	0.9
628	100	18	8	8	0.6	100	19	8	7	0.6
618	100	24	21	22	0.7	100	35	24	28	0.7

Table AIII.1-18 CPD repair in the *RPB2* NTS in the*Δtup1* alpha strain (70J/m^2)

CPDs position	Experiment 1				Experiment 2			
	Repair time (hours)				Repair time (hours)			
	0	1	2	3	0	1	2	3
Top band	920708	1254275	1152718	1224214	1065926	1240259	1201811	1241742
659	16297	16598	5659	2670	X	X	X	X
751	18735	15069	3718	2074	20570	13671	5376	2592
770	19459	25825	9789	4956	16692	16253	6659	3855
810	9403	9067	2462	1044	10350	6281	1204	1336
851	18982	16319	4966	1549	22999	13909	4116	1915
875	5148	4805	2077	1091	6730	4560	1816	1167
891	8652	11088	5316	3001	9990	9352	4577	2055
905	3434	3169	1439	975	3858	3203	1404	899
921	1047	1322	553	868	1388	1252	420	489
945	8302	9595	4752	2669	11699	9684	3731	4460
971	9533	7992	2201	1447	9785	7337	1958	1524
996	14897	15028	5421	2687	13987	10537	3484	1744
1019	7279	7186	3725	2665	7724	5331	2459	2163
1047	3951	4671	2623	1960	4571	4498	1935	2030
1066	13990	16153	6049	3094	14914	12885	4505	2426
1080	7265	8922	3670	2033	7147	6379	2757	1591
1086	5363	5723	1513	840	4578	3814	1015	531
1095	2490	3210	1615	1321	1779	2023	1120	877
1099	3058	3067	966	738	2636	2033	649	379
1109	2463	2611	903	736	4885	3710	999	590
1129	17561	20163	7841	4729	14563	12496	4429	2011
Sum	1118016	1461856	1229976	1267361	1256770	1389468	1256423	1276374
Ratio	1.00	1.31	1.10	1.13	1.00	1.11	1.00	1.02

Table AIII.1-18 Adjusted CPD repair in the *RPB2* NTS in the*Δtup1* alpha strain (70J/m^2)

CPDs position	Experiment 1				Experiment 2			
	Repair time (hours)				Repair time (hours)			
	0	1	2	3	0	1	2	3
659	16297	12694	5144	2356				
751	18735	11524	3379	1830	20570	12366	5377	2552
770	19459	19751	8898	4372	16692	14701	6661	3795
810	9403	6934	2238	921	10350	5681	1204	1315
851	18982	12481	4514	1366	22999	12580	4118	1885
875	5148	3675	1888	962	6730	4124	1816	1149
891	8652	8480	4832	2648	9990	8459	4578	2023
905	3434	2423	1308	861	3858	2897	1405	885
921	1047	1011	503	766	1388	1132	420	482
945	8302	7338	4320	2354	11699	8759	3732	4392
971	9533	6112	2001	1276	9785	6636	1959	1500
996	14897	11494	4928	2370	13987	9531	3485	1717
1019	7279	5496	3386	2351	7724	4822	2459	2129
1047	3951	3572	2384	1729	4571	4068	1936	1999
1066	13990	12354	5499	2729	14914	11654	4506	2388
1080	7265	6824	3336	1793	7147	5770	2758	1567
1086	5363	4377	1375	741	4578	3450	1015	523
1095	2490	2455	1468	1165	1779	1830	1121	864
1099	3058	2346	878	651	2636	1839	649	374
1109	2463	1997	821	650	4885	3356	999	580
1129	17561	15421	7127	4172	14563	11303	4430	1981

Table AIII.1-18 Signal remaining (%)

CPDs position	Experiment 1					Experiment 2				
	Repair time (hours)				$T_{50\%}$	Repair time (hours)				$T_{50\%}$
	0	1	2	3		0	1	2	3	
659	100	78	32	14	1.6					
751	100	62	18	10	1.2	100	60	26	12	1.2
770	100	100	46	22	2.3	100	88	40	23	2.0
810	100	74	24	10	1.5	100	55	12	13	1.0
851	100	66	24	7	1.4	100	55	18	8	1.1
875	100	71	37	19	1.7	100	61	27	17	1.2
891	100	98	56	31	2.5	100	85	46	20	2.0
905	100	71	38	25	1.7	100	75	36	23	1.7
921	100	97	48	73	2.0	100	82	30	35	1.7
945	100	88	52	28	2.3	100	75	32	38	1.6
971	100	64	21	13	1.3	100	68	20	15	1.2
996	100	77	33	16	1.7	100	68	25	12	1.4
1019	100	75	47	32	1.9	100	62	32	28	1.3
1047	100	90	60	44	2.7	100	89	42	44	2.0
1066	100	88	39	20	1.8	100	78	30	16	1.6
1080	100	94	46	25	1.9	100	81	39	22	1.9
1086	100	82	26	14	1.7	100	75	22	11	1.4
1095	100	99	59	47	2.8	100	100	63	49	2.8
1099	100	77	29	21	1.7	100	70	25	14	1.4
1109	100	81	33	26	1.8	100	69	20	12	1.3
1129	100	88	41	24	2.1	100	78	30	14	1.6

AIII.2 CPD repair in the *MFA2* in Chapter 4

Table AIII.2-1 CPD repair in the *MFA2* TS in the *Δrad16* α strain

CPDs position	Experiment 1				Experiment 2			
	Repair time (hours)				Repair time (hours)			
	0	1	2	3	0	1	2	3
Top band	2064671	1757725	1926147	2179106	777839	552320	777490	748515
2	8757	14624	15467	16780	3702	4007	5456	4234
-16	5486	10134	10451	10800	2586	2670	3644	3043
-37	4098	5640	4286	4264	6725	5221	6437	5198
-48	8840	11061	9079	10366	3132	2190	2930	2644
-108	11926	18169	19715	18199	5116	4418	4805	4428
-119	8559	16341	18628	17087	3698	3270	3929	2827
-133	7079	14840	17145	16313	3446	3912	4448	3941
-155	46292	89195	76017	77273	22809	23297	24934	17801
-164	22936	40432	33508	35656	10514	9459	10498	9810
-174	53550	107164	100692	96889	26008	26086	27615	19964
-193	14653	23511	22840	24660	6573	6028	7118	6105
-198	22364	39533	32788	35858	8847	9068	10492	7611
-205	12171	25802	28263	25327	5059	6213	6795	4904
-215	4310	9105	9882	9629	1521	2163	2680	1610
-231	7396	17629	16787	16218	3517	3844	4768	3402
-255	27616	53344	49442	50797	13836	13357	16692	12720
-262	10231	20139	21650	23371	5169	5450	8080	6539
-293	6311	11874	13261	14450	3334	3374	4751	3561
-309	8222	8719	7250	8044	2949	2539	2509	2149
-316	2523	4487	7142	5712	1082	1223	1660	1120
-320	4571	7022	10531	8106	2370	2267	2734	1940
-346	7477	9949	7579	8469	3015	2278	2542	2477
-358	25905	37543	31684	35037	11474	8344	9673	9146
-362	13241	20276	18094	18628	5543	4731	5101	5585
-382	20307	32118	28124	28749	8448	6479	7138	7285
Sum	2429492	2406378	2536451	2795789	948312.9	714207.7	964920	897560.5
Ratio	1.00	0.99	1.04	1.15	1.00	0.75	1.02	0.95

Table AIII.2-1 Adjusted CPD repair in the *MFA2* TS in the *Δrad16* α strain

CPDs position	Experiment 1				Experiment 2			
	Repair time (hours)				Repair time (hours)			
	0	1	2	3	0	1	2	3
2	8757	14765	14815	14582	3702	5320	5362	4474
-16	5486	10231	10011	9385	2586	3546	3582	3215
-37	4098	5694	4105	3705	6725	6933	6327	5492
-48	8840	11167	8696	9008	3132	2908	2879	2793
-108	11926	18343	18884	15814	5116	5867	4722	4674
-119	8559	16498	17842	14848	3698	4342	3862	2987
-133	7079	14982	16422	14175	3446	5194	4372	4163
-155	46292	90052	72811	67149	22809	30933	24505	18807
-164	22936	40821	32095	30984	10514	12559	10318	10365
-174	53550	108194	96446	84195	26008	34637	27140	21092
-193	14653	23737	21877	21429	6573	8004	6995	6450
-198	22364	39913	31405	31160	8847	12041	10311	8041
-205	12171	26050	27071	22009	5059	8250	6678	5182
-215	4310	9192	9465	8368	1521	2872	2634	1701
-231	7396	17798	16079	14094	3517	5104	4686	3595
-255	27616	53856	47357	44141	13836	17736	16404	13439
-262	10231	20332	20737	20309	5169	7236	7941	6909
-293	6311	11988	12702	12557	3334	4480	4669	3762
-309	8222	8802	6944	6990	2949	3371	2466	2270
-316	2523	4530	6841	4964	1082	1624	1632	1184
-320	4571	7089	10087	7044	2370	3010	2687	2050
-346	7477	10045	7259	7359	3015	3025	2499	2617
-358	25905	37904	30348	30447	11474	11079	9506	9663
-362	13241	20471	17331	16188	5543	6281	5014	5901
-382	20307	32427	26938	24983	8448	8602	7015	7696

Table AIII.2-1 Signal remaining (%)

CPDs Position	Experiment 1					Experiment 2				
	Repair time (hours)				$T_{50\%}$	Repair time (hours)				$T_{50\%}$
	0	1	2	3		0	1	2	3	
2	100	100	100	100	6.0	100	100	100	100	6.0
-16	100	100	100	100	6.0	100	100	100	100	6.0
-37	100	100	100	90	6.0	100	100	94	82	6.0
-48	100	100	98	100	6.0	100	93	92	89	6.0
-108	100	100	100	100	6.0	100	100	92	91	6.0
-119	100	100	100	100	6.0	100	100	100	81	6.0
-133	100	100	100	100	6.0	100	100	100	100	6.0
-155	100	100	100	100	6.0	100	100	100	82	6.0
-164	100	100	100	100	6.0	100	100	98	99	6.0
-174	100	100	100	100	6.0	100	100	100	81	6.0
-193	100	100	100	100	6.0	100	100	100	98	6.0
-198	100	100	100	100	6.0	100	100	100	91	6.0
-205	100	100	100	100	6.0	100	100	100	100	6.0
-215	100	100	100	100	6.0	100	100	100	100	6.0
-231	100	100	100	100	6.0	100	100	100	100	6.0
-255	100	100	100	100	6.0	100	100	100	97	6.0
-262	100	100	100	100	6.0	100	100	100	100	6.0
-293	100	100	100	100	6.0	100	100	100	100	6.0
-309	100	100	84	85	6.0	100	100	84	88	6.0
-316	100	100	100	100	6.0	100	100	100	100	6.0
-320	100	100	100	100	6.0	100	100	100	86	6.0
-346	100	100	97	98	6.0	100	100	83	87	6.0
-358	100	100	100	100	6.0	100	97	83	84	6.0
-362	100	100	100	100	6.0	100	100	90	100	6.0
-382	100	100	100	100	6.0	100	100	83	91	6.0

Table AIII.2-2 CPD repair in the *MFA2* NTS in the *Δrad16* α strain

CPDs position	Experiment 1				Experiment 2			
	Repair time (hours)				Repair time (hours)			
	0	1	2	3	0	1	2	3
Top band	275277	255338	256126	248376	391895	377454	376446	282698
-431	10208	12031	11407	11552	19014	19308	19263	14886
-369	4842	5717	4803	4696	7293	7788	6883	5536
-330	1765	2115	1773	1901	2480	3205	2487	2044
-308	12005	13388	11776	12460	17062	19051	18957	14388
-275	1252	1085	1016	1256	1646	1968	1781	1246
-264	3836	4009	3551	3781	5749	5700	5530	4203
-240	8741	9468	8239	7591	12284	13074	12767	8837
-140	264	338	276	329	535	457	625	553
-137	337	396	347	357	488	485	521	381
-129	3519	3969	3418	3872	4455	5276	5051	3349
-98	3942	4153	3905	3476	5717	5612	5242	3759
-93	4936	5175	4380	4562	7111	6694	6461	4963
-88	917	928	721	814	1388	1288	1237	976
-82	7782	8521	7554	7397	9645	10079	9311	6621
-72	787	897	826	869	1043	1230	1372	913
-68	744	931	719	732	1285	1141	1314	851
-60	734	908	786	726	1072	1184	1108	834
-54	601	723	642	628	689	658	878	715
-51	774	817	740	686	1152	1200	1023	888
-25	4586	5147	4450	3735	5744	6751	6463	4365
Sum	347847	336056	327456	319798	497748	489602	484722	363006
Ratio	1.00	0.97	0.94	0.92	1.00	0.98	0.97	0.73

Table AIII.2-2 Adjusted CPD repair in the *MFA2* NTS in the *Δrad16* α strain

CPDs Position	Experiment 1				Experiment 2			
	Repair time (hours)				Repair time (hours)			
	0	1	2	3	0	1	2	3
-431	10208	12453	12118	12566	19014	19629	19780	20412
-369	4842	5918	5102	5108	7293	7918	7068	7591
-330	1765	2189	1884	2068	2480	3258	2553	2803
-308	12005	13857	12509	13553	17062	19368	19467	19728
-275	1252	1123	1079	1366	1646	2001	1829	1709
-264	3836	4149	3772	4113	5749	5794	5679	5763
-240	8741	9800	8752	8257	12284	13292	13111	12116
-140	264	350	293	358	535	465	642	759
-137	337	410	369	388	488	493	535	522
-129	3519	4108	3631	4212	4455	5364	5186	4591
-98	3942	4299	4148	3781	5717	5705	5383	5154
-93	4936	5357	4653	4962	7111	6805	6635	6805
-88	917	961	766	886	1388	1310	1271	1339
-82	7782	8820	8025	8046	9645	10246	9561	9078
-72	787	928	878	945	1043	1250	1409	1251
-68	744	964	764	797	1285	1160	1349	1167
-60	734	940	835	790	1072	1204	1138	1144
-54	601	749	682	683	689	669	902	980
-51	774	846	786	746	1152	1220	1051	1218
-25	4586	5328	4727	4063	5744	6863	6637	5985

Table AIII.2-2 Signal remaining (%)

CPDs Position	Experiment 1					Experiment 2				
	Repair time (hours)				$T_{50\%}$	Repair time (hours)				$T_{50\%}$
	0	1	2	3		0	1	2	3	
-431	100	100	100	100	6.0	100	100	100	100	6.0
-369	100	100	100	100	6.0	100	100	97	100	6.0
-330	100	100	100	100	6.0	100	100	100	100	6.0
-308	100	100	100	100	6.0	100	100	100	100	6.0
-275	100	90	86	100	6.0	100	100	100	100	6.0
-264	100	100	98	100	6.0	100	100	99	100	6.0
-240	100	100	100	94	6.0	100	100	100	99	6.0
-140	100	100	100	100	6.0	100	87	100	100	6.0
-137	100	100	100	100	6.0	100	100	100	100	6.0
-129	100	100	100	100	6.0	100	100	100	100	6.0
-98	100	100	100	96	6.0	100	100	94	90	6.0
-93	100	100	94	100	6.0	100	96	93	96	6.0
-88	100	100	84	97	6.0	100	94	92	96	6.0
-82	100	100	100	100	6.0	100	100	99	94	6.0
-72	100	100	100	100	6.0	100	100	100	100	6.0
-68	100	100	100	100	6.0	100	90	100	91	6.0
-60	100	100	100	100	6.0	100	100	100	100	6.0
-54	100	100	100	100	6.0	100	97	100	100	6.0
-51	100	100	100	96	6.0	100	100	91	100	6.0
-25	100	100	100	89	6.0	100	100	100	100	6.0

Table AIII.2-3 CPD repair in the *MFA2* TS in the *Δrad16tup1* α strain

CPDs position	Experiment 1				Experiment 2			
	Repair time (hours)				Repair time (hours)			
	0	1	2	3	0	1	2	3
Top band	769114	747081	916882	801777	1643791	1353409	1186155	1411581
2	3133	1894	1152	1146	15020	8452	3079	3083
-16	1473	472	378	585	9350	4752	1469	1247
-37	3479	1097	700	866	14703	4918	1308	1506
-48	1563	1190	1255	1330	3747	3292	1752	2998
-108	3789	2665	1719	1524	19042	14018	5491	4376
-119	2722	1965	1403	1229	15295	11380	4707	3725
-133	2401	1607	1517	1950	10068	8462	4523	5328
-155	9760	7066	3583	2904	54633	34007	11630	9036
-164	4155	2944	1329	1063	24896	14416	5085	3603
-174	11337	8533	4482	3683	62818	45254	17548	14352
-193	4492	4050	2861	2260	20244	16089	8392	7807
-198	6621	6189	4205	3593	37619	27701	13364	12676
-205	2628	2274	1455	1101	16541	14954	6390	5151
-215	1951	1701	1330	1149	8735	7908	3862	3714
-231	2603	2648	1304	1174	10614	10630	3804	3442
-255	8663	8400	6155	5335	49119	38033	18641	16125
-262	2315	2650	2870	3127	13190	11999	8525	9415
-293	3098	2849	2707	2169	12935	11675	6588	6598
-309	1891	1202	969	741	8748	4495	1981	2338
-316	598	561	398	383	3545	4000	1566	1264
-320	1030	626	529	537	3972	3399	1316	1332
-346	1422	879	453	436	8959	3883	1379	1225
-358	3934	2333	1641	1375	25546	11701	3916	3524
-362	3154	2004	959	927	19238	10593	3505	3271
-382	5147	2574	1482	1256	37551	16676	6314	5439
Sum	862473	817453	963717	843620	2149919	1696097	1332289	1544155
Ratio	1.00	0.95	1.12	0.98	1.00	0.79	0.62	0.72

Table AIII.2-3 Adjusted CPD repair in the *MFA2* TS in the *Δrad16tup1* α strain

CPDs position	Experiment 1				Experiment 2			
	Repair time (hours)				Repair time (hours)			
	0	1	2	3	0	1	2	3
2	3133	1998	1031	1172	15020	10713	4969	4293
-16	1473	498	338	598	9350	6023	2370	1736
-37	3479	1158	626	886	14703	6234	2111	2096
-48	1563	1256	1123	1360	3747	4173	2827	4173
-108	3789	2811	1539	1559	19042	17768	8861	6092
-119	2722	2073	1256	1256	15295	14425	7595	5186
-133	2401	1696	1358	1993	10068	10726	7299	7419
-155	9760	7455	3207	2969	54633	43106	18768	12581
-164	4155	3106	1189	1087	24896	18273	8205	5017
-174	11337	9003	4011	3765	62818	57363	28317	19982
-193	4492	4274	2560	2311	20244	20393	13542	10869
-198	6621	6529	3763	3674	37619	35112	21565	17648
-205	2628	2399	1302	1125	16541	18955	10312	7172
-215	1951	1794	1191	1174	8735	10024	6232	5170
-231	2603	2794	1167	1200	10614	13474	6138	4793
-255	8663	8863	5508	5455	49119	48210	30080	22451
-262	2315	2796	2569	3197	13190	15209	13757	13108
-293	3098	3006	2422	2217	12935	14799	10631	9187
-309	1891	1268	867	757	8748	5698	3196	3256
-316	598	592	356	391	3545	5070	2527	1760
-320	1030	660	473	549	3972	4309	2124	1854
-346	1422	928	406	446	8959	4922	2225	1706
-358	3934	2462	1469	1405	25546	14832	6319	4906
-362	3154	2115	859	948	19238	13427	5657	4554
-382	5147	2716	1326	1284	37551	21138	10189	7573

Table AIII.2-3 Signal remaining (%)

CPDs Position	Experiment 1					Experiment 2				
	Repair time (hours)				$T_{50\%}$	Repair time (hours)				$T_{50\%}$
	0	1	2	3		0	1	2	3	
2	100	64	33	37	1.3	100	71	33	29	1.5
-16	100	34	23	41	0.7	100	64	25	19	1.2
-37	100	33	18	25	0.8	100	42	14	14	0.8
-48	100	80	72	87	6.0	100	100	75	100	6.0
-108	100	74	41	41	1.8	100	93	47	32	2.0
-119	100	76	46	46	2.0	100	94	50	34	2.0
-133	100	71	57	83	2.2	100	107	73	74	2.4
-155	100	76	33	30	1.6	100	79	34	23	1.7
-164	100	75	29	26	1.5	100	73	33	20	1.6
-174	100	79	35	33	1.8	100	91	45	32	2.0
-193	100	95	57	51	2.8	100	100	67	54	3.0
-198	100	99	57	55	3.0	100	93	57	47	2.7
-205	100	91	50	43	2.0	100	100	62	43	2.2
-215	100	92	61	60	3.4	100	100	71	59	3.2
-231	100	100	45	46	2.6	100	100	58	45	2.7
-255	100	100	64	63	3.0	100	98	61	46	2.7
-262	100	100	100	100	6.0	100	100	100	99	6.0
-293	100	97	78	72	4.4	100	100	82	71	4.0
-309	100	67	46	40	1.8	100	65	37	37	1.4
-316	100	99	60	65	2.2	100	100	71	50	3.0
-320	100	64	46	53	1.6	100	100	53	47	2.0
-346	100	65	29	31	1.3	100	55	25	19	1.1
-358	100	63	37	36	1.4	100	58	25	19	1.2
-362	100	67	27	30	1.3	100	70	29	24	1.4
-382	100	53	26	25	1.1	100	56	27	20	1.2

Table AIII.2-4 CPD repair in the *MFA2* NTS in the *Δrad16tup1* α strain

CPDs position	Experiment 1				Experiment 2			
	Repair time (hours)				Repair time (hours)			
	0	1	2	3	0	1	2	3
Top band	1370646	1075598	989626	1099902	293561	306647	314295	290416
-431	114425	79563	42569	31325	9562	8802	6368	4942
-369	35457	27152	20018	18813	3161	3515	2998	2606
-330	15351	11747	8595	7927	2204	2425	2016	1560
-308	69141	61147	47844	46321	8792	9958	8781	6946
-275	2678	4510	3373	3416	591	700	750	701
-264	16825	17364	12632	11995	1714	2029	2031	1746
-240	56665	48631	35403	31617	6563	7107	5795	4128
-140	1713	2161	1612	1365	193	283	275	217
-137	5009	4107	2959	2264	449	587	508	412
-129	34901	24629	16217	12429	2494	2404	2053	1271
-98	33604	24050	13551	10057	2652	2237	1612	1219
-93	42052	33065	19568	14750	3482	3258	2387	1721
-88	7263	6856	4278	3522	578	698	582	526
-82	66437	48301	28323	20313	5199	4508	3131	2074
-72	5425	6780	4570	2851	430	438	286	214
-68	5805	6027	3660	2794	527	542	500	435
-60	7093	4385	2751	1867	548	517	373	275
-54	4523	4441	2789	2113	240	322	194	230
-51	7519	4486	3059	2314	584	600	422	435
-25	36466	32699	21709	18393	3026	3275	3145	2663
Sum	1938998	1527701	1285103	1346349	346549	360853	358501	324738
Ratio	1.00	0.79	0.66	0.69	1.00	1.04	1.03	0.94

Table AIII.2-4 Adjusted CPD repair in the *MFA2* NTS in the *Δrad16tup1* α strain

CPDs Position	Experiment 1				Experiment 2			
	Repair time (hours)				Repair time (hours)			
	0	1	2	3	0	1	2	3
-431	114425	100984	64229	45113	9562	8453	6156	5274
-369	35457	34462	30204	27095	3161	3376	2898	2782
-330	15351	14909	12968	11417	2204	2329	1948	1664
-308	69141	77610	72188	66711	8792	9563	8489	7412
-275	2678	5725	5089	4920	591	672	725	748
-264	16825	22039	19059	17275	1714	1949	1964	1863
-240	56665	61724	53417	45535	6563	6826	5602	4406
-140	1713	2743	2433	1966	193	272	265	232
-137	5009	5212	4464	3260	449	563	491	439
-129	34901	31259	24468	17900	2494	2309	1984	1357
-98	33604	30525	20445	14484	2652	2148	1559	1301
-93	42052	41967	29524	21243	3482	3129	2307	1837
-88	7263	8702	6454	5073	578	670	563	561
-82	66437	61305	42735	29255	5199	4330	3027	2213
-72	5425	8606	6895	4107	430	420	277	228
-68	5805	7649	5522	4023	527	521	483	464
-60	7093	5566	4151	2689	548	496	360	294
-54	4523	5637	4208	3043	240	309	188	246
-51	7519	5693	4615	3332	584	577	408	464
-25	36466	41502	32754	26489	3026	3145	3040	2842

Table AIII.2-4 signal remaining (%)

CPDs Position	Experiment 1					Experiment 2				
	Repair time (hours)				$T_{50\%}$	Repair time (hours)				$T_{50\%}$
	0	1	2	3		0	1	2	3	
-431	100	88	56	39	2.4	100	88	64	55	3.3
-369	100	97	85	76	4.7	100	100	92	88	6.0
-330	100	97	84	74	4.4	100	100	88	76	4.1
-308	100	100	100	96	6.0	100	100	97	84	4.8
-275	100	100	100	100	6.0	100	100	100	100	6.0
-264	100	100	100	100	6.0	100	100	100	100	6.0
-240	100	100	94	80	4.4	100	100	85	67	3.6
-140	100	100	100	100	6.0	100	100	100	100	6.0
-137	100	100	89	65	3.4	100	100	100	98	6.0
-129	100	90	70	51	3.0	100	93	80	54	3.2
-98	100	91	61	43	2.6	100	81	59	49	2.8
-93	100	100	70	51	2.9	100	90	66	53	3.0
-88	100	100	89	70	3.7	100	100	97	97	6.0
-82	100	92	64	44	2.7	100	83	58	43	2.5
-72	100	100	100	76	3.9	100	98	64	53	3.0
-68	100	100	95	69	3.6	100	99	92	88	6.0
-60	100	78	59	38	2.4	100	91	66	54	3.1
-54	100	100	93	67	3.5	100	100	78	103	2.7
-51	100	76	61	44	2.6	100	99	70	79	2.5
-25	100	100	90	73	3.9	100	100	100	94	6.0

Table AIII.2-5 CPD repair in the *RPB2* TS in the *Δrad16* α strain

CPDs position	Experiment 1				Experiment 2			
	Repair time (hours)				Repair time (hours)			
	0	1	2	3	0	1	2	3
	1085685	1170302	1274268	1004145	1101562	1308174	1194202	1182095
936	9426	3123	921	646	10518	3024	1053	617
934	24983	2804	2422	1465	29845	2887	1544	1317
926	70778	16059	7673	3772	81229	18153	5166	5036
918	13985	3170	2877	3259	14517	4918	1979	2199
910	9677	1737	3934	3620	6628	1085	247	1541
895	27820	2392	2059	1955	24456	4685	2498	2852
887	19030	3369	4119	2177	14738	5182	2168	2216
882	6631	992	966	570	7331	2494	1313	1408
860	5213	2261	4117	2732	6357	727	2635	2546
833	8403	1383	493	974	11753	1640	775	708
810	19168	3278	2973	1724	23593	4222	3235	3594
784	10096	1304	1154	830	10765	1755	900	1326
767	7247	1058	1018	546	7285	1128	779	613
746	3823	1544	1835	1127	4762	2274	1571	1443
737	28190	3802	1553	880	28213	3761	1085	1131
714	17926	2776	2766	1777	19607	3274	2067	2122
699	2685	607	592	439	2977	1114	723	742
682	51682	8827	2973	1510	51394	10115	2365	2185
672	4171	595	350	258	3521	453	139	384
660	8605	1598	1110	570	8443	1894	651	599
646	7337	742	483	509	5328	465	371	376
636	3501	1416	1215	677	2852	1117	657	710
628	41077	5155	1721	1512	36288	4261	789	755
618	9050	2077	2464	1487	8324	2010	1432	1563
Sum	1496191	1242368	1326055	1039160	1522284	1390812	1230344	1220076
Ratio	1.00	0.83	0.89	0.69	1.00	0.91	0.81	0.80

Table AIII.2-5 Adjusted CPD repair in the *RPB2* TS in the *Δrad16* α strain

CPDs position	Experiment 1				Experiment 2			
	Repair time (hours)				Repair time (hours)			
	0	1	2	3	0	1	2	3
936	9426	3761	1039	930	10518	3310	1303	770
934	24983	3377	2733	2109	29845	3160	1911	1643
926	70778	19340	8657	5431	81229	19868	6392	6284
918	13985	3817	3246	4692	14517	5383	2449	2743
910	9677	2092	4439	5212	6628	1187	305	1922
895	27820	2880	2323	2814	24456	5128	3091	3559
887	19030	4057	4648	3135	14738	5672	2682	2764
882	6631	1194	1090	820	7331	2730	1624	1757
860	5213	2723	4645	3933	6357	796	3261	3176
833	8403	1665	556	1402	11753	1795	959	883
810	19168	3947	3354	2483	23593	4621	4003	4484
784	10096	1570	1302	1195	10765	1921	1113	1655
767	7247	1275	1148	786	7285	1235	964	765
746	3823	1860	2070	1622	4762	2489	1944	1801
737	28190	4578	1752	1266	28213	4116	1342	1411
714	17926	3344	3121	2559	19607	3584	2558	2647
699	2685	731	668	632	2977	1219	894	926
682	51682	10630	3354	2174	51394	11072	2926	2726
672	4171	716	395	372	3521	496	173	479
660	8605	1925	1252	821	8443	2073	806	748
646	7337	894	545	733	5328	509	459	469
636	3501	1705	1371	975	2852	1223	812	886
628	41077	6208	1942	2178	36288	4664	976	942
618	9050	2501	2780	2142	8324	2200	1772	1950

Table AIII.2-5 Signal remaining (%)

CPDs position	Experiment 1					Experiment 2				
	Repair time (hours)				$T_{50\%}$	Repair time (hours)				$T_{50\%}$
	0	1	2	3		0	1	2	3	
936	100	40	11	10	0.8	100	31	12	7	0.7
934	100	14	11	8	0.6	100	11	6	6	0.6
926	100	27	12	8	0.7	100	24	8	8	0.7
918	100	27	23	34	0.7	100	37	17	19	0.8
910	100	22	46	54	0.7	100	18	5	29	0.6
895	100	10	8	10	0.6	100	21	13	15	0.6
887	100	21	24	16	0.7	100	38	18	19	0.8
882	100	18	16	12	0.6	100	37	22	24	0.8
860	100	52	89	75	1.1	100	13	51	50	0.5
833	100	20	7	17	0.6	100	15	8	8	0.6
810	100	21	17	13	0.7	100	20	17	19	0.6
784	100	16	13	12	0.6	100	18	10	15	0.6
767	100	18	16	11	0.6	100	17	13	10	0.6
746	100	49	54	42	1	100	52	41	38	1.1
737	100	16	6	4	0.6	100	15	5	5	0.6
714	100	19	17	14	0.6	100	18	13	14	0.6
699	100	27	25	24	0.7	100	41	30	31	0.9
682	100	21	6	4	0.6	100	22	6	5	0.6
672	100	17	9	9	0.6	100	14	5	14	0.6
660	100	22	15	10	0.7	100	25	10	9	0.7
646	100	12	7	10	0.6	100	10	9	9	0.6
636	100	49	39	28	1	100	43	28	31	0.9
628	100	15	5	5	0.6	100	13	3	3	0.6
618	100	28	31	24	0.8	100	26	21	23	0.7

Table AIII.2-6 CPD repair in the *RPB2* NTS in the *Δrad16* α strain

CPDs position	Experiment 1				Experiment 2			
	Repair time (hours)				Repair time (hours)			
	0	1	2	3	0	1	2	3
Top band	1233795	1164206	907382	1108629	1749586	1513326	1694917	1495828
751	50662	40680	29040	31943	86363	66300	73597	51410
770	42612	35466	25423	28417	72794	56247	60392	44124
810					38919	28815	30464	21412
851	39318	32507	22674	26718	76938	57618	59705	41102
875	12778	10836	8659	10531	20433	16796	18187	14371
891	19846	16544	11733	13771	31009	23771	25945	18151
905	5969	4053	3700	4633	11242	8348	10382	7285
921	2606	1715	1534	2261	5004	4369	6602	5419
945	18259	16050	11661	13757	34910	28324	35804	28276
971	23886	21545	15722	17717	42242	34964	35047	26437
996	29647	24614	16972	18460	57308	44215	41460	32329
1019	10662	9108	6300	6976	17847	13853	14509	10309
1047	8164	7019	4799	5714	14353	11759	14185	8933
1066	34218	28825	20280	23394	56386	42404	48157	32750
1080	13082	11379	7662	8774	24140	18586	23716	14636
1086	14091	12276	8395	9461	25125	18601	20276	13897
1095	7929	7231	5368	6136	15293	12399	15479	12700
1099	3959	3766	2714	2990	7361	5327	6570	4425
1109	12027	10439	7590	8638	19885	14881	17053	11363
1129	43396	38349	27762	31168	67010	53565	58452	41843
Sum	1626907	1496608	1145370	1380089	2539216	2126203	2360113	1968917
Ratio	1.00	0.92	0.70	0.85	1.00	0.84	0.93	0.78

Table AIII.2-6 Adjusted CPD repair in the *RPB2* NTS in the *Δrad16* α strain

CPDs position	Experiment 1				Experiment 2			
	Repair time (hours)				Repair time (hours)			
	0	1	2	3	0	1	2	3
751	50662	44221	41249	37656	86363	79179	79182	66301
770	42612	38554	36112	33499	72794	67172	64975	56904
810					38919	34412	32776	27614
851	39318	35337	32206	31496	76938	68810	64235	53007
875	12778	11780	12299	12415	20433	20058	19568	18533
891	19846	17984	16666	16234	31009	28388	27914	23409
905	5969	4406	5255	5461	11242	9969	11170	9395
921	2606	1864	2179	2666	5004	5218	7103	6989
945	18259	17448	16564	16218	34910	33826	38521	36466
971	23886	23421	22332	20886	42242	41756	37707	34094
996	29647	26757	24108	21762	57308	52804	44606	41693
1019	10662	9901	8948	8223	17847	16544	15610	13295
1047	8164	7630	6817	6736	14353	14043	15262	11520
1066	34218	31334	28806	27577	56386	50641	51811	42236
1080	13082	12369	10883	10343	24140	22196	25516	18875
1086	14091	13345	11925	11153	25125	22215	21814	17923
1095	7929	7861	7625	7234	15293	14807	16654	16379
1099	3959	4094	3854	3525	7361	6361	7069	5707
1109	12027	11348	10782	10183	19885	17772	18347	14655
1129	43396	41688	39434	36742	67010	63970	62888	53962

Table AIII.2-6 Signal remaining (%)

CPDs position	Experiment 1					Experiment 2				
	Repair time (hours)				$T_{50\%}$	Repair time (hours)				$T_{50\%}$
	0	1	2	3		0	1	2	3	
751	100	88	82	75	6.0	100	92	92	77	6.0
770	100	91	85	79	6.0	100	92	89	78	6.0
810						100	88	84	71	5.4
851	100	90	82	81	6.0	100	89	83	69	5.2
875	100	93	97	98	6.0	100	98	96	91	6.0
891	100	91	85	83	6.0	100	92	90	75	6.0
905	100	74	89	92	6.0	100	89	99	84	6.0
921	100	72	84	100	5.4	100	100	100	100	6.0
945	100	96	91	90	6.0	100	97	100	100	6.0
971	100	99	94	88	6.0	100	99	89	81	5.0
996	100	91	82	74	6.0	100	92	78	73	6.0
1019	100	93	85	78	6.0	100	93	87	74	6.0
1047	100	94	84	83	6.0	100	98	100	80	6.0
1066	100	92	85	81	6.0	100	90	92	75	6.0
1080	100	95	84	80	6.0	100	92	100	78	6.0
1086	100	95	85	80	6.0	100	88	87	71	5.8
1095	100	100	97	92	6.0	100	97	100	100	6.0
1099	100	100	98	90	5.8	100	86	96	78	6.0
1109	100	95	90	85	6.0	100	89	92	74	6.0
1129	100	97	91	85	6.0	100	95	94	81	6.0

Table AIII.2-7 CPD repair in the *RPB2* TS in the *Δrad16tup1* α strain

CPDs position	Experiment 1				Experiment 2			
	Repair time (hours)				Repair time (hours)			
	0	1	2	3	0	1	2	3
Top band	576140	579382	549191	450786	653801	753725	882751	671334
936	3499	638	570	376	2201	426	486	769
934	8343	622	387	188	7878	547	1228	900
926	29797	3678	3434	2228	34420	4282	4190	3406
918	3801	863	743	580	4671	750	1902	1121
910					3183	584	1071	1542
895	8415	781	596	408	9309	732	1150	1531
887	6644	688	600	651	7050	962	1673	2118
882	2041	544	808	353	2620	369	442	829
860					4421	3251	2605	3349
833	2591	511	700	809	3379	635	293	582
810	4908	1028	860	798	7627	2082	2348	1828
784	3332	573	413	461	3674	970	858	684
767	2040	319	329	176	2621	396	390	350
746	1387	557	569	494	2068	840	948	643
737	11275	1007	838	553	15132	1068	839	798
714	8404	1829	2609	2485	11304	1996	1426	2261
699	691	271	332	247	934	475	659	544
682	10447	1039	782	439	11873	1639	1661	1079
672	1447	182	333	124	1225	200	222	236
660	2970	455	554	413	3189	750	779	468
646	2547	277	516	236	1805	212	401	310
636	1112	422	855	494	1230	448	502	411
628	9931	1108	1105	732	11760	1123	1037	771
618	3150	998	1242	1010	3603	1151	1293	984
Sum	715495	606134	577602	472841	810977	779614	911153	698848
Ratio	1.00	0.85	0.81	0.66	1.00	0.96	1.12	0.86

Table AIII.2-7 Adjusted CPD repair in the *RPB2* TS in the *Δrad16tup1* α strain

CPDs position	Experiment 1				Experiment 2			
	Repair time (hours)				Repair time (hours)			
	0	1	2	3	0	1	2	3
936	3499	753	707	569	2201	443	432	892
934	8343	735	479	285	7878	569	1093	1044
926	29797	4341	4254	3371	34420	4455	3729	3953
918	3801	1019	920	877	4671	780	1693	1300
910					3183	607	953	1789
895	8415	922	738	617	9309	762	1024	1777
887	6644	812	744	985	7050	1000	1489	2458
882	2041	643	1001	534	2620	383	394	962
860					4421	3382	2319	3887
833	2591	603	867	1225	3379	661	261	675
810	4908	1214	1065	1208	7627	2166	2090	2121
784	3332	677	511	698	3674	1009	764	794
767	2040	376	408	267	2621	412	348	407
746	1387	657	704	748	2068	873	843	747
737	11275	1189	1038	836	15132	1111	747	926
714	8404	2159	3232	3760	11304	2077	1270	2624
699	691	320	412	374	934	494	586	631
682	10447	1226	968	664	11873	1705	1478	1252
672	1447	215	412	187	1225	208	197	274
660	2970	537	687	625	3189	781	693	544
646	2547	327	639	357	1805	221	357	360
636	1112	498	1059	748	1230	466	446	477
628	9931	1308	1368	1108	11760	1168	923	895
618	3150	1178	1538	1529	3603	1198	1151	1142

Table AIII.2-7 Signal remaining (%)

CPDs position	Experiment 1					Experiment 2				
	Repair time (hours)				$T_{50\%}$	Repair time (hours)				$T_{50\%}$
	0	1	2	3		0	1	2	3	
936	100	22	20	16	0.7	100	20	20	41	0.6
934	100	9	6	3	0.6	100	7	14	13	0.6
926	100	15	14	11	0.6	100	13	11	11	0.6
918	100	27	24	23	0.7	100	17	36	28	0.5
910						100	19	30	56	0.6
895	100	11	9	7	0.5	100	8	11	19	0.5
887	100	12	11	15	0.6	100	14	21	35	0.6
882	100	31	49	26	0.7	100	15	15	37	0.6
860						100	77	52	88	2.1
833	100	23	33	47	0.7	100	20	8	20	0.6
810	100	25	22	25	0.7	100	28	27	28	0.7
784	100	20	15	21	0.6	100	27	21	22	0.7
767	100	18	20	13	0.7	100	16	13	16	0.6
746	100	47	51	54	1.0	100	42	41	36	1.0
737	100	11	9	7	0.5	100	7	5	6	0.5
714	100	26	38	45	0.7	100	18	11	23	0.6
699	100	46	60	54	0.9	100	53	63	68	1.2
682	100	12	9	6	0.6	100	14	12	11	0.6
672	100	15	29	13	0.7	100	17	16	22	0.6
660	100	18	23	21	0.7	100	24	22	17	0.7
646	100	13	25	14	0.6	100	12	20	20	0.6
636	100	45	95	67	0.9	100	38	36	39	0.9
628	100	13	14	11	0.6	100	10	8	8	0.6
618	100	37	49	49	0.7	100	33	32	32	0.8

Table AIII.2-8 CPD repair in the *RPB2* NTS in the *Δrad16tup1* α strain

CPDs position	Experiment 1				Experiment 2			
	Repair time (hours)				Repair time (hours)			
	0	1	2	3	0	1	2	3
Top band	746239	685690	708811	467791	1105208	810872	880939	639775
659	9176	10661	12361	6235	18185	17548	18579	12595
751	16874	17066	23257	12779	29839	24834	29273	17358
770	13727	13072	19243	10797	23197	19236	21618	13435
810	8077	7317	10975	5902	12217	9575	11093	6828
851	14741	14937	19111	9664	23447	18126	20505	13854
875	5725	5850	7507	4470	8599	7099	7970	5517
891	8311	8111	11488	5902	10605	8366	9033	5679
905	2775	2285	3154	1772	4873	3491	4269	2850
921	1069	828	1374	700	2794	1924	2861	1592
945	5994	6447	9161	5599	12321	9368	12945	7691
971	7720	8617	11168	6044	11887	9564	10709	7317
996	10777	10852	14545	7991	18228	14076	15018	9709
1019	3060	3731	5032	2877	4842	3729	4029	2545
1047	2481	3117	4193	2468	4113	3179	3579	2622
1066	11123	13192	17323	9134	17993	14237	15382	10035
1080	4915	5885	7194	4084	10336	8042	9035	5688
1086	4579	6085	7559	4188	8118	6384	6644	4303
1095	2898	3481	4360	2401	6170	4958	6458	3926
1099	1755	2231	2500	1627	3157	2643	2700	1950
1109	4299	5278	6410	3919	6469	5566	5737	3994
1129	15154	18096	23918	12781	21953	17745	18770	13139
Sum	901469	852829	930644	589126	1364552	1020559	1117148	792403
Ratio	1.00	0.95	1.03	0.65	1.00	0.75	0.82	0.58

Table AIII.2-8 Adjusted CPD repair in the *RPB2* NTS in the *Δrad16tup1* α strain

CPDs position	Experiment 1				Experiment 2			
	Repair time (hours)				Repair time (hours)			
	0	1	2	3	0	1	2	3
659	9176	11269	11974	9541	18185	23462	22694	21689
751	16874	18040	22528	19554	29839	33204	35756	29891
770	13727	13818	18639	16522	23197	25720	26406	23136
810	8077	7734	10631	9031	12217	12803	13550	11758
851	14741	15788	18512	14788	23447	24235	25046	23858
875	5725	6183	7272	6840	8599	9491	9735	9500
891	8311	8574	11128	9031	10605	11185	11033	9779
905	2775	2416	3055	2712	4873	4667	5215	4907
921	1069	875	1331	1072	2794	2572	3495	2741
945	5994	6814	8874	8567	12321	12525	15812	13245
971	7720	9108	10818	9248	11887	12787	13080	12601
996	10777	11471	14089	12227	18228	18820	18344	16720
1019	3060	3943	4874	4403	4842	4985	4921	4383
1047	2481	3294	4062	3777	4113	4251	4372	4514
1066	11123	13944	16780	13977	17993	19036	18789	17281
1080	4915	6221	6968	6249	10336	10753	11036	9795
1086	4579	6432	7322	6409	8118	8536	8116	7410
1095	2898	3679	4224	3674	6170	6630	7888	6760
1099	1755	2359	2421	2490	3157	3534	3298	3358
1109	4299	5579	6209	5996	6469	7442	7007	6878
1129	15154	19128	23168	19557	21953	23726	22927	22626

Table AIII.2-8 Signal remaining (%)

CPDs position	Experiment 1					Experiment 2				
	Repair time (hours)				$T_{50\%}$	Repair time (hours)				$T_{50\%}$
	0	1	2	3		0	1	2	3	
659	100	100	100	100	6.0	100	100	100	100	6.0
751	100	100	100	100	6.0	100	100	100	100	6.0
770	100	100	100	100	6.0	100	100	100	100	6.0
810	100	96	100	100	6.0	100	100	100	96	6.0
851	100	107	100	100	6.0	100	100	100	100	6.0
875	100	108	100	100	6.0	100	100	100	100	6.0
891	100	103	100	100	6.0	100	100	100	92	6.0
905	100	87	100	98	6.0	100	96	100	100	6.0
921	100	82	100	100	6.0	100	92	100	98	6.0
945	100	100	100	100	6.0	100	100	100	100	6.0
971	100	100	100	100	6.0	100	100	100	100	6.0
996	100	100	100	100	6.0	100	100	100	92	6.0
1019	100	100	100	100	6.0	100	100	100	91	6.0
1047	100	100	100	100	6.0	100	100	100	100	6.0
1066	100	100	100	100	6.0	100	100	100	96	6.0
1080	100	100	100	100	6.0	100	100	100	95	6.0
1086	100	100	100	100	6.0	100	100	100	91	6.0
1095	100	100	100	100	6.0	100	100	100	100	6.0
1099	100	100	100	100	6.0	100	100	100	100	6.0
1109	100	100	100	100	6.0	100	100	100	100	6.0
1129	100	100	100	100	6.0	100	100	100	100	6.0

AIII.3 CPD repair in the *MFA2* in Chapter 5

Table AIII.3-1 CPD repair in the *MFA2* TS in the *Δgcn5* a strain

CPDs position	Experiment 1				Experiment 2			
	Repair time (hours)				Repair time (hours)			
	0	1	2	3	0	1	2	3
Top band	576892	447077	640678	838991	180204	139245	156333	187611
2	3630	1769	1525	2293	553	511	307	82
-16	4718	2770	2201	2717	964	645	610	333
-37	2242	1163	740	947	524	415	278	258
-48	4373	3037	2413	3253	1211	1009	906	677
-108	14779	10678	10792	11246	4207	3475	3341	2555
-119	11689	7822	7212	7345	3115	2285	2282	1651
-133	3815	2550	2780	3064	907	726	621	436
-155	39841	26065	24623	23721	9899	7721	6763	5000
-164	15168	9619	8998	8094	3715	2673	2327	1676
-174	47820	34378	30815	30237	12138	9969	8656	6207
-193	9177	6253	7042	6779				
-198	16168	11900	11494	12743	4212	3213	3138	2497
-205	18084	11463	11189	11125	4380	3703	2890	2375
-215	6919	4736	5185	5308	1407	1137	854	701
-231	11645	8037	9498	10261	2774	2575	2517	2143
-255	29575	21835	23889	25898	8593	7343	7354	6021
-262	7623	5221	5580	5784	1961	1525	1559	1232
-293	7185	3398	3099	3257	1967	1345	1275	959
-309	1915	660	458	243	649	442	304	221
-316	5736	3386	3274	2821	1482	1152	970	748
-320	7611	4739	3987	4088	1812	1386	1058	758
-346	4697	2507	2354	2375	970	657	593	416
-358	16209	9467	9493	9695	3692	2853	2703	2189
-362	14995	8067	8294	8149	2871	2180	2002	1489
-382	29095	16274	14421	13828	6683	4489	3975	2915
Sum	911602	664872	852034	1054264	260887	202674	213613	231149
Ratio	1.00	0.73	0.93	1.16	1.00	0.78	0.82	0.89

Table AIII.3-1 Adjusted CPD repair in the *MFA2* TS in the *Δgcn5* a strain

CPDs position	Experiment 1				Experiment 2			
	Repair time (hours)				Repair time (hours)			
	0	1	2	3	0	1	2	3
2	3630	2426	1632	1983	553	658	375	92
-16	4718	3798	2354	2349	964	831	745	376
-37	2242	1595	791	819	524	534	340	291
-48	4373	4164	2582	2813	1211	1299	1107	764
-108	14779	14641	11547	9725	4207	4474	4080	2884
-119	11689	10724	7716	6351	3115	2941	2786	1863
-133	3815	3496	2974	2650	907	935	758	492
-155	39841	35737	26345	20511	9899	9939	8260	5644
-164	15168	13188	9627	6999	3715	3440	2842	1892
-174	47820	47136	32970	26146	12138	12832	10571	7005
-193	9177	8574	7534	5861				
-198	16168	16317	12298	11019	4212	4136	3832	2818
-205	18084	15717	11971	9619	4380	4767	3529	2681
-215	6919	6494	5548	4590	1407	1463	1043	791
-231	11645	11020	10162	8873	2774	3315	3074	2418
-255	29575	29938	25559	22394	8593	9452	8981	6796
-262	7623	7158	5970	5001	1961	1963	1904	1390
-293	7185	4659	3316	2816	1967	1731	1557	1083
-309	1915	905	490	210	649	568	372	249
-316	5736	4643	3503	2440	1482	1483	1185	845
-320	7611	6497	4266	3534	1812	1784	1292	855
-346	4697	3437	2518	2054	970	846	724	469
-358	16209	12981	10157	8383	3692	3672	3302	2471
-362	14995	11061	8874	7046	2871	2806	2445	1681
-382	29095	22313	15429	11957	6683	5779	4854	3290

Table AIII.3-1 signal remaining (%)

CPDs position	Experiment 1					Experiment 2				
	Repair time (hours)				$T_{50\%}$	Repair time (hours)				$T_{50\%}$
	0	1	2	3		0	1	2	3	
2	100	67	45	55	1.8	100	100	68	17	2.4
-16	100	81	50	50	2.6	100	86	77	39	2.7
-37	100	71	35	37	1.6	100	100	65	56	2.2
-48	100	95	59	64	3.6	100	100	91	63	3.4
-108	100	99	78	66	3.6	100	100	97	69	3.6
-119	100	92	66	54	3.1	100	94	89	60	3.3
-133	100	92	78	69	3.4	100	100	84	54	3.2
-155	100	90	66	51	3.0	100	100	83	57	3.2
-164	100	87	63	46	2.8	100	92	77	51	3.0
-174	100	99	69	55	3.1	100	100	87	58	3.2
-193	100	93	82	64	3.6					
-198	100	100	76	68	3.8	100	98	91	67	3.6
-205	100	87	66	53	3.2	100	100	81	61	3.3
-215	100	94	80	66	3.8	100	100	74	56	3.2
-231	100	95	87	76	4.8	100	100	100	87	4.9
-255	100	100	86	76	4.2	100	100	100	79	4.1
-262	100	94	78	66	3.8	100	100	97	71	3.6
-293	100	65	46	39	1.7	100	88	79	55	3.2
-309	100	47	26	11	1.0	100	87	57	38	2.4
-316	100	81	61	43	2.6	100	100	80	57	3.1
-320	100	85	56	46	2.6	100	98	71	47	2.8
-346	100	73	54	44	2.3	100	87	75	48	2.9
-358	100	80	63	52	3.2	100	99	89	67	3.5
-362	100	74	59	47	2.7	100	98	85	59	3.2
-382	100	77	53	41	2.3	100	86	73	49	3.0

Table AIII.3-2 CPD repair in the *MFA2* NTS in the *Δgcn5* a strain

CPDs position	Experiment1				Experiment 2			
	Repair time (hours)				Repair time (hours)			
	0	1	2	3	0	1	2	3
Top band	1969105	1439439	1414952	1808597	113320	86415	96689	119974
-431	248389	144098	131019	161600	14016	10818	11128	13060
-369	63639	34139	35517	47443	3450	2604	2840	3375
-330	29325	16514	17064	18741	1646	1370	1328	1471
-308	154919	91140	80948	102500	8359	6816	6819	7450
-275	11825	6296	6269	8163	632	455	560	687
-264	47705	26544	22470	27564	3134	2572	2594	3180
-240	142376	76373	64787	91922	9104	7090	7168	8556
-140	4947	2941	2615	2909	410	318	349	322
-137					510	362	348	323
-129	62052	32121	26372	34945	3761	3155	2862	3210
-98	64040	32842	27035	33903	4769	3734	3528	4020
-93	76881	40858	31837	40323	4915	3634	3552	3705
-88	13840	7628	6891	8872	715	612	593	558
-82	112768	60483	47281	57623	5082	3750	3588	3528
-72	12568	7954	7624	10169	523	458	430	486
-68	10730	5885	5164	6876	407	360	330	333
-60	9320	4950	3276	4787	332	332	224	276
-54	8667	5465	7565	6489	1856	1343	956	1363
-51	9706	5354	6451	4435	922	646	524	631
-25	55803	31898	28482	35018	4295	3355	3517	3520
Sum	3108605	2072922	1973619	2512879	182158	140199	149927	180030
Ratio	1.00	0.67	0.63	0.81	1.00	0.77	0.82	0.99

Table AIII.3-2 CPD repair in the *MFA2* NTS in the *Δgcn5* a strain

CPDs position	Experiment 1				Experiment 2			
	Repair time (hours)				Repair time (hours)			
	0	1	2	3	0	1	2	3
-431	248389	216093	206365	199911	14016	14056	13520	13214
-369	63639	51196	55943	58690	3450	3384	3451	3415
-330	29325	24764	26877	23184	1646	1780	1613	1489
-308	154919	136677	127499	126799	8359	8856	8285	7538
-275	11825	9442	9874	10098	632	591	681	695
-264	47705	39806	35391	34098	3134	3341	3151	3217
-240	142376	114530	102044	113714	9104	9212	8708	8657
-140	4947	4410	4119	3599	410	413	423	326
-137					510	470	423	327
-129	62052	48170	41538	43229	3761	4099	3477	3248
-98	64040	49251	42583	41940	4769	4851	4286	4068
-93	76881	61272	50145	49882	4915	4721	4316	3748
-88	13840	11439	10854	10976	715	795	720	565
-82	112768	90701	74471	71284	5082	4873	4360	3570
-72	12568	11928	12009	12580	523	595	522	492
-68	10730	8825	8134	8506	407	467	401	337
-60	9320	7423	5161	5921	332	432	272	280
-54	8667	8196	11915	8028	1856	1745	1162	1379
-51	9706	8029	10160	5487	922	839	637	638
-25	55803	47835	44862	43320	4295	4360	4273	3562

Table AIII.3-2 signal remaining (%)

CPDs position	Experiment 1					Experiment 2				
	Repair time (hours)				$T_{50\%}$	Repair time (hours)				$T_{50\%}$
	0	1	2	3		0	1	2	3	
-431	100	87	83	81	6.0	100	100	96	94	6.0
-369	100	81	88	92	6.0	100	98	100	99	6.0
-330	100	85	92	79	4.7	100	108	98	90	6.0
-308	100	88	82	82	6.0	100	106	99	90	5.7
-275	100	80	84	86	6.0	100	93	108	110	6.0
-264	100	84	74	72	5.4	100	107	101	103	6.0
-240	100	81	72	80	6.0	100	101	96	95	6.0
-140	100	89	83	73	5.8	100	101	103	80	4.0
-137						100	92	83	64	3.6
-129	100	78	67	70	5.0	100	109	92	86	5.8
-98	100	77	67	66	4.3	100	102	90	85	6.0
-93	100	80	65	65	4.2	100	96	88	76	4.6
-88	100	83	79	79	6.0	100	111	101	79	4.1
-82	100	81	66	63	4.1	100	96	86	70	4.0
-72	100	95	96	100	6.0	100	114	100	94	6.0
-68	100	82	76	79	6.0	100	115	99	83	4.5
-60	100	80	55	64	4.2	100	130	82	84	4.9
-54	100	95	138	93	6.0	100	94	63	74	4.6
-51	100	83	105	57	3.5	100	91	69	69	4.6
-25	100	86	81	78	6.0	100	102	99	83	4.5

Table AIII.3-3 CPD repair in the *MFA2* TS in the *Δtup1gcn5* a strain

CPDs position	Experiments 1				Experiment 2			
	Repair time (hours)				Repair time (hours)			
	0	1	2	3	0	1	2	3
Top band	174567	177783	260547	282866	69127	87179	80712	102184
2	1648	970	733	449	548	577	228	227
-16	2004	1080	945	498	673	608	374	269
-37	829	435	370	139	252	297	103	76
-48	1975	1233	869	524	666	711	383	269
-108	4496	3884	3298	2201	1612	1896	1294	1046
-119	3360	2401	1863	1059	1232	1227	661	523
-133	1146	973	928	622				
-155	10941	8377	6047	3668	4055	4250	2356	1725
-164	4007	2503	1754	956	1425	1252	580	408
-174	14383	10451	7063	4334	5128	5426	2829	1997
-193	2832	2426	1858	1245	1195	1314	873	632
-198	5131	3980	3185	2092	1815	1907	1113	974
-205	5235	3386	2122	1336	1982	1807	962	671
-215	2033	1687	1262	804	799	882	478	437
-231	3773	3187	2985	2139	1292	1541	1092	989
-255	10150	8567	7632	5390	3670	4401	3098	2590
-262	2697	1921	1884	1328	858	946	646	545
-293	2533	1331	917	591	885	725	403	283
-309	734	226	121	99	280	120	104	95
-316	1896	1041	563	351	707	573	301	221
-320	2348	1291	672	434	863	726	345	237
-346	1197	802	528	318	452	413	220	166
-358	4064	2688	2223	1353	1430	1310	742	564
-362	3708	2394	1612	1006	1465	1301	688	474
-382	7020	4346	2992	1851	2860	2281	1269	921
Sum	274708	249362	314973	317653	105271	123669	101854	118523
Ratio	1.00	0.91	1.15	1.16	1.00	1.17	0.97	1.13

Table AIII.3-3 CPD repair in the *MFA2* TS in the *Δtup1gcn5* a strain

CPDs position	Experiment 1				Experiment 2			
	Repair time (hours)				Repair time (hours)			
	0	1	2	3	0	1	2	3
2	1648	1069	639	388	548	492	236	201
-16	2004	1190	824	431	673	517	386	239
-37	829	480	323	120	252	253	106	67
-48	1975	1358	758	453	666	605	395	239
-108	4496	4279	2877	1904	1612	1614	1337	929
-119	3360	2645	1625	916	1232	1044	683	465
-133	1146	1072	809	538				
-155	10941	9228	5274	3172	4055	3618	2435	1533
-164	4007	2757	1530	826	1425	1066	599	363
-174	14383	11513	6160	3748	5128	4619	2924	1774
-193	2832	2673	1621	1077	1195	1118	902	561
-198	5131	4385	2778	1809	1815	1623	1150	865
-205	5235	3730	1851	1155	1982	1538	994	596
-215	2033	1859	1101	695	799	751	495	388
-231	3773	3511	2603	1850	1292	1311	1129	878
-255	10150	9437	6656	4661	3670	3746	3202	2301
-262	2697	2117	1643	1148	858	805	667	484
-293	2533	1466	800	511	885	617	417	252
-309	734	249	105	86	280	102	108	85
-316	1896	1146	491	303	707	488	312	196
-320	2348	1422	586	375	863	618	356	211
-346	1197	884	461	275	452	352	227	147
-358	4064	2961	1939	1170	1430	1116	767	501
-362	3708	2637	1406	870	1465	1108	711	421
-382	7020	4787	2609	1601	2860	1942	1311	818

Table AIII.3-3 signal remaining (%)

CPDs position	Experiment 1					Experiment 2				
	Repair time (hours)				$T_{50\%}$	Repair time (hours)				$T_{50\%}$
	0	1	2	3		0	1	2	3	
2	100	65	39	24	1.6	100	90	43	37	1.9
-16	100	59	41	21	1.5	100	77	57	36	2.3
-37	100	58	39	14	1.4	100	100	42	27	1.9
-48	100	69	38	23	1.6	100	91	59	36	2.2
-108	100	95	64	42	2.7	100	100	83	58	3.2
-119	100	79	48	27	2.0	100	85	55	38	2.3
-133	100	94	71	47	2.8					
-155	100	84	48	29	2.1	100	89	60	38	2.4
-164	100	69	38	21	1.6	100	75	42	25	1.8
-174	100	80	43	26	1.9	100	90	57	35	2.2
-193	100	94	57	38	2.5	100	94	76	47	2.8
-198	100	85	54	35	2.3	100	89	63	48	2.4
-205	100	71	35	22	1.6	100	78	50	30	2.0
-215	100	91	54	34	2.4	100	94	62	49	2.3
-231	100	93	69	49	2.9	100	101	87	68	3.2
-255	100	93	66	46	2.8	100	102	87	63	3.2
-262	100	78	61	43	2.6	100	94	78	56	3.1
-293	100	58	32	20	1.2	100	70	47	28	1.8
-309	100	34	14	12	0.8	100	36	39	30	0.9
-316	100	60	26	16	1.2	100	69	44	28	1.6
-320	100	61	25	16	1.2	100	72	41	24	1.6
-346	100	74	38	23	1.7	100	78	50	33	2.0
-358	100	73	48	29	1.9	100	78	54	35	2.2
-362	100	71	38	23	1.6	100	76	49	29	2.0
-382	100	68	37	23	1.6	100	68	46	29	1.7

Table AIII.3-4 CPD repair in the *MFA2* NTS in the *Δtup1gcn5* a strain

CPDs position	Experiment 1				Experiment 2			
	Repair time (hours)				Repair time (hours)			
	0	1	2	3	0	1	2	3
Top band	166582	193168	218061	235513	74658	65799	56922	97506
-431	20153	18421	12759	8335	10574	8243	5028	5083
-369	4675	4293	3384	2535	2556	2051	1441	1524
-330	2281	2158	1441	1288	1223	976	527	625
-308	11081	9914	6369	4805	5685	4432	2683	2709
-275	1673	998	577	407				
-264					2445	1791	881	1296
-240	10611	9579	8003	7110	5412	4430	3009	3629
-140	837	617	267	276	522	322	148	132
-137	447	239	135	79	336	132	72	62
-129	3203	2823	1955	1587	1985	1400	808	902
-98	5390	4931	2966	2710	3354	2775	1399	1530
-93	5776	5210	3530	2536	3096	2340	1402	1355
-88	1293	1380	844	733	660	567	345	405
-82	7930	7196	4520	3225	4214	3288	1873	1778
-72	1558	2161	1001	2006	995	922	471	656
-68	941	1123	764	831	523	511	230	416
-60	651	706	412	567				
-51					349	335	130	203
-25	6186	4606	4314	2707	2180	1745	1050	1169
Sum	251266	269524	271301	277251	120768	102058	78418	120978
Ratio	1.00	1.07	1.08	1.10	1.00	0.85	0.65	1.00

Table AIII.3-4 CPD repair in the *MFA2* NTS in the *Δtup1gcn5* a strain

CPDs position	Experiment 1				Experiment 2			
	Repair time (hours)				Repair time (hours)			
	0	1	2	3	0	1	2	3
-431	20153	17173	11817	7554	10574	9754	7744	5074
-369	4675	4002	3134	2297	2556	2427	2219	1521
-330	2281	2012	1335	1167	1223	1155	811	624
-308	11081	9242	5899	4354	5685	5244	4133	2704
-275	1673	931	534	369				
-264					2445	2120	1357	1294
-240	10611	8930	7412	6444	5412	5242	4633	3623
-140	837	575	248	250	522	381	228	131
-137	447	223	125	72	336	156	111	62
-129	3203	2632	1811	1438	1985	1657	1244	900
-98	5390	4597	2747	2456	3354	3284	2155	1527
-93	5776	4857	3269	2298	3096	2769	2159	1353
-88	1293	1287	781	665	660	671	532	404
-82	7930	6708	4186	2922	4214	3891	2884	1775
-72	1558	2015	927	1818	995	1091	726	655
-68	941	1047	708	753	523	605	354	415
-60	651	658	381	514				
-51					349	397	200	203
-25	6186	4294	3996	2454	2180	2064	1616	1167

Table AIII.3-4 signal remaining (%)

CPDs position	Experiment 1					Experiment 2				
	Repair time (hours)				$T_{50\%}$	Repair time (hours)				$T_{50\%}$
	0	1	2	3		0	1	2	3	
-431	100	85	59	37	2.4	100	92	73	48	2.9
-369	100	86	67	49	2.9	100	95	87	60	3.3
-330	100	88	59	51	2.2	100	94	66	51	2.9
-308	100	83	53	39	2.1	100	92	73	48	2.8
-275	100	56	32	22	1.2					
-264						100	87	56	53	2.2
-240	100	84	70	61	3.6	100	97	86	67	3.6
-140	100	69	30	30	1.8	100	73	44	25	1.8
-137	100	50	28	16	1.0	100	46	33	18	1.0
-129	100	82	57	45	2.3	100	84	63	45	2.6
-98	100	85	51	46	2.1	100	98	64	46	2.7
-93	100	84	57	40	2.4	100	89	70	44	2.7
-88	100	99	60	51	2.8	100	100	81	61	3.3
-82	100	85	53	37	2.2	100	92	68	42	2.6
-72	100	100	60	100	2.2	100	100	73	66	3.4
-68	100	100	75	80	2.5	100	100	68	79	2.2
-60	100	100	59	79	2.0					
-51						100	100	57	58	2.0
-25	100	69	65	40	2.4	100	95	74	54	3.1

Table AIII.3-5 CPD repair in the *MFA2* TS in the *Δgcn5* α strain

CPDs position	Experiment 1				Experiment 2			
	Repair time (hours)				Repair time (hours)			
	0	1	2	3	0	1	2	3
Top band	181046	232298	198869	238855	56276	81538	77266	96762
2	1482	1644	1155	1159	566	725	646	658
-16	1847	2068	1479	1478	607	751	735	644
-37	945	1048	728	624	281	343	311	283
-48	1761	1798	1229	1002	617	707	509	438
-108	3843	4318	3221	3336	1436	1807	1655	1615
-119	3383	3807	2948	2894	1191	1544	1401	1343
-133	1136	1218	928	957	503	613	574	640
-155	16654	19235	13561	13337	6049	7794	6807	6396
-164	5833	6645	4496	4324	2173	2612	2156	1964
-174	19792	21659	15141	15040	7472	9162	7875	7324
-193	3260	3656	2820	2701	1197	1551	1406	1340
-198	5252	6187	4467	4124	1955	2379	2048	2018
-205	5814	5482	3524	3201	2600	3035	2550	2156
-215	1913	1947	1420	1333	715	893	884	715
-231	3228	3658	2773	2709	1408	1898	1713	1661
-255	10408	11876	8540	8867	4142	5369	4925	4727
-262	3255	3690	2732	2818	1246	1511	1388	1264
-293	2547	2556	1794	1549	1013	1123	930	825
-309	867	818	478	385	383	396	279	259
-316	1678	1474	1014	915	871	906	769	662
-320	2380	2048	1414	1348	1271	1430	1113	978
-346	1530	1649	1133	1102	734	751	666	598
-358	5658	6271	4487	4294	2641	2989	2617	2514
-362	4001	4189	2963	2810	1936	2047	1817	1801
-382	7994	7573	4961	4561	3235	3164	2572	2348
Sum	297506	358813	288274	325723	102518	137039	125611	141931
Ratio	1.00	1.21	0.97	1.09	1.00	1.34	1.23	1.38

Table AIII.3-5 CPD repair in the *MFA2* TS in the *Δgcn5* α strain

CPDs position	Experiment 1				Experiment 2			
	Repair time (hours)				Repair time (hours)			
	0	1	2	3	0	1	2	3
2	1482	1363	1192	1059	566	542	528	475
-16	1847	1715	1527	1350	607	562	600	465
-37	945	869	752	570	281	257	254	204
-48	1761	1491	1268	915	617	529	415	316
-108	3843	3580	3324	3047	1436	1352	1351	1166
-119	3383	3156	3043	2644	1191	1155	1144	970
-133	1136	1010	957	874	503	459	468	462
-155	16654	15948	13995	12182	6049	5831	5555	4620
-164	5833	5509	4640	3950	2173	1954	1759	1419
-174	19792	17958	15626	13737	7472	6854	6427	5290
-193	3260	3031	2910	2467	1197	1160	1147	968
-198	5252	5130	4610	3767	1955	1780	1671	1457
-205	5814	4546	3637	2924	2600	2271	2081	1557
-215	1913	1615	1466	1218	715	668	721	516
-231	3228	3033	2861	2474	1408	1420	1398	1200
-255	10408	9847	8814	8099	4142	4017	4020	3415
-262	3255	3060	2819	2574	1246	1131	1133	913
-293	2547	2119	1851	1415	1013	840	759	596
-309	867	678	493	351	383	297	228	187
-316	1678	1223	1047	835	871	678	628	478
-320	2380	1698	1459	1231	1271	1070	908	706
-346	1530	1367	1170	1007	734	562	543	432
-358	5658	5200	4630	3922	2641	2236	2136	1816
-362	4001	3473	3058	2566	1936	1531	1483	1301
-382	7994	6279	5120	4166	3235	2367	2099	1696

Table AIII.3-5 signal remaining (%)

CPDs position	Experiment 1					Experiment 2				
	Repair time (hours)				$T_{50\%}$	Repair time (hours)				$T_{50\%}$
	0	1	2	3		0	1	2	3	
2	100	92	80	71	4.9	100	96	93	84	5.8
-16	100	93	83	73	4.9	100	93	99	77	4.3
-37	100	92	80	60	3.4	100	91	90	73	4.3
-48	100	85	72	52	3.1	100	86	67	51	3.0
-108	100	93	87	79	6.0	100	94	94	81	5.2
-119	100	93	90	78	5.1	100	97	96	81	4.7
-133	100	89	84	77	6.0	100	91	93	92	6.0
-155	100	96	84	73	4.4	100	96	92	76	4.3
-164	100	94	80	68	4.0	100	90	81	65	4.0
-174	100	91	79	69	4.7	100	92	86	71	4.3
-193	100	93	89	76	4.7	100	97	96	81	4.6
-198	100	98	88	72	3.9	100	91	86	75	5.2
-205	100	78	63	50	3.0	100	87	80	60	3.5
-215	100	84	77	64	4.6	100	93	100	72	3.8
-231	100	94	89	77	4.8	100	100	99	85	4.7
-255	100	95	85	78	5.8	100	97	97	82	4.7
-262	100	94	87	79	6.0	100	91	91	73	4.4
-293	100	83	73	56	3.4	100	83	75	59	3.8
-309	100	78	57	41	2.4	100	77	59	49	2.8
-316	100	73	62	50	3.0	100	78	72	55	3.6
-320	100	71	61	52	3.0	100	84	71	56	3.4
-346	100	89	76	66	4.3	100	77	74	59	3.6
-358	100	92	82	69	4.3	100	85	81	69	5.0
-362	100	87	76	64	4.3	100	79	77	67	4.5
-382	100	79	64	52	3.2	100	73	65	52	3.0

Table AIII.3-6 CPD repair in the *MFA2* NTS in the *Δgcn5* α strain

CPDs position	Experiment 1				Experiment 2			
	Repair time (hours)				Repair time (hours)			
	0	1	2	3	0	1	2	3
Top band	183320	246535	148577	245236	103474	108707	127976	132012
-431	17346	20174	11658	14633	9513	9838	9958	8529
-369	7537	8628	5455	6698	3274	3647	3845	3348
-330	2469	2947	1740	2149	1229	1233	1273	1149
-308	17799	22108	12935	16164	8216	9103	9504	8867
-275	850	1018	634	679	1008	725	713	617
-264	6801	8115	4444	5414	4256	3832	3969	3520
-240	12577	15812	9599	11989	5586	5765	6176	6024
-140	887	928	525	663	271	338	320	336
-137	371	460	294	343	904	910	945	882
-129	3840	4702	2992	3901	1853	2206	2309	2385
-98	6034	6608	4084	5084	3199	3544	3789	3550
-93	7808	8325	5378	6594	3978	4252	4342	4192
-88	1424	1221	922	1160	801	817	884	810
-82	10529	11110	7031	8120	5285	5516	5500	5003
-72	1503	1495	877	1085	852	828	819	728
-68	1380	1511	924	1113	629	720	679	588
-60	972	1109	638	729	404	404	415	304
-54	827	855	561	641	535	514	500	507
-51	855	970	490	523				
-25	5748	5816	3540	3681	3399	3203	3058	2837
Sum	290879	370448	223300	336599	158669	166105	186973	186189
Ratio	1.00	1.27	0.77	1.16	1.00	1.05	1.18	1.17

Table AIII.3-6 Adjusted CPD repair in the *MFA2* NTS in the *Δgcn5* α strain

CPDs position	Experiment 1				Experiment 2			
	Repair time (hours)				Repair time (hours)			
	0	1	2	3	0	1	2	3
-431	17346	15841	15186	12645	9513	9398	8451	7269
-369	7537	6775	7107	5788	3274	3484	3263	2853
-330	2469	2314	2267	1857	1229	1178	1080	979
-308	17799	17360	16850	13968	8216	8696	8065	7556
-275	850	799	826	587	1008	693	605	525
-264	6801	6372	5789	4679	4256	3660	3368	3000
-240	12577	12416	12504	10361	5586	5507	5241	5134
-140	887	729	684	573	271	323	272	287
-137	371	361	383	297	904	869	802	752
-129	3840	3692	3898	3371	1853	2108	1959	2032
-98	6034	5188	5320	4393	3199	3385	3215	3025
-93	7808	6537	7005	5698	3978	4062	3685	3572
-88	1424	959	1202	1003	801	781	750	690
-82	10529	8724	9158	7017	5285	5270	4667	4264
-72	1503	1174	1143	938	852	791	695	620
-68	1380	1187	1203	962	629	688	576	501
-60	972	870	831	630	404	386	352	259
-54	827	671	731	554	535	491	424	432
-51	855	762	638	452				
-25	5748	4567	4612	3181	3399	3060	2595	2418

Table AIII.3-6 signal remaining (%)

CPDs position	Experiment 1					Experiment 2				
	Repair time (hours)				$T_{50\%}$	Repair time (hours)				$T_{50\%}$
	0	1	2	3		0	1	2	3	
-431	100	91	88	73	4.5	100	99	89	77	4.3
-369	100	90	94	77	4.8	100	100	100	87	4.9
-330	100	94	92	75	4.4	100	96	88	80	5.3
-308	100	98	95	78	4.3	100	106	98	92	6.0
-275	100	94	97	69	3.7	100	69	60	52	3.0
-264	100	94	85	69	3.9	100	86	79	71	5.0
-240	100	99	99	82	4.5	100	99	94	92	6.0
-140	100	82	77	65	4.3	100	100	100	100	6.0
-137	100	97	100	80	4.8	100	96	89	83	6.0
-129	100	96	100	88	5.6	100	100	100	100	6.0
-98	100	86	88	73	5.5	100	100	100	95	6.0
-93	100	84	90	73	6.0	100	102	93	90	6.0
-88	100	67	84	70	4.8	100	98	94	86	6.0
-82	100	83	87	67	5.0	100	100	88	81	4.9
-72	100	78	76	62	4.0	100	93	82	73	4.9
-68	100	86	87	70	4.6	100	100	92	80	4.5
-60	100	90	85	65	3.8	100	96	87	64	3.6
-54	100	81	88	67	4.6	100	92	79	81	6.0
-51	100	89	75	53	3.1					
-25	100	79	80	55	3.4	100	90	76	71	5.0

Table AIII.3-7 CPD repair in the *MFA2* TS in the *Δtup1gcn5* α strain

CPDs position	Experiment 1				Experiment 2			
	Repair time (hours)				Repair time (hours)			
	0	1	2	3	0	1	2	3
Top band	105271	122747	120449	119711	86043	72008	71099	102079
2	915	582	245	101	713	435	222	122
-16	1087	682	368	180	853	503	248	201
-37	444	303	109	59	361	575	84	243
-48	993	732	374	192	930	514	236	215
-108	2451	2126	1298	683	2175	1468	956	797
-119	1650	1214	613	333	1716	956	502	387
-133	593	574	355	218	505	404	306	219
-155	5979	5056	2436	1225	5851	3378	1859	1369
-164	2256	1600	661	357	2205	989	538	371
-174	7592	6283	2837	1446	7481	4217	2098	1604
-193	1317	1202	637	360	1374	884	492	391
-198	2646	2378	1310	632	2979	1645	975	808
-205	3078	2275	1016	515	2749	1525	802	598
-215	1142	1135	640	311	1183	762	507	404
-231	1709	1809	1336	795	1757	1316	1004	975
-255	5315	5413	3919	2463	5906	4087	3198	2922
-262	1157	1111	765	495	1451	866	659	598
-293	1243	914	458	281	1471	680	398	353
-309	361	161	52	65	381	125	62	69
-316	1013	735	327	174	980	507	289	241
-320	1181	811	353	177	1069	567	282	231
-346	708	527	265	108	808	377	211	197
-358	1954	1620	903	489	2334	1166	718	604
-362	1584	1213	628	299	1909	911	518	424
-382	4364	3117	1523	812	4670	2117	1230	1020
Sum	158004	166321	143879	132478	139854	102982	89493	117444
Ratio	1.00	1.05	0.91	0.84	1.00	0.74	0.64	0.84

Table AIII.3-7 Adjusted CPD repair in the *MFA2* TS in the *Δtup1gcn5* α strain

CPDs position	Experiment 1				Experiment 2			
	Repair time (hours)				Repair time (hours)			
	0	1	2	3	0	1	2	3
2	915	553	269	121	713	591	347	146
-16	1087	648	404	214	853	683	388	240
-37	444	288	120	71	361	781	132	290
-48	993	695	411	229	930	698	369	256
-108	2451	2020	1426	815	2175	1994	1493	949
-119	1650	1154	673	397	1716	1299	785	460
-133	593	545	390	259	505	549	478	261
-155	5979	4804	2675	1461	5851	4587	2905	1630
-164	2256	1520	726	425	2205	1343	841	442
-174	7592	5969	3116	1724	7481	5727	3278	1910
-193	1317	1142	699	429	1374	1200	769	466
-198	2646	2259	1438	753	2979	2235	1524	962
-205	3078	2162	1116	614	2749	2071	1253	713
-215	1142	1078	703	370	1183	1034	792	482
-231	1709	1718	1468	949	1757	1788	1569	1161
-255	5315	5142	4304	2938	5906	5550	4997	3479
-262	1157	1055	840	591	1451	1176	1030	712
-293	1243	868	503	335	1471	923	623	421
-309	361	153	58	77	381	170	97	82
-316	1013	698	359	207	980	688	452	287
-320	1181	770	388	211	1069	769	441	275
-346	708	501	291	129	808	512	329	235
-358	1954	1539	991	583	2334	1583	1123	720
-362	1584	1152	689	356	1909	1238	809	505
-382	4364	2961	1672	968	4670	2874	1922	1214

Table AIII.3-7 signal remaining (%)

CPDs position	Experiment 1					Experiment 2				
	Repair time (hours)				$T_{50\%}$	Repair time (hours)				$T_{50\%}$
	0	1	2	3		0	1	2	3	
2	100	60	29	13	1.3	100	83	49	20	2.0
-16	100	60	37	20	1.4	100	80	45	28	1.9
-37	100	65	27	16	1.3	100	100	36	80	1.7
-48	100	70	41	23	1.7	100	75	40	28	1.8
-108	100	82	58	33	2.3	100	92	69	44	2.7
-119	100	70	41	24	1.7	100	76	46	27	1.9
-133	100	92	66	44	2.7	100	100	95	52	3.0
-155	100	80	45	24	2.0	100	78	50	28	2.0
-164	100	67	32	19	1.4	100	61	38	20	1.4
-174	100	79	41	23	1.8	100	77	44	26	1.9
-193	100	87	53	33	2.2	100	87	56	34	2.3
-198	100	85	54	28	2.1	100	75	51	32	2.0
-205	100	70	36	20	1.6	100	75	46	26	1.9
-215	100	94	62	32	2.4	100	87	67	41	2.6
-231	100	100	86	56	3.1	100	100	89	66	3.4
-255	100	97	81	55	3.1	100	94	85	59	3.4
-262	100	91	73	51	3.0	100	81	71	49	3.0
-293	100	70	40	27	1.7	100	63	42	29	1.6
-309	100	42	16	21	0.8	100	45	25	22	0.9
-316	100	69	35	20	1.5	100	70	46	29	1.8
-320	100	65	33	18	1.4	100	72	41	26	1.7
-346	100	71	41	18	1.7	100	63	41	29	1.6
-358	100	79	51	30	2.0	100	68	48	31	1.8
-362	100	73	44	22	1.8	100	65	42	26	1.6
-382	100	68	38	22	1.6	100	62	41	26	1.5

Table AIII.3-8 CPD repair in the *MFA2* NTS in the *Δtup1gcn5* α strain

CPDs position	Experiment 1				Experiment 2			
	Repair time (hours)				Repair time (hours)			
	0	1	2	3	0	1	2	3
Top band	80784	117130	124867	152238	140444	140292	142171	156359
-431	8648	9513	5579	3683	12792	10315	6143	3600
-369	2065	2476	1626	1278	2827	2466	1604	1088
-330	1032	1255	692	434	1782	1572	858	527
-308	5491	6140	3318	2253	7926	6840	3924	2266
-275	464	510	269	174	650	589	297	196
-264	2305	2211	1066	670	3433	3117	1955	706
-240	4909	5753	3921	3421	7548	7447	5461	3607
-140	546	437	178	128	537	368	134	117
-137	333	180	81	42	453	204	91	63
-129	1812	1718	888	635	2474	1792	1018	629
-98	2966	2592	1218	818	3517	2695	1599	755
-93	3207	2839	1409	979	3791	2961	1641	947
-88	737	687	366	266	746	662	355	188
-82	4521	3962	1910	1247	4778	3688	1949	999
-72	766	871	514	306	577	607	334	250
-68	598	601	323	223	613	572	365	222
-60	393	363	196	101	457	434	215	131
-54	337	411	244	256	504	718	474	195
-51					628	487	328	194
-25	2581	2945	1609	1299	2739	2700	1625	1131
Sum	124834	162903	150423	170530	199215	190524	172542	174170
Ratio	1.00	1.30	1.20	1.37	1.00	0.96	0.87	0.87

Table AIII.3-8 Adjusted CPD repair in the *MFA2* NTS in the *Δtup1gcn5* α strain

CPDs position	Experiment 1				Experiment 2			
	Repair time (hours)				Repair time (hours)			
	0	1	2	3	0	1	2	3
-431	8648	7290	4630	2696	12792	10786	7093	4118
-369	2065	1898	1350	935	2827	2578	1852	1245
-330	1032	962	574	318	1782	1643	991	603
-308	5491	4705	2753	1649	7926	7152	4531	2592
-275	464	391	223	128	650	615	343	224
-264	2305	1694	884	491	3433	3259	2257	807
-240	4909	4409	3254	2504	7548	7787	6306	4126
-140	546	335	148	94	537	384	154	134
-137	333	138	67	30	453	213	105	73
-129	1812	1317	737	465	2474	1873	1175	720
-98	2966	1986	1011	599	3517	2818	1846	863
-93	3207	2175	1169	716	3791	3096	1895	1084
-88	737	527	303	195	746	692	410	215
-82	4521	3036	1585	913	4778	3856	2251	1143
-72	766	667	427	224	577	634	385	286
-68	598	460	268	163	613	598	422	254
-60	393	278	162	74	457	453	248	149
-54	337	315	202	188	504	751	547	222
-51					628	509	379	222
-25	2581	2257	1335	951	2739	2824	1876	1293

Table AIII.3-8 signal remaining (%)

CPDs position	Experiment 1					Experiment 2				
	Repair time (hours)				$T_{50\%}$	Repair time (hours)				$T_{50\%}$
	0	1	2	3		0	1	2	3	
-431	100	84	54	31	2.2	100	84	55	32	2.3
-369	100	92	65	45	2.8	100	91	66	44	2.7
-330	100	93	56	31	2.4	100	92	56	34	2.4
-308	100	86	50	30	2.0	100	90	57	33	2.4
-275	100	84	48	28	2.0	100	95	53	35	2.3
-264	100	73	38	21	1.7	100	95	66	24	2.4
-240	100	90	66	51	3.0	100	100	84	55	3.0
-140	100	61	27	17	1.2	100	72	29	25	1.4
-137	100	41	20	9	0.9	100	47	23	16	1.0
-129	100	73	41	26	1.7	100	76	47	29	1.9
-98	100	67	34	20	1.4	100	80	52	25	2.0
-93	100	68	36	22	1.5	100	82	50	29	2.1
-88	100	71	41	26	1.7	100	93	55	29	2.2
-82	100	67	35	20	1.5	100	81	47	24	1.9
-72	100	87	56	29	2.3	100	100	67	50	3.0
-68	100	77	45	27	1.9	100	98	69	41	2.7
-60	100	71	41	19	1.7	100	99	54	33	2.1
-54	100	94	60	56	3.2	100	100	100	44	3.0
-51						100	81	60	35	2.4
-25	100	87	52	37	2.2	100	100	68	47	2.9

References

Acton T. B., Zhong H., Vershon A. K. (1997) DNA-binding specificity of Mcm1: operator mutations that alter DNA-bending and transcriptional activities by a MADS box protein. *Mol Cell Biol*, **17**(4), 1881-1889.

Acton T. B., Mead J., Steiner A. M., Vershon A. K. (2000) Scanning mutagenesis of Mcm1: residues required for DNA binding, DNA bending, and transcriptional activation by a MADS-box protein. *Mol Cell Biol* **20**(1), 1-11.

Agalioti, T., Chen, G., and Thanos, D. (2002). Deciphering the transcriptional histone acetylation code for a human gene. *Cell* **111**(3), 381–392.

Alland L., Muhle R., Hou H. Jr, Potes J., Chin L., Schreiber-Agus N., DePinho R.A. (1997) Role for N-CoR and histone deacetylase in Sin3-mediated transcriptional repression. *Nature* **387**(6628), 49-55.

Andressoo, J. O., Hoeijmakers, J. H. (2005) Transcription-coupled repair and premature ageing. *Mutat Res* **577**(1-2), 179-194.

Aravind, L., Iyer L. M., and Koonin E. V. (2003) Scores of RINGS but no PHDs in ubiquitin signaling. *Cell Cycle* **2**(2), 123–126.

Axelrod, J. D., Reagan, M. S., and Majors, J. (1993) *GAL4* disrupts a repressing nucleosome during activation of *GAL1* transcription *in vivo*. *Genes Dev*, 7(5), 857-869.

Bang D. D., Verhage R., Goosen N., Brouwer J., van de Putte P. (1992) Molecular cloning of RAD16, a gene involved in differential repair in *Saccharomyces cerevisiae*, *Nucl Acids Res* **20**(15), 3925–3931.

Bannister A. J., Kouzarides T. (1996) The CBP co-activator is a histone acetyltransferase. *Nature* **384**(6610), 641-643.

Bardwell A. J., Bardwell L., Tomkinson A. E., Friedberg E. C. (1994) Specific cleavage of model recombination and repair intermediates by the yeast Rad1-Rad10 DNA endonuclease. *Science* **265**(5181), 2082-2085.

Beato M., Eisfeld K. (1997) Transcription factor access to chromatin. *Nucleic Acids Res* **25**(18), 3559-3563.

Becker P. B., and Horz W. (2002) ATP-dependent nucleosome remodeling. *Annu Rev*

Biochem, **71**, 247-273.

Becker, M. M. and Wang, J. C. (1984) Use of light for footprinting DNA *in vivo*. *Nature*, **309** (5970), 682-687.

Berger, S. L. (2002) Histone modifications in transcriptional regulation. *Curr Opin Genet Dev* **12**(2), 142-148.

Bhatia P. K., Wang Z., Friedberg E. C. (1996) DNA repair and transcription. *Curr Opin Genet Dev* **6**(2), 146-150.

Bird, A. W., Yu, D. Y., Pray-Grant, M. G., Qiu, Q., Harmon, K. E., Megee, P. C., Grant, P. A., Smith, M. M., Christman, M. F. (2002) Acetylation of histone H4 by Esa1 is required for DNA double-strand break repair. *Nature* **419**(6905), 411-415.

Biswas, D., Imbalzano, A. N., Eriksson, P., Yu, Y., Stillman, D. J. (2004) Role for Nhp6, Gcn5, and the Swi/Snf complex in stimulating formation of the TATA-binding protein-TFIIA-DNA complex. *Mol Cell Biol* **24**(18), 8312-8321.

Bohr, V. A., Smith, C. A., Okumoto, D. S., Hanawalt, P. C. (1985) DNA repair in an active gene: removal of pyrimidine dimers from the DHFR gene of CHO cells is much more efficient than in the genome overall. *Cell* **40**(2), 359-369.

Bohr, V.A., Hanawalt, P.C. (1987) Enhanced repair of pyrimidine dimers in coding and non-coding genomic sequences in CHO cells expressing a prokaryotic DNA repair gene. *Carcinogenesis* **8**(9), 1333-1336.

Bohr, V. A. (1991) Gene specific DNA repair. *Carcinogenesis* **12**(11), 1983–1992.

Bonenfant, D., Coulot, M., Towbin, H., Schindler, P., van Oostrum, J. (2005) Characterization of histones H2A and H2B variants and their post-translational modifications by mass spectrometry. *Mol Cell Proteomic*s, Nov. 30 (Eprint)

Boukaba, A., Georgieva, E. I., Myers, F. A., Thorne, A. W., López-Rodas, G., Crane-Robinson, C., and Franco, L.(2004). A short-range gradient of histone H3 acetylation and Tup1p redistribution at the promoter of the *Saccharomyces cerevisiae SUC2* gene. *J Bio Chem* **279**(9), 7678–7684.

Brownell, J. E., Allis, C. D. (1996) Special HATs for special occasions: linking histone acetylation to chromatin assembly and gene activation. *Curr Opin Genet Dev* **6**(2), 176-184.

Brownell, J. E., Zhou, J., Ranalli, T., Kobayashi, R., Edmondson, D. G., Roth, S. Y., Allis, C. D. (1996) Tetrahymena histone acetyltransferase A: a homolog to yeast

Gcn5p linking histone acetylation to gene activation. *Cell* **84**(6), 843-851.

Bucheli, M., Lommel, L., Sweder, K. (2001) The defect in transcription-coupled repair displayed by a Saccharomyces cerevisiae rad26 mutant is dependent on carbon source and is not associated with a lack of transcription. *Genetics* **158**(3), 989-997.

Carlson, M. (1997) Genetics of transcriptional regulation in yeast: connections to the RNA polymerase II CTD. *Annu Rev Cell Dev Biol* **13**, 1-23.

Cheung, P., Tanner, K. G., Cheung, W. L., Sassone-Corsi, P., Denu, J. M., Allis, C. D. (2000) Synergistic coupling of histone H3 phosphorylation and acetylation in response to epidermal growth factor stimulation. *Mol Cell* **5**(6), 905-915.

Christ, C., Tye, B. K. (1991) Functional domains of the yeast transcription/replication factor MCM1. *Genes Dev* **5**(5), 751-763.

Chu, G. and Chang, E. (1988) Xeroderma pigmentosum group E cells lack a nuclear factor that binds to damaged DNA. *Science* **242** (1988), 564–567.

Clements, A., Poux, A. N., Lo, W. S., Pillus, L., Berger, S. L., and Marmorstein, R. (2003) Structural basis for histone and phosphohistone binding by the GCN5 histone acetyltransferase. *Mol Cell* **12**(2), 461–473.

Cline, S. D., Hanawalt, P. C. (2003) Who's on first in the cellular response to DNA damage? *Nat Rev Mol Cell Biol* **4**(5), 361-372.

Cooper, J. P., Roth, S. Y., Simpson, R. T. (1994) The global transcriptional regulators, SSN6 and TUP1, play distinct roles in the establishment of a repressive chromatin structure. *Genes Dev* **8**(12), 1400-1410.

Cordonnier, A. M., Lehmann, A. R., Fuchs, R. P. (1999) Impaired translesion synthesis in xeroderma pigmentosum variant extracts. *Mol Cell Biol* **19**(3), 2206-2211.

Cosma, M. P., Tanaka, T., Nasmyth, K. (1999) Ordered recruitment of transcription and chromatin remodeling factors to a cell cycle- and developmentally regulated promoter. *Cell* **97**(3), 299-311.

Costa, R. M., Chigancas, V., Galhardo, Rda S., Carvalho, H., Menck, C. F. (2003) The eukaryotic nucleotide excision repair pathway. *Biochimie* **85**(11), 1083-1099.

Daniel, J. A., Torok, M. S., Sun, Z. W., Schieltz, D., Allis, C. D., Yates, J. R. 3rd, Grant, P. A. (2004) Deubiquitination of histone H2B by a yeast acetyltransferase complex regulates transcription. *J Biol Chem* **279**(3), 1867-1871.

Datta, A., Bagchi, S., Nag, A., Shiyanov, P., Adami, G. R., Yoon, T. and Raychaudhuri, P. (2001) The p48 subunit of the damaged-DNA binding protein DDB associates with the CBP/p300 family of histone acetyltransferase. *Mutat Res* **486**, 89–97.

Davie, J. K., Trumbly, R. J., Dent, S. Y. (2002) Histone-dependent association of Tup1-Ssn6 with repressed genes in vivo. *Mol Cell Biol* **22**(3), 693-703

de Boer, J., Andressoo, J. O., de Wit, J, Huijmans, J., Beems, R. B., van Steeg, H., Weeda, G., van der Horst, G. T., van Leeuwen, W., Themmen, A. P., Meradji, M., Hoeijmakers, J. H. (2002) Premature Aging in Mice Deficient in DNA Repair and Transcription. *Science* **296**(5571), 1276-1279.

de Boer, J., Hoeijmakers, J. H. (2000) Nucleotide excision repair and human syndromes. *Carcinogenesis* **21**(3), 453-460.

Deckert, J., Struhl, K. (2001) Histone acetylation at promoters is differentially affected by specific activators and repressors. *Mol Cell Biol* **21**(8), 2726-2735.

de la Cruz, X., Lois, S., Sanchez-Molina, S., Martinez-Balbas, M. A. (2005) Do protein motifs read the histone code? *Bioessays* **27**(2), 164-175.

de Laat, W. L., Appeldoorn, E., Sugasawa, K., Weterings, E., Jaspers, N. G., Hoeijmakers, J. H. (1998) DNA-binding polarity of human replication protein A positions nucleases in nucleotide excision repair. *Genes Dev* **12**(16), 2598-2609.

de Laat, W. L., Jaspers, N. G., Hoeijmakers, J. H. (1999) Molecular mechanism of nucleotide excision repair. *Genes Dev* **13**(7), 768-785.

Del Bigio, M. R., Greenberg, C. R., Rorke, L. B., Schnur, R., McDonald-McGinn, D. M., Zackai, E. H. (1997) Neuropathological findings in eight children with cerebro-oculo-facio-skeletal (COFS) syndrome. *J Neuropathol Exp Neurol* **56**(10), 1147-1157.

Dhalluin, C., Carlson, J. E., Zeng, L., He, C., Aggarwal, A. K., and Zhou, M. M. (1999). Structure and ligand of a histone acetyltransferase bromodomain. *Nature* **399**(6735), 491–496.

Diffey, B. (2004) Climate change, ozone depletion and the impact on ultraviolet exposure of human skin. *Phys Med Biol* **49**(1), R1-11.

Donahue, B. A., Yin, S., Taylor, J. S., Reines, D., Hanawalt, P. C. (1994) Transcript cleavage by RNA polymerase II arrested by a cyclobutane pyrimidine dimer in the DNA template. *Proc Natl Acad Sci U S A.* **91**(18), 8502-8506.

Downs, J. A., Kosmidou, E., Morgan, A., Jackson, S. P. (2003) Suppression of homologous recombination by the Saccharomyces cerevisiae linker histone. *Mol Cell* **11**(6), 1685-1692.

Dranginis, A. M. (1990) Binding of yeast a1 and alpha 2 as a heterodimer to the operator DNA of a haploid-specific gene. *Nature* **347**(6294), 682-685.

Ducker, C. E. and Simpson, R. T. (2000) The organized chromatin domain of the repressed yeast a cell-specific gene *STE6* contains two molecules of the corepressor Tup1p per nucleosome. *EMBO J* **19**(3), 400–409.

Dunphy, E. L, Johnson, T., Auerbach, S. S, Wang, E. H. (2000) Requirement for TAF(II)250 acetyltransferase activity in cell cycle progression. *Mol Cell Biol* **20**(4), 1134-1139.

Durrin, L.K., Mann, R.K., Kayne, P. S., Grunstein, M. (1991) Yeast histone H4 N-terminal sequence is required for promoter activation in vivo. *Cell* **65**(6), 1023-1031.

Dvir, A., Conaway, R. C., Conaway, J. W. (1997) A role for TFIIH in controlling the activity of early RNA polymerase II elongation complexes. *Proc Natl Acad Sci U S A.* **94**(17), 9006-9010.

Edmondson, D. G., Smith, M. M., and Roth, S. Y. (1996) Repression domain of the yeast global repressor Tup1 interacts directly with histones H3 and H4. *Genes Dev* **10**(10), 1247–1259.

Edmondson, D. G., Zhang, W., Watson, A., Xu, W., Bone, J. R., Yu, Y., Stillman, D., Roth, S. Y. (1998) In vivo functions of histone acetylation/deacetylation in Tup1p repression and Gcn5p activation. *Cold Spring Harb Symp Quant Biol* **63**, 459-468.

Eisen, J. A., Sweder K. S., and Hanawalt P. C. (1995) Evolution of the SNF2 family of proteins: subfamilies with distinct sequences and functions. *Nucleic Acids Res* **23**(14), 2715–2723.

Eisenmann, D. M., Arndt, K. M., Ricupero, S. L., Rooney, J. W., Winston, F. (1992) SPT3 interacts with TFIID to allow normal transcription in *Saccharomyces cerevisiae*. *Genes Dev* **6**(7), 1319-1331.

Evans, E., Moggs, J. G., Hwang, J. R., Egly, J. M., Wood, R. D. (1997) Mechanism of open complex and dual incision formation by human nucleotide excision repair factors. *EMBO J* **16**(21), 6559-6573.

Feaver, W. J., Svejstrup, J. Q., Bardwell, L., Bardwell, A. J., Buratowski, S., Gulyas,

K. D., Donahue, T. F., Friedberg, E. C., Kornberg, R. D. (1993) Dual roles of a multiprotein complex from *S. cerevisiae* in transcription and DNA repair. *Cell* **75**(7), 1379-1387.

Feaver, W. J., Svejstrup, J. Q., Henry, N. L., Kornberg, R. D. (1994) Relationship of CDK-activating kinase and RNA polymerase II CTD kinase TFIIH/TFIIK. *Cell* **79**(6), 1103-1109.

Feaver, W. J., Huang, W., Friedberg, E. C. (1999) The TFB4 subunit of yeast TFIIH is required for both nucleotide excision repair and RNA polymerase II transcription. *J Biol Chem* **274**(41), 29564-29567.

Feaver, W. J., Huang, W., Gileadi, O., Myers, L., Gustafsson, C. M., Kornberg, R. D., Friedberg, E. C. (2000) Subunit interactions in yeast transcription/repair factor TFIIH. Requirement for Tfb3 subunit in nucleotide excision repair. *J Biol Chem 275*(8), 5941-5946.

Feng, Z., Hu, W., Chasin, L. A., Tang, M. S. (2003) Effects of genomic context and chromatin structure on transcription-coupled and global genomic repair in mammalian cells. *Nucleic Acids Res* **31**(20), 5897-5906.

Ferreiro, J. A., Powell, N. G., Karabetsou, N., Kent, N. A., Mellor, J., Waters, R. (2004) Cbf1p modulates chromatin structure, transcription and repair at the *Saccharomyces cerevisiae* MET16 locus. *Nucleic Acids Res* **32**(5), 1617-1626.

Filetici, P., Aranda, C., Gonzalez, A., Ballario, P. (1998) GCN5, a yeast transcriptional coactivator, induces chromatin reconfiguration of HIS3 promoter *in vivo*. *Biochem Biophys Res Commun* **242**(1), 84-87.

Fitzpatrick, D. R., Wilson, C. B. (2003) Methylation and demethylation in the regulation of genes, cells, and responses in the immune system. *Clin Immunol* **109**(1), 37-45.

Franklin, W. A., Doetsch, P. W., and Haseltine, W. A. (1985) Structural determination of the ultraviolet light-induced thymine-cytosine pyrimidine-pyrimidone (6-4) photoproduct. *Nucleic Acids Res* **13**(14), 5317-5325.

Friedberg, E. C., Walker G. C. and Siede W. (1995) DNA repair and Mutagenesis. *American Society of Microbiology Press, Washington DC.*

Friedberg, E. C. (1996) Relationships between DNA repair and transcription. *Annu Rev Biochem* **65**, 15-42.

Friedberg, E. C. (2001) How Nucleotide Excision Repair Protects Against Cancer.

Nature Reviews Cancer **1**(1), 22-33.

Friedberg, E. C. (2003) DNA damage of repair. *Nature* **421**(6921), 436-440.

Friedberg, E. C., McDaniel, L. D., Schultz, R. A. (2004) The role of endogenous and exogenous DNA damage and mutagenesis. *Curr Opin Genet Dev* **14**(1), 5-10.

Gale, J. M. and Smerdon, M. J. (1990) UV induced (6-4) photoproducts are distributed differently than cyclobutane dimmers in nucleosomes. *Photochem Photobiol*, **51**(4), 411-417.

Gavin, I. M., Kladde, M. P., Simpson, R. T. (2000) Tup1p represses Mcm1p transcriptional activation and chromatin remodeling of an a-cell-specific gene. *EMBO J* **19**(21), 5875-5883.

Georgakopoulos, T., Thireos, G. (1992) Two distinct yeast transcriptional activators require the function of the GCN5 protein to promote normal levels of transcription. *EMBO J* **11**(11), 4145-4152.

Gillette, T. G., Huang, W., Russell, S. J., Reed, S. H., Johnston, S. A., Friedberg, E. C. (2001) The 19S complex of the proteasome regulates nucleotide excision repair in yeast. *Genes Dev* **15**(12), 1528-1539.

Goodrich, J. A., Tjian, R. (1994) Transcription factors IIE and IIH and ATP hydrolysis direct promoter clearance by RNA polymerase II. *Cell* **77**(1), 145-156.

Gorbalenya, A. E., Koonin, E. V., Donchenko, A. P., Blinov, V. M. (1989) Two related superfamilies of putative helicases involved in replication, recombination, repair and expression of DNA and RNA genomes, *Nucl Acids Res* **17**(12), 4713–4730.

Gordon, L. K., Haseltine, W. A. (1982) Quantitation of cyclobutane pyrimidine dimer formation in double- and single-stranded DNA fragments of defined sequence. *Radiat Res* **89**(1), 99-112

Graham Jr., J. M., Anyane-Yeboa, K., Raams, A., Appeldoorn, E., Kleijer, W. J., Garritsen, V. H., Busch, D., Edersheim, T. G., Jaspers, N. G. (2001) Cerebro-oculo-facio-skeletal syndrome with a nucleotide excision-repair defect and a mutated XPD gene, with prenatal diagnosis in a triplet pregnancy. *Am J Hum Genet* **69**, 291–300.

Grant, P. A., Duggan, L., Cote, J., Roberts, S. M., Brownell, J. E., Candau, R., Ohba, R., Owen-Hughes, T., Allis, C. D., Winston, F., Berger, S. L., Workman, J. L. (1997) Yeast Gcn5 functions in two multisubunit complexes to acetylate nucleosomal

histones: characterization of an Ada complex and the SAGA (Spt/Ada) complex. *Genes Dev* **11**(13), 1640-1650.

Grant, P. A., Eberharter, A., John, S., Cook, R. G., Turner, B. M. and Workman, J. L. (1999) Expanded lysine acetylation specificity of Gcn5 in native complexes. *J Biol Chem*, **274**(9), 5895-5900.

Grant, P. A., Schieltz, D., Pray-Grant, M. G., Steger, D. J., Reese, J. C., Yates, J. R. 3rd, Workman, J. L. (1998) A subset of TAF(II)s are integral components of the SAGA complex required for nucleosome acetylation and transcriptional stimulation. *Cell* **94**(1), 45-53.

Gromoller, A., Lehming, N. (2000) Srb7p is a physical and physiological target of Tup1p. *EMBO J* **19**(24), 6845-6852.

Grunstein, M., Hecht, A., Fisher-Adams, G., Wan, J., Mann, R. K., Strahl-Bolsinger, S., Laroche, T., Gasser, S. (1995) The regulation of euchromatin and heterochromatin by histones in yeast. *J Cell Sci Suppl* **19**, 29-36.

Grunstein, M. (1997) Histone acetylation in chromatin structure and transcription. *Nature* **389**(6649), 349-352.

Guarente, L. (1995) Transcriptional coactivators in yeast and beyond. *Trends Biochem.. Sci* **20**(12), 517-521.

Guzder, S. N., Bailly, V., Sung, P., Prakash, L., Prakash, S. (1995a) Yeast DNA repair protein RAD23 promotes complex formation between transcription factor TFIIH and DNA damage recognition factor RAD14. *J Biol Chem* **270**(15), 8385-8388

Guzder, S. N., Habraken, Y., Sung, P., Prakash, L., Prakash, S. (1995b) Reconstitution of yeast nucleotide excision repair with purified Rad proteins, replication protein A, and transcription factor TFIIH. *J Biol Chem* **270**(22), 12973-12976

Guzder, S. N., Sung, P., Prakash, L., Prakash, S. (1993) Yeast DNA-repair gene RAD14 encodes a zinc metalloprotein with affinity for ultraviolet-damaged DNA. *Proc Natl Acad Sci U S A.* **90**(12), 5433-5437.

Guzder, S. N., Qiu, H., Sommers, C. H., Sung, P., Prakash, L., Prakash, S. (1994 a) DNA repair gene RAD3 of S. cerevisiae is essential for transcription by RNA polymerase II. *Nature* **367**(6458), 91-94.

Guzder, S. N., Sung, P., Bailly, V., Prakash, L., Prakash, S. (1994 b) RAD25 is a DNA helicase required for DNA repair and RNA polymerase II transcription. *Nature*

369(6481), 578-581.

Guzder, S. N., Sung, P., Prakash, L., and Prakash, S. (1997) Yeast Rad7-Rad16 complex, specific for the nucleotide excision repair of the nontranscribed DNA strand, is an ATP-dependent DNA damage sensor. *J Biol Chem* **272**(35), 21665–21668.

Guzder, S. N., Sung, P., Prakash, L., Prakash, S. (1998a) The DNA-dependent ATPase activity of yeast nucleotide excision repair factor 4 and its role in DNA damage recognition. *J Biol Chem* **273**(11), 6292-6296.

Guzder, S. N., Sung, P., Prakash, L., Prakash, S. (1998b) Affinity of yeast nucleotide excision repair factor 2, consisting of the Rad4 and Rad23 proteins, for ultraviolet damaged DNA. *J Biol Chem* **273**(47), 31541-31546.

Hamilton, K. K., Kim, P. M., Doetsch, P. W. (1992) A eukaryotic DNA glycosylase/lyase recognizing ultraviolet light-induced pyrimidine dimers. *Nature* **356**(6371), 725-728.

Hanawalt, P., and Mellon, I. (1993) Stranded in an active gene. *Curr Biol* **3**(1), 67-69.

Hanawalt, P. C. (1994) Transcription-coupled repair and human disease. *Science* **266**(5193), 1957-1958.

Hanawalt, P. C. (2000) DNA repair. The bases for Cockayne syndrome. *Nature* **405**(6785), 415-416

Hanawalt, P. C. (2001) Controlling the efficiency of excision repair. *Mutat Res* **485**(1), 3-13.

Hanawalt, P. C. (2002) Subpathways of nucleotide excision repair and their regulation. *Oncogene* **21**(58), 8949-8956.

Hanawalt, P. C. (2003) Four decades of DNA repair: from early insights to current perspectives. *Biochimie* **85**(11), 1043-1052.

Hara, R., Mo, J., Sancar, A. (2000) DNA damage in the nucleosome core is refractory to repair by human excision nuclease. *Mol Cell Biol* **20**(24), 9173-9181.

Harrington, J. J., Lieber, M. R. (1994) Functional domains within FEN-1 and RAD2 define a family of structure-specific endonucleases: implications for nucleotide excision repair. *Genes Dev* **8**(11), 1344-1355.

Harvey, A. C., Downs, J. A. (2004) What functions do linker histones provide? *Mol Microbiol* **53**(3), 771-775.

Hassan, A. H., Prochasson, P., Neely, K. E., Galasinski, S. C., Chandy, M., Carrozza, M. J., and Workman, J. L. (2002) Function and selectivity of bromodomains in anchoring chromatin-modifying complexes to promoter nucleosomes. *Cell* **111**(3), 369-379.

Hassig, C. A., Fleischer, T. C., Billin, A. N., Schreiber, S. L., Ayer, D. E. (1997) Histone deacetylase activity is required for full transcriptional repression by mSin3A. *Cell* **89**(3), 341-347.

Hasty, P., Vijg, J. (2002) Aging: Genomic priorities in aging. *Science* **296**(5571), 1250-1251.

Havas, K., Flaus, A., Phelan, M., Kingston, R., Wade, P. A., Lilley, D. M., Owen-Hughes, T. (2000) Generation of superhelical torsion by ATP-dependent chromatin remodeling activities. *Cell* **103**(7), 1133-1142.

Hebbes, T. R, Thorne, A. W, Crane-Robinson, C. (1988) A direct link between core histone acetylation and transcriptionally active chromatin. *EMBO J* **7**(5), 1395-1402.

Heinzel, T., Lavinsky, R.M., Mullen, T. M., Soderstrom, M., Laherty, C. D., Torchia, J., Yang, W. M., Brard, G., Ngo, S. D., Davie, J. R., Seto, E., Eisenman, R. N., Rose, D. W., Glass, C. K., Rosenfeld, M. G. (1997) A complex containing N-CoR, mSin3 and histone deacetylase mediates transcriptional repression. *Nature* **387**(6628), 43-48.

Henikoff, S., and Ahmad, K. (2005) Assembly of Variant Histones into Chromatin. *Annu Rev Cell Dev Biol* **12**, 133-153.

Herschbach, B. M., Arnaud, M. B., Johnson, A. D. (1994) Transcriptional repression directed by the yeast alpha 2 protein in vitro. *Nature* **370**(6487), 309-311.

Herschbach, B. M., Johnson, A. D. (1993) Transcriptional repression in eukaryotes. *Annu. Rev Cell Biol* **9**, 479-509.

Herskowitz, I.(1989) A regulatory hierarchy for cell specialization in yeast. *Nature* **342**(6251), 749-757.

Hess, M. T., Schwitter, U., Petretta, M., Giese, B., Naegeli, H. (1997) Bipartite substrate discrimination by human nucleotide excision repair. *Proc Natl Acad Sci USA* **94**(13), 6664-6669.

Ho. Y., Gruhler. A., Heilbut, A., Bader, G. D., Moore, L., Adams, S.L., Millar, A., Taylor, P., Bennett, K., Boutilier, K., Yang, L., Wolting, C., Donaldson, I., Schandorff, S., Shewnarane, J., Vo, M., Taggart, J., Goudreault, M., Muskat, B., Alfarano, C., Dewar, D., Lin, Z., Michalickova, K., Willems, A. R., Sassi, H., Nielsen, P. A.,

Rasmussen, K. J., Andersen, J. R., Johansen, L. E., Hansen, L. H., Jespersen, H., Podtelejnikov, A., Nielsen, E., Crawford, J., Poulsen, V., Sorensen, B. D., Matthiesen, J., Hendrickson, R.C., Gleeson, F., Pawson, T., Moran, M. F., Durocher, D., Mann, M., Hogue, C. W., Figeys, D., Tyers, M. (2002) Systematic identification of protein complexes in *Saccharomyces cerevisiae* by mass spectrometry. *Nature* **415**(6868), 180–183.

Hochstrasser, M. (1996) Ubiquitin-dependent protein degradation. *Annu Rev Genet* **30**, 405–439.

Hoeijmakers, J. H. (2001) Genome maintenance mechanisms for preventing cancer. *Nature*, **411**(6835), 366-374.

Holstege, F. C., Jennings, E. G., Wyrick, J. J., Lee, T. I., Hengartner, C. J., Green, M. R., Gloub, T. R., Lander, E. S., and Young, R. A. (1998) Dissecting the regulatory circuitry of a eukaryotic genome. *Cell* **95**(5), 717-728.

Hu, W., Feng, Z., Chasin, L. A., Tang, M. S. (2002) Transcription-coupled and transcription-independent repair of cyclobutane pyrimidine dimers in the dihydrofolate reductase gene. *J Biol Chem* **277**(41), 38305-38310.

Huang, M., Zhou, Z., Elledge, S. J. (1998) The DNA replication and damage checkpoint pathways induce transcription by inhibition of the Crt1 repressor. *Cell* **94**(5), 595–605.

Hwang-Shum, J. J., Hagen, D. C., Jarvis, E. E., Westby, C. A., Sprague, G. F., Jr. (1991) Relative contributions of MCM1 and STE12 to transcriptional activation of a- and alpha-specific genes from *Saccharomyces cerevisiae. Mol Gen Genet* **227**(2), 197-204.

Ichihashi, M., Ueda, M., Budiyanto, A., Bito, T., Oka, M., Fukunaga, M., Tsuru, K., Horikawa, T. (2003) UV-induced skin damage. *Toxicology* **189**(1-2), 21-39.

Imbalzano, A. N., Kwon, H., Green, M. R., Kingston, R. E. (1994) Facilitated binding of TATA-binding protein to nucleosomal DNA. *Nature* **370**(6489), 481-485.

Jacobson, R. H., Ladurner, A. G., King, D. S., and Tjian, R. (2000). Structure and function of a human TAFII250 double bromodomain module. *Science* **288**(5470), 1422–1425.

Jenuwein, T. and Allis, C. D. (2001) Translating the Histone Code. *Science* **293**(5532), 1074-1080.

Joazeiro, C. A., and Weissman A. M. (2000) RING finger proteins: mediators of

ubiquitin ligase activity. *Cell* **102**(5), 549–552.

Jones, C. J., Wood, R. D. (1993) Preferential binding of the xeroderma pigmentosum group A complementing protein to damaged DNA. *Biochemistry* **32**(45), 12096-12104.

Kadosh, D. and Struhl, K. (1997) Repression by Ume6 involves recruitment of a complex containing Sin3 corepressor and Rpd3 histone deacetylase to target promoters. *Cell* **89**(3), 365-371.

Kadosh, D. and Struhl, K. (1998) Targeted recruitment of the Sin3-Rpd3 histone deacetylase complex generates a highly localized domain of repressed chromatin *in vivo*. *Mol Cell Biol* **18**(9), 5121-5127.

Katan-Khaykovich, Y., Struhl, K. (2002) Dynamics of global histone acetylation and deacetylation in vivo: rapid restoration of normal histone acetylation status upon removal of activators and repressors. *Genes Dev* **16**(6), 743–752.

Keleher, C. A., Redd, M. J., Schultz, J., Carlson, M., Johnson, A. D. (1992) Ssn6-Tup1 is a general repressor of transcription in yeast. *Cell* **68**(4), 709-719.

Khorasanizadeh, S. (2004) The nucleosome: from genomic organization to genomic regulation. *Cell* **116**(2), 259–272.

Kim, J. K., Patel, D. and Choi, B. S. (1995) Contrasting structural impacts induced by *cis-syn* cyclobutane dimer and (6-4) adduct in DNA duplex deccamers: implication in mutagenesis and repair activity. *photochem Photobiol*, **62** (1), 44-50.

Kornberg, R. D. Lorch, Y. (1999) Chromatin-modifying and -remodeling complexes. *Curr Opin Genet Dev* **9**(2), 148-151.

Krebs, J. E., Kuo, M. H., Allis, C. D., Peterson, C. L. (1999) Cell cycle-regulated histone acetylation required for expression of the yeast HO gene. *Genes Dev* **13**(11), 1412-1421.

Krebs, J. E., and Peterson, C. L. (2000) Understanding "active" chromatin: a historical perspective of chromatin remodeling. *Crit Rev Eukaryot Gene Expr* **10**(1), 1–12.

Krokan, H. E., Standal, R. and Slupphaug, G. (1997) DNA glycosylases in the base excision repair of DNA. *Biochem J* **325**, 1-16.

Kuchin, S., Carlson, M. (1998) Functional relationships of Srb10-Srb11 kinase, carboxy-terminal domain kinase CTDK-I, and transcriptional corepressor Ssn6-Tup1.

Mol Cell Biol **18**(3), 1163-1171.

Kuo, M. H., and Allis, C. D. (1998) Roles of histone acetyltransferases and deacetylases in gene regulation. *Bioessays* **20**(8), 615–626.

Kuo, M. H., Brownell, J. E., Sobel, R. E., Ranalli, T. A., Cook, R. G., Edmondson, D. G., Roth, S. Y., Allis, C. D. (1996) Transcription-linked acetylation by Gcn5p of histones H3 and H4 at specific lysines. *Nature* **383**(6597), 269-272.

Kuo, M. H., vom Baur, E., Struhl, K., Allis, C. D. (2000) Gcn4 activator targets Gcn5 histone acetyltransferase to specific promoters independently of transcription. *Molecular Cell* **6**(6), 1309–1320.

Kuo, M. H., Zhou, J., Jambeck, P., Churchill, M. E., Allis, C. D. (1998) Histone acetyltransferase activity of yeast Gcn5p is required for the activation of target genes in vivo. *Genes Dev.* **12**(5), 627-639.

Kuras, L., and Struhl, K. (1999) Binding of TBP to promoters in vivo is stimulated by activators and requires Pol II holoenzyme. *Nature* **399**(6736), 609–613.

Kurdistani, S. K., Tavazoie, S., Grunstein, M. (2004) Mapping global histone acetylation patterns to gene expression. *Cell* **117**(6), 721–733.

Kusumoto, R., Masutani, C., Sugasawa, K., Iwai, S., Araki, M., Uchida, A., Mizukoshi, T., Hanaoka, F. (2001) Diversity of the damage recognition step in the global genomic nucleotide excision repair *in vitro*. *Mutat Res* **485**(3), 219-227.

Laherty, C. D., Yang, W. M., Sun, J. M., Davie, J. R., Seto, E., Eisenman, R. N. (1997) Histone deacetylases associated with the mSin3 corepressor mediate mad transcriptional repression. *Cell* **89**(3), 349-356.

Landsman, D. (1996) Histone H1 in Saccharomyces cerevisiae: a double mystery solved? *Trends Biochem Sci* **21**(8), 287-288.

Leadon, S. A., Lawrence, D. A. (1991) Preferential repair of DNA damage on the transcribed strand of the human metallothionein genes requires RNA polymerase II. *Mutat Res* **255**(1), 67-78.

Leadon, S. A., Lawrence, D. A. (1992) Strand-selective repair of DNA damage in the yeast GAL7 gene requires RNA polymerase II. *J Biol Chem* **267**(32), 23175-23182.

Lee, D. Y., Hayes, J. J., Pruss, D., Wolffe, A. P. (1993) A positive role for histone acetylation in transcription factor access to nucleosomal DNA. *Cell* **72**(1), 73-84.

Lee, M., Chatterjee, S., Struhl, K. (2000) Genetic analysis of the role of Pol II holoenzyme components in repression by the Cyc8-Tup1 corepressor in yeast. *Genetics* **155**(4), 1535-1542.

Lee, S. K., Yu, S. L., Prakash, L., Prakash, S. (2001) Requirement for yeast RAD26, a homolog of the human CSB gene, in elongation by RNA polymerase II. *Mol Cell Biol* **21**(24), 8651-8656.

Lee, S. K., Yu, S. L., Prakash, L., Prakash, S. (2002) Yeast RAD26, a homolog of the human CSB gene, functions independently of nucleotide excision repair and base excision repair in promoting transcription through damaged bases. *Mol Cell Biol* **22**(12), 4383-4389.

Lehmann, A. R. (2000) Replication of UV-damaged DNA: new insights into links between DNA polymerases, mutagenesis and human disease. *Gene* **253**(1), 1-12.

Lehmann, A. R. (2001) The xeroderma pigmentosum group D (XPD) gene: one gene, two functions, three diseases. *Genes Dev.* **15**(1), 15-23.

Lehmann, A. R., Bootsma, D., Clarkson, S. G., Cleaver, J. E., McAlpine, P. J., Tanaka, K., Thompson, L. H., Wood, R. D. (1994) Nomenclature of human DNA repair genes. *Mutat Res* **315**(1), 41-42.

Li, B., Reese, J. C. (2001) Ssn6-Tup1 regulates RNR3 by positioning nucleosomes and affecting the chromatin structure at the upstream repression sequence. *J Biol Chem* **276**(36), 33788-33797.

Li, S., Livingstone-Zatchej, M., Gupta, R., Meijer, M., Thoma, F., Smerdon, M. J. (1999) Nucleotide excision repair in a constitutive and inducible gene of a yeast minichromosome in intact cells. *Nucleic Acids Res* **27**(17), 3610-3620.

Li, S., Smerdon, M. J. (2002) Rpb4 and Rpb9 mediate subpathways of transcription-coupled DNA repair in *Saccharomyces cerevisiae*. *EMBO J* **21**(21), 5921-5929.

Li, S., Smerdon, M. J. (2004) Dissecting transcription-coupled and global genomic repair in the chromatin of yeast GAL1-10 genes. *J Biol Chem* **279**(14), 14418-14426.

Li, S., Waters, R. (1996) Nucleotide level detection of cyclobutane pyrimidine dimers using oligonucleotides and magnetic beads to facilitate labelling of DNA fragments incised at the dimers and chemical sequencing reference ladders. *Carcinogenesis* **17**(8), 1549-1552.

Lindahl, T. (1982) DNA repair enzymes. *Annu Rev Biochem* **51**, 61-87.

Lindahl, T. (1993) Instability and decay of the primary structure of DNA. *Nature* **362**(6422), 709–715.

Lippke, J. A., Gordon, L. K., Brash, D. E. and Haseltine, W. A. (1981) Distribution of UV light-induced damage in a defined sequence of human DNA: detection of alhaline-sensitive lesions at pyrimidine nucleotide-cytidine sequences. *Proc Natl Acad Sci USA*, **78**(6), 3388-3392.

Livingstone-Zatchej, M., Thoma, F. (1999) Mapping of nucleosome positions in yeast. *Methods Mol Biol* **119**, 363-378.

Lloyd, R. S. (1998) Base excision repair of cyclobutane pyrimidine dimmers. *Mutat Res* **408**(3), 159-170.

Lorick, K. L., Jensen, J. P., Fang, S., Ong, A. M., Hatakeyama, S., Weissman, A. M. (1999) RING fingers mediate ubiquitin-conjugating enzyme (E2)-dependent ubiquitination. *Proc Natl Acad Sci USA*. **96**(20), 11364–11369.

Luger, K., Mader, A. W., Richmond, R. K., Sargent, D. F., Richmond, T. J. (1997) Crystal structure of the nucleosome core particle at 2.8 A resolution. *Nature* **389**(6648), 251-260.

Mann, R. K., Grunstein, M. (1992) Histone H3 N-terminal mutations allow hyperactivation of the yeast GAL1 gene *in vivo*. *EMBO J* **11**(9), 3297-3306.

Martens, J. A., Winston, F. (2002) Evidence that Swi/Snf directly represses transcription in *S. cerevisiae*. *Genes Dev* **16**(17), 2231-2236.

Martens, J. A., Winston, F. (2003) Recent advances in understanding chromatin remodeling by Swi/Snf complexes. *Curr Opin Genet Dev* **13**(2), 136-142.

Martin, C., Zhang, Y. (2005) The diverse functions of histone lysine methylation. *Nat Rev Mol Cell Biol* **6**(11), 838-849.

McCullough, A. K., Dodson, M. L., Lloyd, R. S. (1999) Initiation of base excision repair: glycosylase mechanisms and structures. *Annu Rev Biochem* **68**, 255-285.

Mead, J., Zhong, H., Acton, T. B., Vershon, A. K. (1996) The yeast alpha2 and Mcm1 proteins interact through a region similar to a motif found in homeodomain proteins of higher eukaryotes. *Mol Cell Biol* **16**(5), 2135-2143.

Mellon, I., Hanawalt, P. C. (1989) Induction of the Escherichia coli lactose operon selectively increases repair of its transcribed DNA strand. *Nature* **342**(6245), 95-98.

Mellon, I., Spivak, G. and Hanawalt, P. C. (1987) Selective removal of transcription-blocking DNA damage from the transcribed strand of the mammalian *DHFR* gene. *Cell* **51**(2), 241-249.

Meniel, V., Waters, R. (1999) Spontaneous and photosensitiser-induced DNA single-strand breaks and formamidopyrimidine-DNA glycosylase sensitive sites at nucleotide resolutionin the nuclear and mitochondrial DNA of *Saccharomyces cerevisiae*. *Nucleic Acids Res* **27**(3), 822-830.

Michaelis, S., Chen, P., Berkower, C., Sapperstein, S., Kistler, A. (1992) Biogenesis of yeast a-factor involves prenylation, methylation and a novel export mechanism. *Antonie Van Leeuwenhoek* **61**(2), 115-117.

Michaelis, S., Herskowitz, I. (1988) The a-factor pheromone of Saccharomyces cerevisiae is essential for mating. *Mol Cell Biol* **8**(3), 1309-1318.

Mitchell, D.L., Jen, J. and Cleaver, J.E. (1992) Sequence specificity of cyclobutane pyrimidine dimmers in DNA treated with solar (ultraviolet B) radiation. *Nucleic Acids Res* **20**(2), 225-229.

Mitchell, D. L., Nairn, R. S. (1989) The biology of (6-4) photoproduct. *Photochem Photobiol* **49**(6), 805-819.

Mizzen, C. A., Yang, X. J., Kokubo, T., Brownell, J. E., Bannister, A. J., Owen-Hughes, T., Workman, J., Wang, L., Berger, S. L., Kouzarides, T., Nakatani, Y., Allis, C. D. (1996) The TAF(II)250 subunit of TFIID has histone acetyltransferase activity. *Cell* **87**(7), 1261-1270.

Moggs, J. G., and Almouzni, G. (1999) Chromatin rearrangements during nucleotide excision repair. *Biochimie* **81**(1-2), 45–52.

Morse, N. R., Meniel, V., Waters, R. (2002) Photoreactivation of UV-induced cyclobutane pyrimidine dimers in the *MFA2* gene of *Saccharomyces cerevisiae*. *Nucleic Acids Res* **30**(8), 1799-1807.

Mu, D., Sancar, A. (1997) Model for XPC-independent transcription-coupled repair of pyrimidine dimers in humans. *J Biol Chem* **272**(12), 7570-7573.

Mu, D., Wakasugi, M., Hsu, D. S., Sancar, A. (1997) Characterization of reaction intermediates of human excision repair nuclease. *J Biol Chem* **272**(46), 28971-28979.

Mueller, J. P., Smerdon, M. J. (1995) Repair of plasmid and genomic DNA in a rad7 delta mutant of yeast. *Nucleic Acids Res* **23**(17), 3457-3464.

Murphy, M. R., Shimizu, M., Roth, S. Y., Dranginis, A. M., Simpson, R. T. (1993) DNA-protein interactions at the *S.cerevisiae* alpha 2 operator *in vivo*. *Nucleic Acids Res* **21**(14), 3295-3300.

Myslinski, E., Schuster, C., Huet, J., Sentenac, A., Krol, A., Carbon, P. (1993) Point mutations 5' to the tRNA selenocysteine TATA box alter RNA polymerase III transcription by affecting the binding of TBP. *Nucleic Acids Res* **21**(25), 5852-5858.

Nagy, L., Kao, H. Y., Chakravarti, D., Lin, R. J., Hassig, C. A., Ayer, D. E., Schreiber, S. L., Evans, R. M. (1997) Nuclear receptor repression mediated by a complex containing SMRT, mSin3A, and histone deacetylase. *Cell* **89**(3), 373-380.

Nasmyth, K., Shore, D. (1987) Transcriptional regulation in the yeast life cycle. *Science* **237**(4819), 1162-1170.

Narlikar, G. J., Fan, H. Y., Kingston, R. E. (2002) Cooperation between complexes that regulate chromatin structure and transcription. *Cell* **108**(4), 475-487.

Nehlin, J. O., Carlberg, M., Ronne, H. (1991) Control of yeast GAL genes by MIG1 repressor: a transcriptional cascade in the glucose response. *EMBO J* **10**(11), 3373–3377.

Ng, J. M., Vermeulen, W., van der Horst, G. T., Bergink, S., Sugasawa, K., Vrieling, H., Hoeijmakers, J. H. (2003) A novel regulation mechanism of DNA repair by damage-induced and RAD23-dependent stabilization of xeroderma pigmentosum group C protein. *Genes Dev* **17**(13), 1630-1645.

Niggli, H. J., and Cerutti, P. A. (1982) Nucleosomal distribution of thymine photodimers following far- ad near-ultraviolet irradiation. *Biochem Biophys Res Commun* **105**(3), 1215-1223.

Nightingale, K. P., Wellinger, R. E., Sogo, J. M., Becker, P. B. (1998) Histone acetylation facilitates RNA polymerase II transcription of the Drosophila hsp26 gene in chromatin. *EMBO J* **17**(10), 2865-2876.

Nowak, S. J., Corces, V. G. (2004) Phosphorylation of histone H3: a balancing act between chromosome condensation and transcriptional activation. *Trends Genet* **20**(4), 214-220.

Nusinzon, I., Horvath, C. M. (2005) Unexpected roles for deacetylation in interferon- and cytokine-induced transcription. *J Interferon Cytokine Res* **25**(12), 745-748.

Ogryzko, V. V., Schiltz, R. L., Russanova, V., Howard, B. H., Nakatani, Y. (1996) The transcriptional coactivators p300 and CBP are histone acetyltransferases. *Cell*

87(5), 953-959.

Papamichos-Chronakis, M., Conlan, R. S., Gounalaki, N., Copf, T., Tzamarias, D. (2000) Hrs1/Med3 is a Cyc8-Tup1 corepressor target in the RNA polymerase II holoenzyme. *J Biol Chem* **275**(12), 8397-8403.

Patterton, H. G., Simpson, R. T. (1994) Nucleosomal location of the STE6 TATA box and Mat alpha 2p-mediated repression. *Mol Cell Biol* **14**(6), 4002-4010.

Pazin, M. J., Kadonaga, J. T. (1997) What's up and down with histone deacetylation and transcription? *Cell* **89**(3), 325-328.

Petit, C., Sancar, A. (1999) Nucleotide excision repair: from E. coli to man. *Biochimie* **81**(1-2), 15-25.

Peterson, C. L., and Herskowitz I. (1992) Characterization of the yeast *SWI1*, *SWI2*, and *SWI3* genes, which encode a global activator of transcription. *Cell* **68**(3), 573-583.

Peterson C. L., Workman J. L. (2000) Promoter targeting and chromatin remodeling by the SWI/SNF complex. *Curr Opin Genet Dev* **10**(2), 187–192.

Pfeifer, G. P., Drouin, R., Riggs, A. D. and Holmquist, G. P. (1992) Binding of transcription factors creates hot spots for UV photoproducts in vivo. *Mol Cell Biol* **12**(4), 1798-1804.

Piersen, C. E., Prince, M. A., Augustine, M. L., Dodson, M. L., Lloyd, R. S. (1995) Purification and cloning of Micrococcus luteus ultraviolet endonuclease, an N-glycosylase/abasic lyase that proceeds via an imino enzyme-DNA intermediate. *J Biol Chem* **270**(40), 23475-23484.

Prakash, S., and Prakash, L. (2000) Nucleotide excision repair in yeast. *Mutat Res* **451**(1-2), 13–24.

Prakash, S., Sung, P., and Prakash, L. (1993) DNA repair genes and proteins of *Saccharomyces cerevisiae*. *Annu Rev Genet* **27**, 33–70.

Pray-Grant, M. G., Schieltz, D., McMahon, S. J., Wood, J. M., Kennedy, E. L., Cook, R. G., Workman, J. L., Yates, J. R., 3rd, Grant, P. A. (2002) The novel SLIK histone acetyltransferase complex functions in the yeast retrograde response pathway. *Mol Cell Biol* **22**(24), 8774-8786.

Proft, M., Struhl, K. (2002) Hog1 kinase converts the Sko1-Cyc8-Tup1 repressor complex into an activator that recruits SAGA and SWI/SNF in response to osmotic

stress. *Mol Cell* **9**(6), 1307-1317.

Pruss, D., Bartholomew, B., Persinger, J., Hayes, J., Arents, G., Moudrianakis, E. N., Wolffe, A. P. (1996) An asymmetric model for the nucleosome: a binding site for linker histones inside the DNA gyres. *Science* **274**(5287), 614-617.

Ramsey, K. L., Smith, J. J., Dasgupta, A., Maqani, N., Grant, P., Auble, D. T. (2004) The NEF4 Complex Regulates Rad4 Levels and Utilizes Snf2/Swi2-Related ATPase Activity for Nucleotide Excision Repair. *Mol Cell Biol* **24**(14), 6362–6378.

Rapin, I., Lindenbaum, Y., Dickson, D. W., Kraemer, K. H., Robbins, J. H. (2000) Cockayne syndrome and xeroderma pigmentosum. *Neurology* **55**(10), 1442-1449.

Redd, M. J., Stark, M. R., Johnson, A. D. (1996) Accessibility of alpha 2-repressed promoters to the activator Gal4. *Mol Cell Biol* **16**(6), 2865-2869.

Redd, M. J., Arnaud, M. B., Johnson, A. D. (1997) A complex composed of tup1 and ssn6 represses transcription in vitro. *J Biol Chem* **272**(17), 11193-11197.

Reed, S. H. (2005) Nucleotide excision repair in chromatin: the shape of things to come. *DNA Repair (Amst)*, **4**(8), 909-918.

Reed, S. H., You, Z., and Friedberg, E. C. (1998) The yeast *RAD7* and *RAD16* genes are required for postincision events during nucleotide excision repair. *In vitro* and *in vivo* studies with rad7 and rad16 mutants and purification of a Rad7/Rad16-containing protein complex. *J Biol Chem* **273**(45), 29481–29488.

Reed, S. H., Akiyama, M., Stillman, B., Friedberg, E. C. (1999) Yeast autonomously replicating sequence binding factor is involved in nucleotide excision repair. *Genes Dev* **13**(23), 3052-3058.

Reed, S. H. and Waters, R. (2003) DNA repair. *Nature Encyclopedia of the human Genome*. London, Macmillan Publishers Ltd. Vol 2, pp.148-154.

Rojas, J. R., Trievel, R. C., Zhou, J., Mo, Y., Li, X., Berger, S. L., Allis, C. D., and Marmorstein, R. (1999) Structure of Tetrahymena GCN5 bound to coenzyme A and a histone H3 peptide. *Nature* **401**(6748), 93–98.

Roth, S. Y., Shimizu, M., Johnson, L., Grunstein, M., Simpson, R. T. (1992) Stable nucleosome positioning and complete repression by the yeast alpha 2 repressor are disrupted by amino-terminal mutations in histone H4. *Genes Dev* **6**(3), 411-425.

Roth, S. Y., Denu, J. M., Allis, C. D. (2001) Histone acetyltransferases. *Annu Rev Biochem* **70**, 81-120.

Rundlett, S. E., Carmen, A. A., Kobayashi, R., Bavykin, S., Turner, B. M., Grunstein, M. (1996) HDA1 and RPD3 are members of distinct yeast histone deacetylase complexes that regulate silencing and transcription. *Proc Natl Acad Sci U S A* **93**(25), 14503-14508.

Rundlett, S. E., Carmen, A. A., Suka, N., Turner, B. M., Grunstein, M. (1998) Transcriptional repression by UME6 involves deacetylation of lysine 5 of histone H4 by RPD3. *Nature* **392**(6678), 831-835.

Russell, S. J., Reed, S. H., Huang, W., Friedberg, E. C., Johnston, S. A. (1999) The 19S regulatory complex of the proteasome functions independently of proteolysis in nucleotide excision repair. *Mol Cell* **3**(6), 687-695.

Sancar, A. (1994) Mechanisms of DNA excision repair. *Science* **266**(5193), 1954-1956.

Sancar, A. (1995) Excision repair in mammalian cells. *J Biol Chem* **270**(27), 15915-15918.

Sancar, A. (1996) DNA excision repair. *Annu Rev Biochem* **65**, 43-81.

Sancar, A., Lindsey-Boltz, L. A., Unsal-Kacmaz, K., and Linn, S. (2005) Molecular mechanisms of mammalian DNA repair and the DNA damage checkpoints. *Annu Rev Biochem* **73**, 39-85.

Sauer, R. T., Smith, D. L., Johnson, A. D. (1988) Flexibility of the yeast alpha 2 repressor enables it to occupy the ends of its operator, leaving the center free. *Genes Dev* **2**(7), 807-816.

Saurin, A. J., Borden, K. L., Boddy, M. N., and Freemont, P. S. (1996) Does this have a familiar RING? *Trends Biochem Sci* **21**(6), 208–214.

Schaeffer, L., Moncollin, V., Roy, R., Staub, A., Mezzina, M., Sarasin, A., Weeda, G., Hoeijmakers, J. H., Egly, J. M. (1994) The ERCC2/DNA repair protein is associated with the class II BTF2/TFIIH transcription factor. *EMBO J* **13**(10), 2388-2392.

Schaeffer, L., Roy, R., Humbert, S., Moncollin, V., Vermeulen, W., Hoeijmakers, J. H., Chambon, P., Egly, J. M. (1993) DNA repair helicase: a component of BTF2 (TFIIH) basic transcription factor. *Science* **260**(5104), 58-63.

Schmitt, M. J., Tipper, D. J. (1990) K28, a unique double-stranded RNA killer virus of Saccharomyces cerevisiae. *Mol Cell Biol* **10**(9), 4807-4815.

Seeberg, E., Fuchs, R. P. (1990) Acetylaminofluorene bound to different guanines of

the sequence -GGCGCC- is excised with different efficiencies by the UvrABC excision nuclease in a pattern not correlated to the potency of mutation induction. *Proc Natl Acad Sci USA* **87**(1), 191-194.

Selleck, S. B. and Majors, J. (1987) Photofootprinting *in vivo* detects transcription-dependent changes in yeast TATA boxes. *Nature* **325** (7000), 173-177.

Shimizu, M., Roth, S. Y., Szent-Gyorgyi, C., Simpson, R. T. (1991) Nucleosomes are positioned with base pair precision adjacent to the alpha 2 operator in *Saccharomyces cerevisiae*. *EMBO J* **10**(10), 3033-3041.

Simpson, R. T. (1991) Nucleosome positioning: occurrence, mechanisms, and functional consequences. *Prog Nucleic Acid Res Mol Biol* **40**, 143-184.

Slupphaug, G., Mol, C. D., Kavli, B., Arvai, A. S., Krokan, H. E., Tainer, J. A. (1996) A nucleotide-flipping mechanism from the structure of human uracil-DNA glycosylase bound to DNA. *Nature* **384**(6604), 87-92.

Smerdon, M. J., Conconi, A. (1999) Modulation of DNA damage and DNA repair in chromatin. *Prog Nucleic Acids Res Mol Biol* **62**, 227–255.

Smerdon, M. J., Thoma, F. (1990) Site-specific DNA repair at the nucleosome level in a yeast minichromosome. *Cell*, **61**(4), 675-684.

Smith, C. A., Taylor, J. S. (1993) Preparation and characterization of a set of deoxyoligonucleotide 49-mers containing site-specific cis-syn, trans-syn-I, (6-4), and Dewar photoproducts of thymidylyl(3'-->5')-thymidine. *J Biol Chem* **268**(15), 11143-11151.

Smith, R. L. and Johnson, A. D. (2000) Turning genes off by Ssn6–Tup1: a conserved system of transcriptional repression in eukaryotes. *Trends Biochem Sci* **25**(7), 325-30.

Spivak, G. (2005) UV-sensitive syndrome. *Mutat Res* **577**(1-2), 162-169.

Sterner, D. E. and Berger, S. L. (2000) Acetylation of histones and transcription-related factors. *Microbiology and molecular biology reviews* **64**(2), 435-459.

Sterner, D. E., Grant, P. A., Roberts, S. M., Duggan, L. J., Belotserkovskaya, R., Pacella, L. A., Winston, F., Workman, J. L., Berger, S. L. (1999) Functional organization of the yeast SAGA complex: distinct components involved in structural integrity, nucleosome acetylation, and TATA-binding protein interaction. *Mol Cell Biol* **19**(1), 86-98.

Strahl, B. D. and Allis C. D. (2000) The language of covalent histone modifications. *Nature* **403**(6765), 41–45.

Struhl, K. (1998) Histone acetylation and transcriptional regulatory mechanisms. *Genes Dev* **12**(5), 599–606.
Struhl, K. (1999) Fundamentally different logic of gene regulation in eukaryotes and prokaryotes. *Cell* **98**(1), 1-4.

Sudarsanam, P., Cao, Y., Wu, L., Laurent, B. C., Winston, F. (1999) The nucleosome remodeling complex, Snf/Swi, is required for the maintenance of transcription in vivo and is partially redundant with the histone acetyltransferase, Gcn5. *EMBO J* **18**(11), 3101-3106.

Sudarsanam, P., Winston, F. (2000) The Swi/Snf family nucleosome-remodeling complexes and transcriptional control. *Trends Genet* **16**(8), 345-351.

Sugasawa, K., Okamoto, T., Shimizu, Y., Masutani, C., Iwai, S., Hanaoka, F. (2001) A multistep damage recognition mechanism for global genomic nucleotide excision repair. *Genes Dev* **15**(5), 507-521.

Sugasawa, K., Okuda, Y., Saijo, M., Nishi, R., Matsuda, N., Chu, G., Mori, T., Iwai, S., Tanaka, K., Tanaka, K., Hanaoka, F. (2005) UV-induced ubiquitylation of XPC protein mediated by UV-DDB-ubiquitin ligase complex. *Cell* **121**(3), 387-400.

Sung, P., Bailly, V., Weber, C., Thompson, L. H., Prakash, L., Prakash, S. (1993) Human xeroderma pigmentosum group D gene encodes a DNA helicase. *Nature* **365**(6449), 852-855.

Sung, P., Guzder S. N., Prakash, L., Prakash, S. (1996) Reconstitution of TFIIH and requirement of its DNA helicase subunits, Rad3 and Rad25, in the incision step of nucleotide excision repair. *J Biol Chem* **271**(18), 10821-10826.

Sung, P., Prakash, L., Matson, S. W., Prakash, S. (1987) RAD3 protein of *Saccharomyces cerevisiae* is a DNA helicase. *Proc Natl Acad Sci USA* **84**(24), 8951-8955.

Sung, P., Guzder, S. N., Prakash, L., Prakash, S. (1996) Reconstitution of TFIIH and requirement of its DNA helicase subunits, Rad3 and Rad25, in the incision step of nucleotide excision repair. *J Biol Chem* **271**(18), 10821-10826.

Svejstrup, J. Q. (2002) Mechanisms of transcription-coupled DNA repair. *Nat Rev Mol Cell Biol* **3**(1), 21-29.

Svejstrup, J. Q. (2003) Rescue of arrested RNA polymerase II complexes. *J Cell Sci*

116(pt3), 447-451.

Svejstrup, J. Q., Feaver, W. J., LaPointe, J., Kornberg, R. D. (1994) RNA polymerase transcription factor IIH holoenzyme from yeast. *J Biol Chem* **269**(45), 28044-28048.

Svejstrup, J. Q., Wang, Z., Feaver, W. J., Wu, X., Bushnell, D. A., Donahue, T. F., Friedberg, E. C., Kornberg, R. D. (1995) Different forms of TFIIH for transcription and DNA repair: holo-TFIIH and a nucleotide excision repairosome. *Cell* **80**(1), 21-28.

Sweder, K., Madura, K. (2002) Regulation of repair by the 26S proteasome. *J Biomed Biotechnol* **2**(2), 94-105.

Taunton, J., Hassig, C. A., Schreiber, S. L. (1996) A mammalian histone deacetylase related to the yeast transcriptional regulator Rpd3p. *Science* **272**(5260), 408-411.

Teng, Y. (2000) Nucleotide excision repair in the *Saccharomyces cerevisiae MFA2* gene. PhD thesis. University of Wales, Swansea

Teng Y., Li S., Waters R., Reed S. H.(1997) Excision repair at the level of the nucleotide in the *Saccharomyces cerevisiae MFA2* gene: mapping of where enhanced repair in the transcribed strand begins or ends and identification of only a partial rad16 requisite for repairing upstream control sequences. *J Mol Biol* **267**(2), 324-337.

Teng, Y., Liu, H., Yu, Y., Conlan, S., Reed, S., Waters, R. (2006) Rad16p is not essential for the GGR of all transcribed regions of the yeast genome: absence of Tup1p enhances GGR and Suppresses the Rad16p requisite in certain regulatory regions. *(in preparation)*

Teng, Y., Longhese, M., McDonough, G., Waters, R. (1998) Mutants with changes in different domains of yeast replication protein A exhibit differences in repairing the control region, the transcribed strand and the non-transcribed strand of the *Saccharomyces cerevisiae MFA2* gene. *J Mol Biol* **280**(3), 355-363.

Teng, Y., Waters, R. (2000) Excision repair at the level of the nucleotide in the upstream control region, the coding sequence and in the region where transcription terminates of the *Saccharomyces cerevisiae MFA2* gene and the role of *RAD26*. *Nucleic Acids Res.* **28**(5), 1114-1119.

Teng, Y., Yu, S., Waters, R. (2001) The mapping of nucleosomes and regulatory protein binding sites at the *Saccharomyces cerevisiae MFA2* gene: a high resolution approach. *Nucleic Acids Res* **29**(13), e64-4.

Teng, Y., Yu, Y., Waters, R. (2002) The Saccharomyces cerevisiae histone

acetyltransferase Gcn5 has a role in the photoreactivation and nucleotide excision repair of UV-induced cyclobutane pyrimidine dimers in the *MFA2* gene. *J Mol Biol* **316**(3), 489-499.

Teng, Y., Yu, Y., Ferreiro, J. A., Waters, R. (2005) Histone acetylation, chromatin remodelling, transcription and nucleotide excision repair in *S. cerevisiae*: studies with two model genes. *DNA Repair (Amst)*, **4**(8), 870-883.

Terleth, C., Schenk P., Poot, R., Brouwer, J., and van de Putte, P. (1990) Differential repair of UV damage in rad mutants of Saccharomyces cerevisiae: a possible function of G2 arrest upon UV irradiation. *Mol Cell Biol* **10**(9), 4678–4684.

Thoma, F. (1992) Nucleosome positioning. *Biochim Biophys Acta* **1130**(1), 1-19.

Thoma, F. (1999) Light and dark in chromatin repair: repair of UV-induced DNA lesions by photolyase and nucleotide excision repair. *EMBO J* **18**(23), 6585–6598.

Tijsterman, M., Brouwer, J. (1999) Rad26, the yeast homolog of the cockayne syndrome B gene product, counteracts inhibition of DNA repair due to RNA polymerase II transcription. *J Biol Chem* **274**(3), 1199-1202.

Tijsterman, M., Verhage, R. A., van de Putte, P., Tasseron-de Jong, J. G., Brouwer, J. (1997) Transitions in the coupling of transcription and nucleotide excision repair within RNA polymerase II-transcribed genes of Saccharomyces cerevisiae. *Pro Natl Acad Sci USA* **94**(15), 8027-8032.

Tomkinson, A. E., Bardwell, A. J., Bardwell, L., Tappe, N. J., Friedberg, E. C. (1993) Yeast DNA repair and recombination proteins Rad1 and Rad10 constitute a single-stranded-DNA endonuclease. *Nature* **362**(6423), 860-862.

Tornaletti, S., Rozek, D., Pfeifer, G. P. (1993) The distribution of UV photoproducts along the human p53 gene and its relation to mutations in skin cancer. *Oncogene* **8** (8), 2051-2057.

Tornaletti, S. and Pfeifer, G.P. (1995) UV light as a footprinting agent: modulation of UV-induced DNA damage by transcription factors bound at the promoters of three human genes. *J Mol Biol* **249**(4), 714-728.

Trievel, R. C., Rojas, J. R., Sterner, D. E., Venkataramani, R., Wang, L., Zhou, J., Allis, C. D., Berger, S. L., and Marmorstein R. (1999) Crystal structure and mechanism of histone acetylation of the yeast GCN5 transcriptional coactivator. *Proc Natl Acad Sci USA* **96**(16), 8931–8936.

Tse, C., Sera, T., Wolffe, A. P., Hansen, J. C. (1998) Disruption of higher-order

folding by core histone acetylation dramatically enhances transcription of nucleosomal arrays by RNA polymerase III. *Mol Cell Biol* **18**(8), 4629-4638.

Tsukiyama, T., Ishida, N., Shirane, M., Minamishima, Y. A., Hatakeyama, S., Kitagawa, M., Nakayama, K., Nakayama, K. (2002) Down-regulation of p27Kip1 expression is required for development and function of T cells. *J Immunol* **166**(1), 304-312.

Tsukiyama, T., Palmer, J., Landel, C. C., Shiloach, J., Wu, C. (1999) Characterization of the imitation switch subfamily of ATP-dependent chromatin-remodeling factors in Saccharomyces cerevisiae. *Genes Dev* **13**(6), 686-697.

Tzamarias, D., Struhl, K. (1995) Distinct TPR motifs of Cyc8 are involved in recruiting the Cyc8-Tup1 corepressor complex to differentially regulated promoters. *Genes Dev* **9**(7), 821-831.

Ura, K., Kurumizaka, H., Dimitrov, S., Almouzni, G., Wolffe, A. P. (1997) Histone acetylation: influence on transcription, nucleosome mobility and positioning, and linker histone-dependent transcriptional repression. *EMBO J* **16**(8), 2096-2107.

Urnov, F. D., Wolffe, A. P. (2001) Chromatin remodeling and transcriptional activation: the cast (in order of appearance). *Oncogene* **20**(24), 2991-3006.

van Hoffen, A., Balajee, A. S., van Zeeland, A. A., Mullenders, L. H. (2003) Nucleotide excision repair and its interplay with transcription. *Toxicology* **193**(1-2), 79-90.

van Hoffen, A., Natarajan, A. T., Mayne, L. V., van Zeeland, A. A., Mullenders, L. H., Venema, J. (1993) Deficient repair of the transcribed strand of active genes in Cockayne's syndrome cells. *Nucleic Acids Res* **21**(25), 5890-5895.

van Hoffen, A., Venema, J., Meschini, R., van Zeeland, A. A., Mullenders, L. H. (1995) Transcription-coupled repair removes both cyclobutane pyrimidine dimers and 6-4 photoproducts with equal efficiency and in a sequential way from transcribed DNA in xeroderma pigmentosum group C fibroblasts. *EMBO J* **14**(2), 360-367.

Van Houten, B., Eisen, J. A., Hanawalt, P. C. (2002) A cut above: discovery of an alternative excision repair pathway in bacteria. *Proc Natl Acad Sci USA* **99**(5), 2581-2583.

van Vuuren, A.,J., Vermeulen, W., Ma, L., Weeda, G., Appeldoorn, E., Jaspers, N. G., van der Eb, A. J., Bootsma, D., Hoeijmakers, J. H., Humbert, S., Schaeffer, L.and Egly, J. -M. (1994) Correction of xeroderma pigmentosum repair defect by basal transcription factor BTF2 (TFIIH). *EMBO J* **13**(7), 1645-1653.

Venema, J., Mullenders, L. H., Natarajan, A. T., van Zeeland, A. A., Mayne, L. V. (1990) The genetic defect in Cockayne syndrome is associated with a defect in repair of UV-induced DNA damage in transcriptionally active DNA. *Proc Natl Acad Sci USA* **87**(12), 4707-4711.

Venema, J., van Hoffen, A., Karcagi, V., Natarajan, A. T., van Zeeland, A. A., Mullenders, L. H. (1991) Xeroderma pigmentosum complementation group C cells remove pyrimidine dimers selectively from the transcribed strand of active genes. *Mol Cell Biol* **11**(8), 4128-4134.

Verhage, R., Zeeman, A. M., de Groot, N., Gleig, F., Bang, D. D., van de Putte, P., Brouwer, J. (1994) The RAD7 and RAD16 genes, which are essential for pyrimidine dimer removal from the silent mating type loci, are also required for repair of the nontranscribed strand of an active gene in *Saccharomyces cerevisiae. Mol Cell Biol* **14**(9), 6135-6142.

Vermeulen, W., Rademakers, S., Jaspers, N. G., Appeldoorn, E., Raams, A., Klein, B., Kleijer, W. J., Hansen, L. K., Hoeijmakers, J. H. (2001)A temperature-sensitive disorder in basal transcription and DNA repair in humans. *Nature Genet* **27**(3), 299-303.

Vignali, M., Hassan, A. H., Neely, K. E., and Workman, J. L. (2000) ATP-dependent chromatin-remodeling complexes. *Mol Cell Biol* **20**(6), 1899–1910.

Wahi, M. Johnson, A. D. (1995) Identification of genes required for alpha 2 repression in *Saccharomyces cerevisiae. Genetics* **140**(1), 79-90.

Wang, C. I. and Taylor, J. S. (1991) Site-specific effect of thymine dimmer formation on dAn·dTn tract bending and its biological implications. *Proc Natl Acad Sci USA* **88**(20), 9072-9076.

Wang, L., Mizzen, C., Ying, C., Candau, R., Barlev, N., Brownell, J., Allis, C. D., Berger, S. L. (1997) Histone acetyltransferase activity is conserved between yeast and human GCN5 and is required for complementation of growth and transcriptional activation. *Mol Cell Biol* **17**(1), 519-527.

Wang, Z., Buratowski, S., Svejstrup, J. Q., Feaver, W. J., Wu, X., Kornberg, R. D., Donahue, T. F., Friedberg, E. C. (1995) The yeast TFB1 and SSL1 genes, which encode subunits of transcription factor IIH, are required for nucleotide excision repair and RNA polymerase II transcription. *Mol Cell Biol* **15**(4), 2288-2293.

Wang, Z., Wei, S., Reed, S. H., Wu, X., Svejstrup, J. Q., Feaver, W. J., Kornberg, R. D., and Friedberg, E. C. (1997) The *RAD7*, *RAD16*, and *RAD23* genes of *Saccharomyces cerevisiae*: requirement for transcription-independent nucleotide

excision repair in vitro and interactions between the gene products. *Mol Cell Biol* **17**(2), 635–643.

Waterborg, J. H. (2000) Steady-state levels of histone acetylation in *Saccharomyces cerevisiae*. *J Biol Chem* **275**(17), 13007-13011.

Watson, A. D., Edmondson, D. G., Bone, J. R., Mukai, Y., Yu, Y., Du, W., Stillman, D. J., Roth, S. Y. (2000) Ssn6-Tupl interacts with class I histone deacetylases required for repression. *Genes Dev* **14**(21), 2737-2744.

Weissmann, F., Lyko, F. (2003) Cooperative interactions between epigenetic modifications and their function in the regulation of chromosome architecture. *Bioessays* **25**(8), 792-797.

Wellinger, R. E., Thoma, F. (1997) Nucleosome structure and positioning modulate nucleotide excision repair in the non-transcribed strand of an active gene. *EMBO J* **16**(16), 5046-5056.

Whitehouse, I., Flaus, A., Cairns, B. R., White, M. F., Workman, J. L., Owen-Hughes, T. (1999) Nucleosome mobilization catalysed by the yeast SWI/SNF complex. *Nature* **400**(6746), 784–787.

Wilson, K. L., Herskowitz, I. (1986) Sequences upstream of the STE6 gene required for its expression and regulation by the mating type locus in *Saccharomyces cerevisiae*. *Proc Natl Acad Sci USA* **83**(8), 2536-2540.

Winkler, G. S., Vermeulen, W., Coin, F., Egly, J. M., Hoeijmakers, J. H., Weeda, G. (1998) Affinity purification of human DNA repair/transcription factor TFIIH using epitope-tagged xeroderma pigmentosum B protein. *J Biol Chem* **273**(2), 1092-1098.

Winston, F., and Carlson, M. (1992) Yeast SNF/SWI transcriptional activators and the SPT/SIN chromatin connection. *Trends Genet* **8**(11), 387-391.

Wolffe, A. P. (1994) Transcription: in tune with the histones. *Cell* **77**(1), 13-16.

Wolffe, A. P. (1996) Histone deacetylase: a regulator of transcription. *Science* **272**(5260), 371-372.

Wolffe, A. P. (1998) Packaging principle: how DNA methylation and histone acetylation control the transcriptional activity of chromatin. *J Exp Zool* **282**(1-2), 239-244.

Wolffe, A. P. (2001) Transcriptional regulation in the context of chromatin structure. *Essays Biochem* **37**, 45-57.

Wolffe, A. P., and Hayes, J. J. (1999) Chromatin disruption and modification. *Nucleic Acids Res* **27**(3), 711–720.

Wolffe, A. P., Pruss, D. (1996) Targeting chromatin disruption: Transcription regulators that acetylate histones. *Cell* **84**(6), 817-819.

Wood, R. D. (1996) DNA repair in eukaryotes. *Annu Rev Biochem* **65**, 135-167.

Wood, R. D. (1997) Nucleotide excision repair in mammalian cells. *J Biol Chem* **272**(38), 23465-23468.

Wood, R. D. (1999) DNA damage recognition during nucleotide excision repair in mammalian cells. *Biochimie* **81**(1-2), 39-44.

Workman, J. L., Kingston, R. E. (1992) Nucleosome core displacement in vitro via a metastable transcription factor-nucleosome complex. *Science* **258**(5089), 1780-1784.

Workman, J. L., Yates, J. R. 3rd, Grant, P. A. (2002) The novel SLIK histone acetyltransferase complex functions in the yeast retrograde response pathway. *Mol Cell Biol* **22**(24), 8774-8786.

Woudstra, E. C., Gilbert, C., Fellows, J., Jansen, L., Brouwer, J., Erdjument-Bromage, H., Tempst, P., Svejstrup, J. Q. (2002) A Rad26-Def1 complex coordinates repair and RNA pol II proteolysis in response to DNA damage. *Nature* **415**(6874), 929-933.

Wu, J., Suka, N., Carlson, M., Grunstein, M. (2001) *TUP1* utilizes histone H3/H2B-specific HDA1 deacetylase to repress gene activity in yeast. *Mol Cell* **7**(1), 117-126.

Wu, J., Grunstein, M. (2000) 25 years after the nucleosome model: chromatin modifications. *Trends Biochem Sci* **25**(12), 619-623.

Xu, W., Edmondson, D. G., Evrard, Y. A., Wakamiya, M., Behringer, R. R., Roth, S. Y. (2000) Loss of Gcn5l2 leads to increased apoptosis and mesodermal defects during mouse development. *Nat Genet* **26**(2), 229-232.

Yang X. J., Ogryzko V. V., Nishikawa J., Howard B. H., Nakatani Y. (1996) A p300/CBP-associated factor that competes with the adenoviral oncoprotein E1A. *Nature* **382**(6589), 319-324.

You, Z., Feaver, W. J., Friedberg, E. C. (1998) Yeast RNA polymerase II transcription in vitro is inhibited in the presence of nucleotide excision repair: complementation of inhibition by Holo-TFIIH and requirement for RAD26. *Mol Cell Biol* **18**(5), 2668-2676.

Yu, S. (2001) Nucleotide excision repair and nucleosome positioning in the *Saccharomyces cerevisiae MFA2* gene. PhD thesis. University of Wales, Swansea.

Yu, S., Teng, Y., Lowndes, N. F., Waters, R. (2001) RAD9, RAD24, RAD16 and RAD26 are required for the inducible nucleotide excision repair of UV-induced cyclobutane pyrimidine dimers from the transcribed and non-transcribed regions of the *Saccharomyces cerevisiae MFA2* gene. *Mutat Res* **485**(3), 229-236.

Yu, S., Owen-Hughes, T., Friedberg, E. C., Waters, R., Reed, S. H. (2004) The yeast Rad7/Rad16/Abf1 complex generates superhelical torsion in DNA that is required for nucleotide excision repair. *DNA Repair (Amst)* **3**(3), 277-287.

Yu, Y. (2002) The repair of DNA damage in *Saccharomyces cerevisiae*. PhD thesis. University of Wales, Swansea.

Yu, Y., Teng, Y., Liu, H., Reed, S. H., Waters, R. (2005) UV irradiation stimulates histone acetylation and chromatin remodeling at a repressed yeast locus. *Proc Natl Acad Sci U S A* **102**(24), 8650-8655.

Zaman, Z., Ansari, A. Z., Koh, S. S., Young, R., Ptashne, M. (2001) Interaction of a transcriptional repressor with the RNA polymerase II holoenzyme plays a crucial role in repression. *Proc Natl Acad Sci USA* **98**(5), 2550-2554.

Zhang, W., Bone, J. R., Edmondson, D. G., Turner, B. M., and Roth, S. Y. (1998) Essential and redundant functions of histone acetylation revealed by mutation of target lysines and loss of the Gcn5p acetyltransferase. *EMBO J* **17**(11), 3155-3167.

Zhang, Z., Reese, J. C. (2004) Redundant mechanisms are used by Ssn6-Tup1 in repressing chromosomal gene transcription in *Saccharomyces cerevisiae*. *J Biol Chem* **279**(38), 39240-39250.

Zhou, B. B., Elledge, S. J. (2000) The DNA damage response: putting checkpoints in perspective. *Nature* **408**(6811), 433-439.